INVESTIGATION OF OPTOKINETIC NYSTAGMUS AND THE LINEAR VESTIBULAR-OCULAR REFLEX

By

Juan Carlos Mendoza

B.S., Georgia Institute of Technology (1991)

SUBMITTED TO THE DEPARMENT OF AERONAUTICS AND
ASTRONAUTICS IN PARTIAL FULFILLMENT OF THE REQUIREMENTS FOR
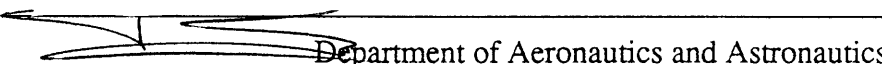THE DEGREE OF MASTER OF SCIENCE

AT THE

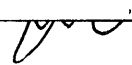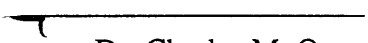MASSACHUSETTS INSTITUTE OF TECHNOLOGY

June 1993

Signature of Author _____
Department of Aeronautics and Astronautics
May 7, 1993

Certified by _____
Dr. Daniel M. Merfeld
Research Scientist and Lecturer
Thesis Supervisor

Certified by _____
Dr. Charles M. Oman
Senior Research Scientist

Certified by _____
Professor Harold Y. Wachman
Chairman, Department Graduate Committee

INVESTIGATION OF OPTOKINETIC NYSTAGMUS AND THE LINEAR VESTIBULAR-OCULAR REFLEX

By
Juan Carlos Mendoza

ABSTRACT

Only recently have humans been exposed to novel environments such as microgravity (space flight) or the high accelerations pilots undergo at takeoff in carrier-based jets. Eye movements during linear acceleration have been measured during and after spaceflight to investigate the process by which humans adapt to microgravity. Characterization of the Linear Vestibulo-Ocular Reflex (LVOR) has remained elusive due to the variability found in previous studies. Its interaction with optokinetic (OK) stimuli induced eye movements could provide information on how the central nervous system (CNS) incorporates multi-sensory information (visual and vestibular) to generate an estimate of body position within an inertial frame. This estimate is expected to help elicit the reflexive eye movements which are needed to keep an image stable on the retina in spite of self-motion.

Six subjects were tested in the upright position and seven supine using the MIT linear sled. Subjects were accelerated sinusoidally (0.4 G peak acc., 0.25Hz) along the inter-aural axis in three different conditions, 1) in darkness, 2) while viewing an OK display placed 74 cm in front of the subject moving at a constant velocity of 71cm/s (60°/s) in four different directions (up, down, right, left), and 3) while viewing this display moving sinusoidally (71cm/s peak vel., 0.25Hz) with a) no sled motion, b) with complementary sled motion (e.g. sled moving to the right, display moving to the left), and c) with anti-complementary sled motion (e.g. sled moving to the right, display moving to the right). Eye movements were measured with the scleral search coil technique.

A new statistical multi-variate method using the Hotelling's T^2 distribution was developed to analyze the slow phase velocity of the ocular response. This addresses the covariance between phase and magnitude which has been overlooked in many previous studies.

Significant ($p < 0.05$) horizontal responses were observed in all conditions. In the upright position, dark responses had an amplitude of 5.2°/s and a phase lead (of eye velocity with respect to velocity of motion) of 30°. The amplitude of the oscillations during constant velocity OK stimulation increased to 7°/s-10°/s and the DC offset of the visual response increased slightly after acceleration began. Phase lead remained in the same range (44°-33°). Complementary sinusoidal stimulation increased both the amplitude (54.8°/s) and the phase lead (19°) compared to OK stimulus only (46.3°/s, 2° lag), while the anti-complementary stimulation also increased the phase lead (13°) and left the amplitude (40°/s) near the OK alone value. Supine responses had similar amplitudes, except for dark which showed a lower amplitude (1.3°/s). During constant velocity OK stimulation the oscillations had amplitudes of 6°/s-8°/s and increased phase leads (40°-85°). Complementary sinusoidal stimulation increased the amplitude (59.2°/s) and phase lead

(19.5°) compared to OK stimulus alone (47.0°/s, 3° lag) while anticomplementary stimulation also increased the phase lead (12°) and left the magnitude (48.0) unchanged with respect to upright.

It is possible that a reciprocal effect of the vestibular and visual systems exists with the gain of each system being enhanced by the other and also modulated by the relative orientation of the gravity vector. A similar protocol to the one developed here will be used on astronauts in the NASA SLS-2 mission to investigate the effects of the CNS adaptation to the microgravity environment

Thesis Supervisor: Dr. Daniel M. Merfeld
Title: Research Scientist and Lecturer

ACKNOWLEDGMENTS

My parents, my sister, my brother and his family have been a primary source of support in since I came to this country. This thesis is for them.

The only true measure of success in life is given by the number of people one impacts in a positive way. Since I started my academical endeavors I have been fortunate to come upon many individuals who understand that.

Dan Merfeld, my thesis advisor, is one of those persons. During innumerable hours he taught and guided me through the paths of real science. Not only has he been a model to me of what a true scientist should be, he is also a model of what an outstanding human being should be.

Dr. Larry Young initiated this adventure by bringing me to the MIT, thanks to him I have had the opportunity to get involved in space research and experience what most students can only dream of doing.

The MVL has been a unique environment, where every single person taught me something important. Sherry constantly nurtured my inner child, Beverly efficiently kept me informed of all those things I needed to know, Kim went through the unbearable pain of hearing my periodical attacks of complaints, and Kristen kept us up with her good humor.

Jim, you have to promise me that sometime you'll drink a scotch with me in California. Thank you by making up for my terrible mechanical skills and discussing existentialist philosophy with me every morning.

My first year here was very hard and I do not know if I would have made it without Valérie's constant reality checks in the office. Michele helped me keep my sanity, being a constant reminder of what caring individuals are.

The rest of graduate students have also been a source of support in one way or another. Corrie is one of the most energetic and caring persons I have met. I have always been fortunate with my officemates. Thanks Karla for periodically stopping by my office to check if I still was alive and Keoki for your Hawaiian mood. Ted and Scott also provided help when needed. During the time he was here, Jock gave invaluable help.

My two favorite post-docs were always a source of inspiration. Ted C-S introduced me to perception psychology and took the time to listen to me. No, we won't into the comedy routine business, at least not for now. Winfried taught me a lot about coils and German humor.

The students I attempted to supervise were always a source of enthusiasm for my work, especially Mike Phillips and Mike Ginsberg.

The people deserve must of the credit for my being able to accomplish this are my friends, who rescued me and took care of me when I was ready to give up.

Yuri has been a true friend and the one who has taken the most from me. We'll celebrate together in Spain! Gemma and Maria always taught me something new about the meaning of life. Isela, Juan, José, MariCarmen, and Mila were a constant source of warmth. If our friendship transcends time and space, we will know what the meaning of the word friend is.

My friends in Atlanta, especially Joe and Shabnam, kept me warm through our telephone link.

Finally, when after reaching all what I have been seeking before I saw what I was lacking, you came into my life and took me into an infinite field of sunflowers. Thanks for holding my hand when I was about to fall. But above all, thanks for being you, Teresa.

7

Chapter 1
Introduction

" But although the [acceleration-related] sensations are so easily accessible to observation, there are nevertheless only a very few isolated and incomplete investigations on the determination of the pertinent facts and laws." So wrote Dr. E. Mach (Mach, 1875) more than a century ago in his classic *Outlines of The Theory of Motor Sensations*. The research needed to make his remark obsolete is still taking place for it deals with some of the most challenging questions scientists may attempt to answer: how does the human brain combine multi-sensory information to generate a representation of the orientation of our body with respect to its surroundings?

Several kinds of information are available to the central nervous system (CNS) to estimate body orientation: vestibular, visual, proprioceptive, and somatosensory. This thesis deals with the interaction between the vestibular and the visual systems and how these modalities of sensory information are used by the CNS to generate ocular movements that attempt to compensate for the new body position in order to keep images stable on the retina. The functional importance of this interaction is sometimes taken for granted but is essential for most daily activities. In the absence of this interaction, humans would see the world moving up and down as they performed activities such as walking. The evolutionary need for this is also evident. For example, rapid head

movements while fixating on a target are essential for a predator which has to pursue its prey.

Not only is the analysis of eye movements important to understand the relationship with the vestibular information, but, putting it in a larger context, it provides a means to infer the higher-level processing occurring within the CNS to produce an estimate of body orientation.

More specifically, I will attempt to characterize the oculomotor responses to linear acceleration along the interaural axis as well as to simultaneous linear dynamic visual stimulation and how these two types of sensory information interact,.

1.1 Motivation for this Study

A characterization of the relationship among different sensory information is related to the perception of orientation and is paramount to our understanding of how the CNS integrates all this information in order to control posture, eye movements, and generate an internal representation of body orientation. The need for this kind of study has become more evident in recent years as humans have been exposed to novel environments such as microgravity (space flight) or the high accelerations that pilots undergo during takeoff in carrier-based jets. Evidence suggests that the CNS shifts the weight given to each sensory channel when erroneous or conflicting information is being provided by one or more of the sensory modalities in these new environments (Young et al., 1986).

The understanding of these processes is still very limited but in the last ten years several studies have been conducted in the Space Shuttle (Young et al., 1986; Oman et al., 1989) aiming at studying the readaptation of the vestibular reflexes in response to microgravity. Further ground studies are needed not only to develop in-flight experimental protocols but also to understand the CNS orientation processes in its more common terrestrial environment.

9

Only by fully characterizing these adaptation mechanism will we be able to suggest ways to prevent or diminish the severity of conditions caused by conflicting sensory information such as motion sickness or serious disorientation. In the particular case of spaceflight, the incidence of space motion syndrome (SMS) is very high. In the first 24 missions of the Shuttle program, almost 70% of the crew members making their first flight reported SMS symptoms (Clément and Reschke, 1992). This condition seriously decreases the performance of the astronauts during the first two or three days of flight, an uncomfortable situation under normal circumstances but a potentially life-threatening one if an emergency situation were to occur during that period of impaired performance.

1.2 Thesis Organization

After this introductory chapter, Chapter 2 will review the anatomical and physiological characteristics of the structures involved in visual-vestibular interaction as well as some of the most relevant previous studies found in the literature.

Chapter 3 describes the methods used to conduct this study. It discusses the experimental protocol, the test subjects, the hardware used, and the way data were processed.

Chapter 4 presents the results in three main parts. First those obtained in the experiments run with the subject in the upright position followed by those obtained in the supine position. The last section presents the statistical analysis of the differences between these two conditions.

Chapter 5 discusses the results, presents the conclusions obtained from the analysis, and suggests future research.

Chapter 2
Background

After a brief historical introduction, this chapter will define the anatomical structures and concepts that this thesis will deal with in the ensuing discussion. The first section will discuss the basic anatomy and physiology of the vestibular system followed by a similar study of the parts of the visual system relevant to vestibular function. The last part of the chapter will discuss the known interaction between these two systems.

Though early anatomists had known of the existence of the vestibular organs, it was not until the middle of the Nineteenth Century that Flourens (1842) correctly postulated some of the functional properties of this system and suggested that it was related in some way to the visual system. He bilaterally severed the semi-circular canals of a pigeon and observed that this deficit caused severe horizontal head movements accompanied by chaotic eye displacements. After this procedure, he sacrificed the animal to prove that the cerebral cortex and especially the cerebellum had remained intact. From this, he concluded that these organs played some role in vertigo and equilibrium disturbances but did not consider them the sensory organs of equilibrium. Some years later, Goltz (1870) performed similar experiments and conclusively stated that the semicircular canals are sensory organs involved in maintaining equilibrium of the body. Mach, in 1875, finished laying the foundations of vestibular research by asserting that the stimulus to those sensory endings is *angular acceleration*, and not angular velocity, as

other researchers had proposed. The relation between ocular motor responses and body movement had been studied even before the function of the vestibular system was identified. Erasmus Darwin observed in the late 18th century the presence of nystagmus during and after rotation (Cohen, 1984), followed by a more systematic study of this phenomenon by Purkinje in 1819 (Grüser, 1984) and the geometrical analysis of eye movements carried out by Helmholtz (Westheimer, 1984).

2.1 The Vestibular System

In the most basic terms, the function of the vestibular system is to transduce linear and angular acceleration, including gravity, into a biological signal that can be fed to the upper neural areas that integrate this and other signals to generate control commands for equilibrium and locomotion as well as an internal representation of body orientation (Baloh and Honrubia, 1979). The mathematical process carried out by the CNS is analogous to the one an inertial guidance system would perform: to take information from multiple sensors and integrate it to determine the orientation and motion states in a way that allows controlled motion in the six degrees of freedom that humans have (three rotational and three translational).

Two main vestibular end organs (Figs. 2.1 and 2.2) are present in this system: the semicircular canals, which primarily transduce angular acceleration and the otolith organs, which primarily transduce linear acceleration. Both sets of organs are bilaterally located in the non-auditory portion of each inner ear, within a membranous labyrinth inside a convoluted space in the temporal bone called the bony labyrinth. The signals transduced by these organs are directed to the central vestibular system via the VIIIth cranial nerve. In addition to these afferent pathways, efferent fibers to the vestibular sensory organs have been also identified.

12

SUPERIOR CANAL

FACIAL NERVE

VESTIBULAR NERVE

UTRICLE

HORIZONTAL CANAL

AUDITORY NERVE

SACCULE

POSTERIOR CANAL
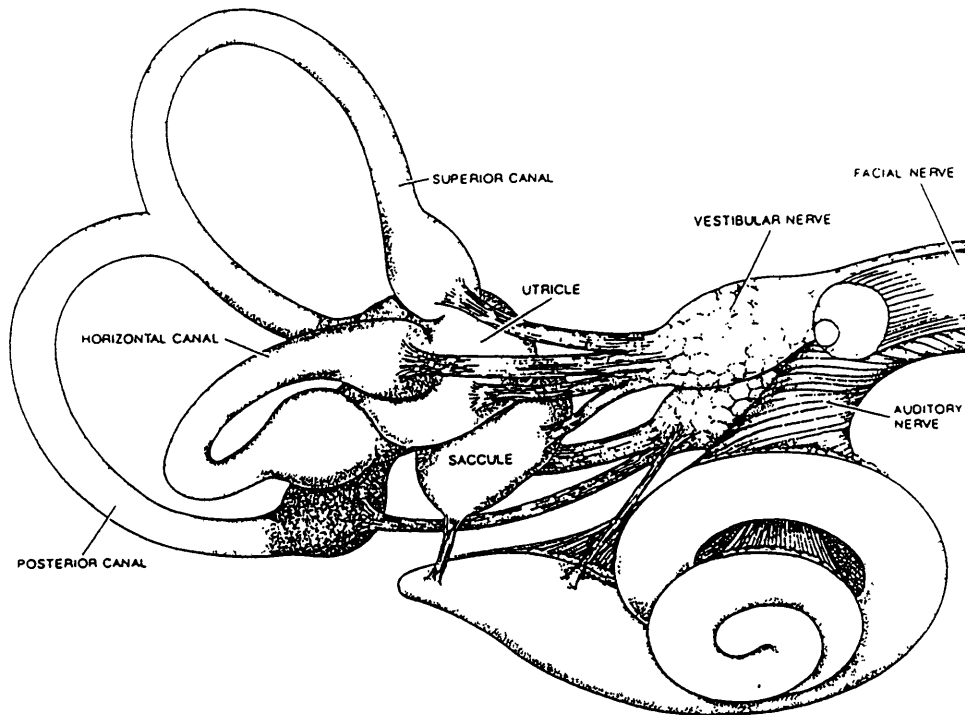
VESTIBULAR APPARATUS consists of a series of fluid-filled sacs and ducts. In this drawing of the human vestibular apparatus the three semicircular canals are at the left; clockwise from the top they are the superior, the horizontal and the posterior canal. They are oriented in the three dimensions of space and respond to angular accelerations of the head. In the center of the drawing are the two otolith receptors: the utricle (top) and the saccule. The fluid known as endolymph fills the apparatus; in the semicircular canals the endolymph functions as an inertial mass analogous to the otoconia crystals in the otolith receptors. Each semicircular canal has a bulge, the ampulla, one of which is shown in color; it is enlarged in the illustration on page 125. At the lower right in the drawing is the cochlea

LEADS TO UTRICLE

AMPULLA

CUPULA

LEADS TO SEMICIRCULAR CANAL
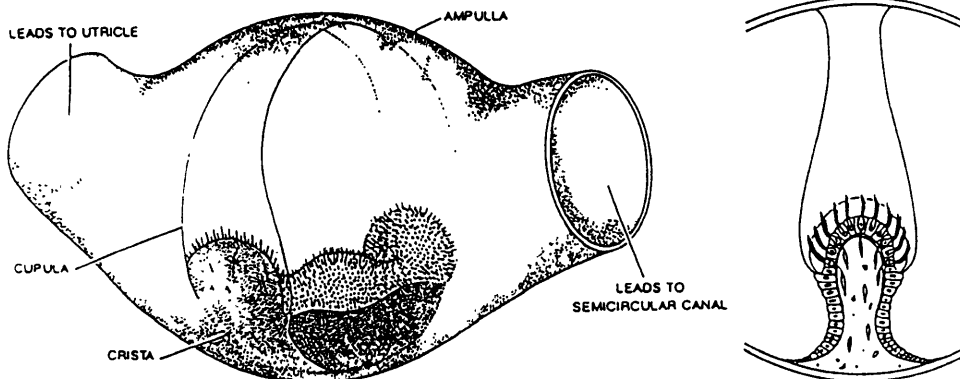
CRISTA

BULGE OF THE SEMICIRCULAR CANAL, the ampulla, is shown in transparent full view (left) and in cross section (right). Hairs anchored in a crest-shaped surface, the crista, project into a gelatinous flap called the cupula (color). The endolymph flows through the canal but is blocked by the flap. When the head is accelerated in the plane of the canal, the fluid remains stationary as the canal, including the gelatinous flap, rotates in the direction in which the head has been accelerated. The flap and the hairs protruding into it are therefore bent in the opposite direction. The bending of the hairs stimulates the transmission of impulses by nerve cells at base of hair cell

Figure 2.1: The Vestibular Apparatus and Schematic of the Ampulla. Taken from Parker (1980).

13
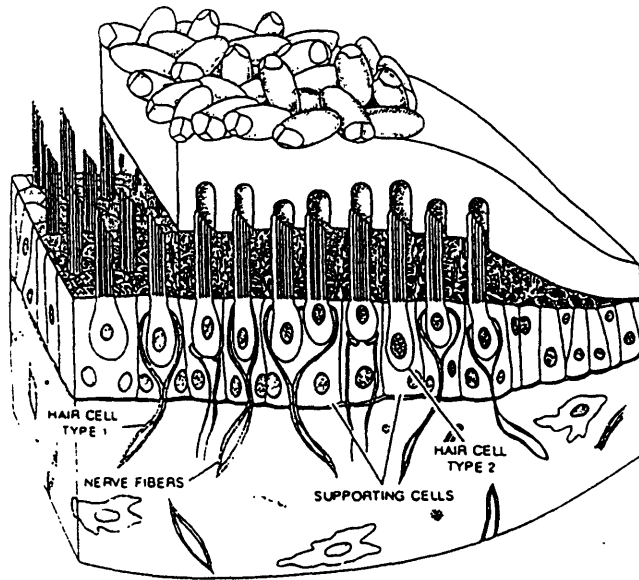
OTOLITH RECEPTOR has bundles of hairs that project into a gelatinous membrane (color). The kinocilium, the longest hair in each bundle, is attached to the side of an opening in the membrane; the shorter stereocilia extend into the opening and do not make contact. Otoconia crystals rest on top of the membrane; the membrane in turn rests on a spongelike surface, the filamentous base. Under the base is a layer of cells. Near the top of this layer are the hair cells; separating the hair cells and extending to the bottom of the layer are supporting cells. Attached to the hair cells are the threadlike nerve fibers that transmit impulses to the central nervous system. Curvature of the bottom layer of tissue corresponds to inside wall of utricle and saccule.

Figure 2.2: The Otolith Receptor. Taken from Parker (1980).

14

2.1.1 Peripheral Vestibular System

2.1.1.1 The Semicircular Canals

The semicircular canals are three membranous tubes with an average cross section diameter of 0.4 mm, each forming about two-thirds of a circle with a diameter of approximately 6.5 mm. The three canals on each side are roughly orthogonal. Each one of them has an epithelium-covered enlargement, the ampulla. This epithelium, called the crista, contains the specialized receptor cells, the vestibular hair cells. The more central area of the crista is richer in type I hair cells, while the proportion of type II cells is higher in the periphery. Type I cells are globular with a single nerve terminal surrounding the base, while type II cells are more cylindrical with multiple nerve terminals at their base. The principal difference between these two kinds of cells, is that type I cells are in contact with just one afferent fibers, while type II cells are in contact with several afferent and efferent nerve endings (Engström and Engström, 1981). The processes of these sensory neurons project into the cupula, a gelatinous mass that fills the space between the crista and the inner walls of the ampulla, and then reach the afferent fibers of the VIIIth nerve.

In principle, the canals are angular acceleration sensors with an overdamped mechanical integrator that delivers angular velocity information. Since measurements are based on acceleration, constant velocities cannot be accurately measured. To understand the physiology of the canals, it is useful to introduce a model that involves a spring restoring force acting on a piston, simulating the cupula. When the system starts rotating, the fluid inside the canal lags with respect to the tube, so that a piston would move a shorter distance than the tube itself. This produces a relative movement of the fluid with respect to the canal which causes displacement of the cupula (Wilson and Melvill-Jones, 1979). This relative movement is the mechanism of stimulation.

2.1.1.2 The Otolith Organs

The otoliths are the two globular cavities in the base of the canals, the utriculus and the sacculus. The sensory area of the otoliths is the macule, a differentiated patch of membrane that lies in the medial wall. The macule of the utricle lies mostly in the horizontal plane with the most anterior part slightly tilted in the dorsal direction and the saccular macula is approximately orthogonal, aligned with the vertical axis. Each macule has an area of less than 1 mm^2 and supports the otolith, a membrane covered by a calcareous deposit, the otoconia, which are calcium carbonate crystals, ranging from 0.5 to 30 microns in diameter. The sensory stereocilia protrude into the otolithic membrane. The striola, a well-defined curved area running through the center of each macula divides them into two areas of physiological relevance.

During motion, the otolithic membrane tends to displace with respect to the macule. The otolith is restrained in its motion by inertial and elastic pendulum-like forces with larger displacements for lower frequencies of acceleration. These displacements excite the nerve fibers innervating this area. Each neuron has a characteristic functional polarization vector that defines the axis of greatest sensitivity and the striola divides each macule into two areas of directional sensitivity. The combined polarization vector of the two macules cover all axes of linear displacement, but the sacculus is predominantly polarized in the saggital plane, while the utriculus shows maximum sensitivity in the horizontal plane (Baloh and Honrubia, 1979). Just as the canals do not sense constant angular velocity, the otolith organs do not accurately measure constant linear velocities.

After describing the sensors needed to measure displacement in the three angular degrees of freedom (the canals) and in the three translational degrees of freedom (the otolith organs), it is necessary to describe the pathways that carry this information and the structures that receive it.

16

2.1.2 Central Vestibular System

The afferent fibers of the vestibular system have their cell bodies in the vestibular ganglion in the internal auditory meatus. These axons join the ones coming from the spiral ganglion (auditory fibers) to form the VIIIth cranial nerve. This nerve runs through the cerebellopontine angle to reach the lateral section of the pons, where the axons enter the vestibular nuclei, except for some primary fibers that continue directly to the cerebellum.

The vestibular nuclear complex occupies a portion of the medulla beneath the floor of the fourth ventricle (Fig. 2.3) and is formed by four distinct nuclei with different connections that give insight into the subject of this thesis, multisensory interaction.

Vestibular Nucleus	Inputs	Outputs
Lateral	Utricle, Cerebellum, and Spinal Cord	Lateral Vestibulospinal Tract, Cerebellum
Medial & Superior	Semicircular Canals	Medial Vestibulospinal Tract: Neck Muscles, Medial Longitudinal Fasciculus, Contralateral Medial & Sup nuclei, Cerebellum.
Inferior	Utricle, Sacculus, Canals, and Cerebellum	Medial Vestibulospinal Tract, Cerebellum

Table 2.1 : Innervation of the Different Parts of the Vestibular Nucleus

17

Superior colliculus

Inferior colliculus

Ascending medial
longitudinal
fasciculus

Vestibular nuclei
(N. VIII):

Superior
Lateral
Medial
Inferior

Oculomotor nucleus (N. III)

Trochlear
nucleus (N. IV)

Abducens
nucleus (N. VI)

Nodule

Uvula

Lateral
vestibulospinal
tract

Medial
vestibulospinal
tract
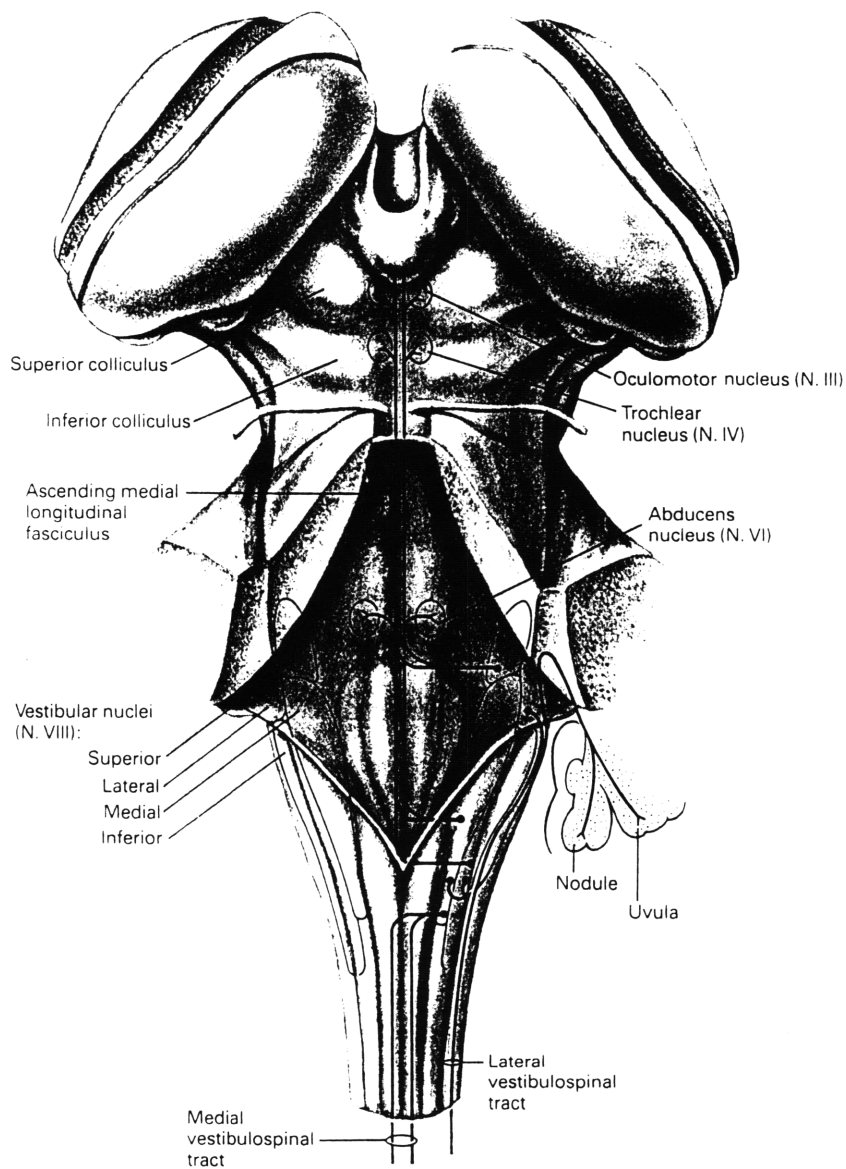
Figure 2.3: Brain Stem Structures Related to the Ocular and Vestibular Systems.
Taken from Kelly (1986)
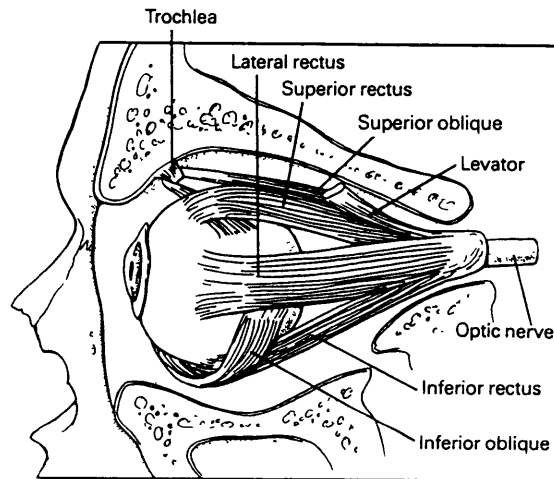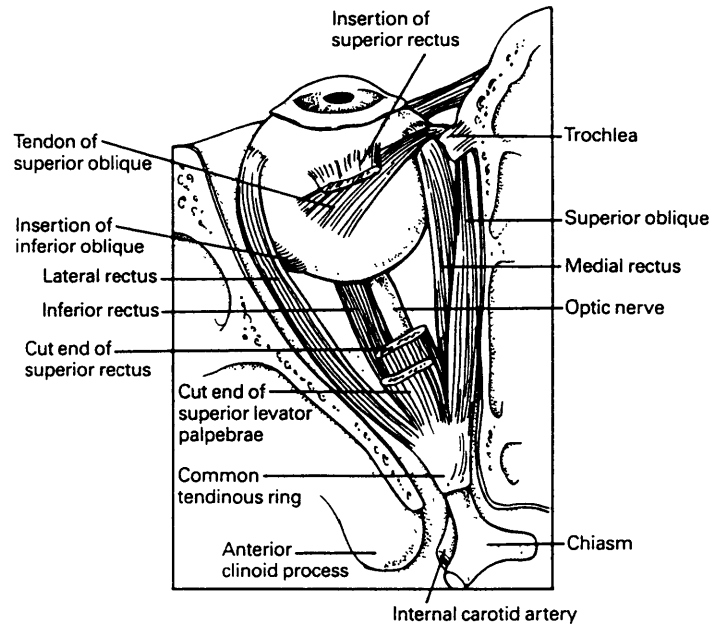
Figure 2.4: Anatomy of Oculomotor Structures. Taken from Kelly (1986)

2.1.2.1 Vestibulospinal Projections

The lateral vestibulospinal tract has a facilitatory effect on motor neurons that innervate antigravity muscles in the limbs and that enables us to maintain an upright body posture. Interaction of vestibular and neck reflexes change the location of the limbs to stabilize the trunk (Roberts, 1973). The medial vestibulospinal tract terminates in more cervical areas of the chord making monosynaptic connections to motor neurons innervating the neck muscles . This tract participates in the vestibulocollic reflex (VCR), a reflex movement of neck muscles in the direction opposite to a rotation of the canals that tends to stabilize the head relative to space.

2.1.2.2 Vestibuloocular Projections

Efferent neurons from the medial and lateral vestibular nuclei project to the abducens nucleus of the oculomotor group. The interneuron located within the abducens nucleus projects contralaterally via the medial longitudinal fasciculus to terminate in the medial rectus, another oculomotor nucleus. Neurons from these two oculomotor nuclei innervate the medial and lateral recti muscles, the two sets of muscles that perform horizontal eye movements. Torsional and vertical eye movements are mediated by neurons that project from the superior and medial vestibular nuclei to the trochlear nucleus and the subgroups of the oculomotor nucleus which innervate the superior and inferior recti and the inferior oblique muscles. There is also an indirect pathway between the vestibular and oculomotor nuclei via a multisynaptic connection involving the reticular substance.

2.1.2.3 Vestibulocerebellar Projections

Vestibular neurons projecting to the vestibulocerebellum (flocculus, nodulus, uvula and ventral paraflocculus) are found in all four vestibular nuclei, and some primary vestibular fibers terminate directly in this area too. These axons enter the cerebellum through the mossy fiber and climbing fiber pathways, ending in both cases

with connections to Purkinje cells either directly (excitatory) or via interneurons (inhibitory). Projections to the vestibular nuclei play a major role in equilibrium and in the control of the axial muscles that are used to maintain balance by maintaining the tone of antigravity muscles (Ghez and Fahn, 1985). In addition, the vestibulocerebellum plays a role on oculomotor reflexes that will be discussed below.

2.1.2.4 Vestibulocommissural Projections

Retrograde tracer studies have shown that comissural vestibular projections exist between the superior and medial vestibular nuclei and their contralateral nuclei (Gacek, 1981). Commisural pathways connect parts of the vestibular nuclei that receive information from synergistic pairs of canals (i.e. those located in the same plane but on opposite sides of the head). The commisural connections excite contralateral type II neurons while contralateral type I neurons are strongly inhibited. It may be concluded from this connection that its function is to enhance the overall response by inhibiting the contralateral canal during ipsilateral stimulation. The commisural system also restores the activity in type I neurons on the affected side after labyrinthine lesion and might play a role in the regulation of nystagmus gain and phase (Precht, 1975).

2.1.2.5 Vestibular Efferent System

The efferent vestibular pathway has a bilateral origin from small neurons located lateral to the abducens nucleus and ventral to the medial vestibular nucleus. The fiber merges with the olivocochlear (auditory) efferent fibers before joining the vestibular nerve root in the brain stem. When they reach the vestibular ganglion they disperse into individual nerve branches supplying vestibular sense organs. These connections seem to be inhibitory and complete a negative feed-back loop that may provide an inhibitory control mechanism which is operative in the case of strong sensory stimulation to prevent a system overflow (Precht, 1975). However, more recent studies suggest that this

inhibitory effect decreases or becomes excitatory as we ascend in the phylogenetic scale (Wilson and Melvill-Jones, 1979) and it is a topic of current research.

2.2 Visual-Vestibular Interaction

Stimulation of the vestibular organ elicits eye movements which are for the most part compensatory: they oppose head movements and act to stabilize the visual information in the retina. In the same way that proprioceptive and vestibular integration is needed to maintain posture, visual-vestibular interaction is essential to ensure stable visual information. This section will only discuss vestibular control of eye movements and not other voluntary eye movements such as smooth pursuit. Since the vestibular stimulus to be used in this thesis is linear, the phenomenon presented in section 2.2.3.2 (Linear Vestibular Ocular Reflex) will be given a more complete treatment.

2.2.1 Anatomy of Eye Movements

The eye movements are controlled by three pairs of muscles (Fig 2.4) :

- Medial and Lateral Recti

- Superior and Inferior Recti

- Superior and Inferior Obliques

The medial and lateral recti contract reciprocally primarily to move the eyes from side to side. The superior and inferior recti primarily contract reciprocally to move the eyes upward or downward. And the oblique muscles function primarily to rotate the eye (torsion). Figure 2.3 also shows the location of the nuclei involved in activating these muscles: the oculomotor, the trochlear and the abducens nuclei. These three nuclei are interconnected through the medial longitudinal fasciculus so the three sets of muscles are reciprocally innervated: one muscle of the pair relaxes while the other contracts.

22

2.2.2 Optokinetic Nystagmus

When a subject observes a visual pattern that covers a good part of the visual field and all the elements of that pattern are moving in the same direction, reflexive eye movements that tend to follow the moving pattern are generated. This reflex consists of a slow phase, when the eye is attempting to follow the stimulus, and a fast phase, that takes place when the eye snaps back to begin tracking again. This combination of rhythmic slow and fast movements in opposite directions in response to a moving visual stimulus is called optokinetic nystagmus (OKN).

OKN can be characterized quantitatively by varying the angular rate (measured at the straight ahead orientation) of the stimulus. Cohen et al. (1977) used rhesus monkeys to study OKN gains. He found that peak values of OKN slow phase velocity (SPV) increased linearly with increases in stimulus velocity with a gain close to unity up to 180°/sec. Above this, OKN gain started falling but the amplitude still increased up to 240°/sec. The cutoff point for a gain of one in humans occurs at velocities 2-3 times slower than in monkeys, which is consistent with studies in humans that report perfect ocular compensation (gain of one) for visual field velocities of up to 60°/sec horizontally (Dichgans, 1973) while for visual field displacement in the vertical direction, perfect OKN compensation can be achieved only up to 30°/sec (Clément and Lathan, 1991).

On turning off the light after maintained exposure to an optokinetic stimulus, the nystagmus continues. This is called after-nystagmus and acts in the same direction as the preceding OKN (Boff and Lincoln, 1988). After one minute of optokinetic stimulation, the resultant decay in SPV shows a long time constant on the order of 24 seconds and a short time constant of approximately 0.8 seconds, when fitted by a two-component exponential equation (Jell et al., 1987).

2.2.3 Optokinetic Neural Pathways

Visual information signaling motion of large parts of the visual field must reach the brain to generate eye movements that will compensate for that motion and must be

also connected to the vestibular nuclei since visual stimulation can generate sensations of motion (generally known as vection) similar to the ones elicited by vestibular stimulation. In the case of rhesus monkeys, units in the vestibular nucleus that fire in response to body rotation in one direction, also fire when the visual field is rotated in the opposite direction while the animal remains stationary. When the two stimuli are combined to enhance the sensation of vection (rotation and motion of the visual field in opposite directions), the rate of firing increased when compared to rotation in front of stationary stripes while the combination of a visual field motion and rotation in the same direction (promotes inhibition of vection) decreased the firing frequency (Henn et al, 1974). One of the principal nuclei that relays visual information in the pretectum (area adjacent to the vestibular nuclei) is the nucleus of the optic tract, and the directional sensitivity that neurons in that area show to large, slowly moving patterns suggest that this is the first relay station for horizontal optokinetic information while the nuclei of the accessory optic tract perform the same function for vertical movements (Henn et al., 1980, Precht and Strata, 1980). However, these studies found no evidence of direct connections between the pretectal and vestibular nuclei but an indirect pathway has been suggested (Henn et al., 1980) via the accessory optic system which receives direct input from the retina and relays visual signals to the vestibulo-cerebellum and via the pretectum, a pathway that also reaches the vestibulocerebellum at the flocculus.

2.2.4 Vestibular Oculomotor Responses and the Three-Neuron Arc

The only way in which the CNS can quickly compensate for self-motion in order to stabilize an image on the retina is by using vestibular information to command oculomotor responses. This is achieved by reflexive movements known as the vestibuloocular reflex (VOR). Basically, these reflexes produce eye movements in the same plane but in direction opposite the head movement. The neural connections mediating this reflex are discussed in section 2.1.2.2 and they are a three neuron arc since

the process of relaying vestibular information to the oculomotor muscles is mediated by three neurons. In the case of rotation in the horizontal plane, a primary afferent vestibular neuron reaches the vestibular nucleus where it synapses with a neuron that projects to the ipsilateral ocular nucleus which directly synapses to an ocular motor neuron innervating the lateral rectus. Another neuron leaves the vestibular nucleus and projects to the contralateral abducens nucleus which sends a motor neuron to the medial rectus. The reciprocal activation of the lateral and medial recti produces compensatory horizontal eye movements, and a similar pathway generates vertical eye movements by stimulating the superior and inferior recti. The pathways from the macula to the extraocular muscles are less defined than those from the semicircular canals. The latency of eye muscle activation after stimulation of the utricular and saccular nerves is similar to that recorded after semicircular canal nerve stimulation, suggesting similar pathway length (Baloh and Honrubia, 1979). Prolonged stimulation of the vestibular system leads to intermittent saccadic repositioning of the eyes, a phenomenon called vestibular nystagmus. Vestibular nystagmus, in similar fashion to OKN, is an eye movement characterized by a slow phase (the vestibuloocular compensatory response) and a quick phase (quick, involuntary movements that counteract the slow-phase movements).

2.2.4.1 Angular Vestibuloocular Reflex (AVOR)

This term refers to the oculomotor responses produced by stimulation of the semicircular canals during angular acceleration of the head. Stimulation of a particular set of canals leads mainly to contraction of one muscle in each eye, the prime mover, and to relaxation of the antagonists. Wilson and Melvill-Jones (1979) have synthesized this as shown in Table 2.2.

Canal Stimulated	Muscles Contracting	Muscles Relaxing
Horizontal	Ipsi medial rectus Contra lateral rectus	Ipsi lateral rectus Contra medial rectus
Anterior	Ipsi superior rectus Contra inferior oblique	Ipsi inferior rectus Contra superior oblique
Posterior	Ipsi superior oblique Contra inferior rectus	Ipsi inferior oblique Contra superior rectus

Table 2.2: **Oculomotor Muscles and the Canals that Activate them**

The ratio of peak compensatory eye velocity to head rotation velocity is called the gain of the VOR. A gain of 1.0 suggests a stable retinal image since eye movements closely compensate for head movements. A gain of 0.0 suggests absence of compensation, with the eyes remaining fixed with respect to the head. Many factors influence the gain of AVOR :

-Visual Stimulus

Even in the dark, when no retinal error signal is available, the AVOR is present. Barr and his associates (1976) measured gains in humans performing an arithmetic task (to avoid directing attention to any other oculomotor task) during rotation in the dark. On average, the gain increased from 0.65 at 0.3 Hz to 0.97 at 1.0 Hz. Gains remained close to 1.0 across frequencies for a visible stationary target, an imaginary stationary target and for the after-image of a stationary target.

- Rotational Stimulus

In addition to the influence of frequency of the rotational stimulus, the AVOR is affected by the velocity of rotation. For stationary visual targets, the gain remains close to unity for velocities up to about 350°/sec. After that the response begins to saturate with a maximum SPV of approximately 500°/sec (Pulaski et al., 1981).

- Object Distance

The influence of this parameter seems related to the level of vergence of the eye, which in turn is defined by object distance. In general, greater convergence increases the VOR, while divergence reduces its gain (Post and Leibowitz, 1982). This is consistent with the functional need for larger compensatory eye movements for near targets.

- Microgravity

The effects of extended weightless on humans have been studied in several space shuttle missions. In these studies, a first order model was fit to the SPV data. Results have shown a decrease in the time constant after exposure to weightlessness (Oman and Kulbaski, 1988; Oman and Weigl, 1989) as well as a decrease in system gain (Balkwill, 1992). However, studies with monkeys have shown an increase in gain (Correia et al, 1992) or a lack of significant changes (Cohen et al., 1992).

- Learning, Adaptation

Lisberger (1988) elicited motor learning in the AVOR by fitting rhesus monkeys with magnifying and miniaturizing spectacles and observed that the SPV's changed so that gains were maintained close to unity. Similar results were obtained by Snyder and King (1988) by varying the velocity of the surrounding visual field during rotation. The adaptation has a somewhat exponential time course and suggests that the AVOR is a plastic system (Miles and Eighmy, 1980).

- Distance to Axis of Rotation

The magnitude of the VOR increases with increasing radius of head rotation. If the canals are purely angular velocity detectors they cannot provide information about the radius of rotation. This suggests that the otoliths must also be involved in the generation of reflexive eye movements (Virre et al., 1986). This will be discussed below, and in general, in the rest of this thesis.

27

2.2.4.2 Linear Vestibuloocular Reflex (LVOR)

This term will be used in this thesis to refer to reflexive horizontal or vertical oculomotor responses to linear acceleration of the head. Eye movements in response to linear acceleration were reported as early as 1946 by Jongkees and the effects of the relative orientation of gravity was characterized in his laboratory in 1963 (Bos et al.). The following sections will define the stimulus being given to the otoliths during linear acceleration, summarize qualitatively previous studies of ocular responses, and their relationship with optokinetic stimuli. A quantitative summary of these studies will be presented in the Discussion section as a comparison tool.

2.2.4.2.1 Gravitoinertial Force

Linear acceleration forces acting upon the head interact with the always present gravitational force. The resultant vector force, the gravitoinertial vector force (GIF) $\vec{f}$ forms an angle θ with the earth vertical. The equivalence principle states that a graviceptor cannot distinguish between gravity and linear acceleration. However, the CNS needs to distinguish between gravity and linear acceleration in order to generate the appropriate responses (e.g. lateral acceleration should not be interpreted as tilt). A hypothesis suggests (Merfeld et al., 1992) that the CNS attempts to decompose the GIF into its two components (Fig. 2.5) by rotating a constant magnitude estimate of the gravity vector and adding a linear acceleration estimate. In the case of sinusoidal linear acceleration, the amplitude of the net GIF varies at twice the frequency of the stimulus which could explain vertical eye oscillations at twice the frequency of the horizontal stimulus which Christie (1992) observed.

This oscillation of the GIF might be interpreted by subjects as if they were traveling over the crest of a hill and is therefore known as the "hilltop" illusion (Christie, 1991). Merfeld (1990) has discussed the functional need for a neural process that will take the GIF and decompose into its linear acceleration and gravity components and the oculomotor response might provide an indication of those neural processes.

28
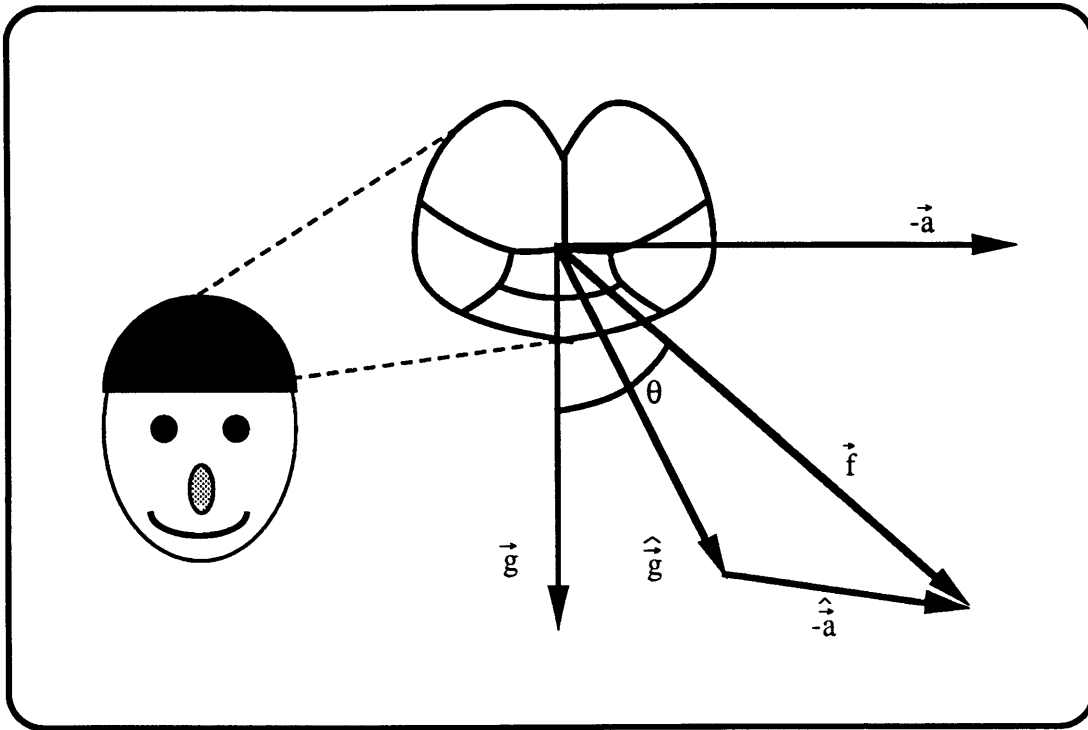
Figure 2.5: Gravitoinertial Force Resolution Hypothesis

2.2.4.2.2 Ocular Responses in the Dark

Some of the first studies of oculomotor responses to linear acceleration were performed by Jongkees and his colleagues in rabbits (Jongkees, 1961; Bos et al., 1963). They used the parallel swing test and electrooculography to measure a horizontal ocular oscillation at the same frequency as the stimulus. Niven and his colleagues (1966) obtained comparable results for horizontal eye movements in humans using motion along a linear track with a peak acceleration of 0.58 G and frequencies ranging from 0.2 to 0.8 Hz, but were unable to elicit vertical eye movements when the vestibular stimulus had components along the foot-to-head axis. Bles and Kapteyn (1973) performed parallel swing experiments in human subjects and did more detailed frequency and phase analysis of the ocular responses. They found that the response was inconsistent in phase (ranging from -180° to 180°. with respect to the stimulus) and in frequency (some subjects showed

29

a response at twice the frequency of the stimulus, probably due to the fact that the parallel swing has a component of motion at that frequency).

Buizza and his associates (1980) used a linear sled to generate a purely linear vestibular stimulus in the dark. They consistently measured linear nystagmus in human subjects seated in the upright position while undergoing linear acceleration. Their experimental setup and results will be discussed further in the following section.

Though Buizza et al. proposed that the linear nystagmus he had measured was intended to compensate for head translation, Hain (1986), based on the fact that linear responses were not always consistent and that SPV was not proportional to translational head velocity, claimed that the linear nystagmus has no purpose, but that it is a side effect of an otolith mechanism that supplements the canals when head orientation with respect to gravity changes. Another study (Berthoz et al., 1987) discredited the compensatory reflexive nature of the LVOR by showing that the required compensatory eye movements during linear acceleration were mediated by the saccadic system. Studies such as that one have led some members of the scientific community to doubt the existence of an LVOR.

However, the most recent studies have further strengthened the concept of LVOR. Baloh (1988) used a more accurate technique to measure eye movements, the scleral search method, on a parallel swing with human subjects. His results were consistent with Buizza's and showed good compensatory behavior with respect to velocity, a phase lag in the order of 160° (where 180° is fully compensatory). Paige and Tomko (1991) observed LVOR responses in all four monkeys that they tested with coils in a linear sled. The most recent experiments in the dark in humans using linear sleds (Shelhamer and Young, 1991; Christie, 1991) showed responses only in some subjects. However some of these experiments used EOG to measure eye movements and these ambivalent results reinforce the need for a set of experiments using a more accurate eye measurement techniques such as coils. Table 2.3 summarizes results for some of the experiments conducted in linear acceleration devices.

The reason for the LVOR variability may be caused by other higher level parameters and in the past few years several research groups have attempted to study these. In similar fashion to AVOR, LVOR can only accomplish (or attempt to accomplish) a functional objective of keeping images stable on the retina during translation by making its gain dependent on the distance of a stationary object to the observer. Skipper and Barnes (1989) used EOG to measure eye movements in a linear sled and they found that the oculomotor response could be heavily modified by the mental task. Subjects performing an arithmetic task in the dark showed a consistent response modulated by the sled sinusoidal acceleration. The magnitude of the eye movements was increased when the subjects imagined a stationary fixed target. Since the response remained smooth for eye velocities of up to 20°/s, they claimed that this was an enhancement of the reflex, not saccades. Paige (1989) was able to increase the vertical LVOR gain in humans just by changing the degree of vergence using spherical lenses during a lighted period right before the run in which subjects underwent self-generated motion along the Z-axis. He proposed that in darkness the brain's estimate of target distance is not infinity, but some other default value to which eye vergence accommodates and this vergence signal is used by the CNS to adjust the LVOR gain. Schwarz and Miles (1991) experimenting with monkeys, found that the LVOR gain with respect to linear sled motion can be varied by changing vergence or accommodation before extinguishing illumination. But a linear sum of the results using these two cues does not predict the normal binocular response, leading them to conclude that neither vergence nor accommodation alone nor a linear combination of both could account for the gain variation in response to viewing distance just before the dark run. More recently, however, Shelhamer and his associates (1993) have found that the LVOR gain does not change when a subject verges his eyes in order to close an auditory feedback loop.

31

Exp./ Technique	Peak Accel. (g)	Frequency (Hz)	Peak SPV (deg/s)
Niven et al.,1966	0.58	0.2	9.2±3.0
(EOG)	0.58	0.4	9.6±2.5
	0.58	0.8	9.3±2.9
Buizza et al.,	0.10	0.2	2.5±1.2
1980 (Corneal	0.10	0.2	1.7±0.6
Reflection.)	0.16	0.2	2.5±1.5
Skipper & Barnes,	0.15	0.2	.85-8.48
1989 (EOG)	0.15	0.8	1.78-5.8
Christie,	0.5	0.25	4.6±1.6
1991	0.5	0.5	6.2±2.5
(Coils)	0.5	1.0	10.±1.4

Table 2.3: *Results of Experiments in the Dark using Interaural Linear Acceleration.* (Subjects performed a mental arithmetic test)

2.2.4.2.3 Influence on Optokinetic Responses

Tokunaga (1977) used a cylinder with black stripes to generate an optokinetic stimulus at constant velocity while human subjects underwent periodic lateral linear acceleration. Ocular responses measured with EOG showed that the observed nystagmus was enhanced when the eye movements elicited by acceleration were in the same direction of the OKN SPV and inhibited in the opposite case. Unfortunately, this study did not present any phase information. Buizza et al. (1980) obtained similar results, quantifying a sinusoidal modulation of the OKN SPV on the order of 9°/s for a sinusoidal stimulus with a peak acceleration of 1.6 m/s^2 and 0.2 Hz frequency. A fairly consistent phase lag of SPV of 90° with respect to sled velocity was reported. Christie (1992) confirmed this vestibularly driven modulation and saw modulations of as high as 50°/s

32

peak-to-peak for an optokinetic stimulus at a constant velocity of 60°/s. His data was consistent with Buizza's suggestion that the modulation increases for subjects with weaker OKN since the retinal slip signal is stronger. More recently, studies have used a sinusoidal optokinetic stimulus to quantify the changes in magnitude and phase that vestibular stimulation cause (Wall et al., 1992 and Lathan et al., 1993) and their preliminary results show enhancement in the response when the visual stimulus moves in complementary fashion with respect to the subject (e.g. subject motion to the left, with visual stimulus motion to the right), and no changes with respect to pure visual stimulation case when the vestibular input is anti-complementary (e.g., both subject and visual field moving in the same direction).

Chapter 3
Methods

In order to study the interaction of LVOR and OKN, subjects were accelerated sinusoidally along the interaural axis. The type of visual stimulation in each trial varied. Subjects were a) in the dark (trials *Dark1* and *Dark2*), b) viewing an optokinetic stimulus moving at a constant linear velocity in four different directions (trials *Right, Left, Up*, and *Down*), or c) viewing an optokinetic stimulus moving sinusoidally in a complementary fashion (e.g., subject moving to the right, visual stimulus moving to the left) or in an anti-complementary mode (e.g., subject moving to the right, visual stimulus moving to the right). These two trials are named respectively *OK+V* and *OK-V*. To obtain information on responses to visual stimuli alone, subjects were also tested viewing the sinusoidal display without acceleration (trial *OK*).

This chapter will describe the paradigms used for these experiments, the equipment used to conduct them, and the way in which the obtained data were analyzed.

3.1 Experimental Parameters

The chosen sled frequency and peak acceleration (0.25 Hz and 0.4 G) are within the ranges that will assure robust responses (this acceleration produces a 21.8° tilt of the GIF vector, and is well above the perceptual threshold of 5mg) and are similar to the ones used by previous researchers (Buizza et al, 1980; Christie, 1991) so that results can be compared. Having a sinusoidal trajectory simplifies the analysis process since this is a

periodic, continuously differentiable function. This type of function, when used as an input to a system, is extremely convenient to model the responses of a linear system.

The visual stimulus used was a "windowshade" (or sometimes referred to as "shade") placed in front of the subject. The windowhade optokinetic pattern is a step grating since transition from one color to the other occurs in a step-like fashion with a spatial frequency of 2.0°. Orientation of the black and yellow stripes, either aligned with the horizontal or with the vertical, assured the highest degree of acuity, a phenomenon known as meridional astigmatism (Howard, 1982). The pattern moved at a constant velocity of 60°/s or sinusoidally with a peak amplitude of 60°/s. This is an intermediate value when compared with those used in previous studies (20°/s-120°/s, Christie, 1991) and below normal levels of OKN saturation.

Illumination was provided by fluorescent lamps that were attached to the sled and were therefore traveling with the subject, except in the trials labeled *Dark1* and *Dark2* which were conducted in complete darkness.

Table 3.1 summarizes the characteristics of the stimuli used in the experiment.

Parameter	Value
Sled Motion	Sinusoid at 0.25 Hz
G-Level	0.4 G peak
Optokinetic Pattern	Physical 60°x60° at 72 cm from eyes Moving at 60°/s (constant vel) or sinusoidally (60°/s peak., 0.25 Hz)
Width of Stripes	2.0°

Table 3.1: Summary of Experimental Parameters

3.2 Experimental Protocol: Description and Purpose of each Trial

Six subjects were tested seated in the upright position while seven were tested supine. In both cases, the dynamic acceleration primarily stimulated the utricular

maculae since acceleration took place along the subject's interaural axis. Figure 3.1 shows

the typical order of trials in each run. *Dark1* and *Dark2* were always respectively the first

and the last trial to be run. For approximately half of the subjects, the order of the trials

was somewhat different than that depicted in fig 3.1, with the three sinusoidal optokinetic

trials (*OK*, *OK+V*, and *OK-V*) being run immediately after *Dark1*.

In order to measure vergence some tests were binocular (coils in both eyes).

Otherwise, measurements were taken from the right eye. Each trial was separated by

approximately 30 seconds (except when the direction of the optokinetic stimulus had to

be changed from horizontal to vertical configuration, a procedure that took about three

minutes).


```
┌─────────────────────────────────┐
│   Calibration                   │
│   (Monocular or Binocular)      │
└─────────────────────────────────┘
              ↓
┌─────────────────────────────────┐
│   Dark1                         │
│   Sled, Task 1                  │
└─────────────────────────────────┘
              ↓
┌─────────────────────────────────┐
│   Right                         │
│   Sled, Constant OK,. Task 2    │
└─────────────────────────────────┘
              ↓
┌─────────────────────────────────┐
│   Left                          │
│   Sled, Constant OK, Task 2     │
└─────────────────────────────────┘
              ↓
┌─────────────────────────────────┐
│   Up                            │
│   Sled, Constant OK, Task 2     │
└─────────────────────────────────┘
              ↓
┌─────────────────────────────────┐
│   Down                          │
│   Sled, Constant OK, Task 2     │
└─────────────────────────────────┘
              ↓
┌─────────────────────────────────┐
│   OK                            │
│   Sinusoidal OK, Task 2         │
└─────────────────────────────────┘
              ↓
┌────────────────────────────────────────────┐
│   OK+V                                      │
│   Sled, Complementary Sinusoidal OK, Task 2 │
└────────────────────────────────────────────┘
              ↓
┌─────────────────────────────────────────────────┐
│   OK-V                                           │
│   Sled, Anti-Complementary Sinusoidal OK, Task 2 │
└─────────────────────────────────────────────────┘
              ↓
┌─────────────────────────────────┐
│   Dark2                         │
│   Sled, Task 3                  │
└─────────────────────────────────┘
```
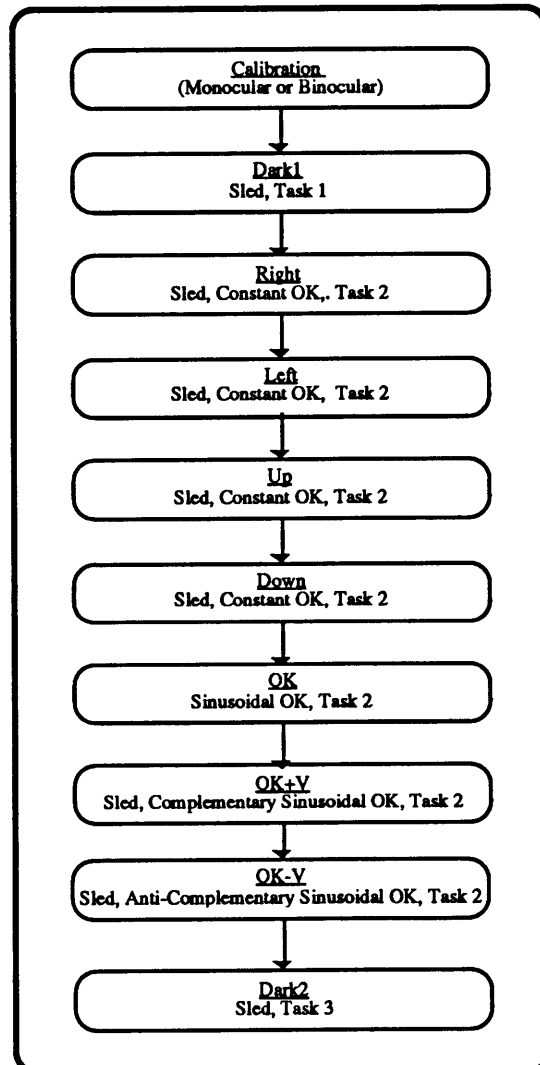
Figure 3.1: Typical Order of Trials

Figure 3.2 describes the time course of sled and windowshade motion in each trial. All runs start with a calibration that relates a known voltage from the coils to a known number of degrees of displacement. Trials can be divided into three basic kinds: dark (*Dark1* and *Dark2*), constant optokinetic (*Right, Left, Up,* and *Down*), and sinusoidal optokinetic (*OK, OK+V,* and *OK-V*). For those trials that involved both optokinetic and vestibular stimulation, the optokinetic stimulus started moving twelve seconds in advance of the sled in order to have a fully developed OKN responses before the vestibular input was added

3.2.1 Calibration

After insertion of the coil (or coils, in the case of binocular trials), a calibration chart was placed in front of the subject at a distance of 36 cm. The calibration procedure varied depending on whether binocular or monocular recordings were being conducted.

- Binocular Calibration

Before the subject was placed in the sled, her interpupillary distance (IPD) was measured by asking the subject to look far away while using a ruler to measure IPD. Figure 3.3 shows a binocular calibration chart (not to scale). The dots labeled *Near Right* and *Near Left* are, respectively, the zero position for the left and right eyes. The other points are chosen so that the maximum range of eye movements remain within twenty degrees from zero, the location of these points is easily calculated using basic trigonometry and the known distance of the chart to the subject's eyes. The subject is instructed to look at each one of the points in the screen and the eye position signals are recorded.

- Monocular Calibration

The procedure is the same as before, but the zero position is *Center* (located in front of the head) and *Near Left* and *Near Right* are absent.

.
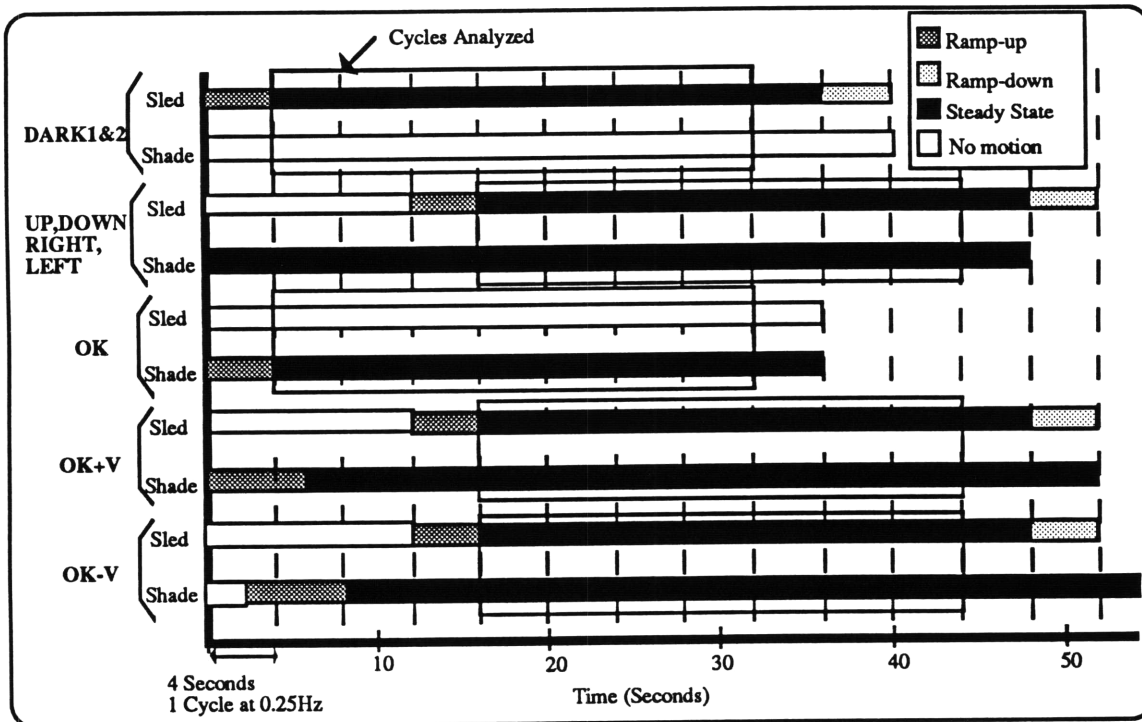
Figure 3.2: Time Course of Trials

The time grid has been divided in period of four seconds to represent a cycle of sled motion (0.25Hz). Cycles enclosed in a square are the ones used for analysis of the response.
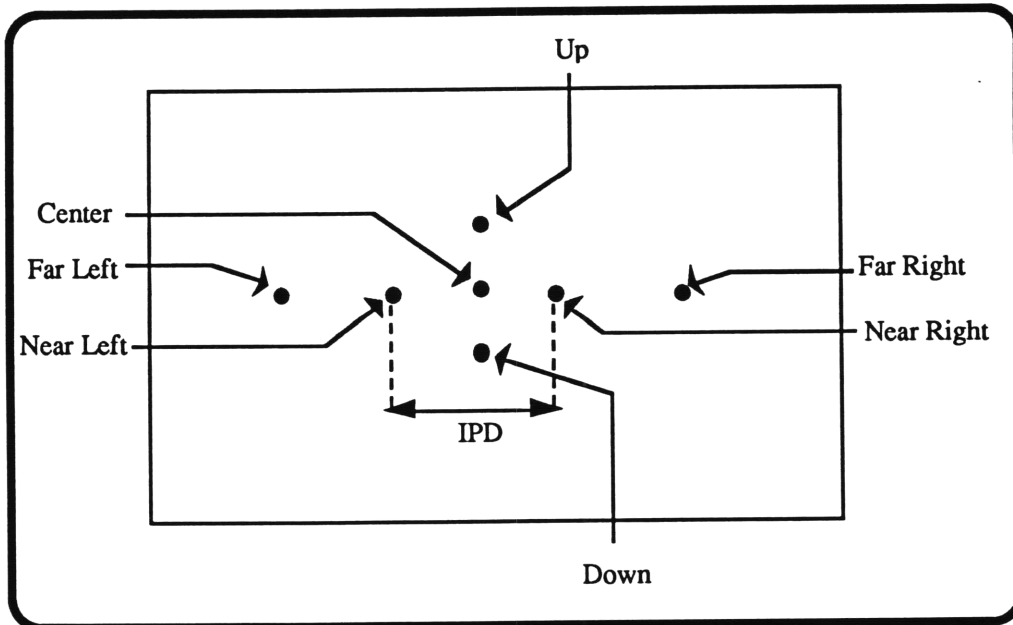
Figure 3.3: Binocular Calibration Chart

The known distance between the points is related to angular displacements of the eyes using simple trigonometry. Near *Left* and Near *Right* are in front of the left and right eye respectively and serve as their zero calibration point.

3.2.2 Dark 1 & 2

The purpose of these two runs is to explore the purely vestibular responses of the oculomotor system. Trials are conducted in darkness with the sled moving sinusoidally at 0.25 Hz and 0.4 G peak acceleration. Two different tasks are given to the subject in these trials. In *Dark1*, subjects are asked to relax and keep their eye open, while in *Dark2* subjects are asked to "count the stripes as they go by even though you cannot see them", referring to the stripes on the optokinetic display that subjects had seen in the previous trials.

As discussed in Chapter 2, the LVOR response can be affected by factors such as vergence and mental task. By measuring vergence and the linear VOR in *Dark1* we intend to assess the responses when no visual stimulus is present. These responses will be compared to those observed in *Dark2*, which may be affected by the subject imagining stripes at some unknown finite distance.

3.2.3 Constant Velocity Optokinetic Displays

These trials combine a constant velocity optokinetic display with a sinusoidal sled motion. In all cases, optokinetic stimulation starts three cycles before sled motion as to have a fully developed OKN before the vestibular component is introduced and the subject is asked to "look straight ahead, count the stripes as they go by but without fixating any stripe in particular". The sled is run in a sinusoidal motion profile at 0.25 Hz and peak acceleration of 0.4 G. The optokinetic stimulus moves at a constant velocity of 60°/s (74cm/s) with the bars traveling in one of the four directions: right, left, up, and down. Figure 3.4 shows the horizontal (*Right* and *Left*) and vertical (*Up* and *Down*) configurations of the visual stimulus.

- Right and Left

In these trials, the stripes are aligned with gravity and travel either to the left or to the right. This condition seeks to emulate experiments performed by Tokunaga (1977), Buizza (1980), and Christie (1992) in order to explore the influence of a periodic vestibular stimulus on the otherwise constant OKN response.
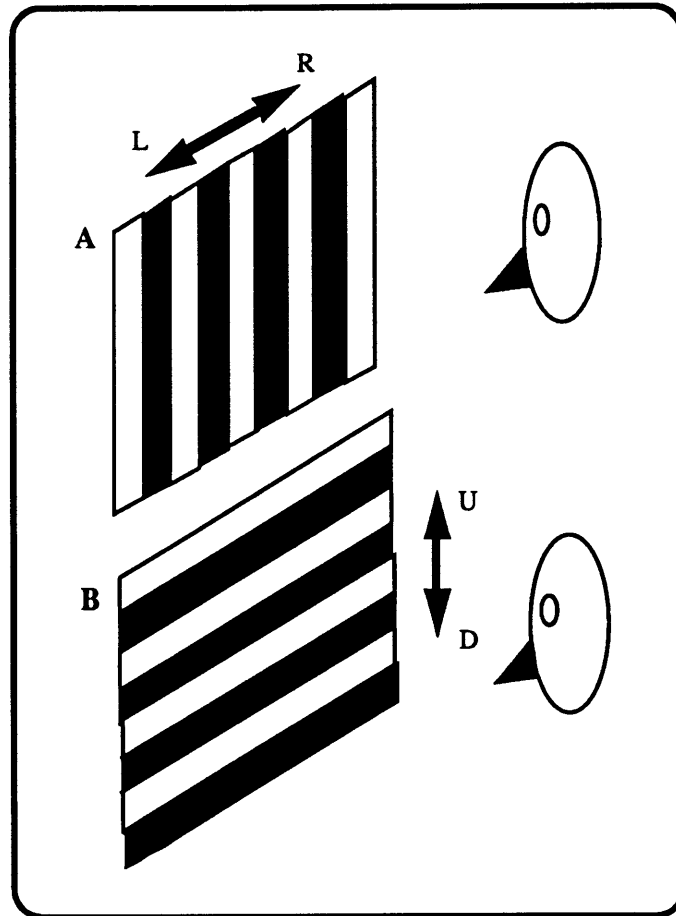
Figure 3.4: **Configurations of the Visual Stimulus.** The optokinetic stimulus can be arranged horizontally for trials *Left, Right OK, OK+V,* and *OK-V* (A), or vertically for trials *Up* and *Down* (B).

- Up and Down

By using this new condition, optokinetic and vestibular responses can be differentiated more easily since the two stimuli are orthogonally directed in space. In addition to this, Christie (1992) observed vertical eye movements in dark trials which suggests interesting effects on vertical optokinetically induced oculomotor responses.

40

3.2.4 Sinusoidal Optokinetic Displays

To study the hypothesis that one of the roles of the vestibular system is to help the visual tracking of objects during linear acceleration, these conditions were designed and are similar to those previously used by Lathan et al. (1993) for acceleration along the head to foot axis. The optokinetic stimulus moves horizontally in a sinusoidal profile at 0.25Hz and peak acceleration of 60°/s (74cm/s). Once again, subjects are asked to "look straight ahead, count the stripes as they go by but without fixating any stripe in particular". Three different trials with sinusoidal displays were implemented, each one having a different vestibular input. These conditions *(OK, OK+V, OK-V)* are briefly described below.

- OK

This is a purely optokinetic trial without sled motion involved. Only the visual system (OKN) is involved in following the stripes.

- OK+V

Both sled and windowshade motion are combined in a complementary manner. In this case the word *complementary* means that the two stimuli are given as they are normally presented in the real world: in opposite directions. When people translate their head to the right, they see the real world moving to the left, and vice-versa for head movements to the left. In this case, both the visual and vestibular system are presented with information that is consistent with every-day experiences.

- OK-V

The two stimuli are *anti-complementary*, meaning that they are contradicting each other when compared to real world situations. Subjects moving to the right see the visual stimulus also moving to the right. This supplies the vestibular and visual systems with information that violates regular behavior of the surrounding world.

41

3.3 Distribution of Subjects in Different Conditions

The previously mentioned protocol was run with subject in the upright and in the supine positions to assess any differences due to different orientation with respect to the gravity vector. In order to maximize the amount of time available while keeping a statistical meaningful pool of data and due to the fact that some subjects were not available in both the upright and the supine sessions (spaced by approximately one month), not all subjects were run in all conditions. Table 3.2 summarizes the conditions in which each subject was run as well as their sex and age. Subjects A, B, C, and H had not been previously tested in the sled, the others had previous experience as subjects. All subjects were volunteers.

Subject	Sex	Age	Upright	Supine
A	F	22	M-B	
B	F	26	M-B	M
C	M	27	M^1	B
D	F	21	M-B	M^2
E	F	23	B	M^2
F	M	24	B^3	M
G	F	24		M
H	M	20		M

Table 3.2: **Distribution of Subjects**

M: Monocular Run. **B:** Binocular Run. **M-B:** Monocular run without *OK-V* and a Binocular run three months later of only *Dark1*, *Dark2*, *OK*, *OK+V*, and *OK-V*. Some conditions were not run due to a thirty-minute time limit in each session. [1] *OK-V* was not run [2]: *Up* and *Down* were not run. [3] *Dark2* was not run.

3.3 Equipment

3.3.1 The MIT Sled Facility

All these experiments were performed at the MIT linear acceleration sled located in the Man-Vehicle Laboratory (Fig 3.5). The sled consists of an aluminum cart supported on parallel rails with a usable length of four meters. Mounted on this rail is a seat which can be arranged in one of the three axis depending on the desired orientation of the stimulation. A football helmet and a subject restraint system minimizes head and body movements relative to the seat.
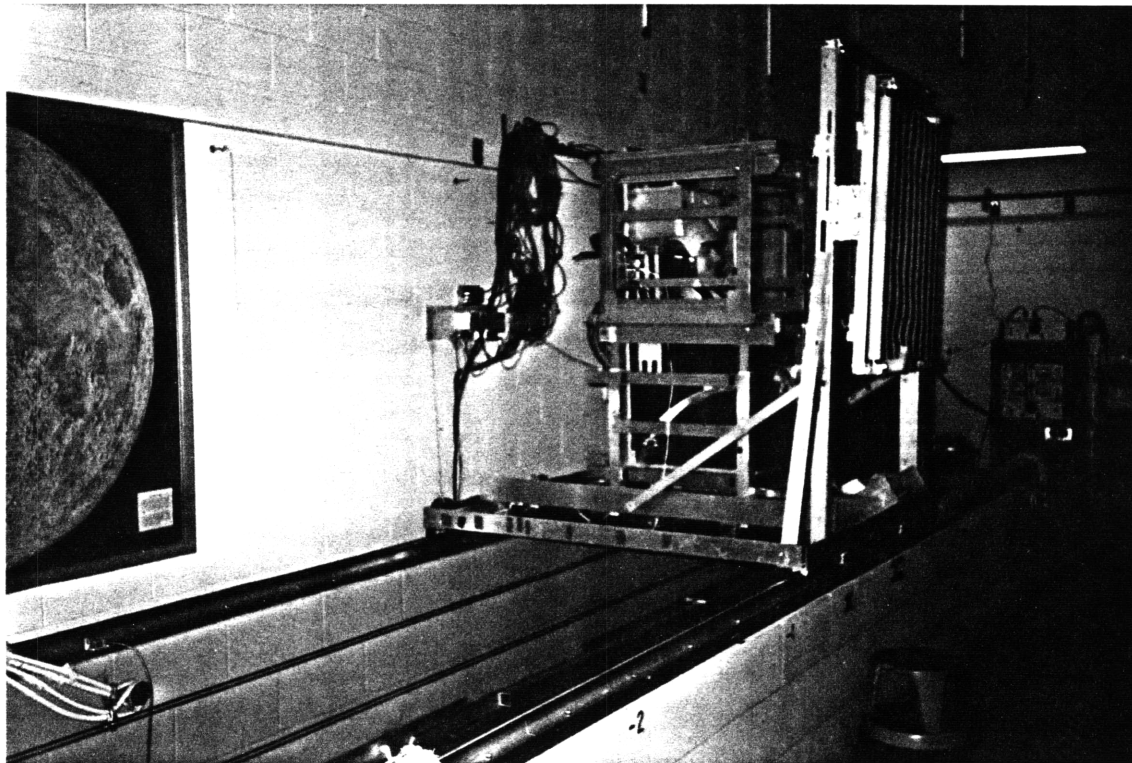
Figure 3.5: **The MIT Sled Facility.** The subject is shown in the upright configuration with the visual display in front of him. The cube surrounding the subject's head contains the magnetic field generators that are part of the eye movement measurement system to be described in the next section.

The system is capable of accelerations of up to 0.9g and 2.0 Hz and the lower limit is set by vibrations, being on the order of 1 mg. Arrott (1985) gives a more detailed description of the system, but two large changes have occurred since then. Law (1991) rebuilt the sled chair with non-metallic materials in order to minimize interference with the eye measurement technique being used, and more recently, Robert Grimes of Payload Systems Inc. (Cambridge, MA) implemented a new control program for the sled.

Visual stimulation is elicited by a square "windowshade", a continuous loop conveyor belt with alternating yellow and black stripes (Refs: Glowing Lemon-Yellow 3104 and Ultra Flat Black 1602, Krylon, Solon, OH) with a width of five centimeters. The windowshade is at a distance of 72 cm from the subject's eyes and subtends an angle of 60°. The windowshade can be arranged with the stripes traveling horizontally or vertically, as shown in Fig. 3.4. This windowshade assembly is mounted in the sled cart and travels with the subject.

3.3.2 Measurement of Eye Movements

Eye movements were measured using the scleral search coil technique (Robinson, 1963). The subject is placed within an alternating magnetic field which generates a voltage in a coil of wire embedded in a scleral contact lens. The induced voltage depends on the relative orientation of the coil with respect to the field.

The system used at MIT was manufactured by C-N-C Engineering (Seattle, WA) and the hardware is extensively discussed by Law (1991). The coil system surrounds the subject's head and is mounted on the sled chair and forms a cube with dimensions of 25" height x 31" width x 30" depth. The coil system consists of two pairs of coils oriented perpendicular to each other. The two coils operate at two different frequencies (60 kHz and 135 kHz). The horizontal coil generates a magnetic field of approximately 0.3 gauss at the center of the cube and the vertical coil generates a field of 0.4 gauss. Typical resolution level for the coil system is 0.15 degrees.

44

The instrument panel consists of a Power Oscillator Driver that drives the two pair of coils at their corresponding frequencies and two Dual Phase Detectors which take the voltage generated in the coils and separate them into measurements of horizontal, vertical, and torsional rotations. For this study, the Detectors were wired so that one would register horizontal and vertical data for the right eye and the other would take these parameters for the left eye. The horizontal/vertical output wires from the coils are connected to a 147 ohm preamplifier located in the back of the chair and from there, a cable connects them to the Detectors. In order to increase the overall gain, eye position signals are amplified once more using an amplifier built by Dr. Winfried Teiwes in 1992 which allows offsets the between +15 and -15V and gain increase between 1 to 10.

The horizontal/vertical coils (Skalar Inc., Netherlands) consist of nine windings of 0.05 mm insulated copper wire embedded in a silicone rubber ring. Coils were inserted in the subject's eye after two drops of a topical ophthalmic anesthesia (Opthetic, proparacaine HCl 0.5%) was administered and the insertion protocol presented in Appendix F of Law's thesis was followed. The main restriction in the use of coils is that they should not remain in the subject's eye for more than thirty minutes to minimize the risk of scleral abrasions.

3.4 Data Acquisition and Methods of Analysis

Figure 3.6 summarizes the data acquisition steps from the hardware point of view while figure 3.7 presents the analysis steps by summarizing the action of each piece of software. The entire process can be divided into three main parts: taking the data into the appropriate format to be analyzed, generating the slow phase velocity using Nysa, and performing frequency and statistical analysis on the SPV.

3.4.1 Data Preparation

Data collection of the eye position information (Horizontal and Vertical) as well as sled and windowshade velocity is done by a 386 Computer using a data collection program written in C language by Dr. Winfried Teiwes, Acquire Version 3.01.

45
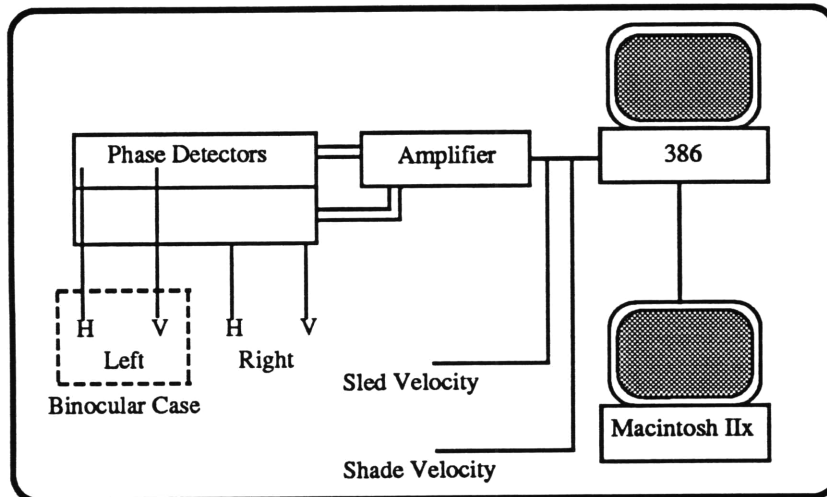
Figure 3.6: **Data Acquisition Steps**
Eye signals from the phase detector are amplified and then collected by a 386 computer from which data is transferred to a Macintosh IIx for analysis.
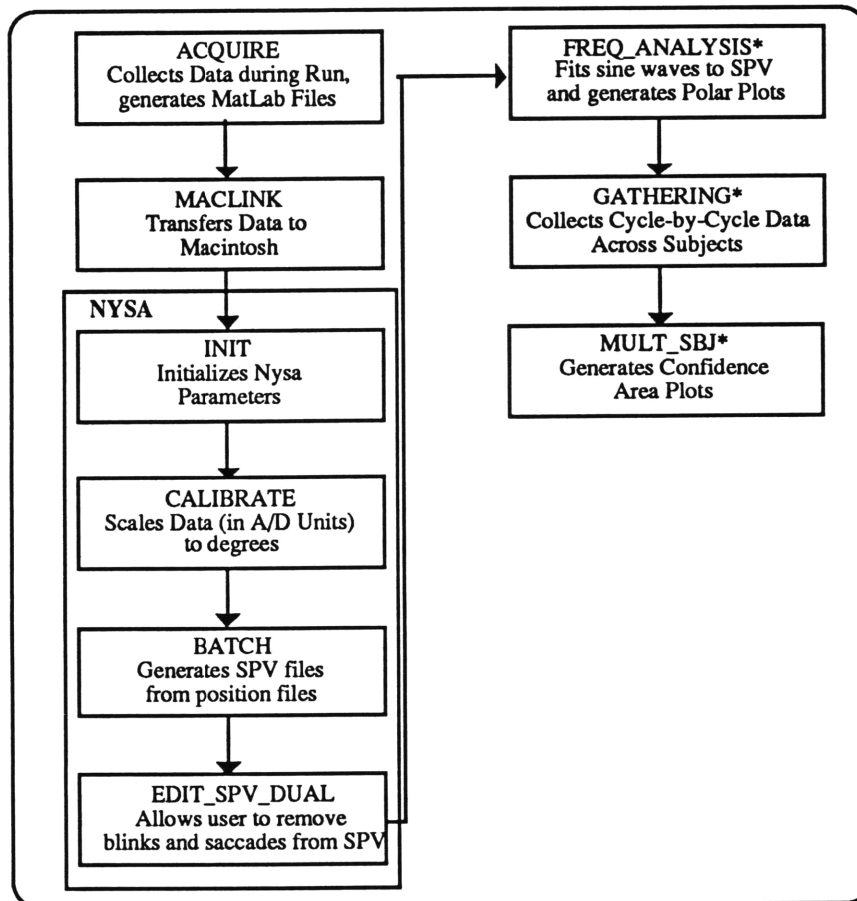
Figure 3.7: **Data Analysis Steps**
Each name in capital letters refers to an individual program that the user has to run, some of which automatically run others. Those with an asterisk are programs written by the author for this project and they are listed in Appendix B.

46

This program generates one MatLab (The MathWorks, Inc., Natick MA) format file per trial in which each column of data corresponds to the input of one of the channels of the computer A/D board. Files are transferred to a Macintosh IIx using a data transmission program, MacLink Plus 4.11 (Data Viz, Inc., Trumbull, CT). Since further processing requires a separate file for each channel, a MatLab script, *Parse*, divides each MatLab file into four (Monocular runs) or six (Binocular runs) individual files using the nomenclature required by Nysa.

3.4.2 Generation of Slow Phase Velocities: Nysa

Obtaining velocity plots from position plots is a relatively simple task when the data are smooth. However, in the case of ocular responses, the need for eliminating the fast phases of the nystagmus and other disturbances such as blinks requires more sophisticated computer algorithms. The term *saccade* will be used to label these discrete events. Most saccade-detector algorithms use either velocity or acceleration thresholds and they were reviewed by Merfeld (1990). Merfeld concluded that an acceleration based algorithm is the most effective method to identify saccades from coil recordings and took the approach initiated by Massoumnia (1983) and expanded it to a method that accounts simultaneously for horizontal, vertical, and torsional eye movements using a spherical coordinate system. The version of Nysa used in this analysis is basically the algorithm implemented by Merfeld as MatLab scripts plus modifications added by Balkwill (1992).

- Init and Calibrate

Init has to be run only once and stores the basic parameters to analyze all the subsequent runs such as the frequency at which the data were sampled. *Calibrate* uses the record of eye position from the Calibration run to scale the data from A/D units to actual degrees of displacement.

- Batch

This is the core of the entire Nysa program. It implements a differentiator using a Remez equal ripple digital filter (a first order derivative plus a low pass filter) that takes

the eye position files and by differentiating twice generates eye velocity and eye acceleration files. Then the acceleration series is scanned and a fast phase is detected when acceleration is above a certain threshold. In this theses, threshold values were automatically calculated using statistical methods. The slow phase velocity file is generated by interpolating across fast phases.

- *Edit_Spv_Dual*

This script allows the user to manually interpolate over saccades that the automatic process may have not detected. All manual editions were performed by the same person to keep consistency in the subjective assessment of what should be considered a saccade. This program displays the two axes (horizontal and vertical) of SPV and the user selects the interpolation points by clicking on them with a mouse.

3.4.3 Frequency Analysis of SPV Responses

Once the SPV file is obtained, the next step is to determine if it has oscillations at the frequency of the stimulus or its harmonics. Christie (1992) concluded that simple Fourier analysis was not an effective approach in this case due to the relatively high noise level, instead he implemented a frequency analysis method using Gauss' Method of Least Squares.

In order to quantify how much response we have at a certain frequency, each cycle in the analyzed region (seven cycles in this study) is taken and fitted by a combination of a sine and a cosine at the desired frequency. The output is seven sets of two orthogonal amplitudes: one for the sine and one for the cosine. These are the two components that define the vector response. This can be interpreted as a problem to be solved using Least Squares, and in the case of this study, four frequencies (the stimulus frequency plus its three first fundamental harmonics) and a DC component will be simultaneously analyzed.

A standard linear system can be written as,

(3.1) $$Ax = B$$

48

In this particular case, the matrix **A** contains the sine and cosine waves to be fitted plus the value 1 to obtain the DC offset value. In this work each cycle is four seconds long and contains 800 data points since data were sampled at 200Hz so this matrix **A** has the form,

(3.2)

$$\begin{pmatrix} 1 & -\sin 2\pi f_1 t_1 & -\sin 2\pi f_2 t_1 & -\sin 2\pi f_3 t_1 & -\sin 2\pi f_4 t_1 & \cos 2\pi f_1 t_1 & \cos 2\pi f_2 t_1 & \cos 2\pi f_3 t_1 & \cos 2\pi f_4 t_1 \\ \vdots & \vdots & \vdots & \vdots & \vdots & \vdots & \vdots & \vdots & \vdots \\ \vdots & \vdots & \vdots & \vdots & \vdots & \vdots & \vdots & \vdots & \vdots \\ 1 & -\sin 2\pi f_1 t_{800} & -\sin 2\pi f_2 t_{800} & -\sin 2\pi f_3 t_{800} & -\sin 2\pi f_4 t_{800} & \cos 2\pi f_1 t_{800} & \cos 2\pi f_2 t_{800} & \cos 2\pi f_3 t_{800} & \cos 2\pi f_4 t_{800} \end{pmatrix}$$

where the four frequencies under consideration are:

(3.3)
$$[f_1 \quad f_2 \quad f_3 \quad f_4] = [0.25 \quad 0.50 \quad 0.75 \quad 1.00]$$

The reason for the negative sign in the sines in Eq. 3.2 is so that the resulting phase difference will be the same as the phase difference with respect to the stimulus since the sled and sinuosidal windowshade velocities are negative sines.

B contains the signal that is being analyzed, in this case it is a column vector containing the series of 800 values of SPV collected during the cycle. The vector **x** entries are the coefficients that we are looking for and which establishes the strength of the signal at each particular frequency as well as the DC offset:

(3.4)
$$x = [DC \quad S_1 \quad S_2 \quad S_3 \quad S_4 \quad C_1 \quad C_2 \quad C_3 \quad C_4]$$

Where DC is the DC offset, S_1 the fundamental frequency sine response, C_1 the fundamental cosine response, S_2 the second harmonic sine response and so on.

This is clearly an overdetermined system and the Least Squares Method gives a solution of the form,

(3.5)
$$x = (A^T A)^{-1} A^T B$$

The Least Squares Method was originally implemented by Christie (1992) in his MatLab script *jc_sines*, and this author modified it under the name *freq_analysis* to generate polar plots of each trial. These polar plots were used to obtain information about the responses in the trial but, when analyzed for each subject, they are not statistically

49

relevant due to the assumption of independence (see section 3.4.4.4). In addition to polar plots, the program also displays the edited slow phase velocity with the curve fitted to it using the Least Squares Method. For each harmonic N in each trial, the program calculates the mean resultant vector.

The mean sine and cosine components are calculated by adding the seven cycles,

(3.6)
$$\overline{S}_N = \sum_{j=1}^{j=7} S_{N_j}/7 \quad ; \quad \overline{C}_N = \sum_{j=1}^{j=7} C_{N_j}/7$$

where N takes a value between one and four to represent each one of the four frequencies.

And the magnitude and phase of the mean resultant vector can be found as,

(3.7)
$$MAG_N = \sqrt{\overline{S}_N{}^2 + \overline{C}_N{}^2}$$

(3.8)
$$PHASE_N = \arctan\left(\frac{\overline{C}_N}{\overline{S}_N}\right)$$

In the polar plots, the radial distance from each response (indicated by an x in Fig. 3.8) represents the magnitude of the response, and the angle that it makes with the 0° axis is the phase difference of the response. Each polar plot shows the seven cycles and the mean resultant vector. Using the convention defined, the phase difference will be 180° when the response is *compensatory,* where compensation means that eye velocity is equal but opposite to sled velocity for those trials in which the phase difference of eye velocity is referenced to sled velocity (dark trials and constant optokinetic trials). When the phase of eye velocity is referenced to the windowshade velocity (sinusoidal optokinetic trials), compensation is attained when the eye velocity is equal and in the same direction as the windowshade velocity.

When the eye velocity leads the compensatory response, the response vector will move in the clockwise direction from 180° while a phase lag will move the response vector in the counterclockwise direction from 180°. This is clearly illustrated in Fig. 3.8 which shows the polar location of responses with a magnitude of 2 units which are

compensatory (A), leading the compensatory response (B), and lagging the compensatory

response (C). Also shown is the location of the major axes (0°, 90°, 180°, and 270°).
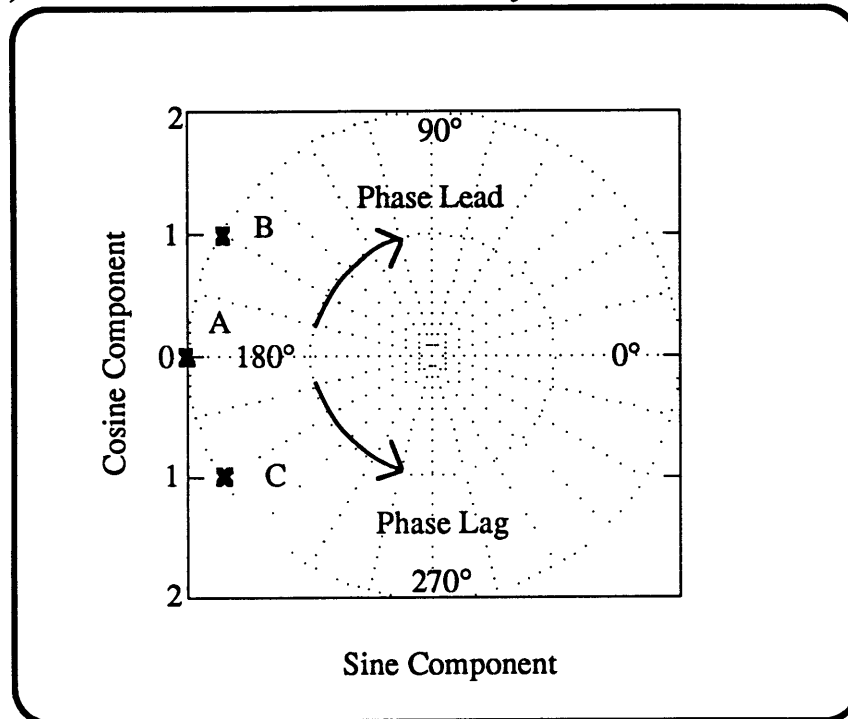
Figure 3.8: **Representation of Phase Information.** Throughout this thesis, a perfectly compensatory ocular response (e.g. sled right, eye left) will be shown as having a phase of 180° (A). Responses leading perfect compensation (B) will appear as a clockwise shift and phase lags (C) as a counter-clockwise shift away from the 180° axis. In this example, B is leading by 30° while C is lagging by the same amount. The radial distance to the origin (2 units) represents the magnitude of the response.

Figure 3.9 and 3.10 show examples of the analysis process as it has been described in the preceding sections for horizontal and vertical eye movements in one subject during three cycles of *Dark1*. The first two panels present the recorded sled velocities and eye position, and the other two panels present the calculated eye velocity, slow phase velocity and curve fit.

3.4.4 Statistical Analysis

Using magnitude and phase information for the different conditions, we (a) verify that the observed responses are statistically different from zero (e.g., the observed eye movement are consistent responses and not just mere random eye movements or noise), and (b) compare the responses in different conditions.

51
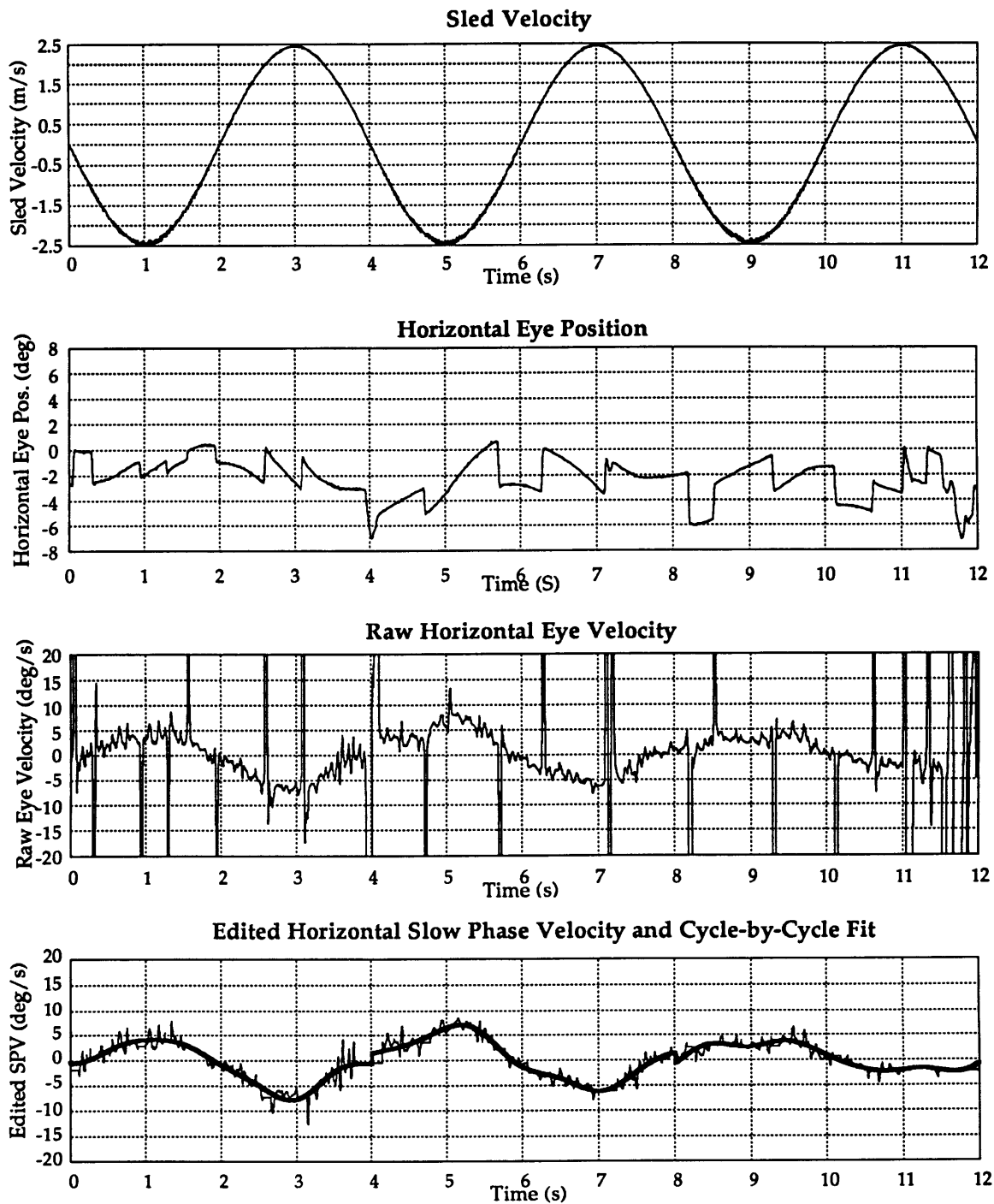
Figure 3.9: Example of Nysa Analysis on Horizontal Eye Movements - Subject E Upright. Dark1. The first two panels are the measured Sled Velocity and the horizontal Eye Position. Nysa differentiates Eye Position to obtain the Raw Eye Velocity, and after taking the fast phases out, it generates the Edited Slow Phase Velocity which is used for further frequency analysis by fitting it to a sum of sines at the first four harmonics of the stimulus (0.25, 0.50, 0.75, and 1.00Hz) by *freq_analysis..*

52
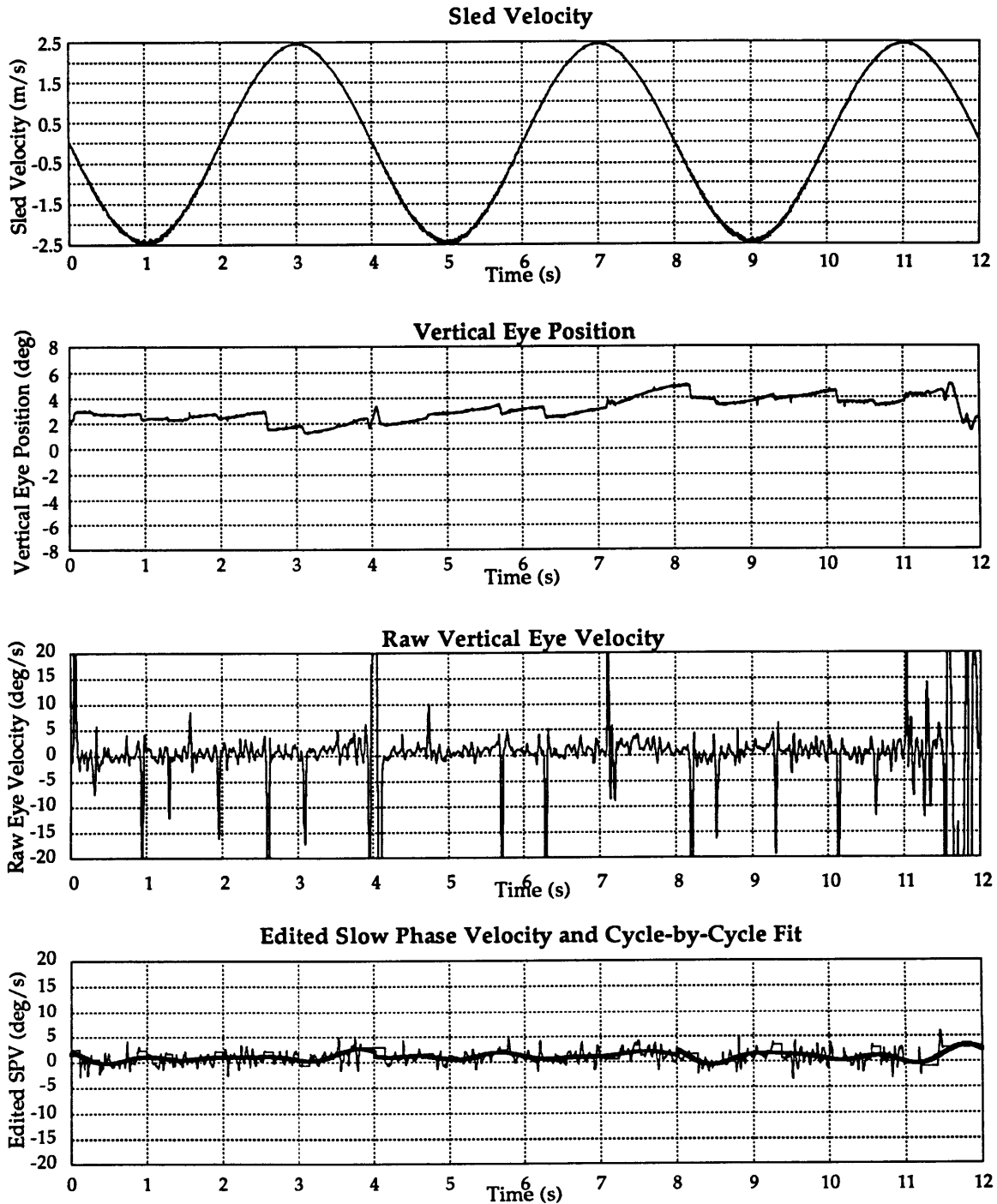
Figure 3.10: Example of Nysa Analysis on Vertical Eye Movements - Subject E Upright Dark1. The first two panels are the measured Sled Velocity and the Vertical Eye Position. Nysa differentiates Eye Position to obtain the Raw Eye Velocity, and after taking the fast phases out, it generates the Edited Slow Phase Velocity which is used for further frequency analysis by fitting it to a sum of sines at the first four harmonics of the stimulus (0.25, 0.50, 0.75, and 1.00Hz) by *freq_analysis.*.

53

3.4.4.1 Statistical Challenges Posed by Data Set

The data obtained in this study could be analyzed using a t-test, to compare the results from different kinds of trials with unknown underlying statistical parameters (Rosner, 1990, pp. 248-292). The two competing hypotheses in this case are,

(3.9) $$H_0: \mu = \mu_0 \text{ against } H_1: \mu \neq \mu_0$$

where μ is the mean of the obtained data, and μ_0 is the overall mean against which it is being compared. The hypothesis H_0 is rejected if |t| exceeds a specified point in a t-distribution. This is equivalent to rejecting it if its square is too large,

(3.10) $$t^2 = \frac{(\overline{X} - \mu_0)^2}{s^2 / n} = n(\overline{X} - \mu_0)(s^2)^{-1}(\overline{X} - \mu_0)$$

where $\overline{X}$ is the numerical mean of the sample, s^2 is the numerical sample variance, and n is the number of samples, and all parameters are scalars.

The measurements taken in this study, however, have two variables, phase and magnitude, which as was seen in Eqs. 3.7 and 3.8 are represented by the mean cosine and sine components. Therefore a multivariate statistical method had to be used to represent the results efficiently (Johnson and Wichern, 1982), We chose Hotellings's T^2 as a multi-variate extension of the t-test.

3.4.4.2 Hotelling's T^2

We need to extend the concept of univariate confidence interval given by the t-test to a multivariate confidence region. Eq. 3.10 can be written in a multivariate form using the statistics T^2 (Eq. 3.11) called Hotelling's T^2 after Harold Hotelling, who first found its distribution (Eq. 3.12).

(3.11) $$T^2 = n(\overline{X} - \mu_0)^T (S)^{-1}(\overline{X} - \mu_0)$$

where $\overline{X}$ is a vector containing the means of each one of the variables in the sample, μ_0 is a vector containing the overall means against which $\overline{X}$ is being compared, and S is the covariance matrix.

(3.12) $$T^2 \text{ is distributed as } \frac{(n-1)p}{(n-p)} F_{p, n-p}$$

54

where p is the number of parameters (two in this study: sine and cosine components), n is the number of samples and F values were obtained from a table for $\alpha = .05$.

Let q be a vector of unknown population parameters, in this case the mean, and Q the set of all possible values of q. A confidence region is a region of likely q values.

The region R(X), where X is the data matrix, is said to be a $100(1-\alpha)\%$ *confidence region* if the probability P,

(3.13)   P[R(X) will cover the true q] = 1 - α

The confidence region of the mean μ_0 of a p-dimensional normal population is shown in Eq. 3.14,

(3.14) $$P\left[n(\overline{X}-\mu_\bullet)^T(S)^{-1}(\overline{X}-\mu_\bullet) \leq \frac{(n-1)p}{n(n-p)}F_{p,n-p}(\alpha)\right] = 1-\alpha$$

The points satisfying 3.14 define a region, an ellipse centered at the mean of the data. In the two-dimensional case under study,

(3.15) $$\overline{X} = \begin{bmatrix} \overline{S}_N & \overline{C}_N \end{bmatrix} \quad S = \begin{bmatrix} \sigma_{S_N S_N} & \sigma_{C_N S_N} \\ \sigma_{S_N C_N} & \sigma_{C_N C_N} \end{bmatrix}$$

Where $\overline{S}_N$ and $\overline{C}_N$ are the mean sine and cosine components and S is the *covariance* matrix of the given data. Note that the bold S refers to this matrix and not to the individual amplitude of the sine component. The resultant ellipse is given by 3.16,

(3.16) $$(\overline{X}-\mu_0)^T S^{-1}(\overline{X}-\mu_0) = \frac{(n-1)p}{n(n-p)}F_{p,n-p}(\alpha)$$

Generation of the ellipses was implemented using the MatLab scripts *Mult_Sbj* and *Conf_Sbj* and an example is presented in Fig. 3.11 using representative data obtained in trials *Right* and *Left* in the upright position. The ellipse is always centered at the resultant mean and most individual measurements are contained in it.

3.4.4.3 Scalar Statistics

In addition to the multi-variate analysis performed on the vector values that represent the ocular responses, estimates of the standard deviation of the amplitude and the phase of each response were obtained. These two parameters are scalars.

55
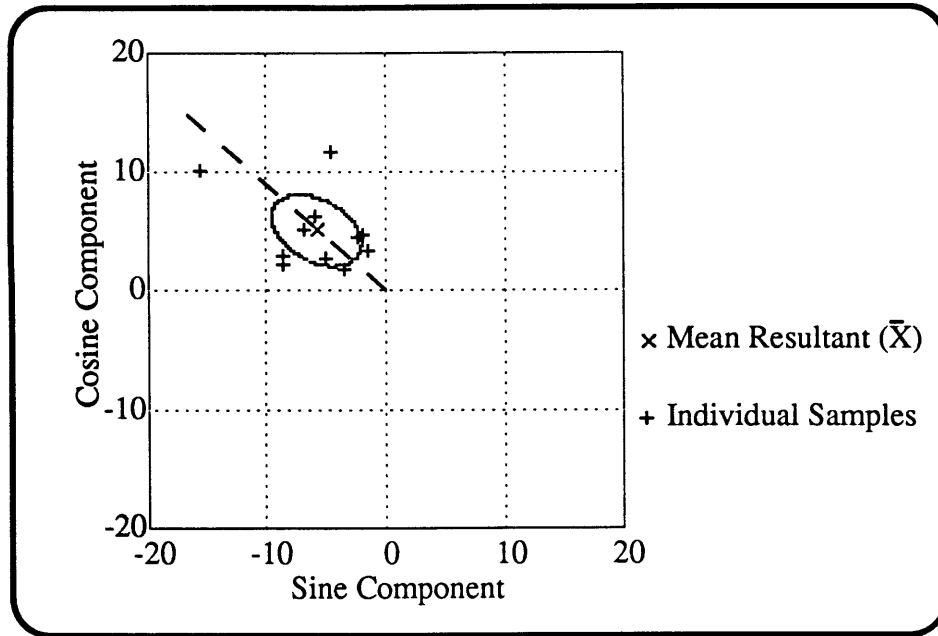
Figure 3.11: Example of the 95% Confidence Area for a Representative set of Data. The ellipse representing the confidence area was obtained from a set of responses in trials *Right* and *Left* upright. The MatLab scripts used to generate the plot take the individual cycle measurements (+) and use them to obtain the confidence area centered at the mean resultant (x). The mean vector response lies along the dashed line.

The standard deviations are presented in the tables in chapter 4, but it should be emphasized that they only provide a rough estimate of the variability of the response since the true response is a vector, not a set of two independent scalars, consequently they were used as a semi-quantitative way of assessing the variance of the magnitude and phase difference of the response.

However, the standard deviation of the amplitude was calculated taking into account the fact that its true variability is affected by the phase. This is accomplished by taking the individual measurements and finding their projections on the line along which the mean response lies (dashed line in fig. 3.11). The standard deviation of the amplitude is taken to be the standard deviation of these projections.

The standard deviation of the phase is calculated directly from the phase values of each cycle.

56

3.4.4.4 Statistical Assumptions

We have taken the observed responses to be normally distributed and that each sample (sine and cosine components of the response) is statistically independent. It is speculative to assume that measurements on successive cycles are independent of one another. Therefore, mean sine and cosine components were averaged for each trial and subject and those means were averaged overall subjects. Ellipses were plotted using the means for each subject as data points since the assumption of independence among subjects can be safely made.

3.4.4.5 Summary of Steps of Statistical Inquiry

Analysis will be done for responses at the frequency of the stimulus in the case of horizontal and vertical eye movements, and responses at the second harmonic will also be studied in order to attempt to replicate some of the results of Christie (1992) where he observed vertical oscillations at twice the frequency of the acceleration stimulus.

Using the confidence area plots, the steps needed to answer these questions will be followed:

a. Is each response different from zero?

b. Are the Dark1 and *Dark2* responses significantly different? *Right* and *Left*? *Up* and *Down*? If they are statistically the same, they will be combined for subsequent analyses

c. Are the responses during each of the constant optokinetic velocity trials (*Right, Left, Up, Down*) different from the Dark trials?

d. Are the *OK+V* and the *OK-V* responses different from the *OK* response and from each other?

In addition to these questions, vergence and DC responses will be analyzed using standard t-tests, since these are univariate parameters.

3.4.5 Control for Possible Sources of Error in Frequency Analysis

To validate the results obtained with the frequency analysis program *freq_analysis,* a dummy file was created containing one cycle of a sinusoidal function generated by,

$$(3.17) \qquad y = A_0\sin(\omega_0 t + \phi_1) + A_1\sin(\omega_1 t + \phi_3) + A_2\sin(\omega_2 t + \phi_3) + A_3\sin(\omega_3 t + \phi_3) + DC$$

Where ω_0 is the fundamental frequency (0.25 Hz in this case) and ω_1, ω_2, and ω_3 are its three next harmonics (0.5, 0.75, and 1.00 Hz respectively). Each sine has an associated amplitude A and phase ϕ.

To further simulate a real SPV response, a random number generator was used to add zero mean noise to the resultant function. Figure 3.12 shows this function and the fit that was obtained with *freq_analysis.* Good accuracy of the algorithm was assured by the high level of agreement between the calculated parameters and the nominal ones (Table 5.1) which showed a difference of less than 2% for the first two harmonics, the ones to be analyzed in the following chapter.

Parameter	Nominal	Calculated
DC Offset	20.0	20.01
A_0	10.0	9.87
ϕ_0	1.0	0.99
A_1	8.0	8.01
ϕ_1	1.7	1.68
A_2	13.0	13.00
ϕ_2	2.0	1.96
A_3	6.0	5.85
ϕ_3	0.8	0.78

Table 3.3: **Comparison between Nominal and Calculated Parameters for Control Run of** *freq_analysis. Nominal* refers to the dummy values used to create the analyzed function, *Calculated* are the values generated by the analysis in the script *freq_analysis.*

58
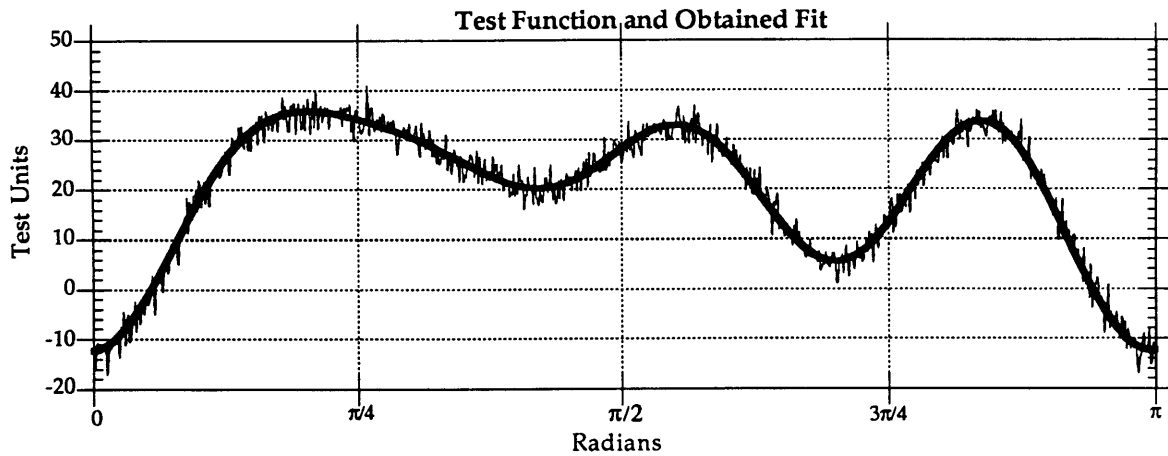
Figure 3.12: **Test Function Generated to Validate freq_analysis and calculated Fit.** The test function is a sum of four sinusoids, a DC offset and zero-mean noise. The bold line superimposed on it is the calculated curve fit.

3.4.6 Vergence and Pre-Acceleration DC Offsets

Vergence measurements were obtained from subjects who wore binocular coils during testing. Vergence was obtained by subtracting the right eye position from the left eye position during the trial. Using this convention, convergence of the eyes (deviation towards the nasal axis) was defined as positive, and divergence (ocular deviation away of the nasal axis) was negative.

In order to compare the change in DC offset of the ocular response to a constant velocity optokinetic display before and after vestibular stimulation, the eight seconds preceding sled motion in the constant velocity optokinetic stimulus trials was averaged and defined as the pre DC offset. Since the windowshade motion begins twelve seconds before the sled motion, this allows four seconds for the OKN to fully develop. This is well above the time for the OKN to rise to steady state which is less than 1 second (Zasorin et al., 1983) in humans. The DC offset during the sled motion is obtained by *freq_analysis* (see section 3.4.3).

59

<u>Chapter 4</u>
Results

This chapter will present the results first for the upright trials and then for the supine ones. In each case, data for one subject is presented followed by those results obtained by pooling all of the subjects. When discussing phase differences of the ocular responses with respect to the stimulus, the stimulus is considered to be sled velocity for the trials in the dark and for the trials with constant velocity visual stimuli. For the trials involving sinusoidal optokinetic stimulation, phases are referenced to windowshade velocity. Responses from each subject are included in Appendix A.

4.1 Upright Condition

A total of six subjects were run in this condition. Five of these subject were tested with coils in both eyes (binocular), but only one, Subject E, was tested through the entire protocol binocularly in a single session (see Table 3.2). Subjects A, B, and D were tested monocularly in a session which did not include the condition *OK-V* and were tested binocularly three months later using a simplified protocol without the constant velocity visual trials. Subject F was run binocularly in a single session following the protocol in Fig. 3.1, but *Dark2* was not run due to time constraints. Subject C was only tested monocularly in one session through the entire protocol, except for the absense of the *OK-V* trial. When showing individual results, this section will present the results of Subject E, while the individual data for the rest of the subjects is in Appendix A. Unless otherwise noted, all measurements were taken from the right eye.

4.1.1 Individual Subject Results: SPV Plots

Figures 4.1 - 4.9 present the traces of the stimulus (sled and/or windowshade), and the final version of slow phase velocity (after manual editing). Since each figure has a similar format, a basic description of each one of the panels follows.

- Sled and Shade Velocities

These channels are directly recorded as voltages coming from the device tachometers. Sled and windowshade velocities are scaled to m/s and deg/s using the respective calibration factors.

- Eye Position

This is the raw eye position channel obtained as a voltage from the magnetic coil system. This voltage is scaled to degrees by substracting an offset value and multiplying by a calibration factor, both of which were determined during the calibration.

- Edited Slow Phase Velocity

Nysa automatically desaccades the raw eye velocity and edit_spv_dual is used to get rid of any saccades missed by the automatic algorithm. All the frequency analysis to be shown is based on these data.

4.1.1.1 *Dark1* and *Dark2* Trials

Dark1 and *Dark2* (Figs. 4.1 and 4.2) were both run in complete darkness and they were respectively the first and the last trial to be run in each session. In the *Dark1* trial, subjects were asked to "relax and keep their eyes open while looking straight-ahead", while in *Dark2* the task was to "count the stripes as they go by even though you cannot see them". The difference in instructions given to the subject does not cause significant changes to the response, in both cases well-defined horizontal oscillations of the eyes were observed at the frequency of the stimulus. The mean response at the frequency of the stimulus in *Dark1* had an amplitude and standard deviation of 4.95±1.28 °/s and a phase difference of -175.1±9.4° with respect to the sled (an average of approximately 5° of phase lag in the response with respect to the ideal compensatory response).
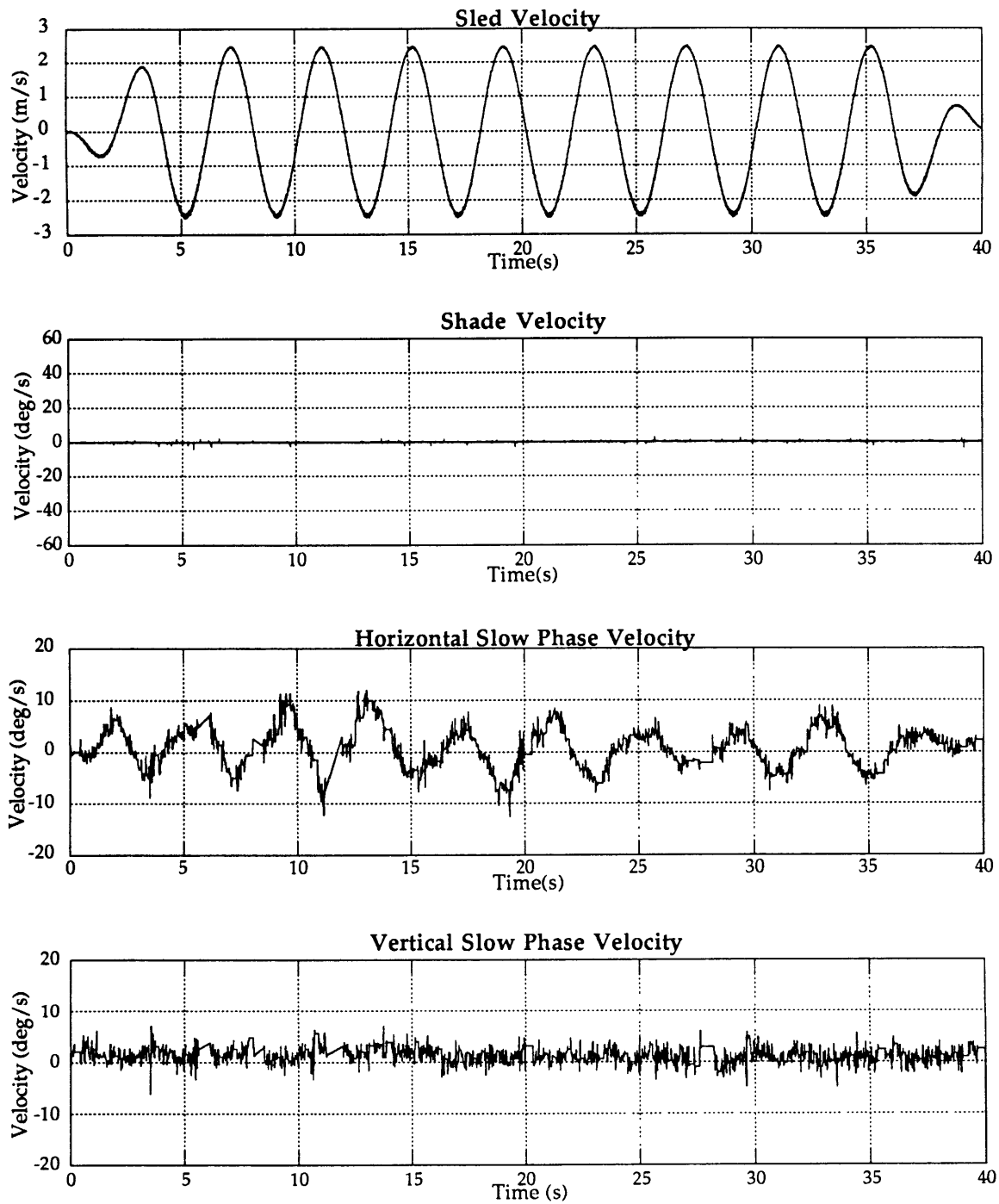
Figure 4.1: Results from trial *Dark1*-Upright in Subject E. Note that the windowshade was not active in this trial. Subjects were instructed to relax and keep their eyes open while undergoing sinusoidal acceleration in completed darkness. Horizontal eye oscillations at the stimulus frequency had a mean amplitude of 4.95 °/s and a mean DC offset of 0.66°/s, while consistent vertical responses were not observed
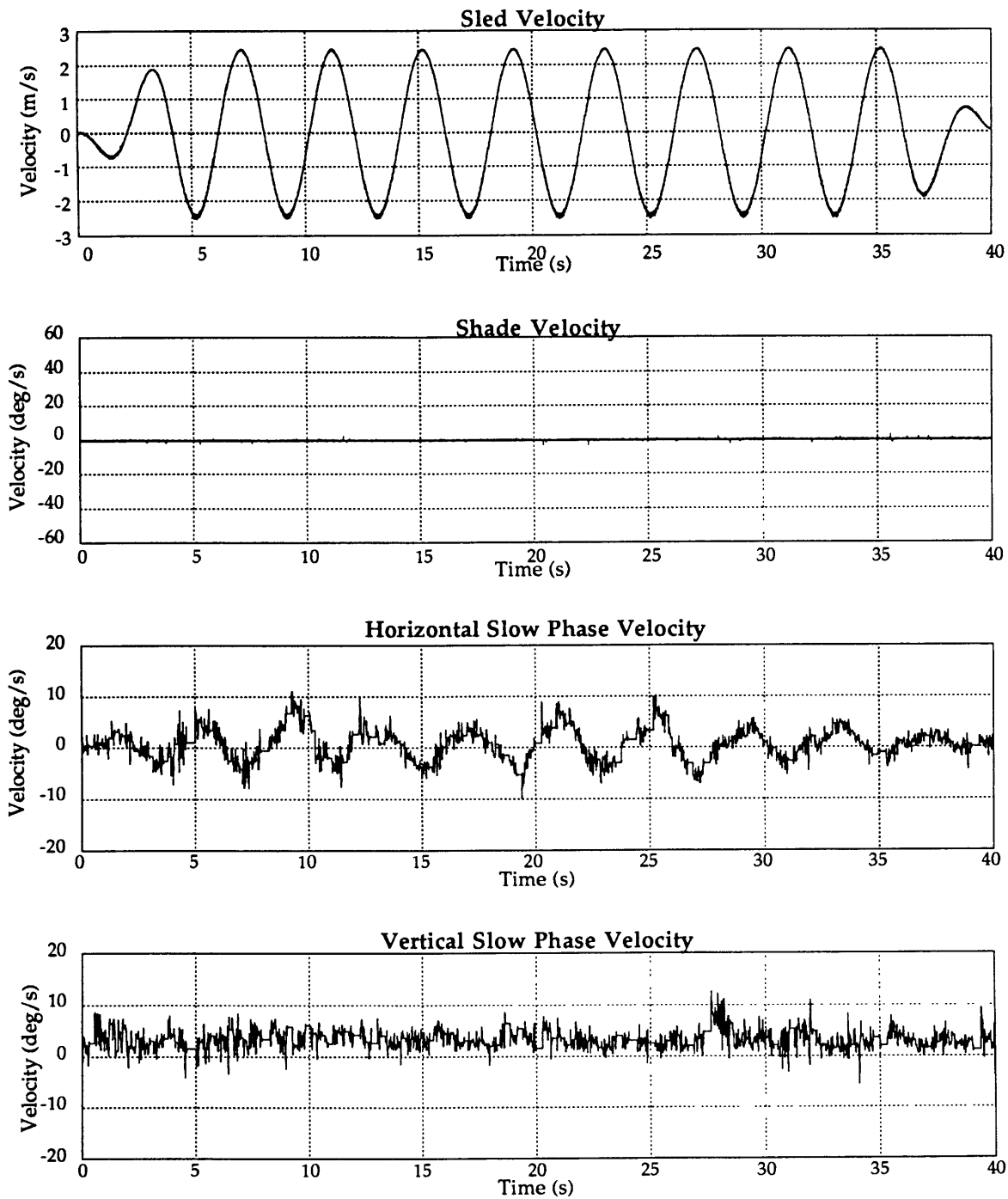
Figure 4.2: Results from trial *Dark2*-Upright in Subject E. Note that the windowshade was not active in this trial. Subjects were instructed to count the stripes in the optokinetic display even though they could not see it while undergoing sinusoidal acceleration in completed darkness. Horizontal eye oscillations at the stimulus frequency had a mean amplitude of 3.97 °/s and a mean DC offset of 0.65°/s, while consistent vertical responses were not observed. These observations were not significantly different from those in *Dark1*.

63

The mean SPV response at the stimulus frequency during *Dark2* had an amplitude of $3.97\pm0.91°/s$ and a phase of $175.9\pm10.0°$(indicating a lead of approximately 5° in the response). Horizontal responses at the other three harmonics in *Dark1* and *Dark2* showed small amplitudes (less than 1°/s) and phase differences with significant variations from cycle to cycle (standard deviations of almost 150°).

Eye motion along the vertical axis did not show consistent responses (phases had standard deviations of approximately 90°) and the observed oscillations in the traces have fairly small amplitudes (less than 0.5°/s for all four frequencies studied).

The DC offset of the horizontal responses was close to zero (mean of 0.65°/s in both *Dark1* and *Dark2*) while the vertical responses showed a somewhat higher upward bias (mean and standard deviation of $1.43\pm0.53°/s$ in *Dark1* and $3.42\pm0.37°/s$).

4.1.1.2 *Right* and *Left* Trials

In these two trials the optokinetic stimulus was moving at a constant velocity of 60°/s horizontally to the left (Fig. 4.3) or to the right (Fig. 4.4). In this case the horizontal movements also showed an oscillation at the frequency of the motion on top of the DC bias produced by the constant velocity of the windowshade, with a larger amplitude than in the dark trials. Responses in the *Right* trial had an amplitude and standard deviation of $5.86\pm5.25°/s$ and a phase difference of $152.27\pm67.16°$ (leading compensatory response by approximately 28°) and the *Left* trial had an amplitude of $9.30\pm3.2°/s$ and phase difference of $160.78\pm14.56°$(lead of about 20°). However, the responses were not as smooth as in the Dark trials and this may be due to OKN irregularities and inconsistencies. The amplitude slightly increased with respect to the Dark trials and the phase advanced by approximately 20 degrees.

Horizontal responses at higher harmonics as well as vertical responses were small (on the order of 1°/s) with phases that spread over more than one quadrant, implying that the responses are very irregular from cycle to cycle.
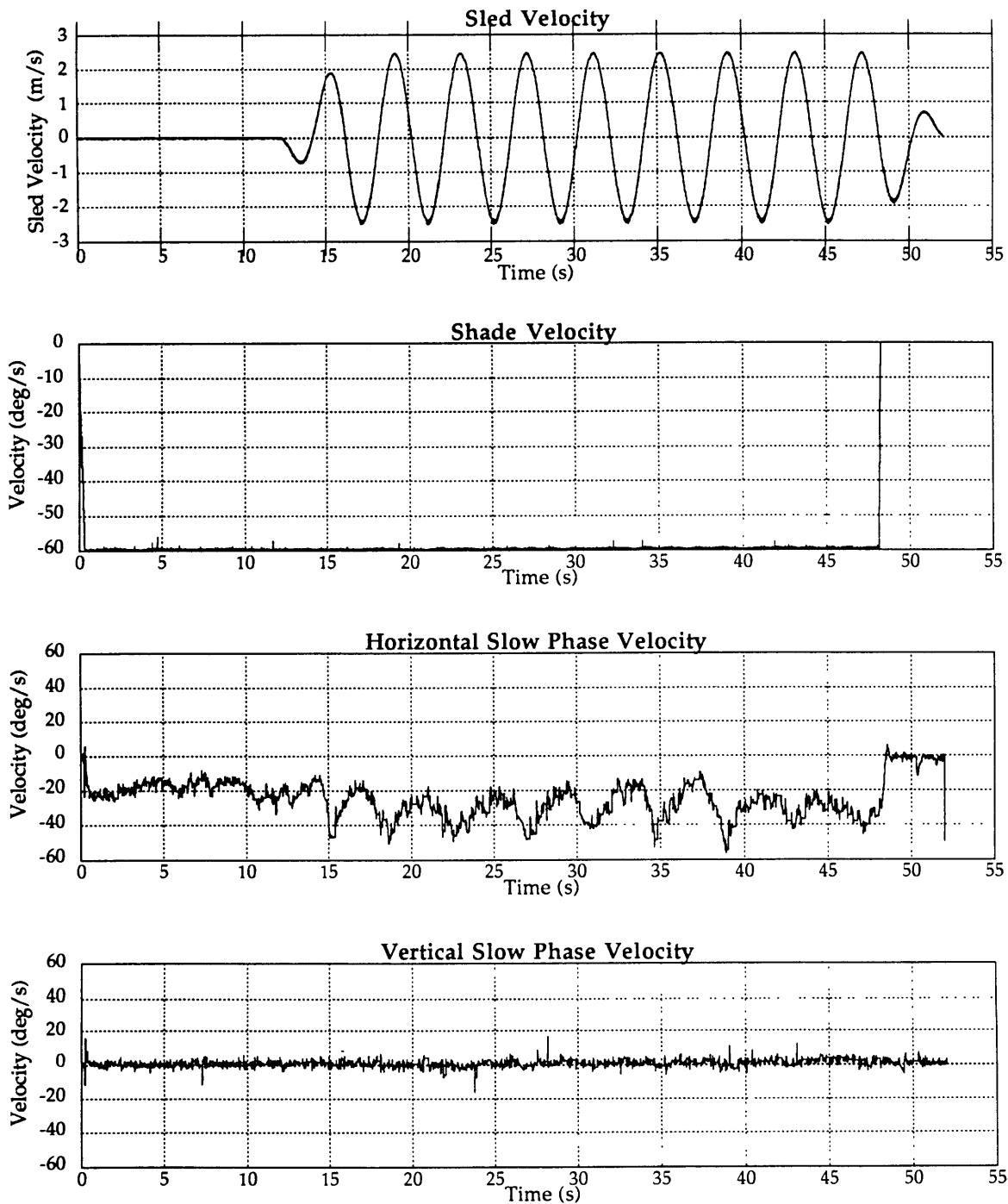
Figure 4.3: Results from trial *Left*-Upright in Subject E. The windowshade is run at a constant velocity of 60 deg/s to the left. After three cycles of only optokinetic stimulation, linear motion begins. Subjects were instructed to count the stripes as they go by without fixating on any one in particular. Eye horizontal oscillations at the stimulus frequency with a mean amplitude of 9.30±3.19°/s and DC bias of -29.97±2.29°/s are observed. Horizontal responses at other frequencies as well as vertical responses have small amplitudes (less than 1-2°/s) and inconsistent phases from cycle to cycle. The offset of the vertical response was close to zero (1.09±0.79°/s).
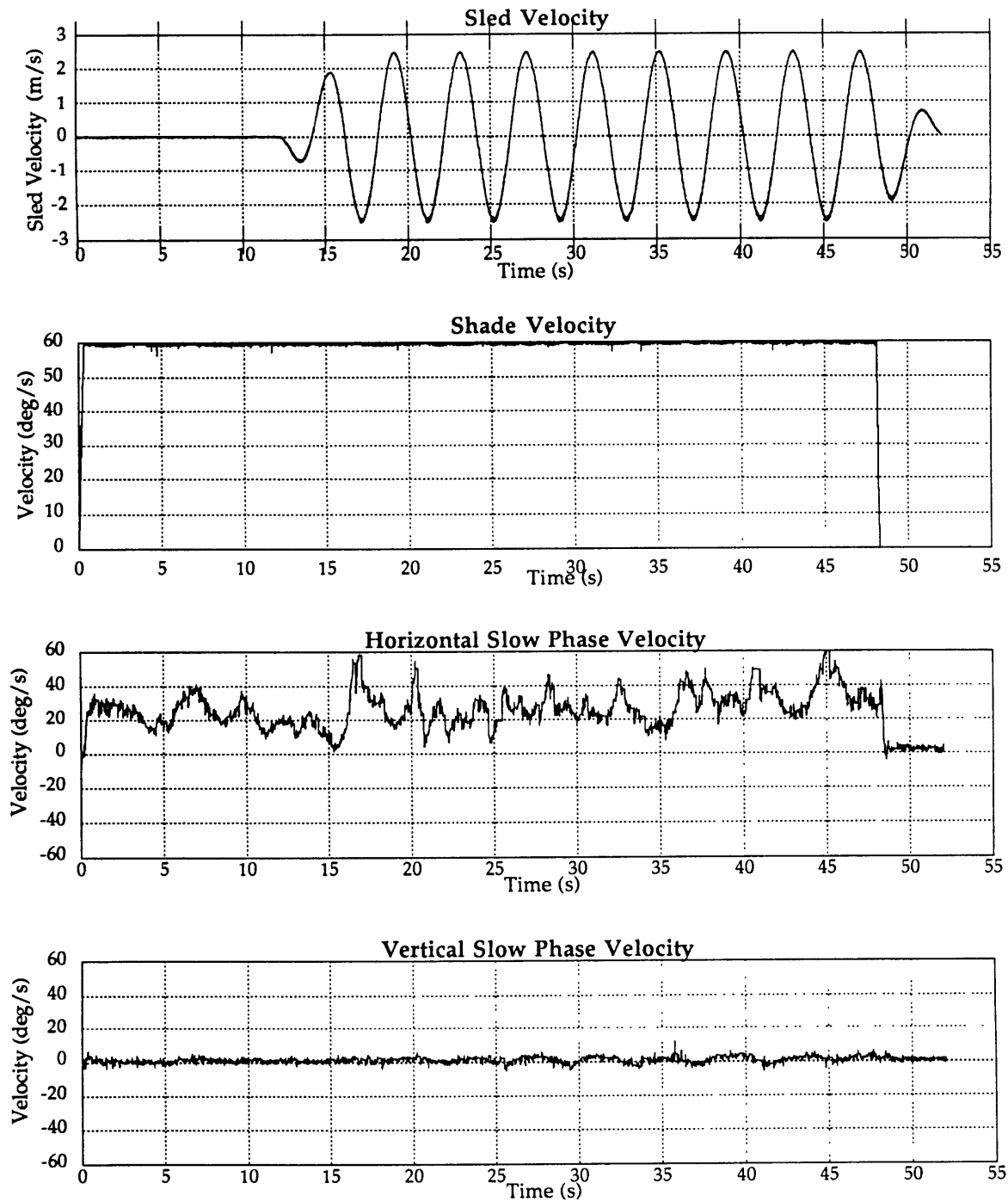
Figure 4.4: Results from trial *Right*-Upright in Subject E. The windowshade is run at a constant velocity of 60 deg/s to the right. After three cycles of only optokinetic stimulation, linear motion begins. Subjects were instructed to count the stripes as they go by without fixating on any one in particular. Eye horizontal oscillations at the stimulus frequency with a mean amplitude of 5.85±5.24°/s and DC bias of 26.60±5.31°/s are observed. Horizontal responses at other frequencies as well as vertical responses have small amplitudes (less than 1-2°/s) and inconsistent phases from cycle to cycle. The offset of the vertical response was close to zero (1.03±0.33°/s).

66

Horizontal DC offsets showed velocities which were approximately 50% of the visual stimulus velocity (26.60±5.31°/s in *Right* and -29.97±2.29°/s in *Left*). Vertical offsets remained close to zero in both cases (1.03±0.33°/s in *Right* and 1.09±0.79°/s in *Left*).

4.1.1.3 *Up* and *Down* Trials

The horizontal oscillations are very well defined in these two trials (Fig. 4.5 and Fig. 4.6) probably due to the absence of visually driven horizontal response variations since the windowshade is moving along the vertical axis.

Horizontal oscillations at the stimulus frequency had an amplitude and standard deviation of 5.65±1.76°/s in *Up* and 4.20±1.30°/s in *Down*. In both trials, the response leads a perfectly compensatory response (phases: 144.89° in *Up* and 152.89° in *Down*). Horizontal responses at the next three harmonics were small (amplitudes of no more than 1.2°/s) and with inconsistent phases (standard deviations of more than 100°). The horizontal DC offset showed small biases in both trials (3.63±0.78°/s in *Up* and -1.88±0.67°/s in *Down*).

Vertical oscillations were again very small and showed large phase variability. The largest vertical response was obtained at the second harmonic during *Up* (2.11±2.48°/s) but the large standard deviation in magnitude, as well as the large variation in phase (standard deviation of 115.10°), shows the lack of consistency of these responses. The DC bias was larger for *Up* (17.36±4.37°/s) than for *Down* (-10.52±4.06°/s) and were smaller than the horizontal bias produced by similar visual stimulation along the that axis.
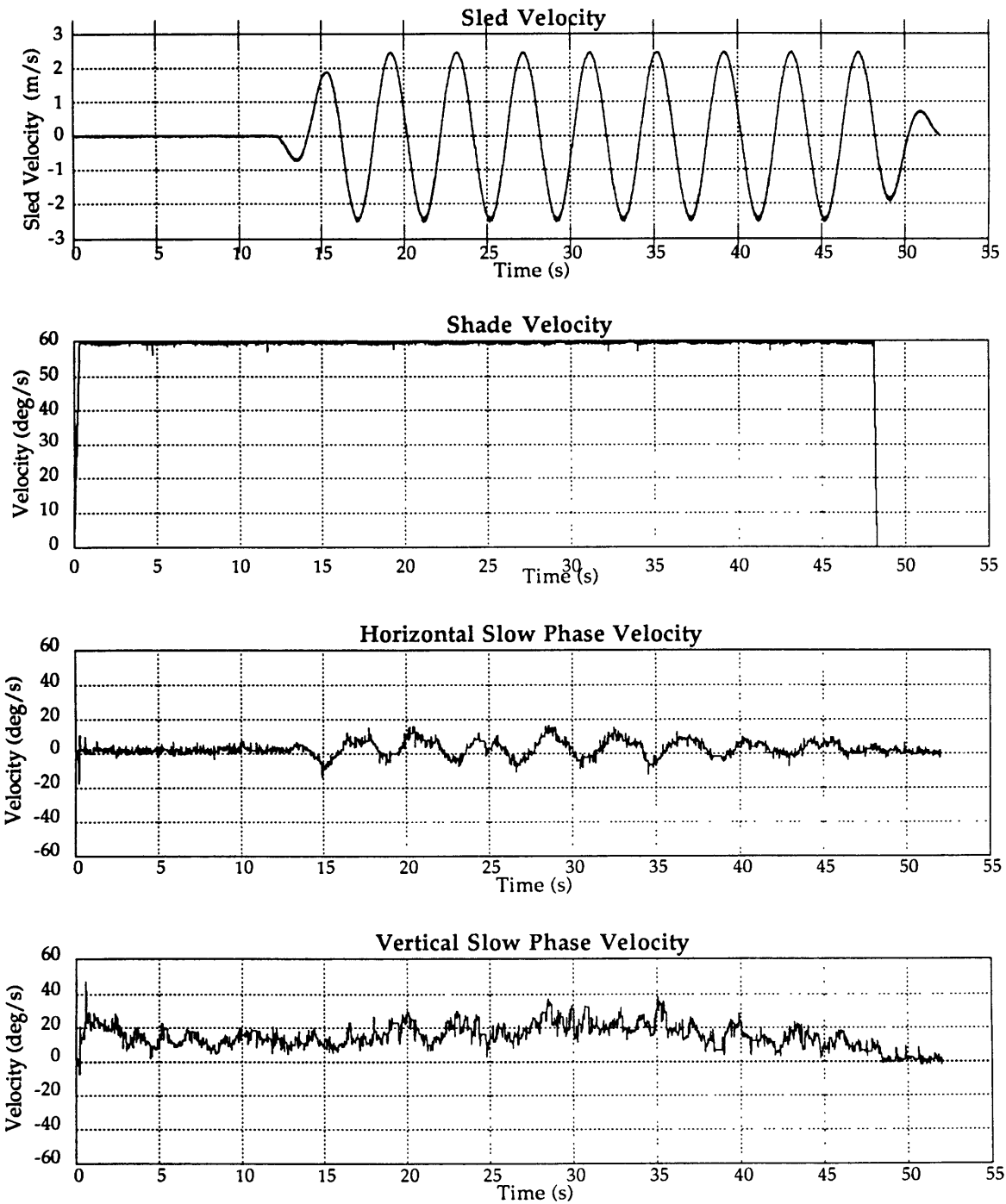
Figure 4.5: Results from trial *Up*-Upright in Subject E. The windowshade is run at a constant velocity of 60 deg/s in the upward direction. After three cycles of only optokinetic stimulation, linear motion begins. Subjects were instructed to count the stripes as they go by without fixating on any one in particular. Eye horizontal oscillations at the stimulus frequency with a mean amplitude of 5.65±1.77°/s and DC bias of 3.63±0.78°/s are observed. Horizontal responses at other frequencies as well as vertical responses have small amplitudes (less than 1-2°/s) and inconsistent phases from cycle to cycle. The offset of the vertical response had a mean amplitude of 17.36±4.37°/s.

68
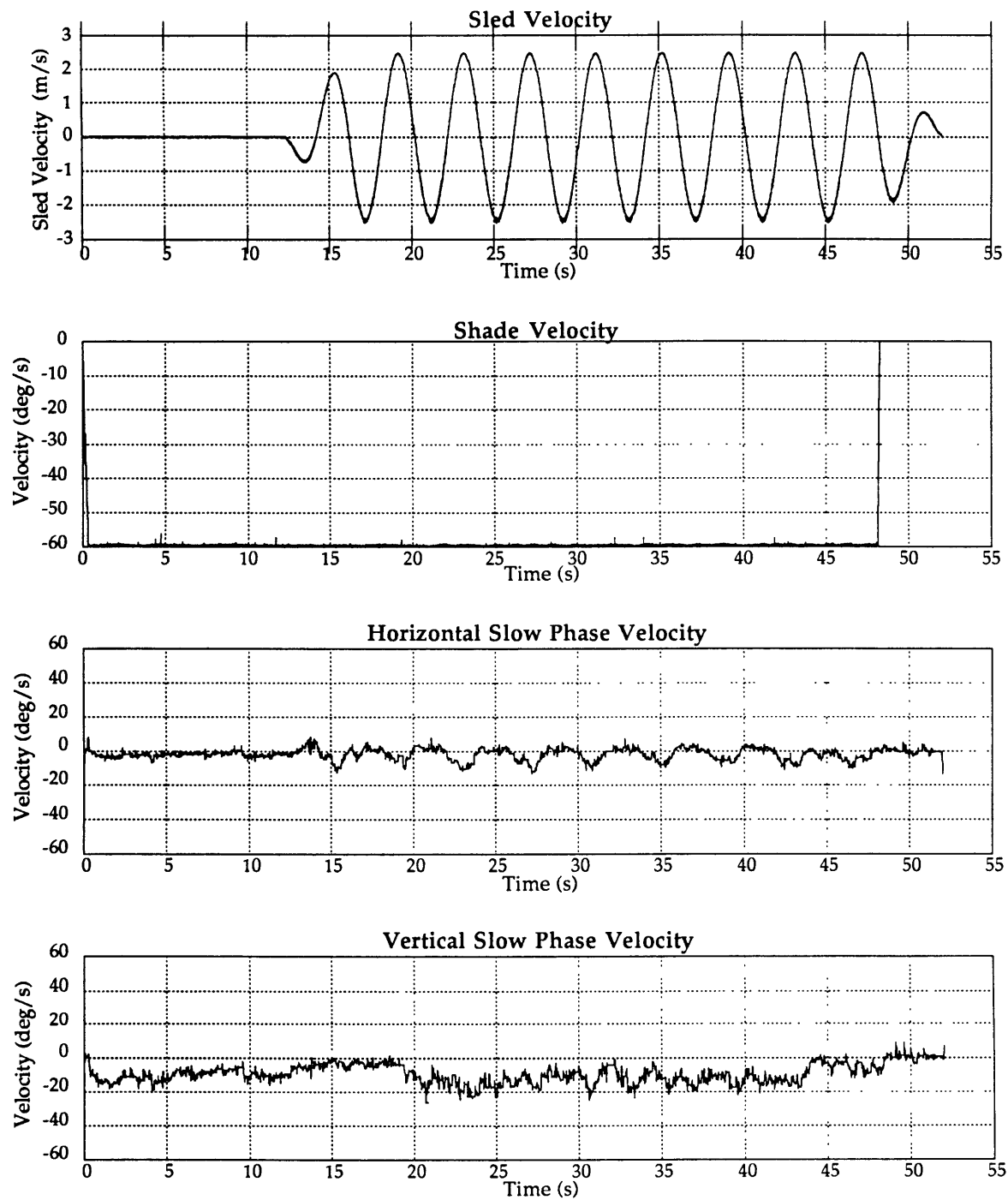
Figure 4.6: Results from trial *Down*-Upright in Subject E. The windowshade is run at a constant velocity of 60 deg/s in the downward direction. After three cycles of only optokinetic stimulation, linear motion begins. Subjects were instructed to count the stripes as they go by without fixating on any one in particular. Eye horizontal oscillations at the stimulus frequency with a mean amplitude of 4.20±1.23°/s and DC bias of -1.88±0.67°/s are observed. Horizontal responses at other frequencies as well as vertical responses have small amplitudes (less than 1-2°/s) and inconsistent phases from cycle to cycle. The offset of the vertical response had a mean amplitude of -10.53±4.06°/s.

69

4.1.1.4 Sinusoidal Optokinetic Stimulus Trials

Figure 4.7 shows the responses in the trial involving only optokinetic stimulation without any sled motion. Unlike the previous results, phase differences are with respect to windowshade velocity and not sled velocity. The response was well synchronized with the windowshade motion as shown by the phase of -179.88° and the mean amplitude is 33.03°/s (gain of 0.55). Horizontal responses at frequencies different from the fundamental and vertical responses were almost non-existent with amplitudes less than 1.2°/s and inconsistent phases. DC offsets were close to zero both in the horizontal (0.08±1.48°/s) and the vertical (0.96±0.26°/s) axes.

When complementary sled motion is incorporated (e.g., sled right - windowshade left), the amplitude of the horizontal response increased to a mean amplitude of 46.16±4.07°/s (Fig. 4.8) and the phase indicated a lead in the response (162.52°). Horizontal responses at the other three frequencies studied as well as vertical responses were small and inconsistent (less than 2°/s). The vertical DC offset was very close to zero (0.05±0.28°/s) while the horizontal offset showed a small bias to the left (-1.46±2.80°/s).

In the anticomplementary case (Fig. 4.9) the amplitude of the horizontal response at the fundamental frequency (33.73±4.68°/s) was similar to the *OK* trial while a phase lead (168.19°) was also observed. As in the other cases, horizontal responses at the next three harmonics as well as all vertical components had small amplitudes (less than 2.4°/s) and large phase variations (standard deviations of more than 100°). Both horizontal (-1.06±0.98°/s) and vertical (1.13±0.34°/s) offsets were close to zero.
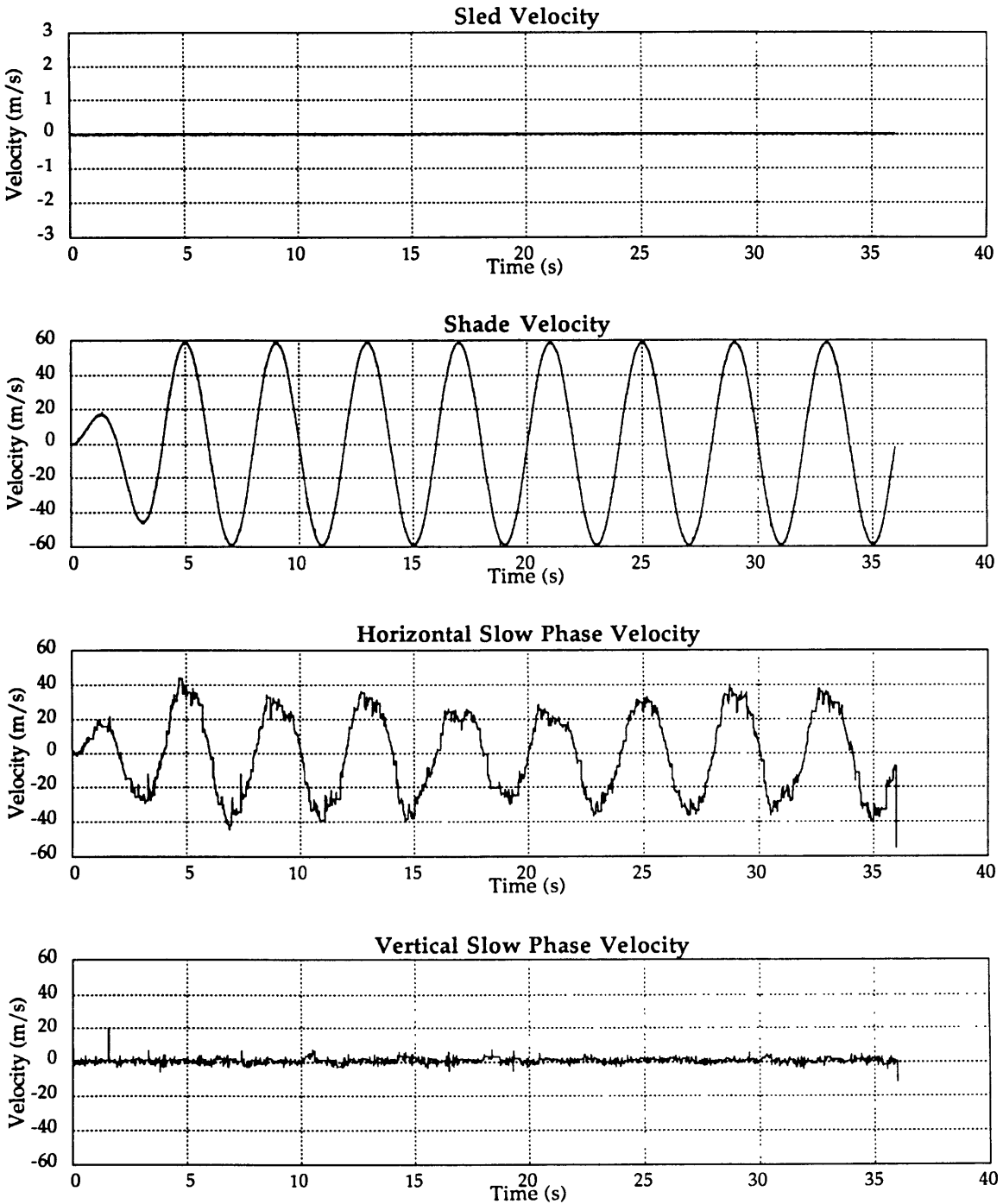
Figure 4.7: Results from trial *OK* - Upright in Subject E. There is only optokinetic stimulation in this trial with the windowshade moving sinusoidally (60°/s 0.25Hz). Subjects were instructed to count the stripes as they go by without fixating on any one in particular. Eye horizontal oscillations at the fundamental frequency had a mean amplitude of 33.03±4.30°/s and phase of -179.88±2.73. Horizontal responses at the other three harmonics analyzed as well as vertical responses were small and inconsistent (amplitudes of less than 1.2°/s). Horizontal (0.95±0.26°/s) and vertical (0.08±1.48°/s) DC offsets are very close to zero.

71
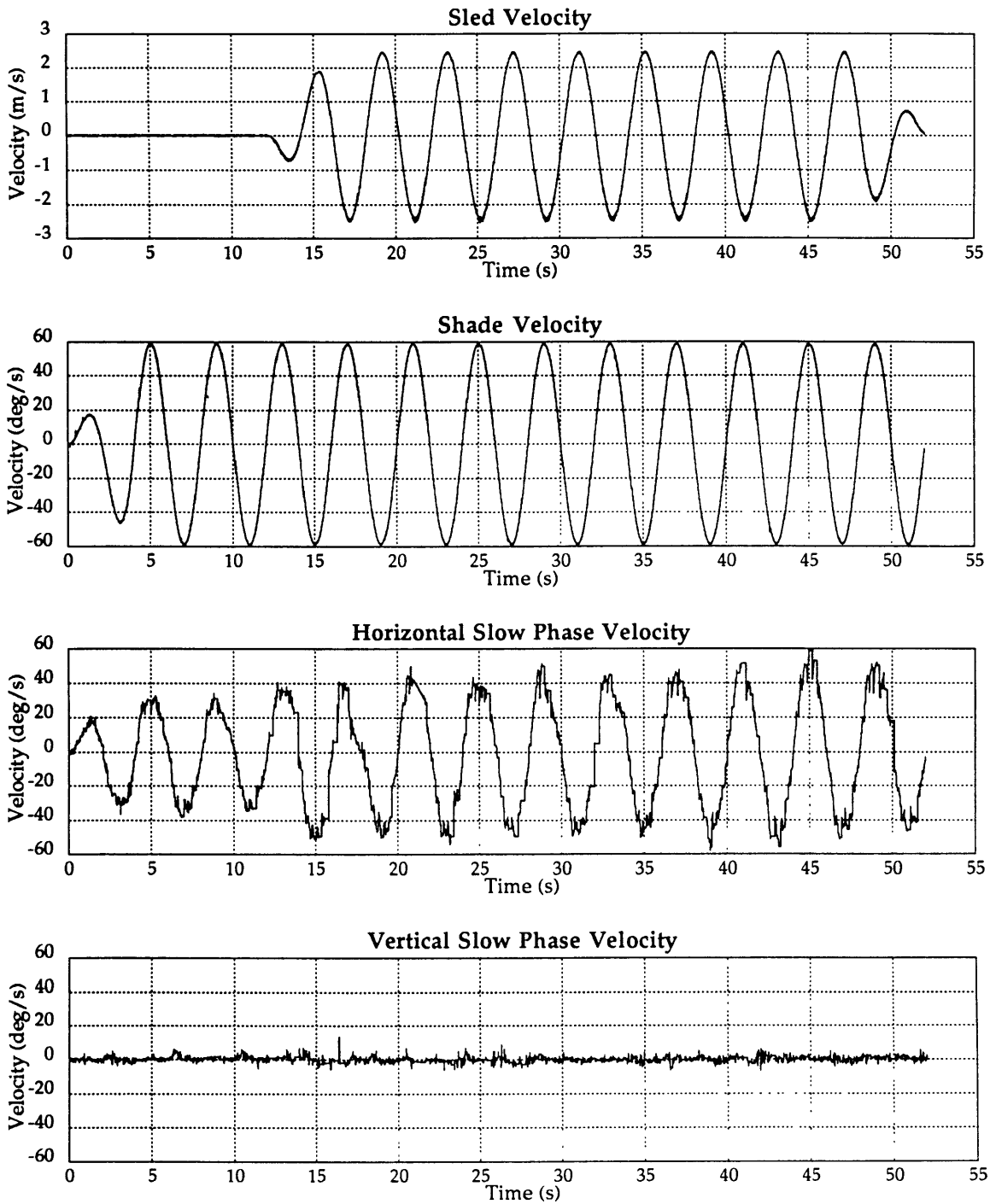
Figure 4.8: Results from trial $OK + V$ - Upright in Subject E. The sled and the windowshade moved in a complementary fashion as in real world motion (e.g. sled right, windowshade left). Subjects were instructed to count the stripes as they go by without fixating on any one in particular. Eye horizontal oscillations at the fundamental frequency had a mean amplitude of 46.16±4.07°/s and phase of 162.52±3.29. Horizontal responses at the other three harmonics analyzed as well as vertical responses were small and inconsistent (amplitudes of less than 2°/s). Horizontal and Vertical biases were within 1.5°/s of zero.
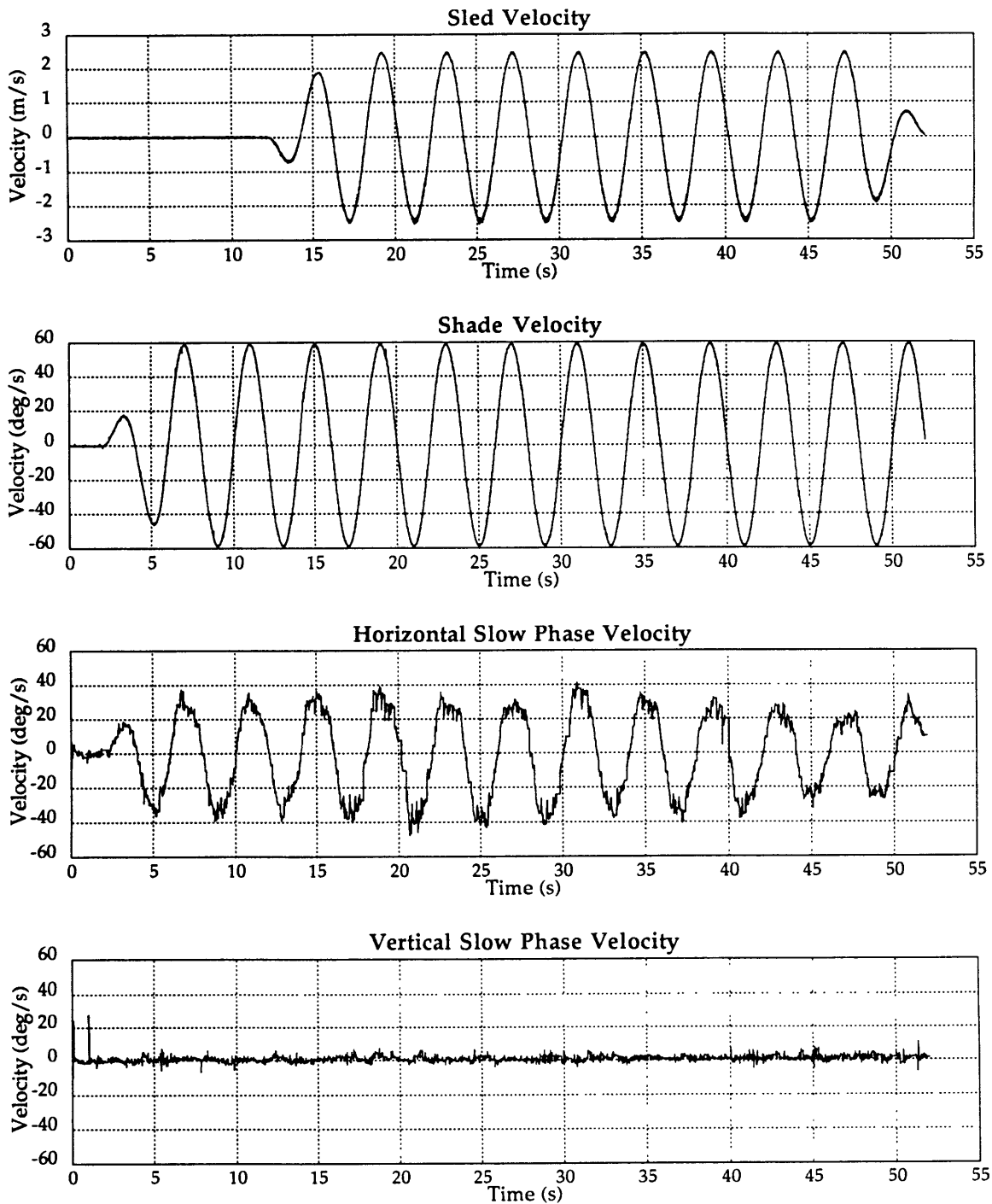
Figure 4.9: Results from trial *OK-V*, subj E upright. The sled and the windowshade moved in an anti-complementary fashion contrary (e.g. sled right, windowshade right) to real world displacements. Subjects were instructed to count the stripes as they go by without fixating on any one in particular. Eye horizontal oscillations at the fundamental frequency had a mean amplitude of 33.73±4.68°/s and phase of 168.19±1.71. Horizontal responses at the other three harmonics analyzed as well as vertical responses were small and inconsistent (amplitudes of less than 2.5°/s). Horizontal and Vertical biases were within 1.2°/s of zero.

4.1.2 Individual Subject Results: Polar Plots

Each response was characterized by the magnitude and phase of the response at each frequency studied. In this case, responses at the fundamental (0.25 Hz) and the second harmonic (0.50 Hz) are presented. Third and fourth harmonics were also studied but no consistent trends were observed.

4.1.2.1 Horizontal Responses

- Responses at the Fundamental Frequency

Figures 4.10 and 4.11 display polar plots (amplitude and phase) of the cycle-by-cycle SPV responses (+) at the stimulus frequency as well as the mean resultant (o) obtained from these single measurements for subject E.

All cycles for the dark trials (*Dark1* and *Dark2*) showed responses within 20 degrees of phase difference with respect to perfect compensation (180 deg) with a small lead in some cases or lag in others and a variation in magnitude of about ±2°/s with respect to the mean resultant response.

Responses in the trials with horizontal optokinetic stimulation (*Right* and *Left*) showed more variability in phase and magnitude which may be caused by variations due to the OKN along this response axis. In the *Right* trial, though most of the responses are within 20° of the 160° phase line, two of the cycles were as far as 180° from the mean, a variation in the overall response that could be attributed to factors such as drop in the attention level of the subject. *Left* responses had more similar phases (responses were approximately within 25° of the mean) which also reflects in the larger mean since single cycles did not cancel each other due to large phase variations.

Horizontal eye movements had a more consistent periodicity in trials with vertical optokinetic motion as seen from the two lower panels in Fig. 4.10. In the *Up* trial, all responses were separated by no more than 15° in phase and *Down* shows a somewhat larger scatter of about 30°. Magnitude variations were also smaller than in the *Right* and *Left* trials, with all responses within 5°/s of the mean.
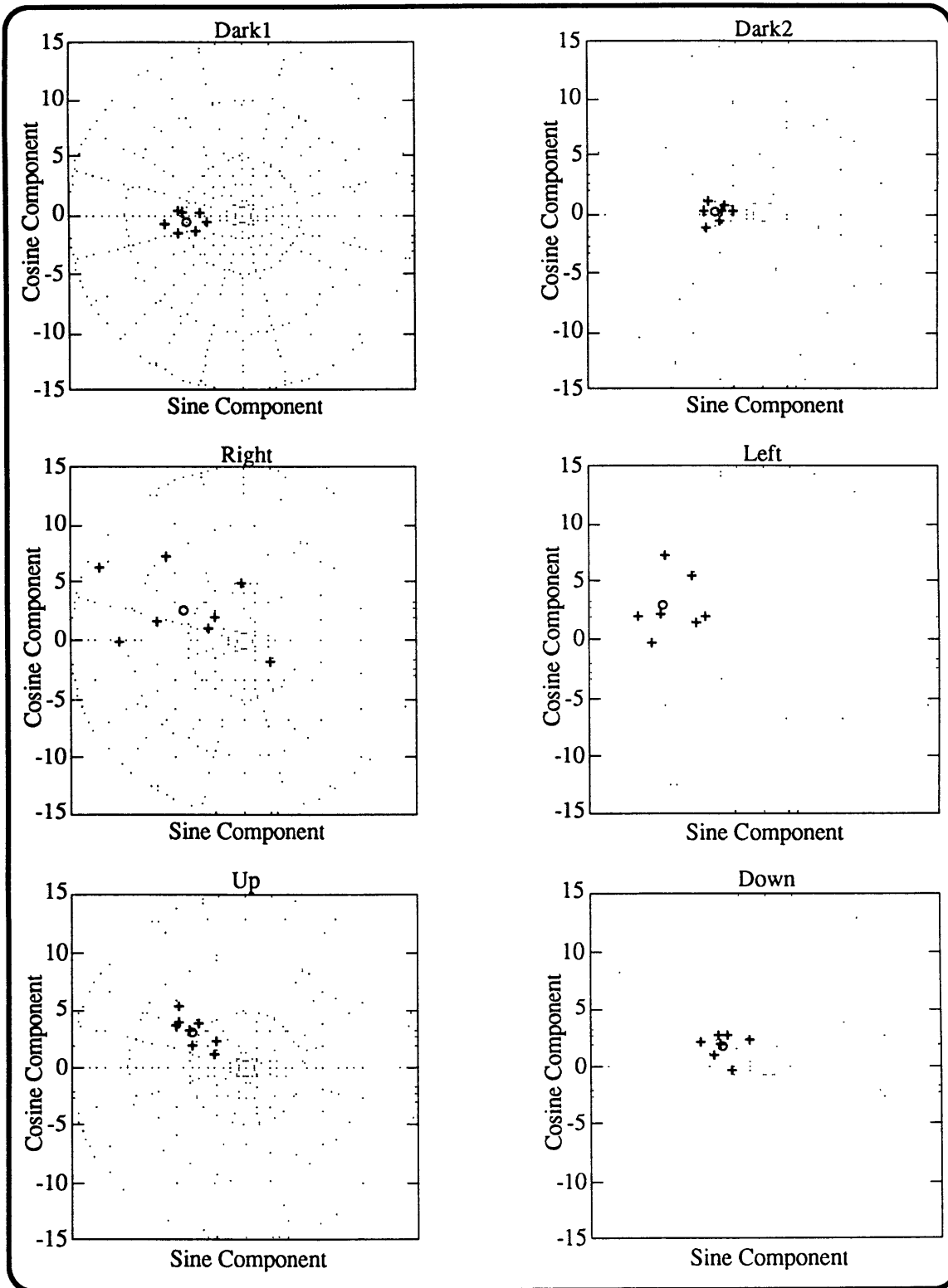
Figure 4.10: Polar Plots for trials *Dark1*, *Dark2*, *Right*, *Left*, *Up*, and *Down*. Amplitude and phase (with respect to sled velocity) of Horizontal SPV responses (+) in deg/s at the fundamental frequency are shown. The mean response (o) calculated from the vector average of the individual cycles is also shown.
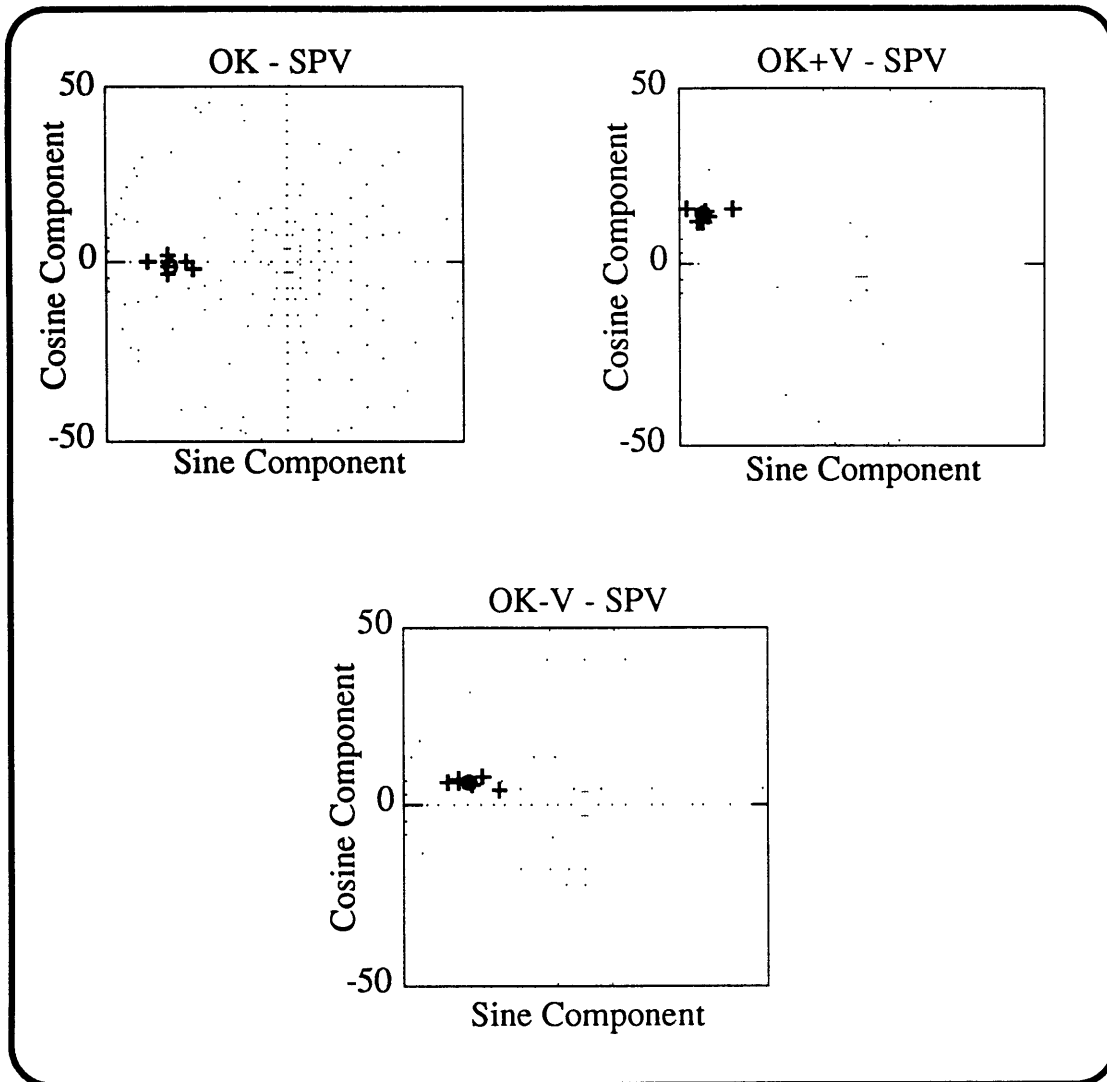
Figure 4.11: Polar Plots trials *OK*, *OK+V*, and *OK-V*. Amplitude and phase (with respect to windowshade velocity) of Horizontal SPV responses (+) in deg/s at the fundamental frequency are shown. The mean response (o) calculated from the vector average of the individual cycles is also shown.

Phases were very consistent in the sinusoidal optokinetic trials with cycles remaining within 10° of the mean in each one of the three trials. Magnitude variations of ±15°/s were observed in all trials. The variation in pattern between the three trials is very consistent. In general, the phase of the *OK* responses was nearly perfectly compensatory (180°) for the windowshade motion. The *OK+V* response a had higher amplitude than the *OK* response and led the windowshade by approximately 20°. The phase in *OK-V* returned closer to the 180° line, but still led the windowshade by approximately 10° and the magnitude decreased to levels similar to the OK responses. It is interesting to note

that the phase shift for the *OK+V* and *OK-V* conditions was in the same direction, despite the fact that the linear acceleration stimuli was shifted by 180° during these trials. This will be discussed more thoroughly in chapter four.

- Responses at the Second Harmonic

Figures 4.12 and 4.13 show the polar plots of the horizontal responses at the second harmonic. In general, these responses had no defined trend, and were characterized by small amplitudes and large phase variability.

Dark1 and *Dark2* trials show responses that are for the most part below 2°/s and separated by as many as 180° of phase difference.

Responses in *Right* and *Left* had somewhat larger amplitudes but the variability in phase is even larger than in the dark trials, suggesting an even more inconsistent series of responses. The phase variability cancels several responses among themselves, generating mean responses close to zero (1.45°/s and 2.19°/s in *Right* and *Left* respectively).

The magnitude of the responses in *Up* and *Down* were as small as those in the dark and showed a similar phase inconsistency which resulted in equally small means (1.27°/s and 1.21°/s in *Up* and *Down* respectively).

Trials with sinusoidal optokinetic stimulation had responses at the second harmonic as inconsistent as the ones previously discussed. In all three cases (*OK, OK+V*, and *OK-V*) phases between responses were separated by as many 180° and mean amplitudes were on the order of 2°/s.
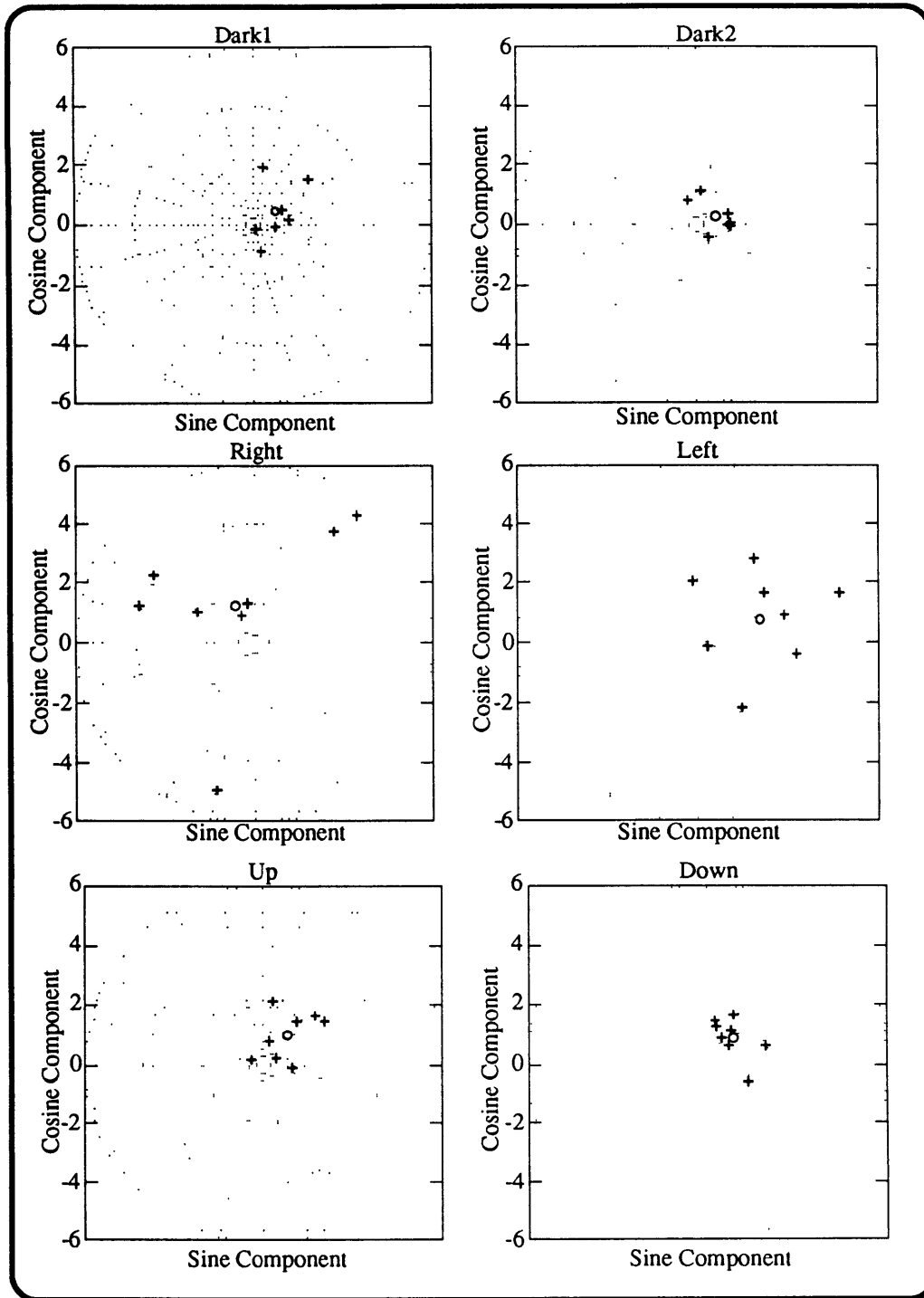
Figure 4.12: Polar Plots trials *Dark1*, *Dark2*, *Right*, *Left*, *Up*, and *Down*. Amplitude and phase (with respect to sled velocity) of Horizontal SPV responses (+) in deg/s at the second harmonic are shown. The mean response (o) calculated from the vector average of the individual cycles is also shown.

78
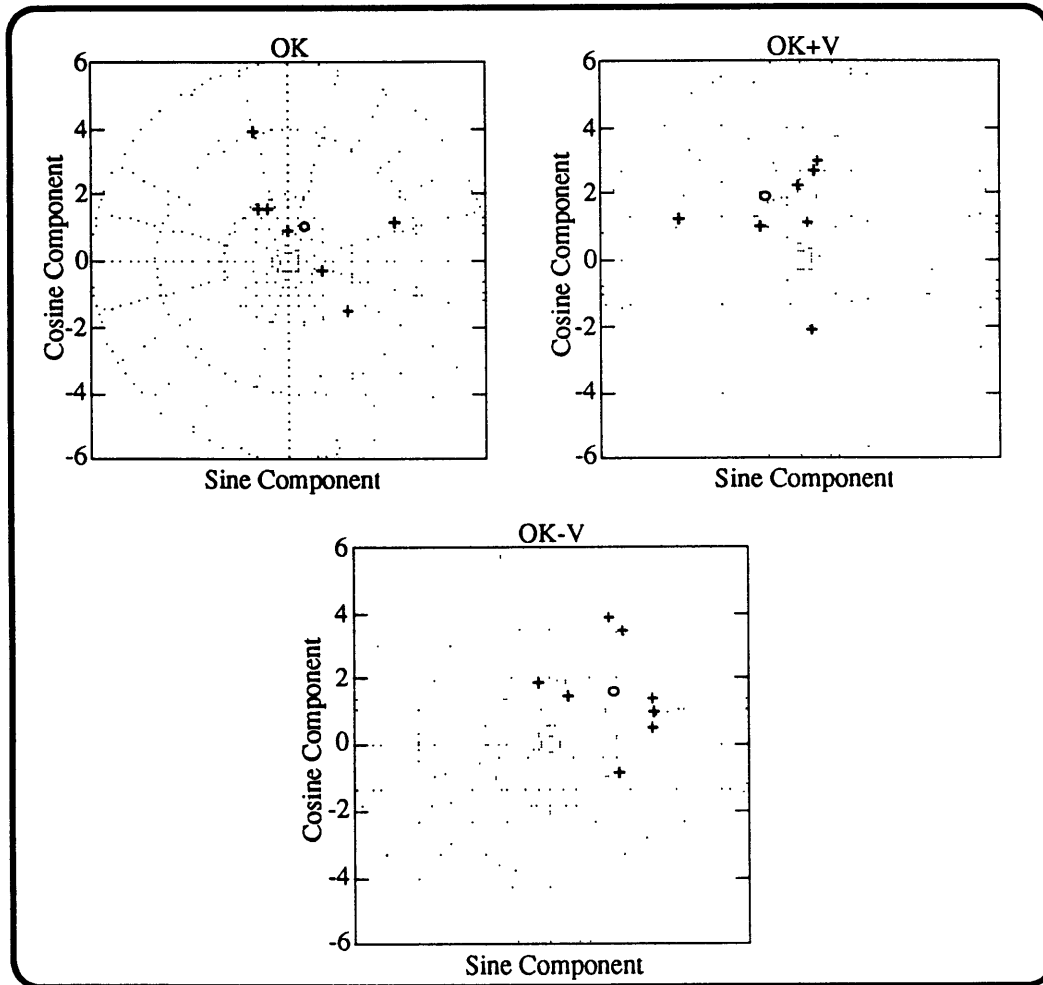
Figure 4.13 Polar Plots trials *OK*, *OK+V*, and *OK-V*. Amplitude and phase (with respect to windowshade velocity) of Horizontal SPV responses (+) in deg/s at the fundamental frequency are shown. The mean response (o) calculated from the vector average of the individual cycles is also shown.

4.1.2.2 Vertical Responses

- Responses at the Fundamental Frequency

Figures 4.14 and 4.15 display the polar location (amplitude and phase) of the cycle-by-cycle vertical SPV responses at the fundamental frequency as well as the mean resultant obtained from these single measurements. In general, all trials showed responses with very small amplitudes and inconsistent phases suggesting that they might represent random oscillations.

The dark trials as well as *Right* and *Left* responses showed very similar characteristics: amplitudes were almost zero (less than 1°/s in all cases) and responses were separated by as much as 180° of phase.

Up and *Down* trials showed responses with larger amplitudes (3°/s-6°/s) but with phases spread over all four quadrants. These responses can be related to the OKN taking place along this axis since the visual stimulus is moving along the vertical.

All responses during the sinusoidal optokinetic stimulus trials had very small amplitudes (below 1°/s) and phases also showed large variations except in the *OK* cases, where responses seem to be aligned near a phase of 300°. However, even then the magnitudes were very low.

- Responses at the Second Harmonic

The vertical responses at the second harmonic (Figs. 4.16 and 4.17) followed a pattern almost identical to the one followed by the responses at the fundamental frequency. The dark trials and *Right* and *Left* showed inconsistent responses with magnitudes very close to zero while *Up* and *Down* responses had somewhat higher magnitudes but also very inconsistent phases (*Up*, for example, had responses in all four quadrants).

Trials with sinusoidal optokinetic stimulus showed responses with very small amplitudes (almost all below 1°/s) though some consistency in phase can be seen in *OK* (-167.88±17.36°) and *OK+V* (116.20±20.92°).
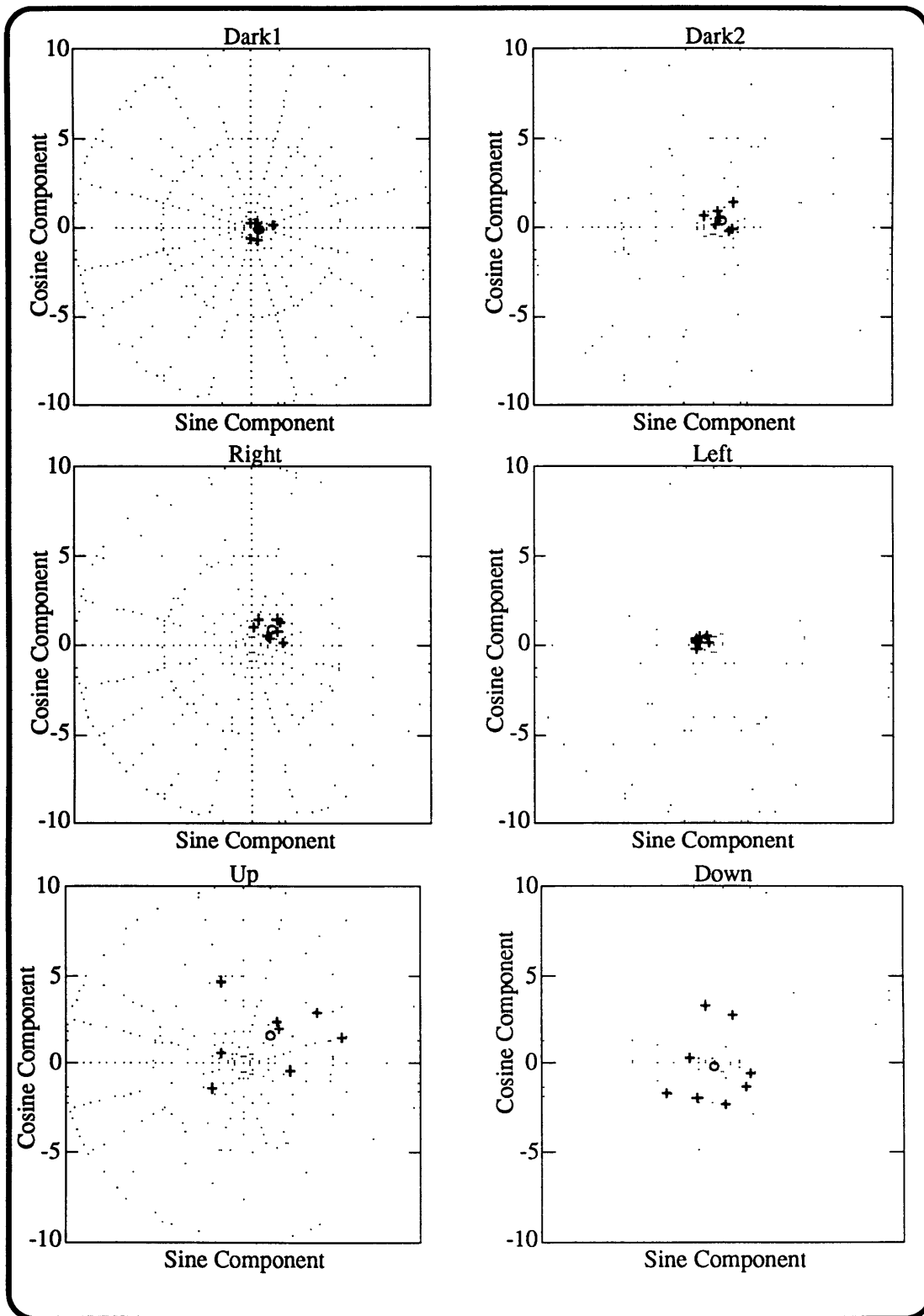
Figure 4.14: Polar Plots trials *Dark1, Dark2, Right, Left, Up,* and *Down.* Amplitude and phase (with respect to sled velocity) of vertical SPV responses (+) in deg/s at the fundamental frequency are shown. The mean response (o) calculated from the vector average of the individual cycles is also shown.
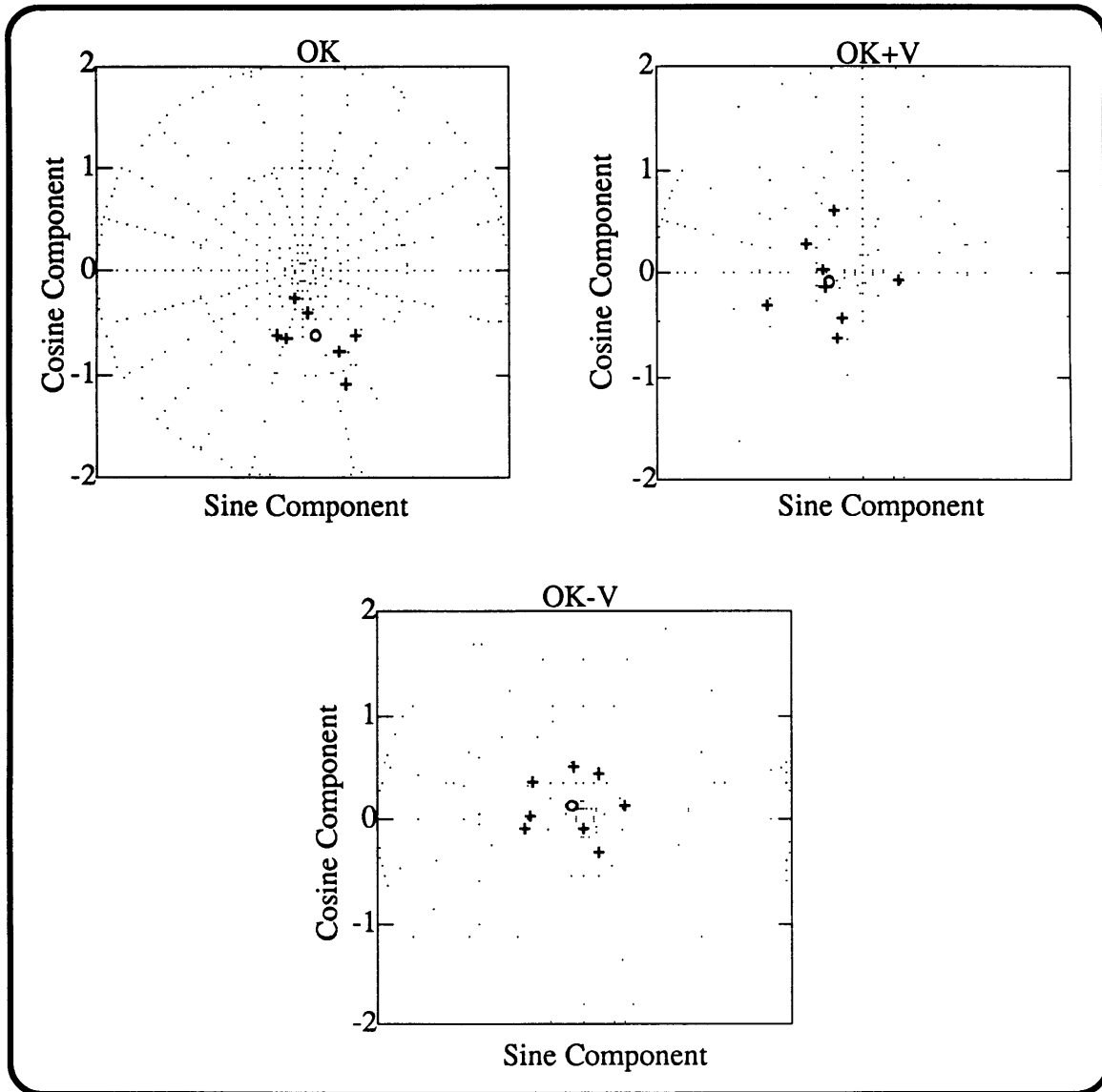
Figure 4.15: Polar Plots trials *OK*, *OK+V*, and *OK-V*. Amplitude and phase (with respect to windowshade velocity) of vertical SPV responses (+) in deg/s at the fundamental frequency are shown. The mean response (o) calculated from the vector average of the individual cycles is also shown.
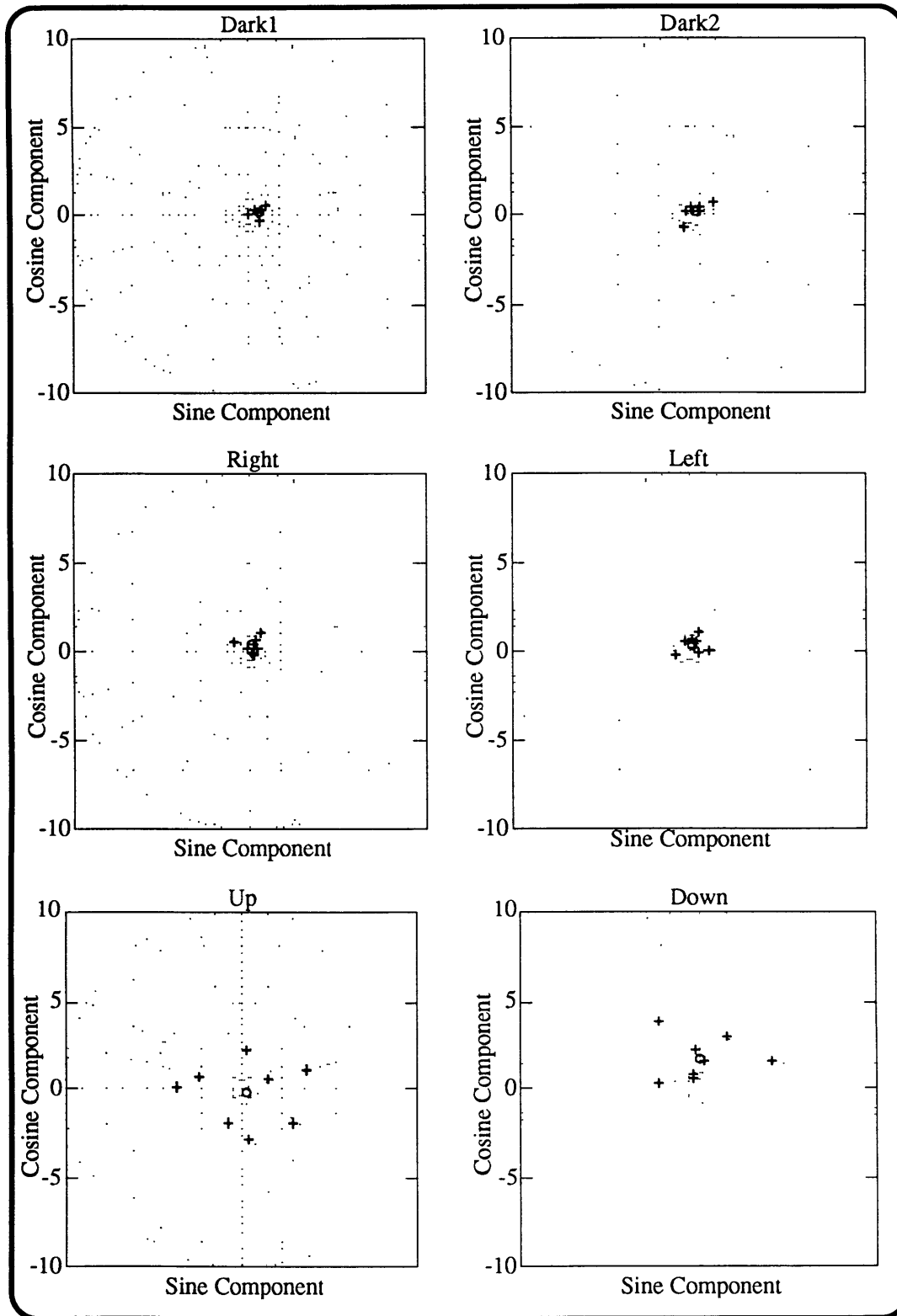
Figure 4.16: Polar Plots trials *Dark1, Dark2, Right, Left, Up,* and *Down.* Amplitude and phase (with respect to sled velocity) of vertical SPV responses (+) in deg/s at the second harmonic are shown. The mean response (o) calculated from the vector average of the individual cycles is also shown.
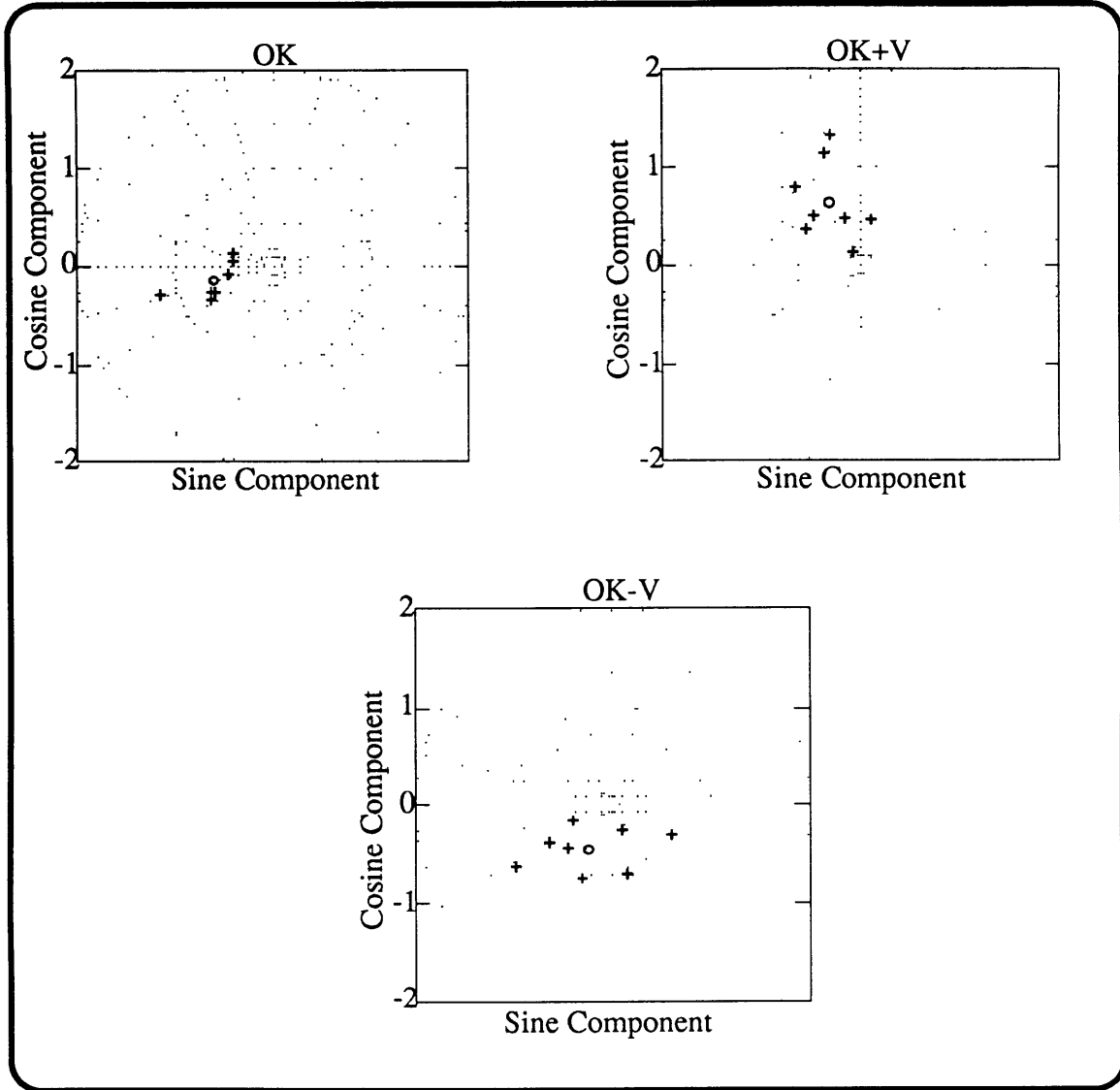
Figure 4.17 Polar Plots trials *OK*, *OK+V*, and *OK-V*. Amplitude and phase (with respect to windowshade velocity) of vertical SPV responses (+) in deg/s at the second harmonic are shown. The mean response (o) calculated from the vector average of the individual cycles is also shown.

4.1.3 Individual Subject Results: Summary

Tables 4.1 and 4.2 summarize the results presented for Subject E. In general consistent horizontal oscillations in SPV were observed in response to vestibular stimulus (sled motion) at the fundamental frequency. These responses in general had a phase lead with respect to sled velocity except in some cases that showed a slight lag (*Dark1*). When comparing the three different kinds of responses in the three sinusoidal optokinetic stimulus trials, it is found that a complementary vestibular input increased the amplitude of the response and increased the phase lead compared to pure visual stimulation while an anti-complementary stimulus showed the same qualitative effect but with smaller changes. Horizontal responses at twice the stimulus frequency were not consistent and had large variances.

Vertical responses were also small and inconsistent except for the DC offset in the Up and Down trials induced by the stimulation along that axis.

In addition to the results presented, tables 4.1 and 4.2 show that the mean vergence in each of the conditions remained approximately constant, and in close agreement with the vergence needed to focus on the windowshade. Vergence will be discussed further in the Pooled Results section (section 4.1.6).

Condition	DC Values		Fundamental Frequency				Vergence		Second Harmonic			
	Ampl	StdDev	Ampl	StdDev	Phase	StdDev	Mean	StdDev	Ampl	StdDev	Phase	StdDev
	(deg/s)	(deg/s)	(deg/s)	(deg/s)	(deg)	(deg)	(deg)	(deg)	(deg/s)	(deg/s)	(deg)	(deg)
Dark1	0.66	1.05	4.95	1.28	-175.10	9.45	6.06	0.78	0.89	0.88	30.88	147.56
Dark2	0.65	0.66	3.97	0.91	175.94	9.99	5.46	0.90	0.67	0.43	25.71	147.80
OK	0.08	1.48	33.03	4.31	-179.88	2.73	4.35	0.40	1.18	1.31	68.14	123.00
OK+V	-1.46	2.81	46.16	4.07	162.52	3.29	4.36	0.51	2.25	2.67	119.60	66.42
OK-V	-1.06	0.98	33.73	4.68	168.19	1.71	4.46	0.60	2.49	1.24	40.58	106.21
Right	26.60	5.31	5.86	5.25	152.27	67.16	4.52	0.49	1.45	2.24	117.58	65.33
Left	-29.97	2.29	9.31	3.20	160.79	14.56	4.48	0.44	2.19	1.61	22.55	152.35
Up	3.64	0.79	5.66	1.78	144.89	7.95	4.91	0.78	1.27	0.97	53.92	108.93
Down	-1.88	0.67	4.20	1.23	152.89	18.86	4.90	0.71	1.21	0.45	49.39	100.37

Table 4.1: Mean resultant amplitude and phase of horizontal responses for subject E - upright. Phase differences are with respect to sled velocity except for trials OK, OK+V, and OK-V where the phase difference with respect to shade velocity is presented.

Condition	DC Values		Fundamental Frequency				Second Harmonic			
	Ampl	StdDev	Ampl	StdDev	Phase	StdDev	Ampl	StdDev	Phase	StdDev
	(deg/s)	(deg/s)	(deg/s)	(deg/s)	(deg)	(deg)	(deg/s)	(deg/s)	(deg)	(deg)
Dark1	1.43	0.53	0.29	0.40	-14.66	139.00	0.58	0.40	28.30	114.04
Dark2	3.42	0.37	0.66	0.57	50.21	138.18	0.41	0.68	36.29	78.52
OK	0.96	0.26	0.62	0.30	-80.37	24.69	0.64	0.28	-167.88	17.37
OK+V	0.05	0.28	0.35	0.35	-169.66	72.90	0.74	0.41	116.20	20.92
OK-V	1.13	0.34	0.20	0.33	136.97	89.46	0.51	0.34	-118.84	47.11
Right	1.04	0.33	1.31	0.47	41.31	28.48	0.42	0.40	90.60	82.64
Left	1.09	0.79	0.88	0.27	165.00	16.50	0.44	0.50	69.81	61.66
Up	17.37	4.37	2.11	2.48	47.53	115.10	0.30	2.18	-46.15	115.74
Down	-10.53	4.06	0.53	1.68	-167.38	93.49	1.74	1.19	89.66	44.86

Table 4.2: Mean resultant amplitude and phase of vertical responses for subject E - upright. Phase differences are with respect to sled velocity except for trials OK, OK+V, and OK-V where the phase difference with respect to shade velocity is presented.

4.1.4 Pooled Results: Sample Size

In order to conservatively analyze the data using statistical methods requiring independent samples, data was summarized across subjects for each condition. A mean response vector for each subject was obtained from the seven cycles analyzed in each trial, and then an overall mean was obtained by obtaining the vector average across subjects for each condition. For subjects tested in two sessions (Subjects A, B, and D), measurements of the same condition in different sessions are considered independent and therefore their means are treated as two independent data points.

The size of the statistical pool varies since not all the subjects were run in all conditions the same number of times. To keep this issue clear, table 4.3 shows the size of the sample in each condition, differentiating between the number of data points used to obtain the DC and the Fundamental and Second Harmonic frequency means (N1) and the one used to calculate vergence (N2) which depend on the number of binocular trials. *D1&D2* refers to the combination of *Dark1* and *Dark2* as a single condition, and *R&L* and *U&D* refers to the same procedure for *Right* and *Left* and *Up* and *Down*. The rationale for these combinations and how they were implemented are discussed in the following section.

Upright Condition	N1	N2
Dark1	9	5
Dark2	8	4
D1&D2	17	9
OK	9	5
OK+V	9	5
OK-V	5	5
Right	6	2
Left	6	2
R&L	12	4
Up	6	2
Down	6	2
U&D	12	4

Table 4.3: Size of the Statistical Pool, Upright Position
N1 is the number of data points used to calculate the DC and fundamental means.
N2 is the number of data points used to calculate the vergence means.

4.1.5 Pooled Results: Confidence Area Plots

4.1.5.1 Horizontal Eye Movements at the Fundamental Frequency

- Dark and Constant Velocity Optokinetic Stimulus

The left panels in Figure 4.18 show the means and the 95% confidence regions for the SPV responses of the dark trials (*Dark1* and *Dark2*) and the trials involving a constant velocity optokinetic stimulus (*Right, Left, Up,* and *Down*). Individual data points are not shown to make figures cleaner and easier to understand (see section 3.4.4.2). Except for the *Left* trial, all pooled responses showed statistical significance since the origin is not encircled by the 95% confidence region. Even the ellipse for *Left* is on the edge of significance as it barely encircles the origin. These three sets of trials had responses with similar characteristics: mean amplitudes ranging from 5°/s to 13°/s and mean phase differences with respect to the sled velocity ranging from 140° to 155°, indicating that the response led the stimulus by 35° to 50°.

To further increase the statistical power of the ensuing analysis, pairs of conditions that were not significantly different were combined. The panels on the right show the confidence area for the vector difference between a number of conditions which may be statistically equal: *Dark1&Dark2, Right&Left,* and *Up&Down.* Each data point used to generate the ellipse was calculated by substracting the mean vectors for each pair of conditions within each subject. The difference ellipses encircled the origin in all three cases, and from this it is concluded that the pairs of conditions are not statistically different and are combined for the rest of the analysis as trials *D1&D2, R&L,* and *U&D.*

It should now be emphasized that the two dark trials had extremely similar means (5.07 °/s vs 5.08 °/s and phases of 155.06° vs 152.45° respectively for *Dark1* and *Dark2*) which suggests that the responses were not dependent on the particular tasks we used.

Dark1 and Dark2 Trials

-Cosine Component

Sine Component

x Dark1

+ Dark2

Difference Dark1-Dark2

-Cosine Component

Sine Component

x D1&D2

Right and Left Trials

-Cosine Component

Sine Component

x Right

+ Left

Difference Right-Left

-Cosine Component

Sine Component

x R&L

Up and Down Trials

-Cosine Component

Sine Component

x Up

+ Down

Difference Up-Down

-Cosine Component

Sine Component

x U&D

Figure 4.18 95 % Confidence Area for *Dark1&Dark2, Right&Left,*and
Up&Down SPV Responses and their Differences (°/s).

Panels in the right represent the confidence area for the difference between the two conditions in the left panels. Each pair of conditions is not statistically different as can be inferred from the fact that the confidence area for their differences enclose the origin. In general, responses with visual stimulus had larger amplitudes and phases of approximately 150 ° (equivalent to a lead of 30 ° with respect to sled velocity)

Right and *Left* also had quite similar means (8.853°/s vs 8.736°/s and phases of 144.20°vs 140.90° respectively) while *Up* and *Down* were somewhat more separated (13.640°/s vs 6.452°/s and phases of 147.71° vs 136.10° respectively) but the difference was not statistically significant due to the large variation in the responses as represented by the large area of the ellipses.

For the ensuing analysis, the two dark runs will be combined under the name *D1&D2*, the combined *Right* and *Left* will be referred to as *R&L*, and the combined *Up* and *Down* will be identified as *U&D*.

The increase in the sample size given by combining these trials generate a smaller confidence area (Fig. 4.19), which indicates a higher level of significance of the response. The final amplitude for *D1&D2* is 5.19°/s and 153.84° of phase difference, for *R&L* is 8.79°/s and 142.56° of phase difference, and for *U&D* is 10.00°/s and 143.99° of phase difference.

After establishing the significance of each of the responses, it is necessary to establish whether or not the responses are different, and especially to investigate if optokinetic stimulation affects the vestibularly driven oscillations obtained in the dark trials. Figure 4.20 shows the two sets of trials involving constant velocity optokinetic stimulation as well as the combined dark trials. By substracting the dark response from the responses in the light for each subject we could investigate the significance of any differences after pooling all subjects together (Fig. 4.21). Neither of the ellipses include the origin, indicating that visual optokinetic stimulation (both along the horizontal or along the vertical axis) does significantly change the response with increases in both amplitude and phase.
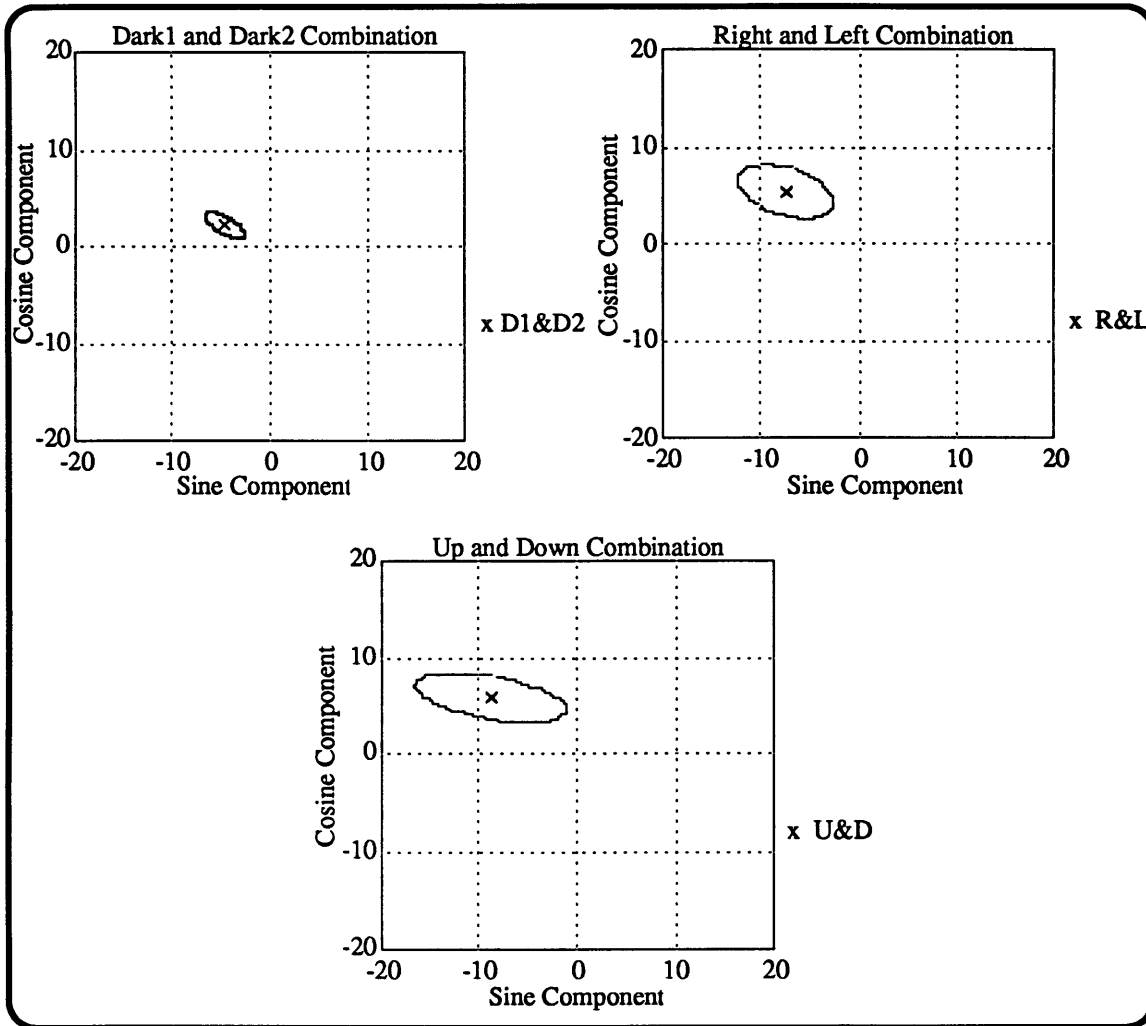
Figure 4.19: **95%** Confidence Areas for the Combinations *Dark1* & *Dark2,Right* & *Left*, and *Up* & *Down* of Fundamental Frequency SPV Responses (°/s).
By combining these pairs of responses, the area of the ellipse decreases (larger N) indicating a more significant result as the ellipse moves further away from zero.
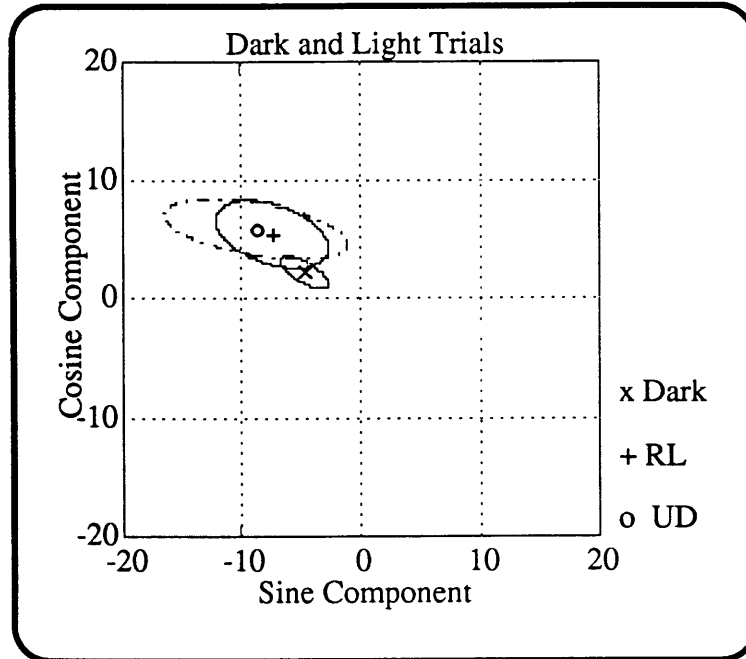
Fig. 4.20 **95% Confidence Areas for Dark and Light Trials (SPV in °/s)**
Optokinetic stimulation at a constant linear velocity tends to increase the magnitude as
well as the lead of the response as seen from the ellipses.
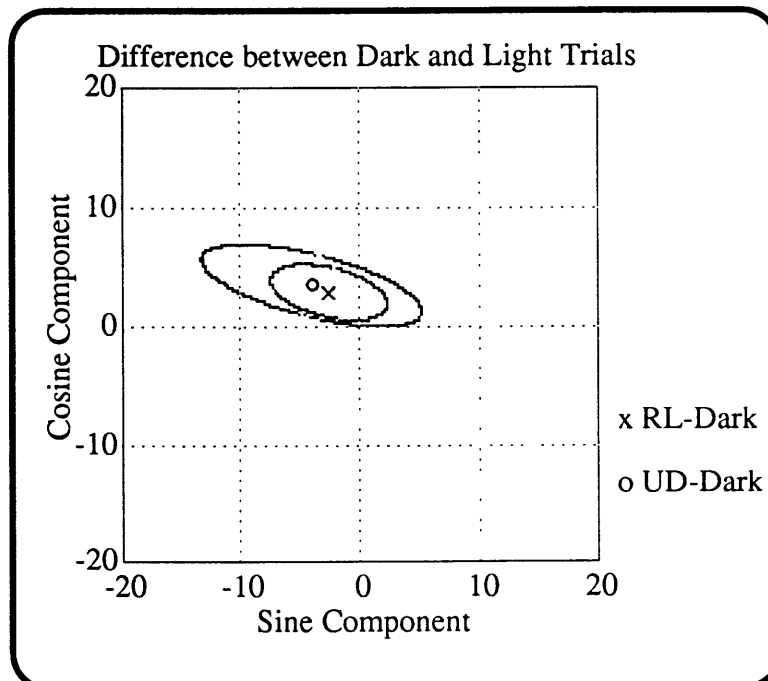
Figure 4.21 **Difference in SPV between Dark and Light Trials**
(95% Confidence Area in °/s)
Difference ellipses are obtained by vector difference of each pair of conditions within
each subject and pooling all results across subjects together. The two ellipses do not
include the origin, indicating that the difference between the light trials and the dark trials
is statistically significant

Sinusoidal Optokinetic Stimulus

To explore how the ocular response is changed by adding a vestibular input to the visual system response, Figs. 4.22 and 4.23 plot the confidence areas for each one of these trials and their differences.

$OK+V$ responses are statistically different from the responses in the purely optokinetic trial OK. Mean amplitude and phases are 54.82°/s and 162.38° in the $OK+V$ case compared to means of 46.35°/s and -178.48° in the OK case. The mean response in the $OK-V$ case (39.45°/s with phase of 168.95°) is not significantly different from the OK responses, but as can be seen, the difference is nearly significant. This suggests that a vestibular stimulus increases the lead of the optokinetic response and that this change is significantly larger when the vestibular input complements the visual input. A complementary stimulus also increases the amplitude of the response while an anticomplementary stimulus may slightly decrease it.

In addition to this, fig. 4.23 also presents the confidence ellipse for the difference between the conditions $OK+V$ and $OK-V$ which indicates that these two responses are significantly different from one another when referenced to the windowshade motion. It is important to remember that the sled stimulation is 180° out of phase during these two conditions.
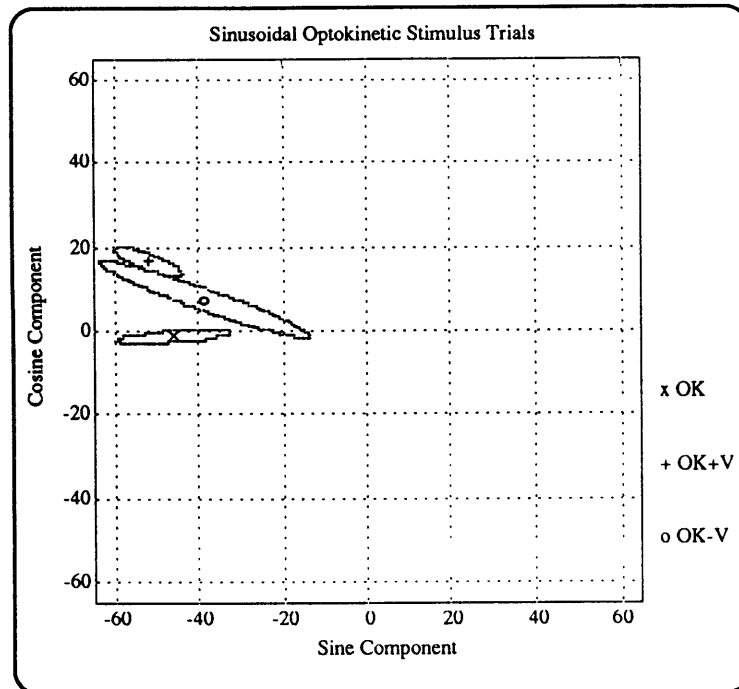
Figure 4.22: **Sinusoidal Optokinetic Stimulus Trials (95% Confidence Areas for SPV Responses in deg/s).** The ellipses for the trials with only optokinetic stimulation (x), complementary visual-vestibular stimuli (+), and anti-complementary visual-vestibular stimuli are shown (o).
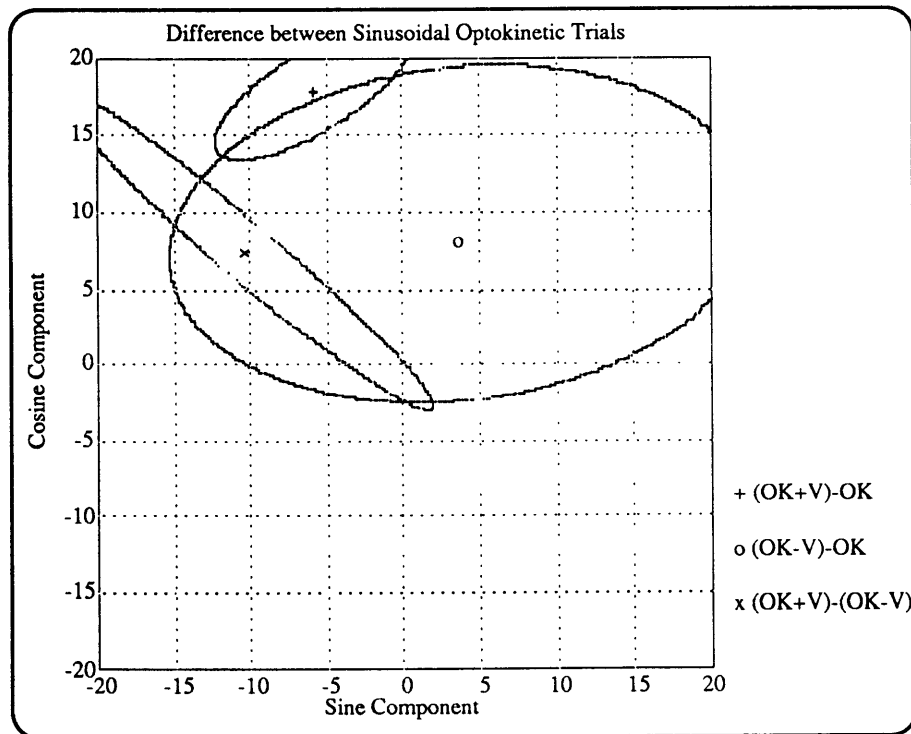
Figure 4.23: **SPV Differences between Sinusoidal Optokinetic Trials (95% Confidence Areas in deg/s).** Differences of Complementary (+) and Anti-Complementary (o) with respect to pure OK. Difference between complementary and anti-complementary trials (x) is also shown.

94

4.1.5.2 Horizontal Eye Movements at the Second Harmonic

To investigate the possibility of significant responses at the second harmonic of the stimulus frequency (0.50 Hz), figure 4.24 shows the confidence area ellipses for responses at that frequency. All responses had small amplitudes and phase differences spread over several quadrants. None of the responses was significantly different from zero (all ellipses enclosed the origin) even after combining equal responses (those whose differences were not significant). Since similar results were found at three and four times the stimulus frequency, this suggests that most horizontal ocular responses occurred almost exclusively at the fundamental frequency.
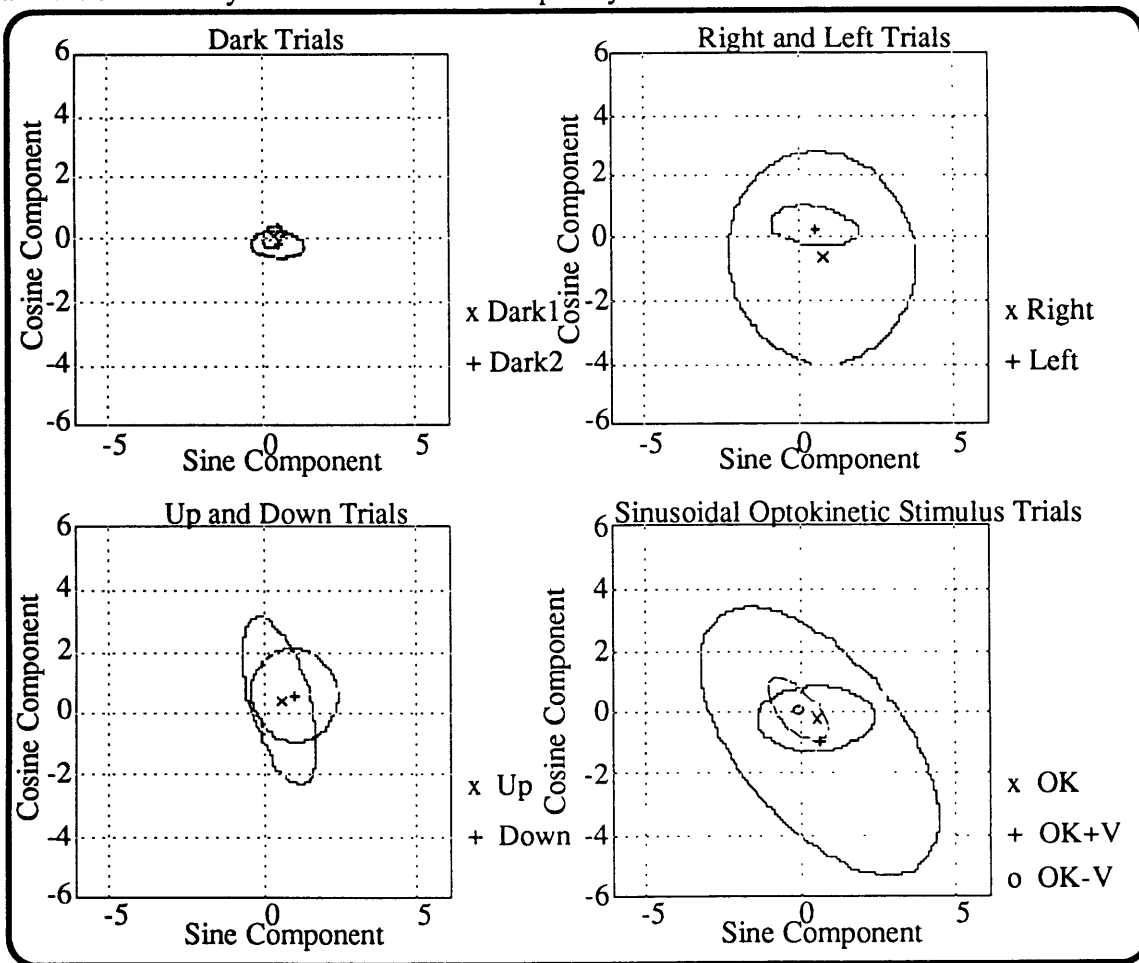
Figure 4.24 95% Confidence Area for Horizontal SPV Responses at the Second Harmonic (deg/s)

In general, responses were not significant and had very small amplitudes. Phases were spread over several quadrants suggesting non-periodical eye movements, all ellipses encircled the origin, therefore the responses were not significantly different from zero.

4.1.5.3 Vertical Eye Movements at the Fundamental Frequency

Vertical responses (fig. 4.25) showed small amplitude oscillations though significant values (at 95%) were found only in the *Dark* and *Right* trials at the fundamental frequency. Combining responses which were not statistically different did not produce other statistically significant conditions, except for the combination of *Dark1* and *Dark2* showed in the figure. The combined dark response had an amplitude of 0.57°/s and a phase lead of 162.11° The other significant response (*Right*), had an amplitude of 1.21°/s and a phase lead of 148.41°. As can be seen from these values, the significant responses were very small but somewhat consistent in phase.

4.1.5.4 Vertical Eye Movements at the Second Harmonic

Responses at the second harmonic were mostly non-significant, with small amplitudes and inconsistent phases. Only the trials *Down* and *OK+V* showed some responses which were on the verge of significance but in both cases their amplitudes were less than 1°/s (0.90°/s of amplitude and 102.38° of phase in *Down*, and 0.62°/s and 135.91° of phase in *OK+V*).

In general, most of the vertical responses were not significantly different from zero. All responses had very small amplitudes and often spread over several quadrants, suggesting that they may be random oscillations and not a consistent oculomotor response.
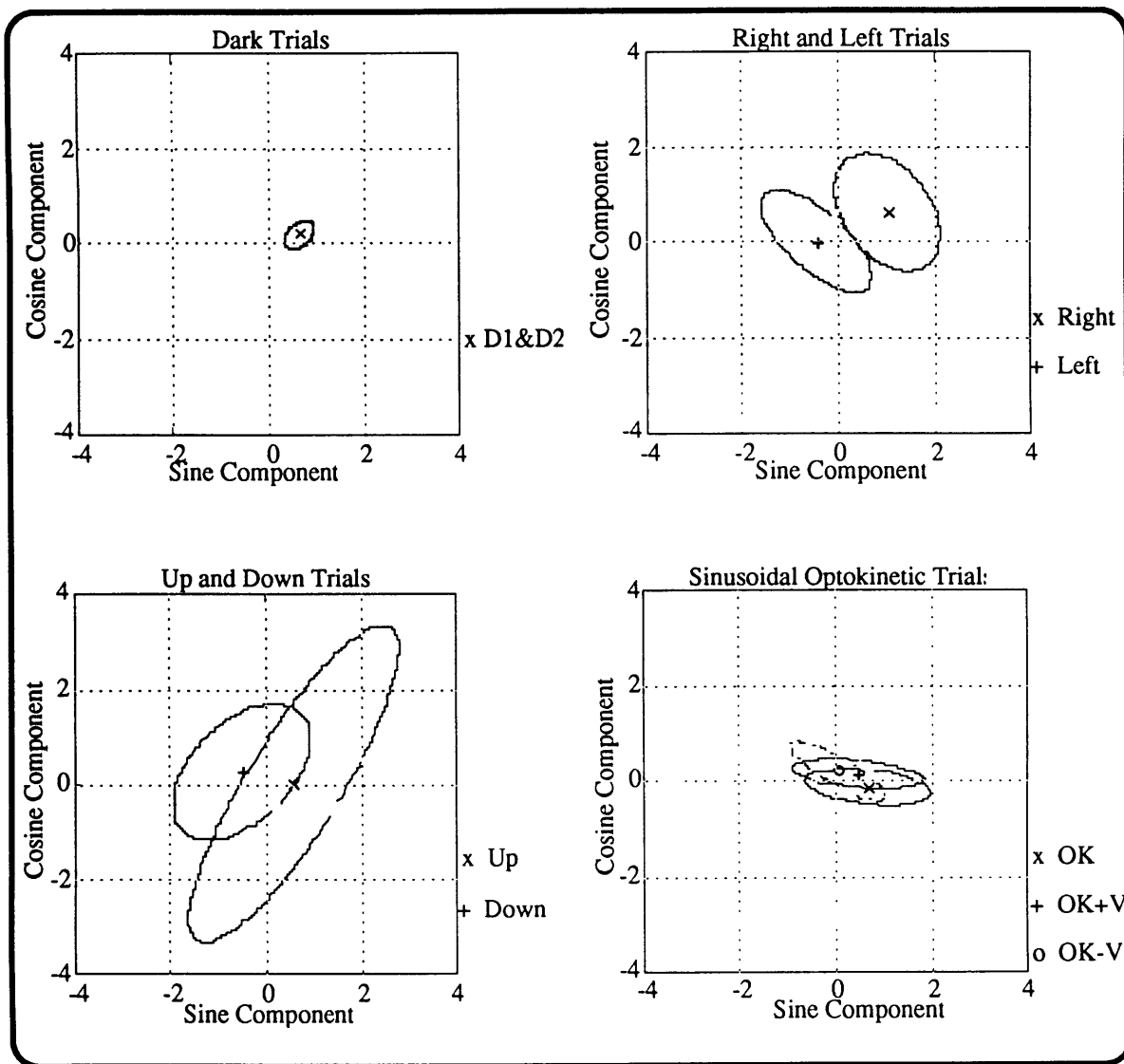
Figure 4.25: **Confidence Interval for Vertical SPV**
Responses at the Fundamental Frequency (°/s)

Most of the responses were not significantly different from zero except for the combination of the dark conditions and *Right*, however, even in those cases, amplitudes were very small.
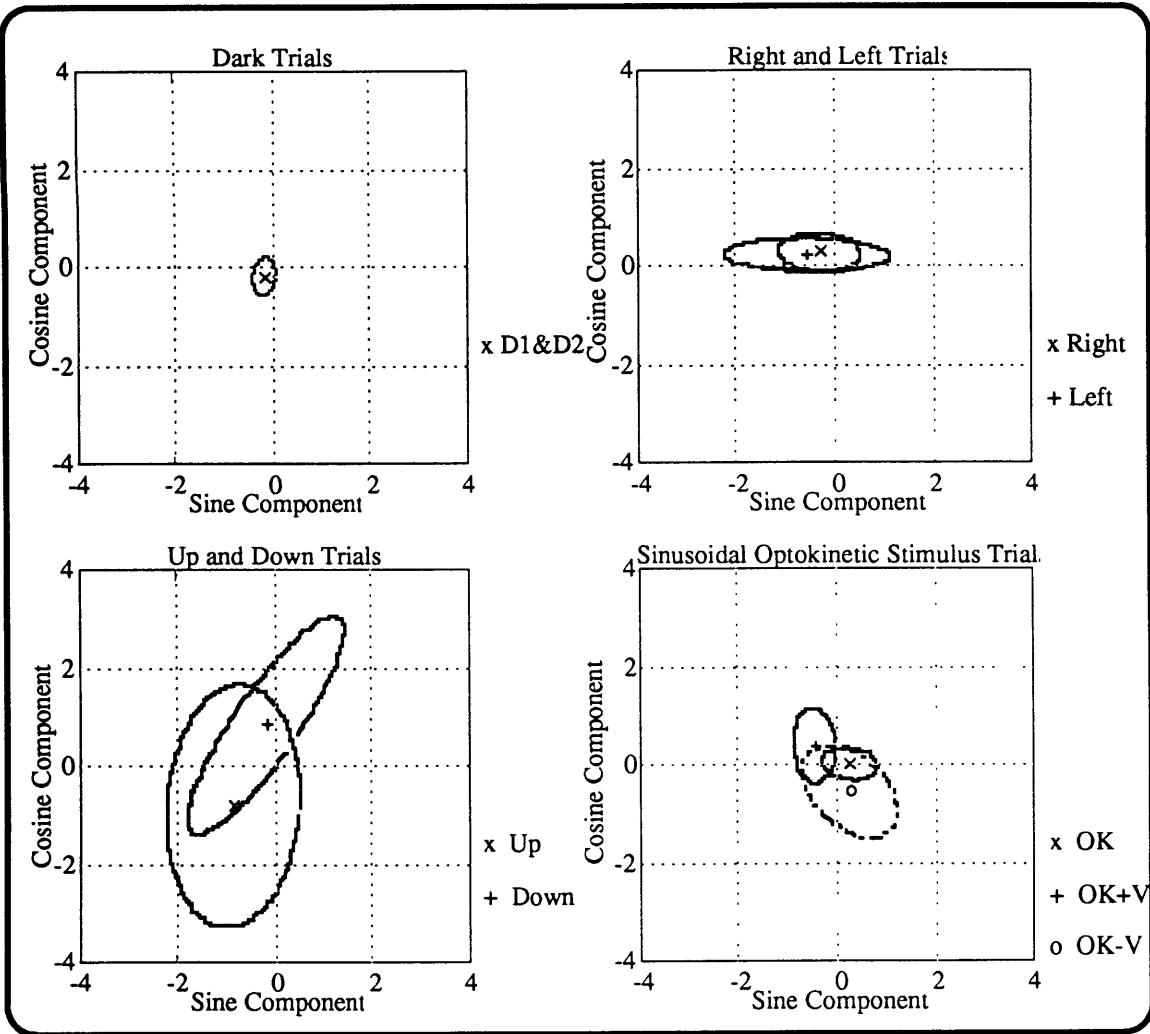
Figure 4.26: **Confidence Interval for Vertical SPV Responses at the <u>Second Harmonic</u> (°/s)**

Most of the responses were not significantly different from zero. Only *OK+V* and *Down* were on the verge of significance, but even in those cases, amplitudes were very small.

4.1.6 Pooled Results: Vergence

Figure 4.27 shows the time course of vergence for Subject E during the dark trials, when the variability was the largest since there was not a specific target that the subject was focusing on. However, even in this case, the vergence remains relatively constant though the presence of blinks can be clearly seen. The observed blinks will act to slightly bias the mean vergence towards convergence, but by no more than approximately 10% as can be seen from the limited number of blinks (upward spikes).
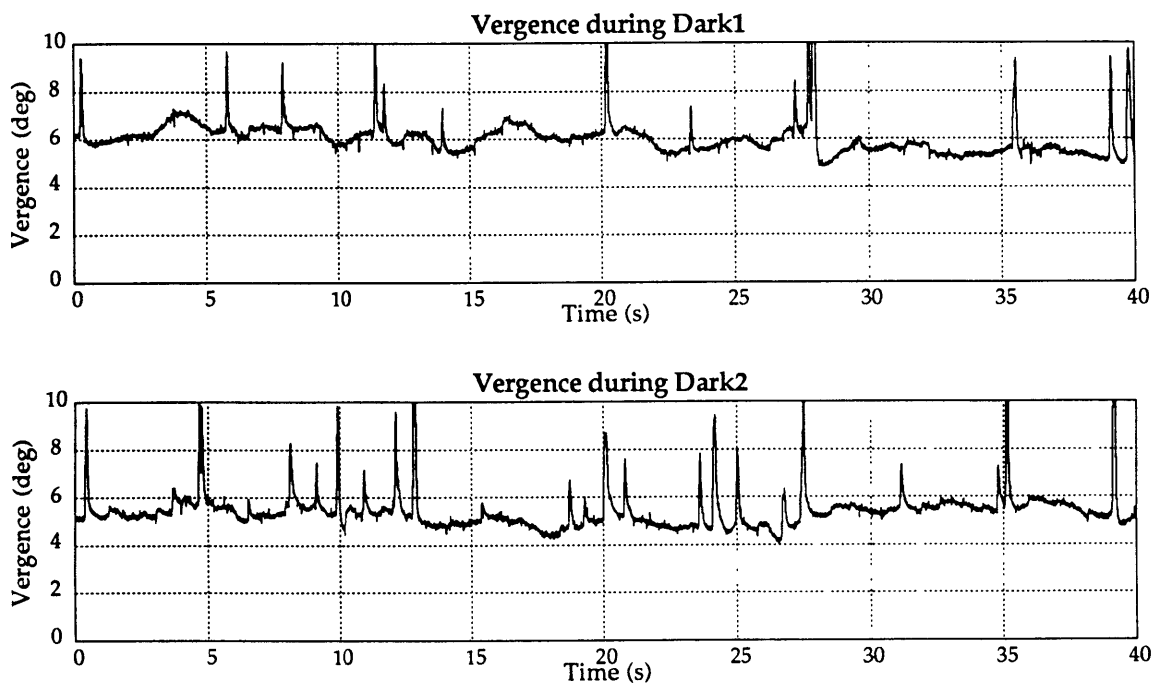
Figure 4.27: Level of Eye Vergence during Dark Trials. Vergence was obtained by substracting right eye position from the left eye position. Positive values indicated convergence, eyes deviated toward the occipitonasal axis.

Figure 4.28 presents the mean values of vergence in each trial for all subjects pooled together. In addition to that, standard error of the means are plotted as well as a line indicating the mean ideal vergence required to focus on the windowshade (5.1°). Though mainly interested in measuring vergence during the dark trials, vergence for all conditions was compared using the paired t-test algorithm provided by Systat 5.2 (Systat,

Inc.,Evanston, IL). No pair of trials showed vergence levels that were statistically different (p<0.05). Table 4.4 shows the p-values for each pair. Unfortunately, the number of subjects run binocularly in each condition varied (N values are listed) and in those cases when paired t-tests were conducted between groups of different size, the number of cases is as small as two. Note that the only cases close to significance, *Dark-Down*, *Dark-Right*, and *Dark-Left*, had a sample size of just two.
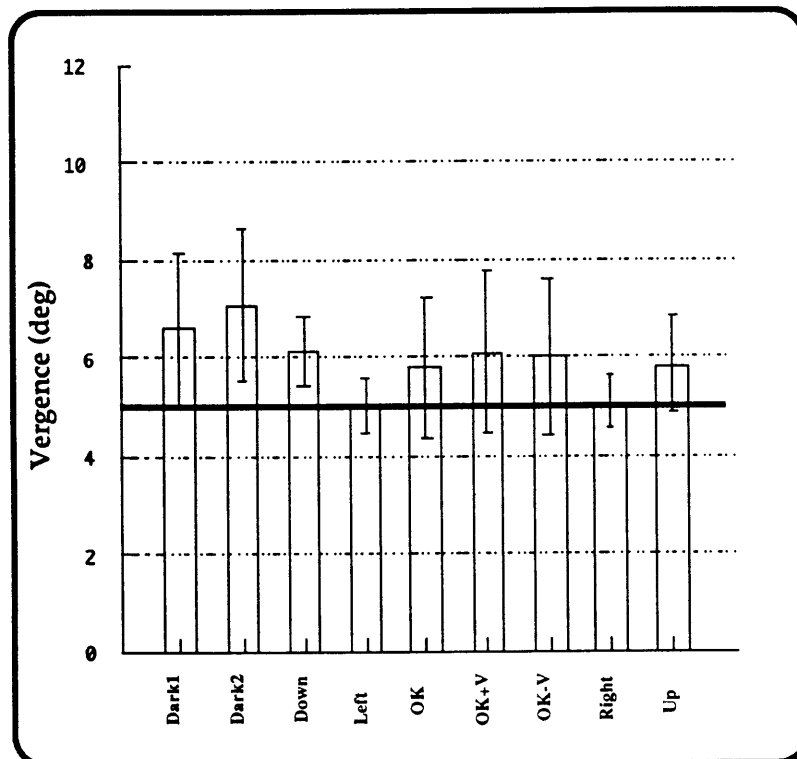
Figure 4.28: Mean Vergence Across Subjects and Comparison with Required Vergence for Focusing on Windowshade

The bars represent mean vergence values after pooling all subjects together, with their respective values of standard error indicated by the vertical lines. The bold horizontal line indicates the mean required vergence (5.1 deg) to focus on the windowshade. Greater vergence is represented by higher values which represent closer targets.

In order to investigate more completely the behavior of vergence in the dark, Table 4.5 shows the values for each subject as well as the average vergence required to focus on the windowshade, which is defined by the distance from the eyes to the windowshade and the interpupillary distance of the subject. The difference between

vergence in *Dark1* and *Dark2* and the required vergence was found not to be statistically different from zero.

Condition	D1	D2	OK	OK+V	OK-V	UP	DOWN	RIGHT	LEFT
Dark1(N=5)		.511	.796	.870	.849	.201	.055	.051	.058
Dark2(N=4)			.734	.829	.802	***	***	***	***
OK(N=5)				.441	.574	.260	.091	.119	.078
OK+V(N=5)					.401	.300	.146	.314	.330
OK-V(N=5)						.330	.164	.421	.463
UP(N=2)							.428	.294	.290
DOWN(N=2)								.086	.093
RIGHT(N=2)									.225
LEFT(N=2)									

Table 4.4: **Statistical p-Values obtained from paired t-test for Mean Vergence difference among trials.** Asterisks (*) are used to indicate that the two conditions were run together only in one subject and therefore t-tests were not performed.

Subject	Req. Verg.	Dark1	Dark2
E	6.740	6.058	5.457
F	4.900	7.402	**********
A	4.290	2.520	5.870
B	4.290	11.750	11.770
D	5.310	5.420	5.340

Table 4.5: Vergence Required to Focus on the Windowshade for each Subject in Dark Trials (degrees). Required vergence for each subject depended on their interpupillary distance and the distance of their eyes to the shade. Asterisks (*) are used to indicate that the condition was not run in that particular subject.

4.1.7 Pooled Results: DC offsets during Constant Velocity OK Stimulation

Table 4.6 and figure 4.29 present the mean DC offset during the eight seconds preceding sled motion (pre) and during sled motion (per) for the horizontal response in *Right* and *Left* combined and for the vertical response in *Up* and *Down* combined. The offsets were combined after using paired t-tests that showed that the two responses were not significantly different. Vestibular stimulation caused the mean DC offset to increase in both cases. The difference in the vertical eye movement DC offset pre and per vestibular stimulation (mean difference of 5.55±3.00°/s) was significant (p<0.001) and was consistent in all six subjects. A similar trend was observed in the offset of the

horizontal movements in *R&L* . However, the significance of this change (4.70±7.35°/s) does not pass the 0.05 confidence though this tendency to increment of the horizontal offset is evident in 4 of 6 subjects.

Condition	Pre (°/s)	Per (°/s)	Mean Change (°/s)	p
RL	34.26±10.49	38.96±9.99	4.70±7.35	0.074
UD	17.08±8.64	22.63±9.10	5.55±3.00	0.001

Table 4.6: **Change in DC offset (mean±sd) between pre and per vestibular stimulation during the *R&L* and *U&D* trials.** The listed p values for the difference were obtained from paired t tests .
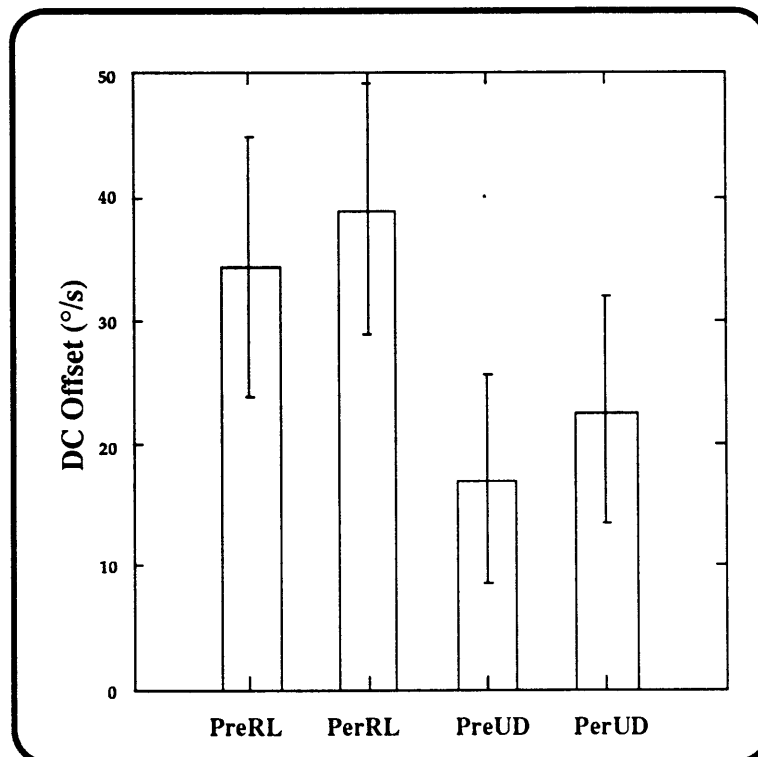
Figure 4.29: **Change in DC offset between pre and per vestibular stimulation during R&L and U&Dtrials in upright.** The small error bars represent the standard deviation of the data.

4.1.8 Pooled Results: General Summary

Tables 4.7 and 4.8 summarize the across subject means found for trials run in the upright condition. In general, horizontal oscillations at the frequency of the sled were found whenever sled motion was present. The addition of a constant velocity optokinetic stimulus increased the magnitude and lag of the response as compared to trials run in the dark. No difference in the oscillation was found which depended on the direction of the constant velocity motion. Sinusoidal optokinetic stimulation which complemented the sled motion (e.g. sled right, windowshade left) increased the amplitude and lead of the eye response as compared to trials without sled motion. On the contrary, anti-complementary visual stimulation kept the response essentially unchanged as compared to the purely visually driven response.

Horizontal oscillations at the second harmonic were not consistent, having irregular phases and small amplitudes. Similar irregularities were observed at the stimulus frequency and twice the stimulus frequency.

These oscillations were superimposed on a relatively constant offset. This DC offset was related to the linear velocity of the visual stimulus, with offsets reaching about 65% of the windowshade constant linear velocity when the stimulus was in the right or left direction. When the stimulus was in the up-down direction, the offset attained approximately 40% of the windowshade velocity. As expected, the offset remained close to zero during runs in the dark and during sinusoidal optokinetic stimulation, since the mean of a sinusoid is zero.

Condition	DC Values		Fundamental Frequency				Vergence		Second Harmonic			
	Ampl	StdDev	Ampl	StdDev	Phase	StdDev	Mean	StdDev	Ampl	StdDev	Phase	StdDev
	(deg/s)	(deg/s)	(deg/s)	(deg/s)	(deg)	(deg)	(deg)	(deg)	(deg/s)	(deg/s)	(deg)	(deg)
Dark1	0.28	0.57	5.08	4.00	155.06	37.75	6.63	3.37	0.35	0.25	26.37	64.26
Dark2	-0.16	0.82	5.08	2.46	152.43	19.74	7.11	3.12	0.47	0.51	-17.14	66.36
D1&D2	0.07	0.71	5.19	3.26	153.84	29.88	6.84	3.06	0.38	0.41	2.50	64.35
OK	0.50	0.91	46.35	12.52	-178.48	1.65	5.83	3.72	0.49	1.33	-25.15	108.58
OK+V	0.58	1.07	54.82	7.90	162.32	1.86	6.10	4.25	0.14	0.78	145.18	125.32
OK-V	0.75	1.81	39.45	11.58	168.95	3.21	6.02	4.14	1.11	2.13	-58.28	126.44
Right	39.82	7.82	8.85	6.16	144.20	23.31	5.08	0.80	0.93	0.99	-40.21	96.26
Left	-39.81	7.76	8.74	5.25	140.90	17.80	5.03	0.77	1.47	1.50	76.40	50.75
R&L	39.81	7.43	8.79	5.46	142.56	20.10	5.05	0.65	0.55	1.19	8.85	86.25
Up	1.63	2.68	13.64	9.90	147.71	14.37	5.87	1.35	0.66	1.05	39.02	80.52
Down	-0.74	4.00	6.45	4.69	136.10	34.85	6.17	1.01	1.15	0.56	32.96	61.05
U&D	0.44	3.47	10.00	8.13	143.99	26.81	6.02	0.99	0.90	0.80	35.17	70.37

Table 4.7: **Mean Responses Across Subjects in Each Condition. Horizontal Eye Movements - Upright Position.** Values were obtained from all six subjects run in this condition. Shaded responses were significant at the 0.05 level. Phase differences are with respect to sled velocity except for trials OK, OK+V, and OK-V where the phase difference with respect to shade velocity is presented.

Condition	DC Values		Fundamental Frequency				First Harmonic Sinusoid			
	Ampl	StdDev	Ampl	StdDev	Phase	StdDev	Ampl	StdDev	Phase	StdDev
	(deg/s)	(deg/s)	(deg/s)	(deg/s)	(deg)	(deg)	(deg/s)	(deg/s)	(deg)	(deg)
Dark1	-0.47	1.36	0.68	0.44	21.15	40.88	0.22	0.18	176.52	145.33
Dark2	-0.20	1.97	0.48	0.53	14.88	68.00	0.46	0.61	-106.01	101.94
OK	-0.54	0.91	0.68	0.59	-10.56	87.80	0.24	0.24	12.87	99.92
OK+V	-0.68	0.75	0.48	0.81	17.22	109.84	0.62	0.49	135.91	126.07
OK-V	-0.19	0.94	0.21	0.36	83.88	68.36	0.57	0.39	-60.79	83.66
Right	-0.78	2.34	1.21	0.60	31.59	47.76	0.48	0.39	133.68	119.54
Left	-0.59	2.13	0.45	0.65	176.87	129.00	0.66	0.76	153.34	68.17
Up	24.03	9.89	0.60	0.99	1.23	83.02	1.16	0.87	-138.56	124.07
Down	-23.06	9.09	0.58	0.90	150.90	120.29	0.90	0.85	102.38	115.11

Table 4.8 **Mean Responses Across Subjects in Each Condition. Vertical Eye Movements - Upright Position.** Values were obtained from all six subjects run in this condition. Shaded responses were significant at the 0.05 level. Phase differences are with respect to sled velocity except for trials OK, OK+V, and OK-V where the phase difference with respect to shade velocity is presented.

4.2 Supine Condition

A total of seven subjects were run in this condition and all them were tested through the entire protocol within the same session, except for subjects D and E who were not tested in the *Up* and *Down* conditions due to the thirty minute test duration constraint. Vergence measurements were taken only from subject C. In similar fashion to section 4.1, results from a representative subject (Subject C) will be presented followed by results pooled together from all seven subjects. Tables presenting individual information for the rest of the subjects are included in appendix A.

4.2.1 Individual Subject Results

Plots of SPV vs time in the supine position were for the most part qualitatively similar to those presented in Figures 4.1-4.9 for the upright condition. Figure 4.30 shows an example of the response in the dark (in *Dark2*) for subject C in the supine position. Note that the amplitude (2.64°/s) is substantially smaller than the equivalent data shown in Figure 4.2 for a subject in the upright position and that the lead in the response is also greater (36.26°±16.86°).

4.2.1.1 Horizontal Responses

4.2.1.1.1 Responses at the Fundamental Frequency

Figures 4.31 and 4.32 display the polar location (amplitude and phase) of the cycle-by-cycle SPV responses at the fundamental frequency as well as the mean resultant obtained from these single measurements.

In general, the magnitudes of these responses were similar to upright, except for responses in the dark which showed a smaller value. Responses also tended to have a larger lead supine.

105
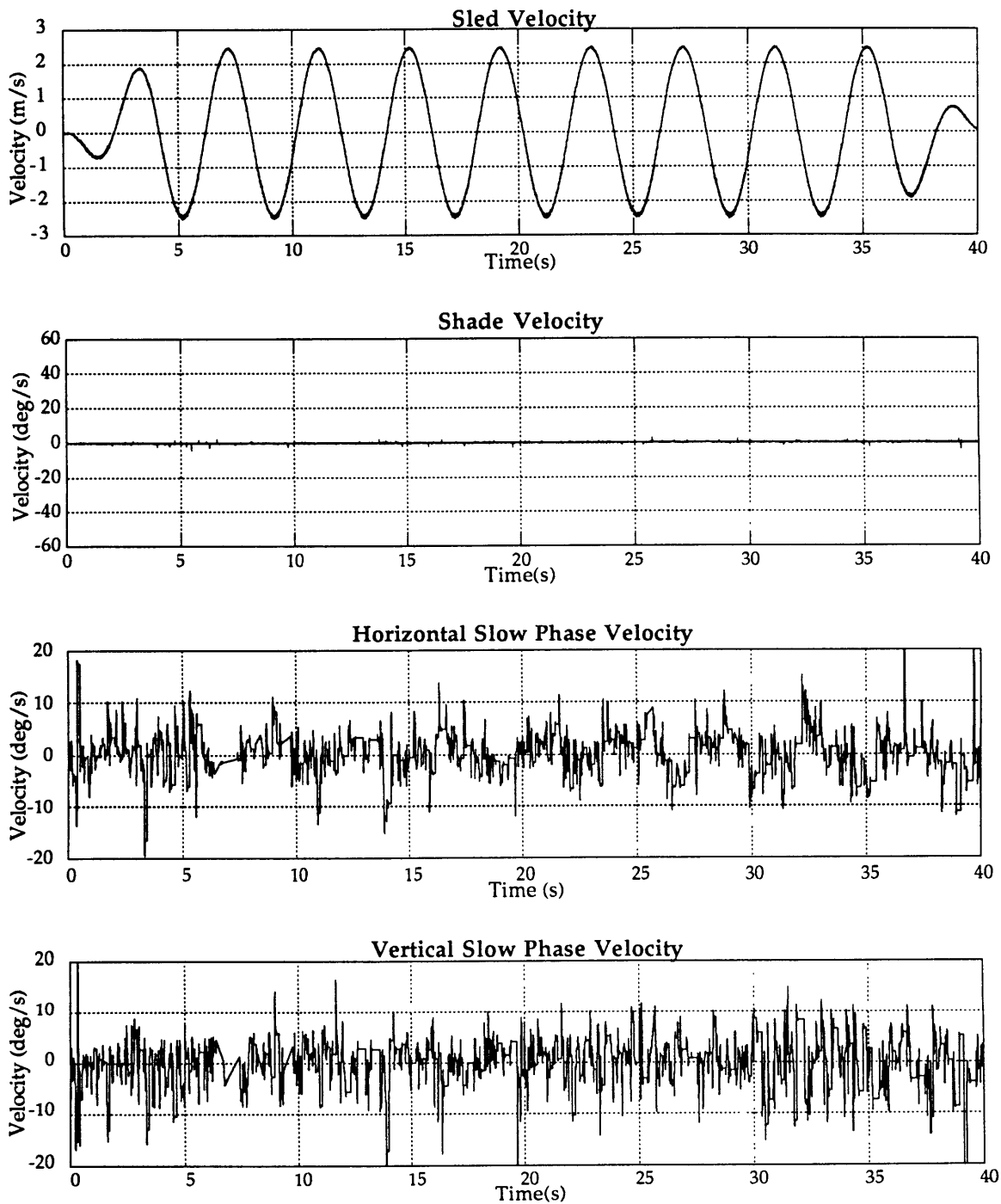
Figure 4.30: Results from trial *Dark2*-Supine in Subject C. Note that the windowshade was not active in this trial. Subjects were instructed to relax and keep their eyes open while undergoing sinusoidal acceleration in completed darkness. Horizontal eye oscillations at the stimulus frequency had a mean amplitude of 2.64 °/s, mean phase of 143.74° and a mean DC offset of 0.36°/s, while consistent vertical responses were not observed. These results can be compared with Figure 4.1 showing results in the dark for a subject in the upright position.

106
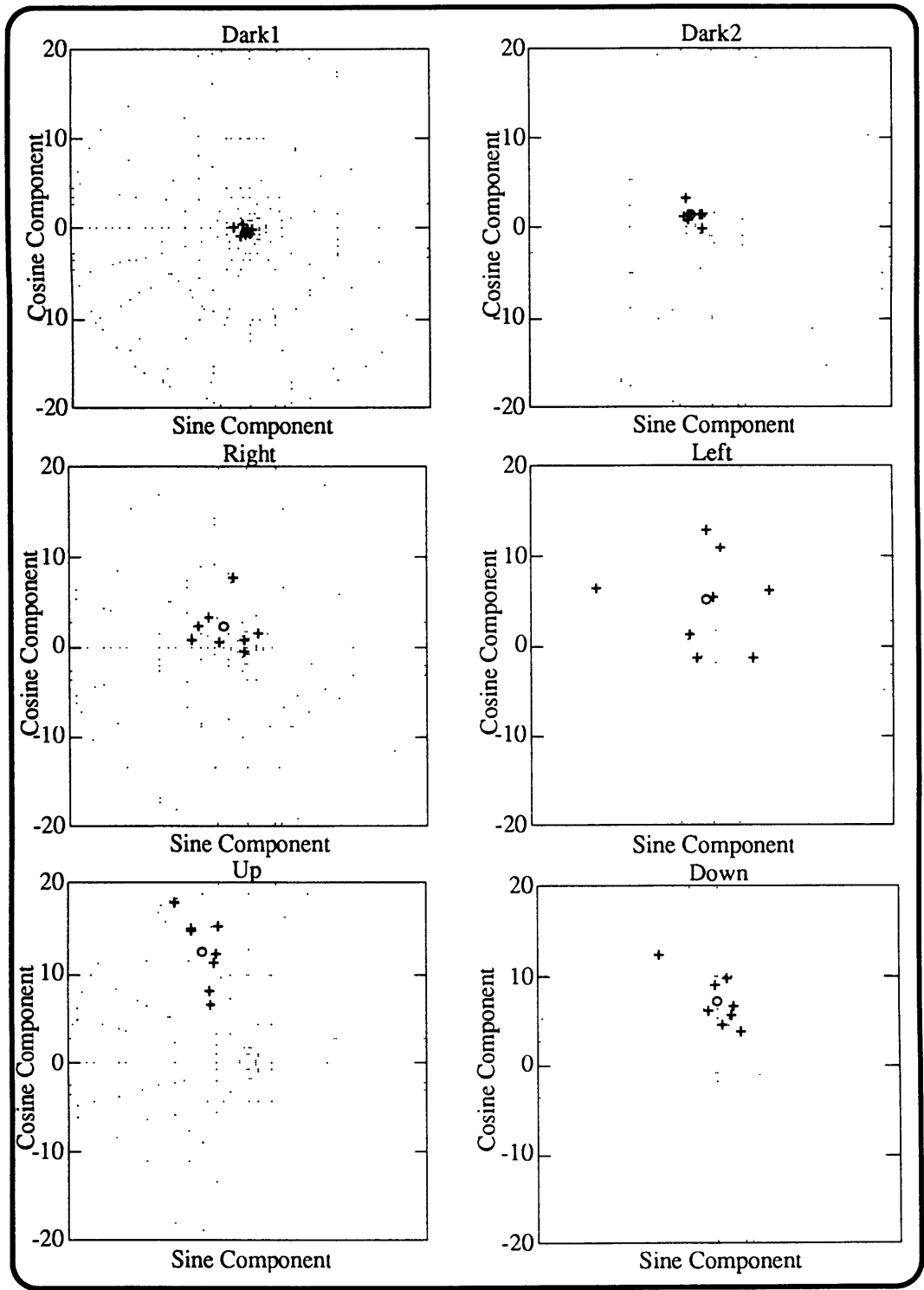
Figure 4.31: Polar Plots trials *Dark1, Dark2, Right, Left, Up,* and *Down.* Amplitude and phase (with respect to sled velocity) of Horizontal SPV responses (+) in deg/s at the fundamental frequency are shown. The mean response (o) calculated from the vector average of the individual cycles is also shown. Note the very small amplitude of the dark responses as opposed to those in the light and the larger variability of the trials producing horizontal OKN as opposed to those eliciting vertical OKN.
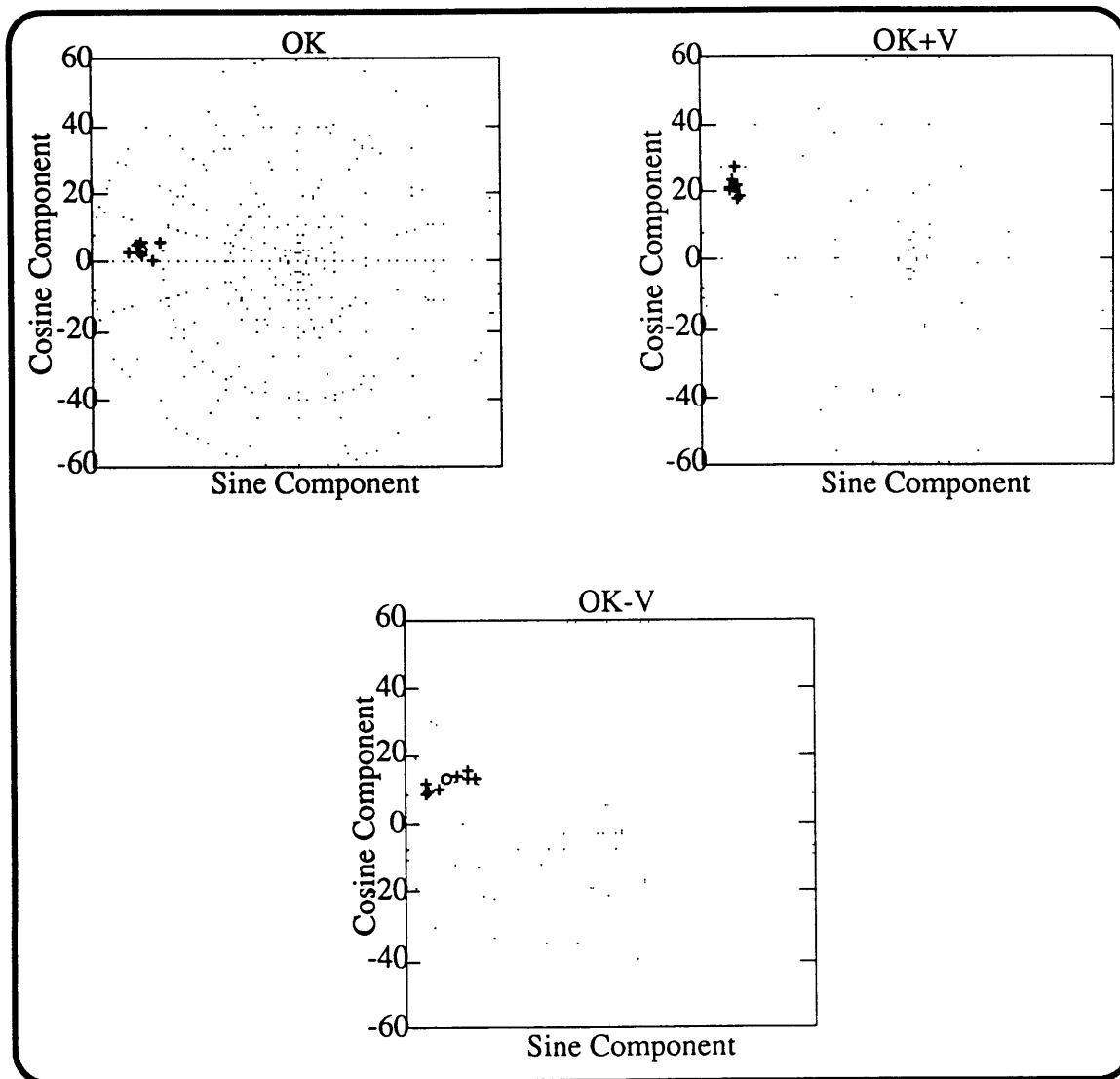
Figure 4.32: Polar Plots trials *OK, OK+V*, and *OK-V*. Amplitude and phase (with respect to windowshade velocity) of Horizontal SPV responses (+) in deg/s at the fundamental frequency are shown. The mean response (o) calculated from the vector average of the individual cycles is also shown. Note the similarity of the pattern with the responses in the upright position for subject E (fig. 4.11).

- Dark1 and Dark2

Both *Dark1* (0.74°/s±0.61°/s) and *Dark2* (2.64°/s±1.04°/s) had very small amplitudes with small leads which increased in the *Dark2* condition (leads were on the order of 30°-40° for most cycles, however two lagging cycles pushed the mean to a lag of 6.22°±57.20° in *Dark1*, while the more consistent cycles of *Dark2* had a resultant mean

108

lead of 36.26°±16.86°). The fact that responses in the dark were small (smaller than in the upright position) was consistent across all subjects.

- Right, Left, Up, and Down

Responses in the light during constant velocity optokinetic stimulation were higher than in the dark. Variability between cycles was higher in trials eliciting horizontal OKN (*Right* and *Left*) with phases distributed over more than one quadrant and magnitudes ranging from 3 to 6 deg/s. This variability is reflected in the large standard deviations in phase. The mean response in *Right* had an amplitude of 3.43°/s±2.70°/s and a phase lead of 39.41°±52.30°. The mean response in *Left* had an amplitude of 5.20°/s±5.44°/s and a phase lead of 80.83°±95.08°.

Oscillations during the *Up* and *Down* trials were substantially more consistent and with amplitudes twice as high as in the *Right* and *Left* cases. The mean amplitude in *Up* was 7.32°/s±2.96°/s and in *Down* was 13.63°/s±4.02°/s. Variability in phase from cycle to cycle was very small, *Up* had a mean lead of 88.31°±18.36° and *Down* had a mean lead of 68.05°±6.87°. Note the large increase in the lead of this response compared to the upright trials.

- OK, OK+V, and OK-V

Responses in the three sinusoidal optokinetic stimulation cases followed the same pattern observed in the upright cases. The *OK+V* responses (mean amplitude of 55.17°/s±1.60°/s and mean phase lead of 23.35°±2.68°) showed higher amplitude and leads with respect to the *OK* case (mean amplitude of 45.90°/s±2.96°/s and mean phase lead of 4.81°±2.60°) while the *OK-V* responses (mean amplitude of 49.21°/s±5.47°/s and lead of 14.20°±4.44°) showed similar effects when compared to *OK* but with smaller increases in amplitude and phase lead.

4.2.1.1.2 Responses at the Second Harmonic

Figures 4.33 and 4.34 show the polar plots of the responses at the second harmonic. In general, amplitudes were again small (less than 2°/s) and the phase

differences were not consistent (observed variations were on the order of 120 degrees within each trial).
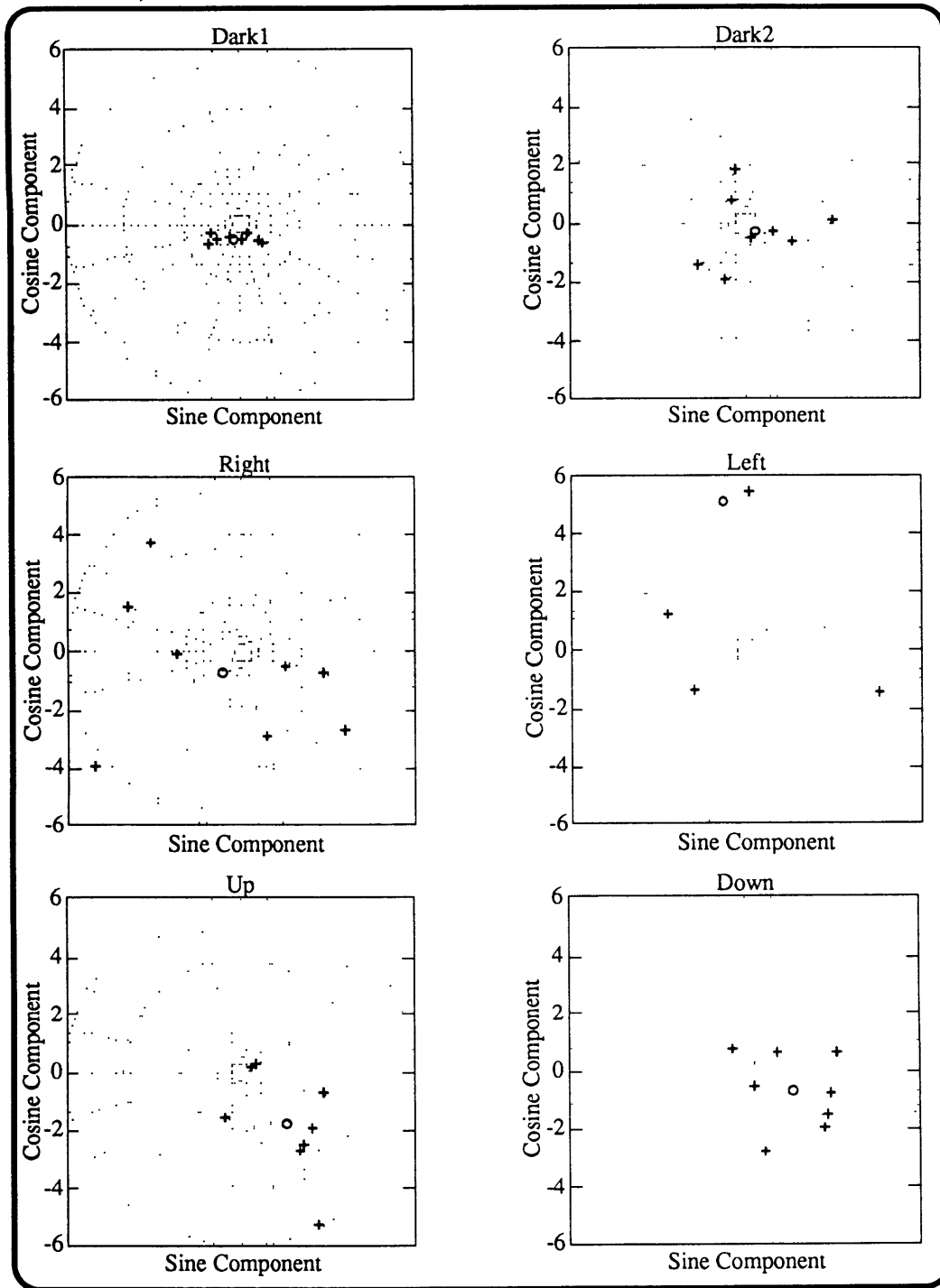
Figure 4.33: Polar Plots trials *Dark1, Dark2, Right, Left, Up,* and *Down.* Amplitude and phase (with respect to sled velocity) of Horizontal SPV responses (+) in deg/s at the second harmonic are shown. The mean response (o) calculated from the vector average of the individual cycles is also shown Amplitudes were in general small (less than 4°/s), and showed large variations in phase (standard deviations of more than 100°).
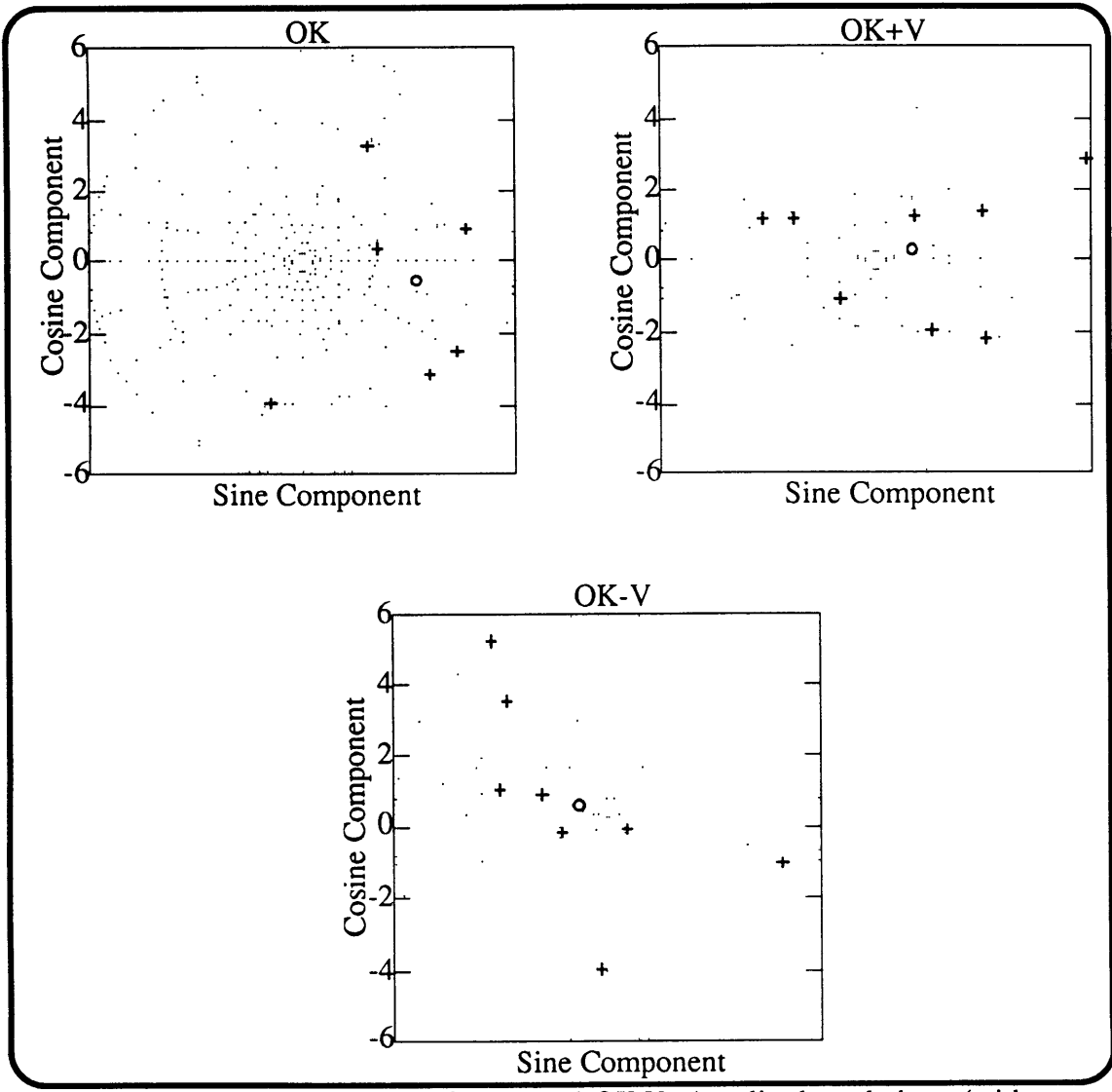
Figure 4.34 Polar Plots trials *OK, OK+V*, and *OK-V*. Amplitude and phase (with respect to sled velocity) of Horizontal SPV responses (+) in deg/s at the fundamental frequency are shown. The mean response (o) calculated from the vector average of the individual cycles is also shown. Amplitudes were in general small (most responses below 4°/s), and showed large variations in phase (standard deviations of more than 120°).

4.2.1.2 Vertical Responses

4.2.1.2.1 Responses at the Fundamental Frequency

Figures 4.35 and 4.36 display the polar location (amplitude and phase) of the cycle-by-cycle vertical SPV responses at the stimulus frequency as well as the mean resultant obtained from these single measurements. Very large variability in phases can be seen in almost all trials (standard deviations were in most cases above 100°), with some consistency seen only in the *Up* and *OK-V* (which respectively had mean phase differences of -97.99° and 174.44°). The mean amplitude of the responses were below 2°/s in all cases.

4.2.1.2.2 Responses at the Second Harmonic

In general all responses (Figs. 4.36 and 4.37) have very small amplitudes (less than 1°/s) and phases spread over several quadrants. This suggest that second harmonic vertical responses are not significant and may be the product of random eye oscillations and measurement noise.
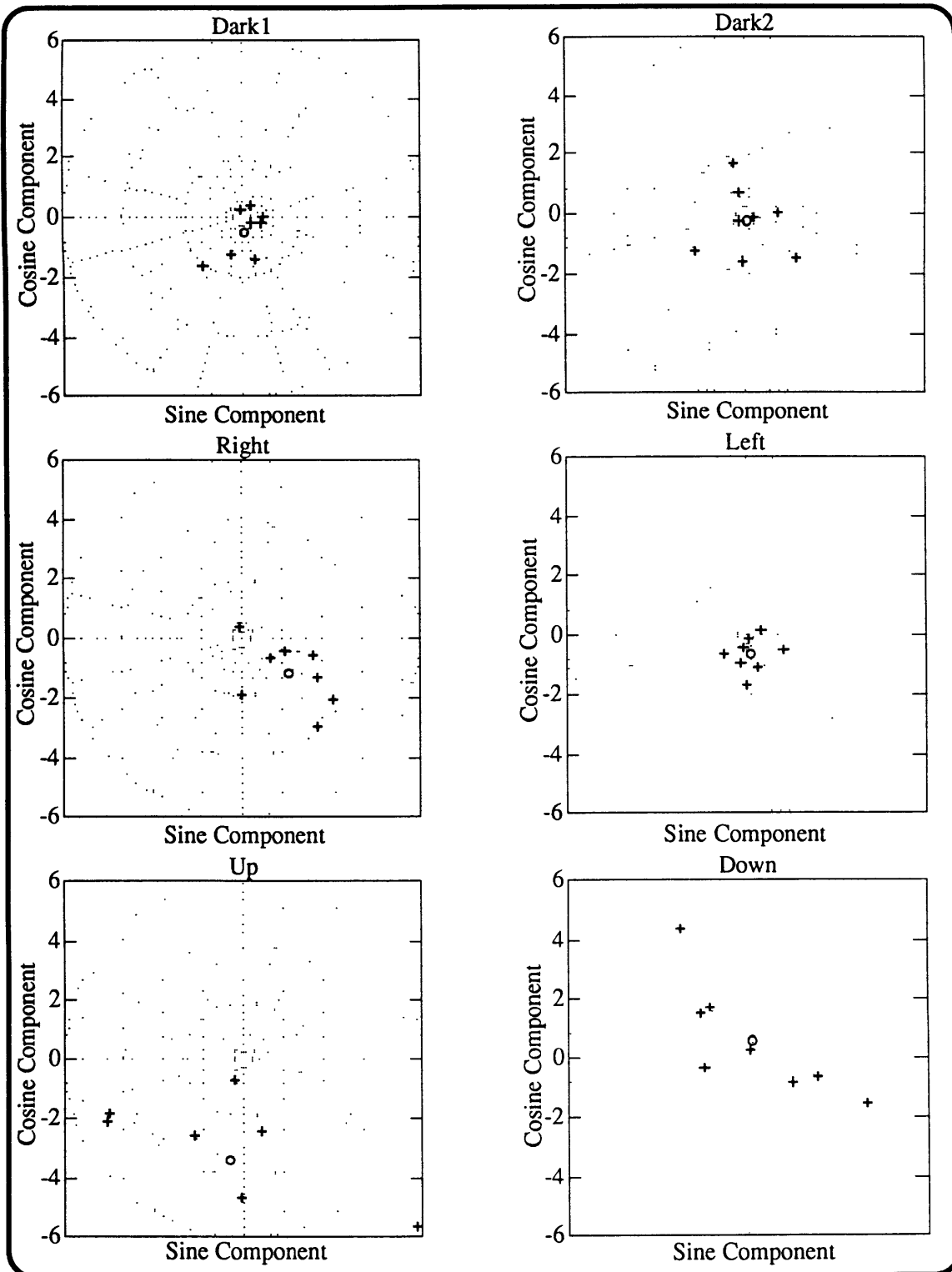
Figure 4.35: Polar Plots trials *Dark1, Dark2, Right, Left, Up*, and *Down*. Amplitude and phase (with respect to sled velocity) of vertical SPV responses (+) in deg/s at the fundamental frequency are shown. The mean response (o) calculated from the vector average of the individual cycles is also shown. Only *Right* seems to show some consistency, but in general, amplitudes are small and phases inconsistent.
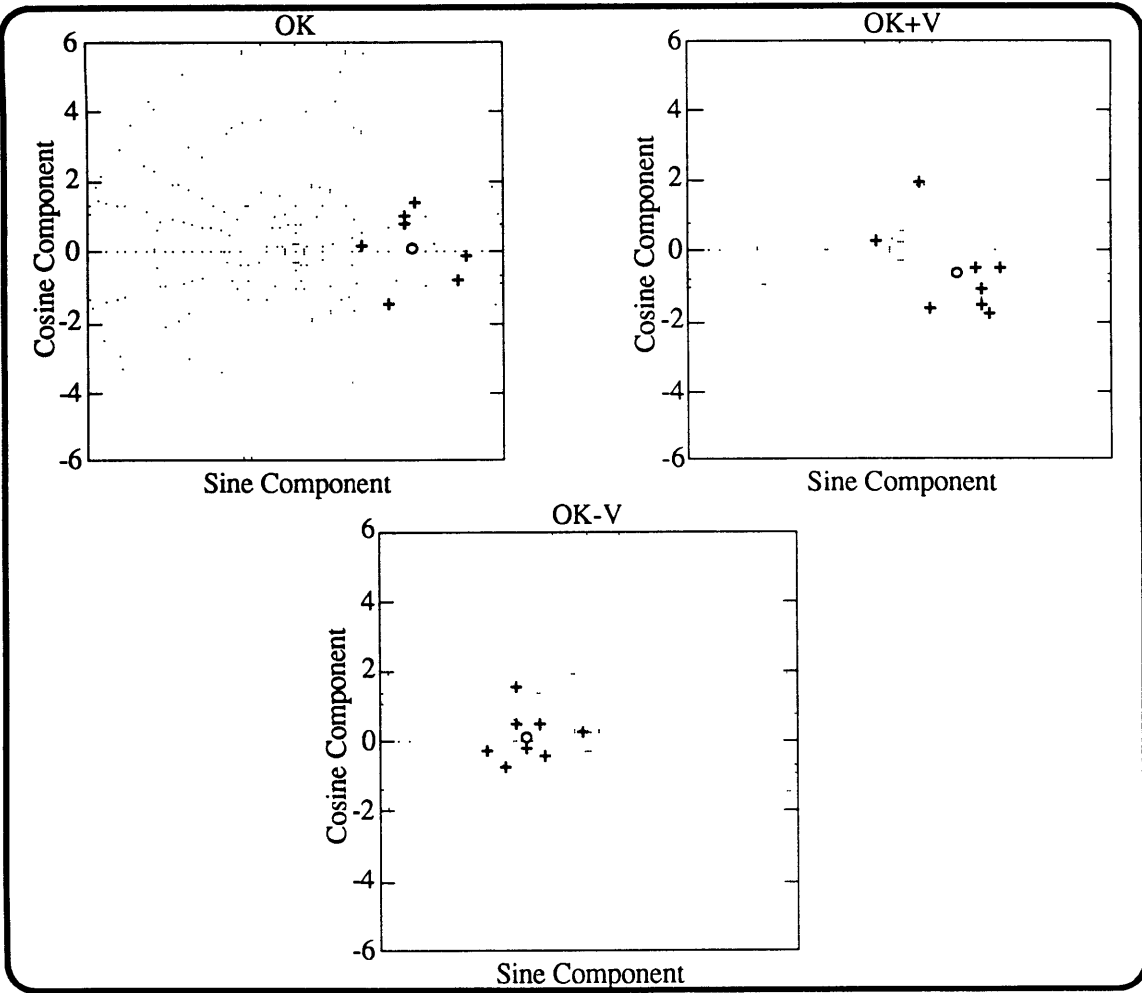
113

Figure 4.36: Polar Plots trials *OK, OK+V,* and *OK-V.* Amplitude and phase (with respect to sled velocity) of vertical SPV responses (+) in deg/s at the fundamental frequency are shown. The mean response (o) calculated from the vector average of the individual cycles is also shown. The small oscillations show some degree of consistency in phase but they have small amplitudes
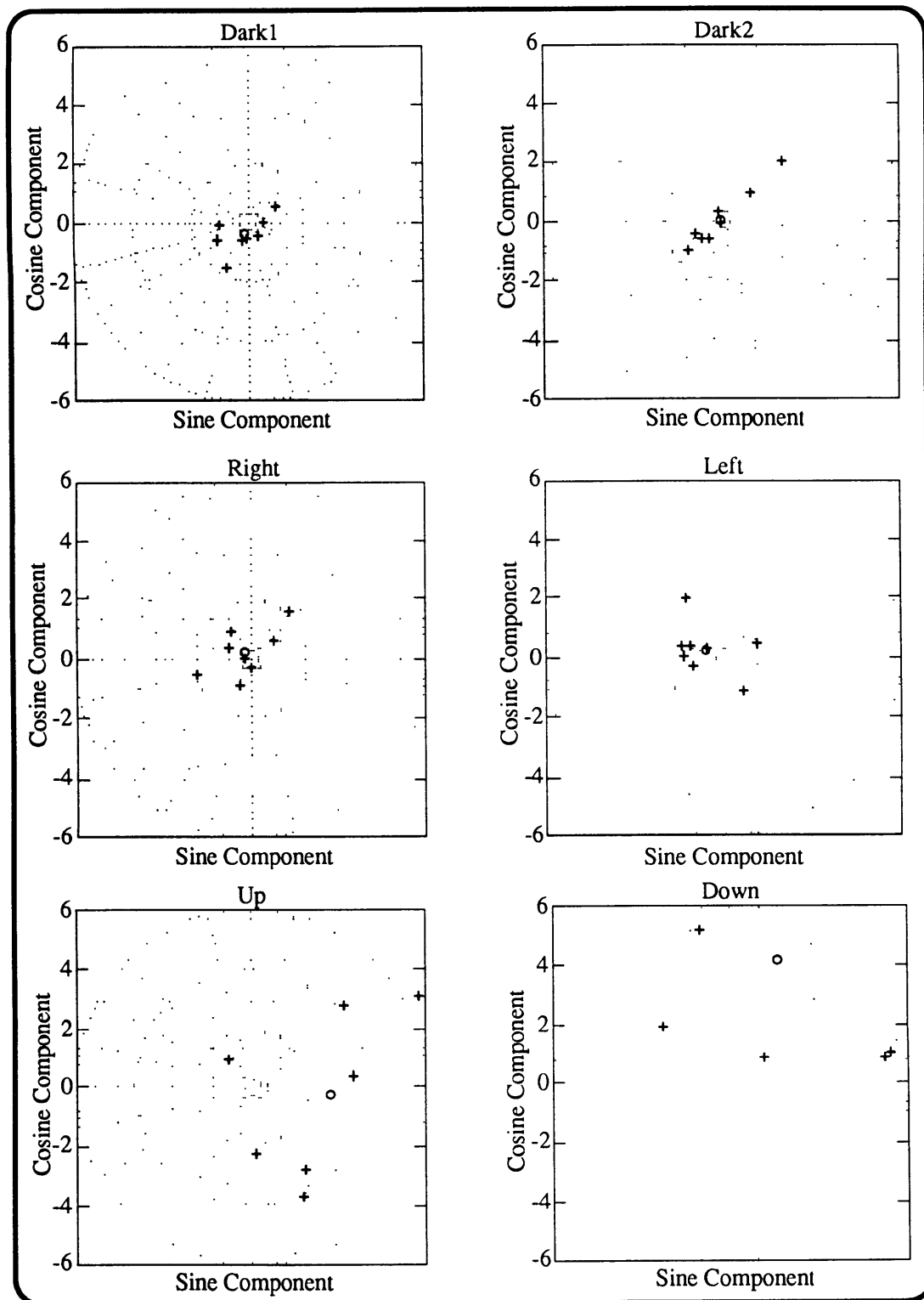
Figure 4.36: Polar Plots trials *Dark1*, *Dark2*, *Right*, *Left*, *Up*, and *Down*. Amplitude and phase (with respect to sled velocity) of vertical SPV responses (+) in deg/s at the second harmonic are shown. The mean response (o) calculated from the vector average of the individual cycles is also shown. Responses do not show a defined pattern in each trial.
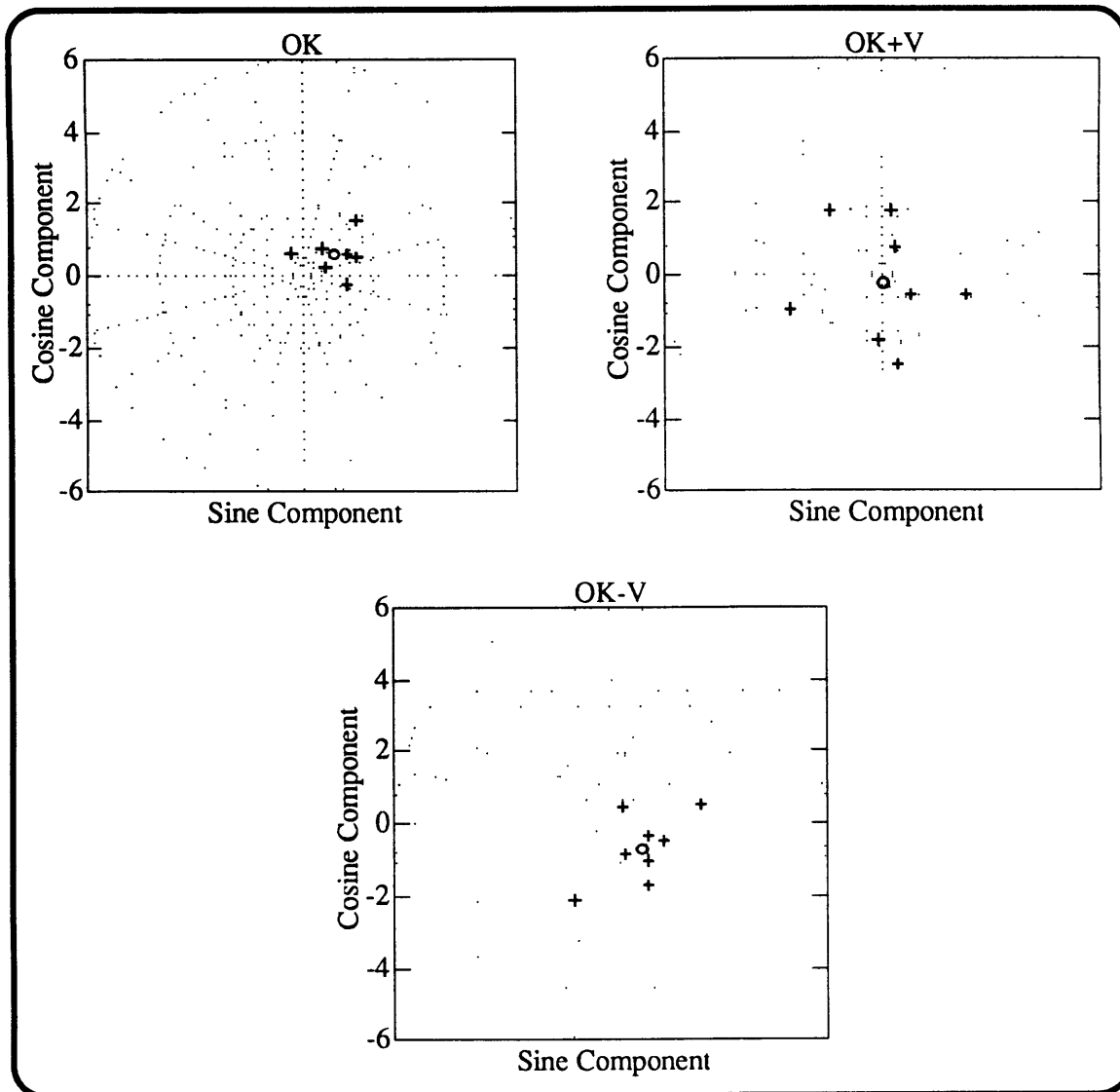
Figure 4.37 Polar Plots trials *OK, OK+V*, and *OK-V*. Amplitude and phase (with respect to sled velocity) of vertical SPV responses (+) in deg/s at the second harmonic are shown. The mean response (o) calculated from the vector average of the individual cycles is also shown. Responses were spread over more than one quadrant, reflecting their lack of consistency.

4.2.1.3 Vergence

Vergence values ranged from 6.1° in the Left trial, to 8.3° in Dark2. This behavior is consistent with the variation in vergence in the pooled result for the upright condition in which the dark trials had slightly greater (not significantly different from the others) vergence than the other trials. Since this is the only measurement of vergence observed in this orientation, no statistical analysis was performed, however the values for Subject C are similar to the pooled vergence values for the subjects in the upright position.

4.2.1.4 General Summary

Tables 4.9 and 4.10 summarize the measured responses for subject C in the supine position. In general horizontal responses at the fundamental frequency of the sled stimuls were observed with very small amplitudes in the dark. These amplitudes increased in the presence of a constant velocity optokinetic stimulus. During sinusoidal optokinetic trials, vestibular stimulation increased the amplitude and phase lead of the response when compared to the purely visual stimulation case.

Clearly defined responses were not consistently found for horizontal responses at the second harmonic or vertical responses at either the fundamental frequency or the second harmonic.

Condition	DC Values		Fundamental Frequency				Vergence		Second Harmonic			
	Ampl (deg/s)	StdDev (deg/s)	Ampl (deg/s)	StdDev (deg/s)	Phase (deg)	StdDev (deg)	Mean (deg)	StdDev (deg)	Ampl (deg/s)	StdDev (deg/s)	Phase (deg)	StdDev (deg)
Dark1	0.42	0.53	0.74	0.61	-173.78	57.20	7.58	0.65	0.51	0.36	-119.01	54.14
Dark2	0.37	0.38	2.64	1.04	143.74	16.86	8.40	0.80	0.40	1.26	-36.04	123.63
OK	0.70	2.41	45.90	2.96	175.19	2.60	6.42	0.50	3.20	2.30	-9.94	151.76
OK+V	0.07	1.74	55.15	1.60	156.65	2.68	6.40	0.56	1.06	2.97	20.26	120.33
OK-V	0.72	2.20	49.21	5.47	165.80	4.44	6.39	0.56	1.12	3.43	-39.48	125.55
Right	34.39	2.58	3.43	2.70	140.59	52.30	6.15	0.64	1.00	2.55	-138.33	87.08
Left	-21.65	6.30	5.20	5.44	99.17	95.08	6.61	0.70	1.21	3.05	-139.49	91.65
Up	-3.54	2.15	7.32	2.96	91.69	18.36	8.06	0.64	1.76	1.47	-21.68	140.25
Down	-0.93	1.81	13.63	4.02	111.95	6.87	8.23	0.70	2.31	1.94	-48.52	128.52

Table 4.9: Mean resultant amplitude and phase of horizontal responses for subject C - supine. Phase differences are with respect to sled velocity except for trials OK, OK+V, and OK-V where the phase difference with respect to shade velocity is presented.

Condition	DC Values		Fundamental Frequency				Second Harmonic			
	Ampl (deg/s)	StdDev (deg/s)	Ampl (deg/s)	StdDev (deg/s)	Phase (deg)	StdDev (deg)	Ampl (deg/s)	StdDev (deg/s)	Phase (deg)	StdDev (deg)
Dark1	-0.15	0.84	0.45	0.75	-83.73	129.73	0.40	0.81	-122.33	107.08
Dark2	0.33	0.54	0.22	1.13	-79.95	118.66	0.12	0.19	129.31	82.93
OK	0.56	0.46	3.38	1.04	2.95	177.41	1.06	0.65	35.63	118.97
OK+V	1.13	1.14	1.70	1.42	-19.77	103.02	0.22	1.58	-92.26	109.16
OK-V	1.96	0.73	1.78	0.82	174.44	26.27	1.09	0.64	-37.18	130.70
Right	0.30	1.05	1.94	1.41	-36.20	80.58	0.37	0.59	135.34	83.16
Left	2.68	0.60	0.63	0.57	-78.37	100.10	0.75	1.09	156.44	75.54
Up	29.27	2.74	3.36	1.87	-98.00	39.82	2.69	2.39	-4.93	142.43
Down	-26.00	3.40	0.61	1.45	75.45	112.76	4.45	2.95	69.42	45.62

Table 4.10: Mean resultant amplitude and phase of vertical responses for subject C - supine. Phase differences are with respect to sled velocity except for trials OK, OK+V, and OK-V where the phase difference with respect to shade velocity is presented.

4.2.2 Pooled Results: Sample Size

As was done in the upright position, a mean response vector for each subject was obtained from the seven cycles analyzed in each trial, and then an overall mean was obtained by determining the vector average across subjects for each condition. In all conditions, the number of samples is seven, except for *Up* and *Down* which have five samples (two subjects were not run in this condition). When two conditions are combined, as for *Dark1* and *Dark2*, N doubles to 14.

4.2.3 Pooled Results: Confidence Area Plots

4.2.3.1 Horizontal Eye Movements at the Fundamental Frequency

The left column in Figure 4.38 shows the 95% confidence areas for the horizontal SPV responses, and the right column shows the difference between each pair of related conditions. Those pairs that are not statistically different are combined in Figure 4.39.

- Dark and Constant Velocity Optokinetic Stimulus

Responses in the absence of optokinetic stimulus (*Dark1* and *Dark2*) were very small and not statistically significant as shown in Fig. 4.38. The difference between the two of them was not significant, but once combined, a significant response is obtained (Fig. 4.39) with an amplitude of just $1.25°/s \pm 1.15°/s$ and a phase lead of $54.4° \pm 77.19°$.

Responses in the light during constant velocity optokinetic stimulation in general showed a larger amplitude ($6°/s$ to $8°/s$) and phase differences ranging from $95°$ to $145°$. Responses in *Right* had a mean amplitude of $6.66°/s \pm 7.08°/s$ and phase lead of $33.17°$. The mean response in *Left* was similar, having an amplitude of $7.63°/s \pm 6.80°/s$ and phase lead of $53.62° \pm 70.54°$. Since the difference between *Right* and *Left* was not significant, the conditions were combined under the name $R\&L$ in Figure 4.39. The resultant response has an amplitude of $7.03°/s \pm 7.14°/s$ and a phase lead of $44.10° \pm 55.89°$.
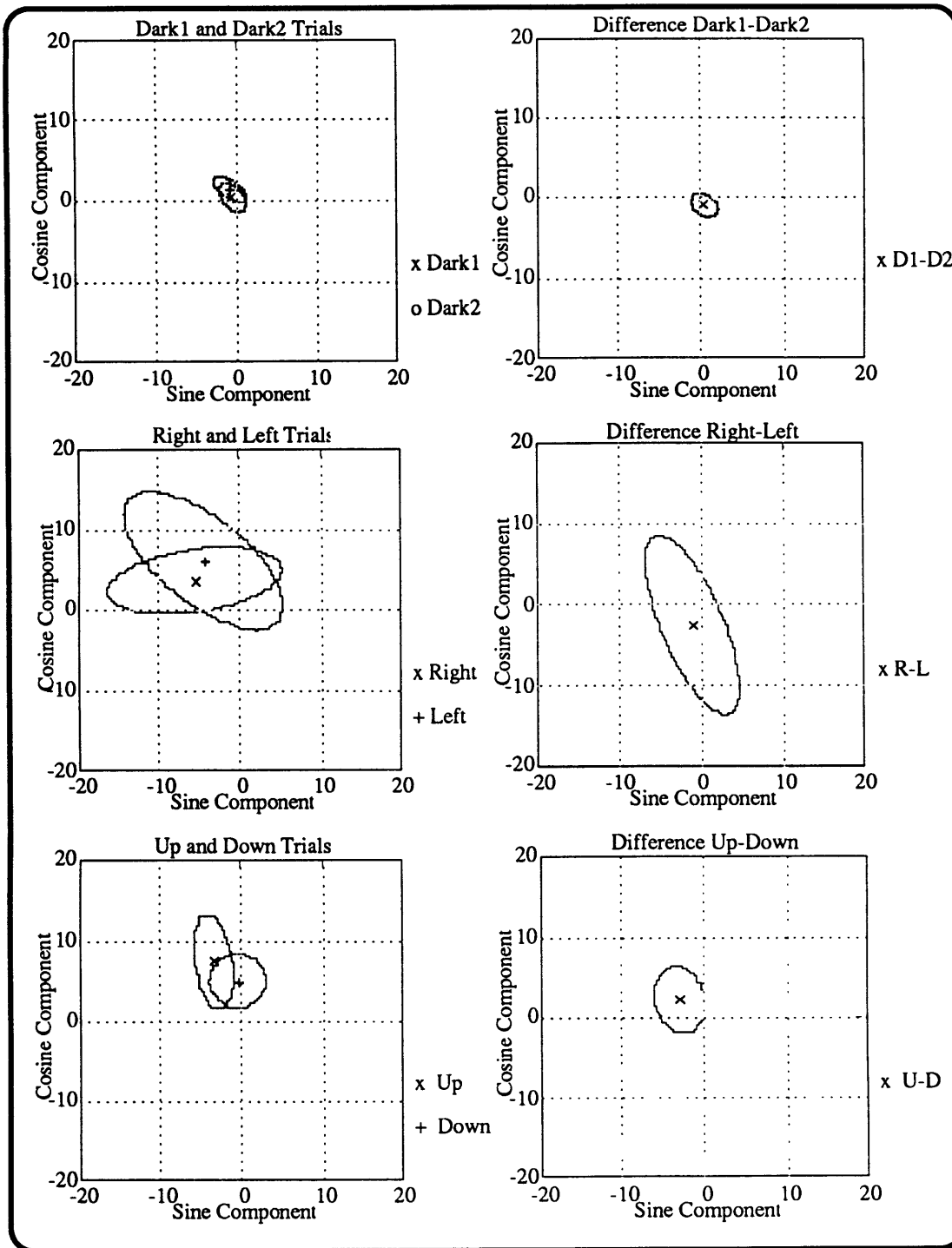
Figure 4.38 95 % Confidence Area for Dark1-Dark2, Right-Left, and Up-Down SPV Responses and their Differences (°/s).

Panels in the right represent the confidence area for the difference between the two conditions in the left panels. The two dark conditions as well as the pair *Right-Left* were not significantly different as can be inferred from their respective difference ellipses which include the origin. The difference ellipse for the pair *Up-Down* did not include the origin, so the two conditions are considered to be different and could not be combined for the rest of the analysis.
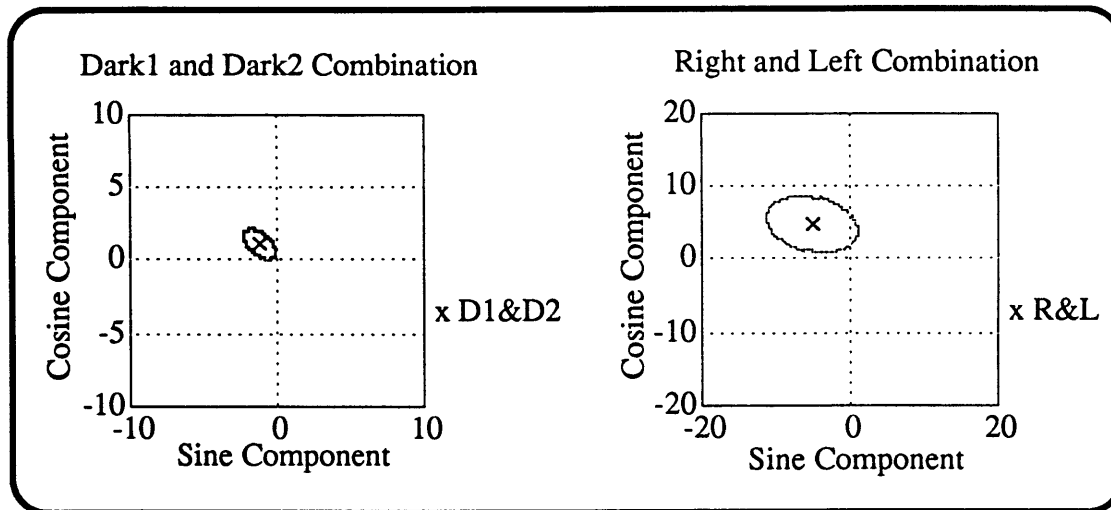
Figure 4.39: 95% Confidence Areas for the Combinations *Dark1&Dark2* and *Right&Left*, of Fundamental Frequency SPV Responses (°/s)

Down responses had an amplitude of $5.08°/s \pm 1.95°/s$ and a phase lead of $84.38° \pm 21.62°$ and *Up* had an amplitude of $8.14°/s \pm 3.21°/s$ and a phase lead of $64.34° \pm 14.35°$.

Two special characteristics of the *Up* and *Down* results should be noted. First, the large and consistent lead of the response, and second, the fact that the difference between the two conditions was statistically significant. Consequently, the two trials will be treated separately in the ensuing analysis.

Figure 4.40 showed the ellipses resulting from the differences between the light and dark trials and none of them encircle the origin, indicating that optokinetic stimulation significantly increase both the magnitude and the lead of the response.

Sinusoidal Optokinetic Stimulus

Figs. 4.41 and 4.42 plot the confidence areas for each one of the trials involving sinusoidal optokinetic stimulation. Note the similar pattern to the one in the upright condition. Both the complementary $(OK+V)$ and the anti-complementary $(OK-V)$ conditions were significantly different from the OK alone condition.

121
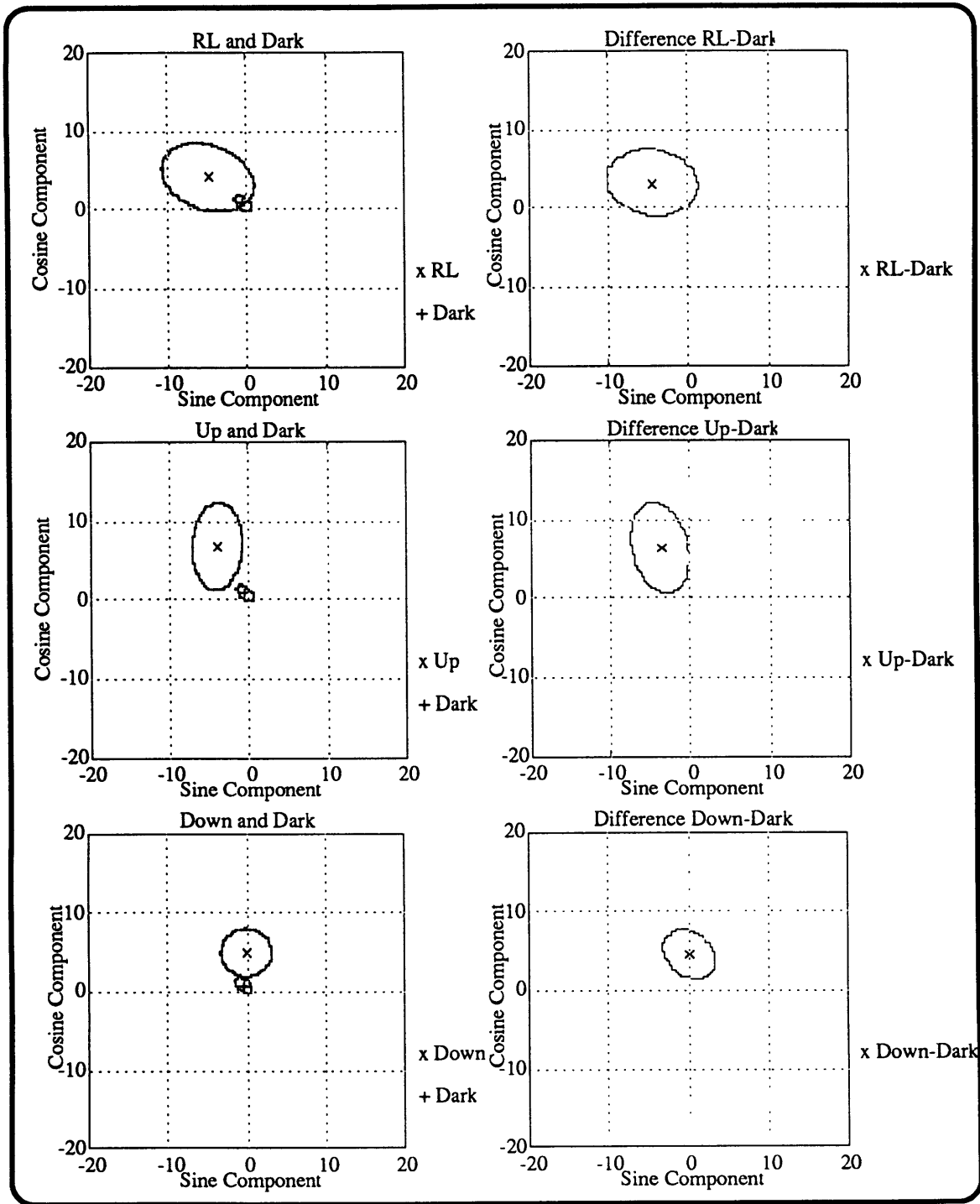
Figure 4.40: **Difference in SPV between Dark and Light Trials (95% Confidence Area in deg/s).** Difference ellipses are obtained by vector difference of each pair of conditions within each subject and pooling all results across subjects together. Neither one of the three ellipses encircle the origin, indicating that the difference between the light and the dark trials is significantly different.

As in the upright case, both the *OK-V* and the *OK+V* trials increased the magnitude and the phase lead of the response. These increases are substantially larger for *OK+V*. While the increase in *OK-V* is smaller, it is still statistically significant. In addition to this, it is observed that the two conditions with vestibular stimulation are also different from each other.
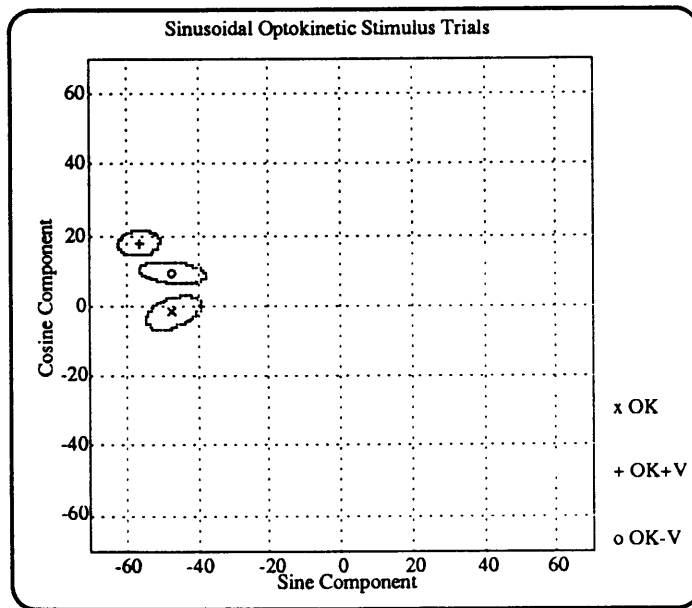
Figure 4.41 **Sinusoidal Optokinetic Stimulus Trials (95% Confidence Areas for SPV Responses in deg/s).** As seen from the position of the ellipses, a vestibular input (complementary or anti-complementary) increases the lead of the response.
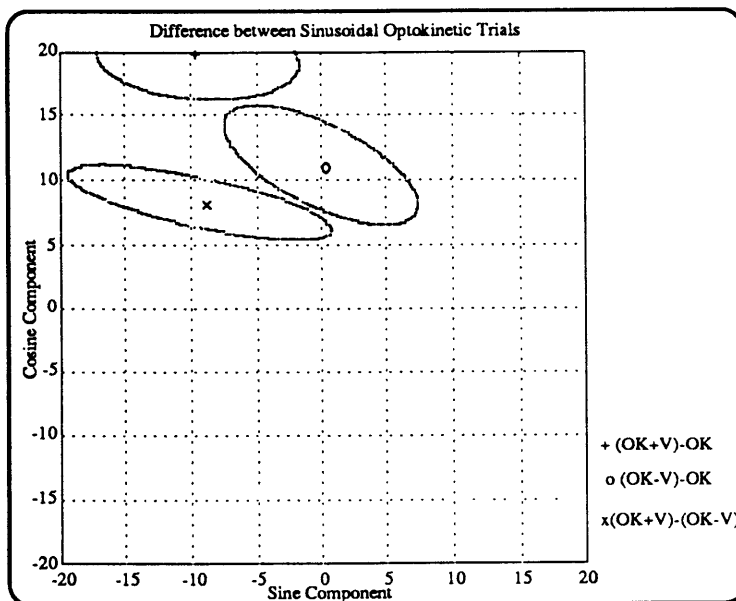
Figure 4.42: **SPV Differences between Sinusoidal Optokinetic Trials (95% Confidence Areas in deg/s).** The origin is not enclosed by any of the ellipses, indicating that the trials were statistically different from one another.

123

4.2.3.2 Horizontal Eye Movements at the Second Harmonic

To investigate the possibility of significant responses at the second harmonic of the stimulus (0.50 Hz), figure 4.43 shows the confidence ellipses for responses at that frequency. In similar fashion to the upright responses at this frequency, responses had small amplitudes and phase differences spread over several quadrants. None of the responses was significantly different from zero (all ellipses enclosed the origin) even after combining equal responses (those whose difference was non-significant) which suggests that horizontal ocular responses primarily occurred at the fundamental frequency.
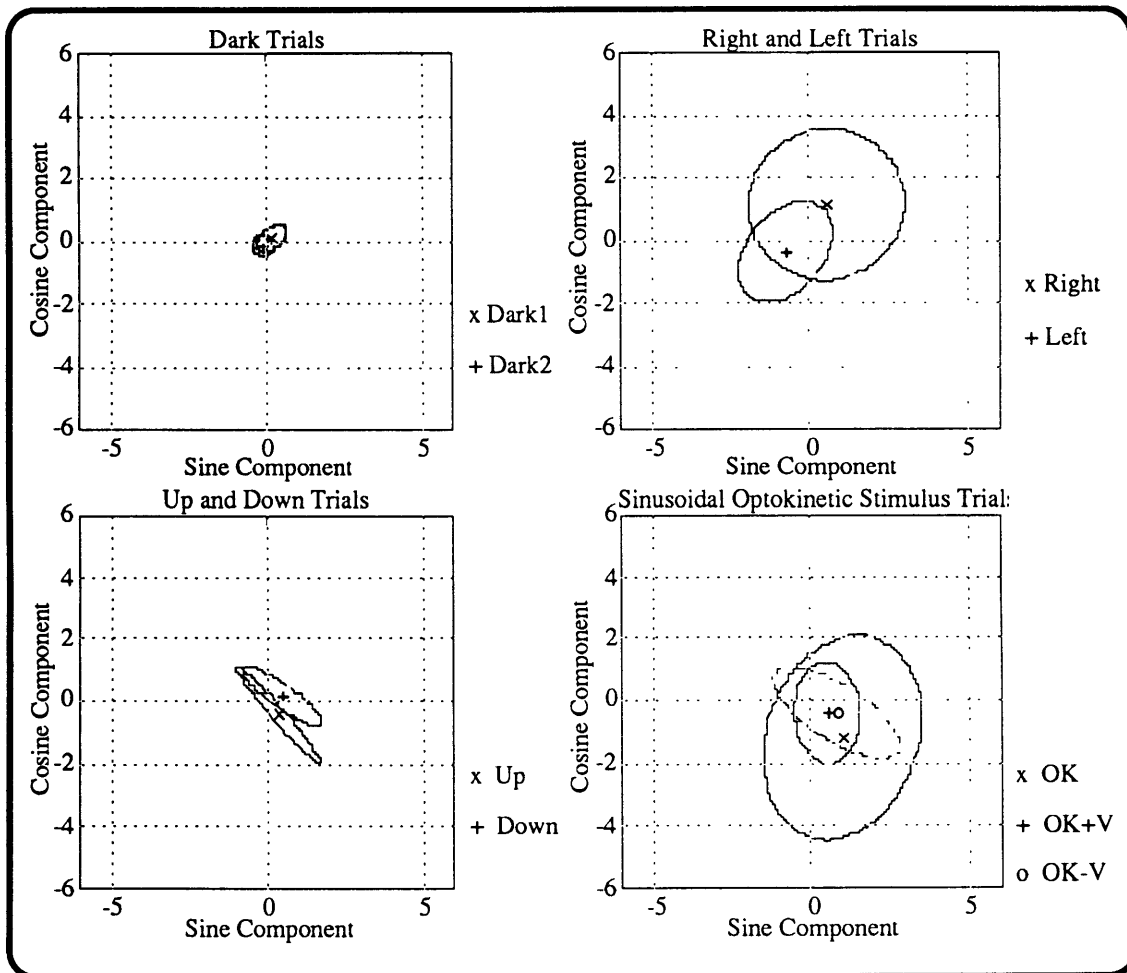
Figure 4.43 95% Confidence Area for Horizontal SPV Responses at the Second Harmonic (deg/s) In general, responses were not significant and had very small amplitudes with phases spread over several quadrants.

4.2.3.3 Vertical Eye Movements at the Fundamental Frequency

Vertical responses (Fig. 4.44) showed small amplitude oscillations (all means were below 2°/s) and they were not significantly different from zero in all cases. The standard deviations of the phase differences were above 100° in most cases, reflecting the large variability of the data (note that most ellipses cover areas in all four of the quadrants).

4.2.3.4 Vertical Eye Movements at the Second Harmonic

Responses at the second harmonic (Fig. 4.45) were mostly non-significant, with small amplitudes and inconsistent phases. Only the trials OK and $OK+V$ showed some responses which were significant but their amplitudes were less than 1 deg/s and with phase differences ranging from 45° to 60°.

In similar fashion to the upright results, none of the vertical responses were consistently and significantly different from zero due to large variability and small amplitude. This suggests that the observed vertical responses may be due to random eye movements and measurement noise.

Dark Trials

Cosine Component
Sine Component

x Dark1
+ Dark2

Right and Left Trials

Cosine Component
Sine Component

x Right
+ Left

Up and Down Trials

Cosine Component
Sine Component

x Up
+ Down

Sinusoidal Optokinetic Stimulus Trial:

Cosine Component
Sine Component

x OK
+ OK+V
o OK-V
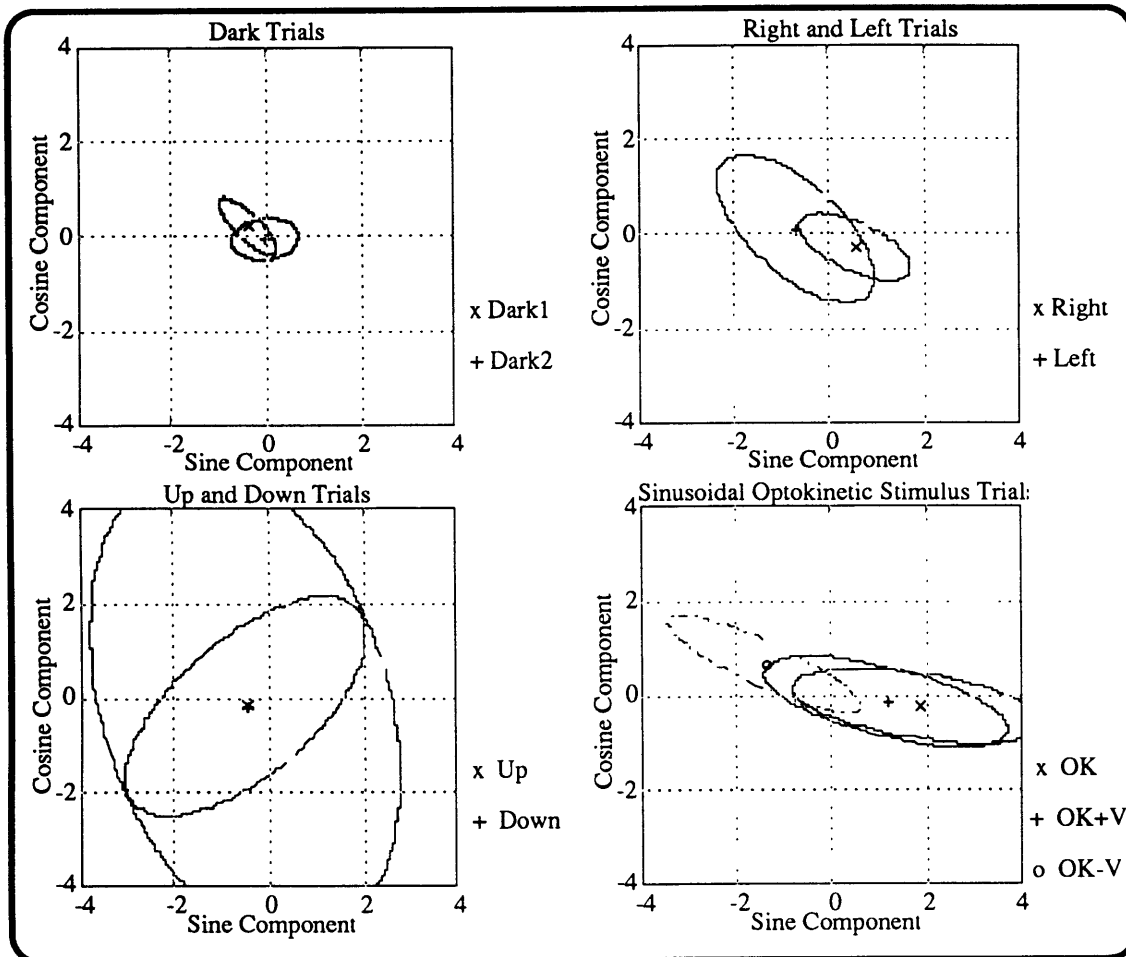
Figure 4.44 Confidence Interval for Vertical SPV
Responses at the Fundamental Frequency (deg/s)

Neither one of the vertical responses at the frequency of the stimulus was significant, as can be seen from the ellipses, all of which encircle the origin.

126
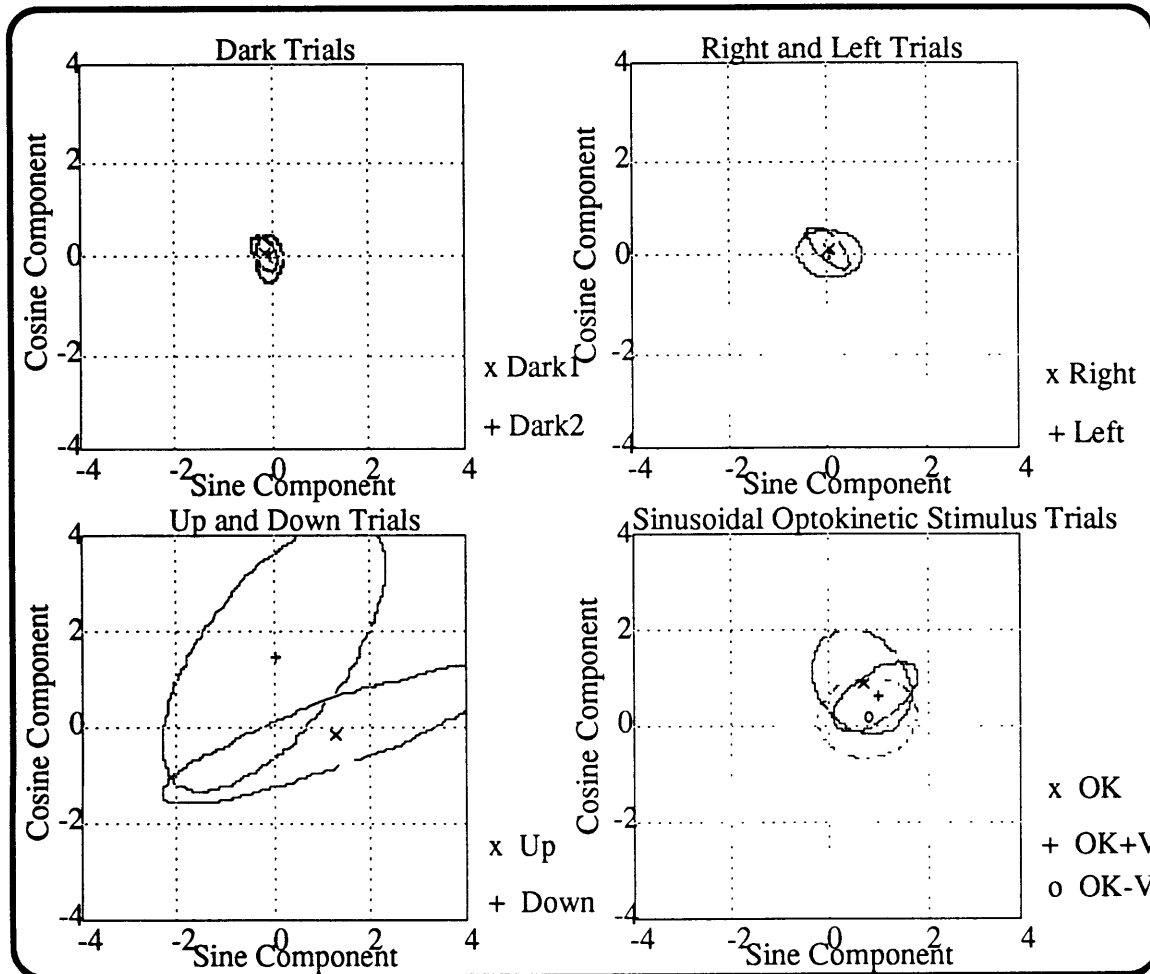
Figure 4.45: **Confidence Interval for Vertical SPV Responses at the <u>Second Harmonic</u> (deg/s)**

Most of the responses were not significantly different from zero. Only *OK+V* and *OK* were significant, however, even in those cases, amplitudes were very small (less than 2°/s).

4.2.4 Pooled Results: DC offsets during Constant Velocity OK Stimulation

Table 4.11 and figure 4.46 present the mean DC offset during the eight seconds preceding sled motion (pre) and during sled motion (per) for the horizontal response in *Right* and *Left* (*R&L*) combined and for the vertical response in *Up* and *Down* (*U&D*) combined. The offsets were combined after using paired t-tests to show that the two responses were not significantly different.

Condition	Pre (°/s)	Per (°/s)	Mean Change (°/s)	p
R&L	31.31±8.38	34.30±9.47	2.99±4.19	0.019
U&D	25.72±11.93	26.71±8.61	-0.98±4.85	0.502

Table 4.11: Change in DC offset (mean±sd) between pre and per vestibular stimulation during the RL trials. The listed p values for the difference were obtained from paired t tests.
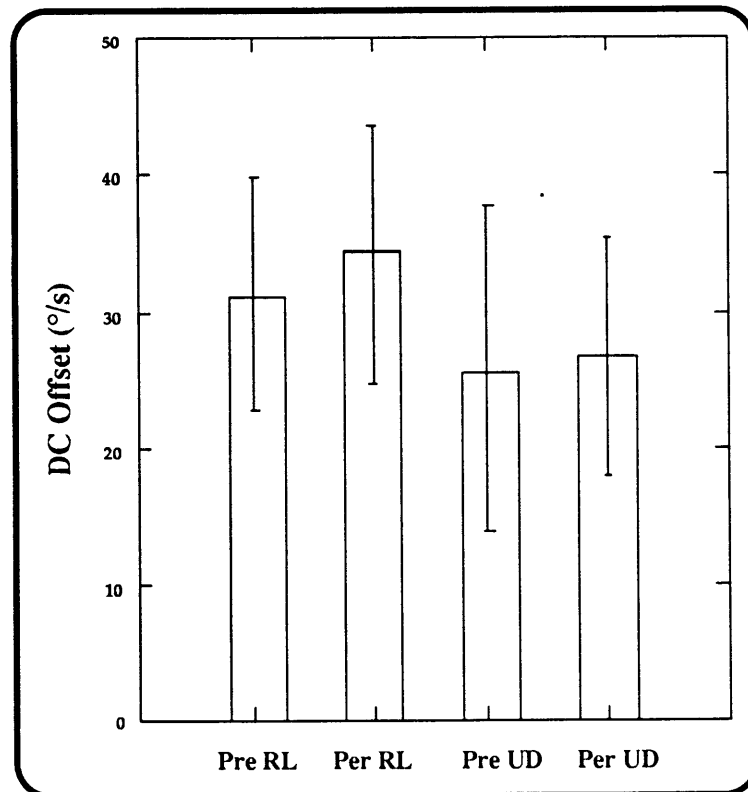
Figure 4.46: Change in DC offset between pre and per vestibular stimulation during *RL* and Combined *Up* and *Down* trials. The small error bars represent the standard deviation of the data.

Vestibular stimulation caused the mean DC offset of the horizontal response in *R&L* to increase significantly (p<0.05) by almost 3°/s. However, it should be noted that this is an increase of the response of less than 10%. On the other hand, the vertical offset during *U&D* did not change significantly. It should be noted that this is opposite to the behavior observed in the upright orientation, where vertical offsets changed more significantly than horizontal offsets.

4.2.5 Pooled Results: General Summary

Tables 4.12 and 4.13 summarize the results presented across subjects for trials run in the supine condition. In general, horizontal oscillations at the frequency of the sled were found whenever sled motion was present but responses in the dark were very small. The addition of an optokinetic stimulus at a constant linear velocity significantly increased the magnitude and lag of the response as compared to trials run in the dark. Sinusoidal optokinetic stimulation which complemented the sled motion (e.g. sled right, shade left) increased the amplitude and lag of the eye response as compared to trials without sled motion. On the contrary, anti-complementary visual stimulation kept the response essentially unchanged as compared to the purely visually driven response. These responses follow the same pattern as that observed for the upright orientation.

Horizontal oscillations at the second harmonic as well as vertical responses at the fundamental and second harmonic frequencies were not consistent, having irregular phases and small amplitudes.

Condition	DC Values		Fundamental Frequency				Second Harmonic			
	Ampl	StdDev	Ampl	StdDev	Phase	StdDev	Ampl	StdDev	Phase	StdDev
	(deg/s)	(deg/s)	(deg/s)	(deg/s)	(deg)	(deg)	(deg/s)	(deg/s)	(deg)	(deg)
Dark1	-0.16	0.38	0.80	0.94	135.82	75.92	0.19	0.30	41.96	88.38
Dark2	-0.22	0.49	1.71	1.37	120.84	71.54	0.19	0.15	-140.18	132.83
D1&D2	-0.19	0.42	1.25	1.15	125.60	77.19	0.00	0.23	118.82	108.44
OK	1.16	1.49	47.00	6.33	-177.87	4.69	1.54	1.86	-50.36	75.16
OK+V	-0.28	1.10	59.24	4.60	162.50	3.23	1.18	0.57	-19.38	60.00
OK-V	-0.21	0.80	48.03	7.72	168.61	2.78	0.90	1.31	-26.65	90.58
Right	36.37	7.45	6.66	7.80	146.83	42.07	1.28	2.09	64.44	101.39
Left	-33.09	10.62	7.63	6.80	126.38	70.54	0.83	1.00	-154.21	121.26
R&L	34.73	8.98	7.03	7.14	135.90	55.89	0.41	1.60	103.45	110.75
Up	1.10	3.39	8.14	3.21	115.66	14.35	0.53	0.86	-51.68	117.40
Down	-2.23	1.47	5.08	1.95	95.65	21.62	0.49	0.56	21.81	60.92

Table 4.12: **Mean Responses Across Subjects in Each Condition. Horizontal Eye Movements - Supine Position.** Values were obtained from all seven subjects run in this condition. Shaded responses were significant at the 0.05 level. Phase differences are with respect to sled velocity except for trials OK, OK+V, and OK-V where the phase difference with respect to shade velocity is presented.

Condition	DC Values		Fundamental Frequency				Second Harmonic			
	Ampl	StdDev	Ampl	StdDev	Phase	StdDev	Ampl	StdDev	Phase	StdDev
	(deg/s)	(deg/s)	(deg/s)	(deg/s)	(deg)	(deg)	(deg/s)	(deg/s)	(deg)	(deg)
Dark1	-0.83	1.74	0.48	0.48	150.95	108.28	0.22	0.22	154.14	118.37
Dark2	-1.25	2.04	0.07	0.35	-145.93	112.28	0.10	0.18	-176.84	118.53
D1&D2	-1.04	1.83	0.26	0.41	157.48	118.87	0.16	0.19	163.43	117.04
OK	-0.66	1.16	1.85	1.56	-6.94	87.66	1.14	0.47	52.85	55.38
OK+V	-0.84	1.42	1.15	1.42	-6.67	90.60	1.16	0.72	32.34	52.65
OK-V	-0.43	1.81	1.56	1.27	154.54	81.53	0.84	0.59	12.11	71.93
Right	-2.74	2.02	0.61	0.70	-26.50	89.08	0.16	0.26	72.92	84.90
Left	-0.96	3.48	0.71	1.16	171.53	133.35	0.07	0.18	38.62	103.72
Up	28.21	4.99	0.52	1.29	-164.09	104.80	1.28	1.51	-5.35	75.14
Down	-25.74	12.07	0.53	1.13	-158.84	124.44	1.50	1.58	90.04	118.48

Table 4.13: **Mean Responses Across Subjects in Each Condition. Vertical Eye Movements - Supine Position.** Values were obtained from all seven subjects run in this condition. Shaded responses were significant at the 0.05 level. Phase differences are with respect to sled velocity except for trials OK, OK+V, and OK-V where the phase difference with respect to shade velocity is presented.

4.3 Comparison of Upright and Supine Results

In order to investigate the affect of body position relative to gravity, the difference between significant responses in the upright and the supine positions will be presented in this section. Only the difference between the horizontal responses at the fundamental frequency will be analyzed since they were the only significant responses observed. When obtaining confidence areas for the differences, only data from the five subjects that were tested in both orientations will be used.

4.3.1 Dark and Constant Velocity OK Trials

Figures 4.47 and 4.48 show the mean amplitude and phase (with standard deviations indicated in each case) in the upright and the supine position. In all cases the same pattern was observed: amplitude was higher in the upright trials, while the lead in the responses was higher supine.

To analyze the statistical significance of these observed trends, Figure 4.49 presents the confidence areas of the vector differences of the responses in each kind of trial between upright and supine positions. Since *Dark1* and *Dark2* as well as *Right* and *Left* were combined in the two positions, the combined conditions were used to generate Fig. 4.48 (combined conditions were first averaged within each subject). On the other hand, *Up* and *Down* were not combined in the supine position, so the individual conditions are used for comparison

Only the difference in *Dark* responses was statistically different. In the upright condition, the oscillations at the fundamental frequency had an amplitude of $5.18 \pm 3.26°/s$ and a phase of $153.83° \pm 29.88°$. In the supine condition the amplitude was $1.25 \pm 1.15°/s$ with a phase of $125.60° \pm 77.18°$.

These results suggest that the new orientation with respect to gravity vin the supine position, decreases the gain of the vestibular pathways (lower LVOR in the dark) which might be brought back to their upright value by optokinetic stimulation (unchanged responses in *R&L, Up,* and *Down*).

131
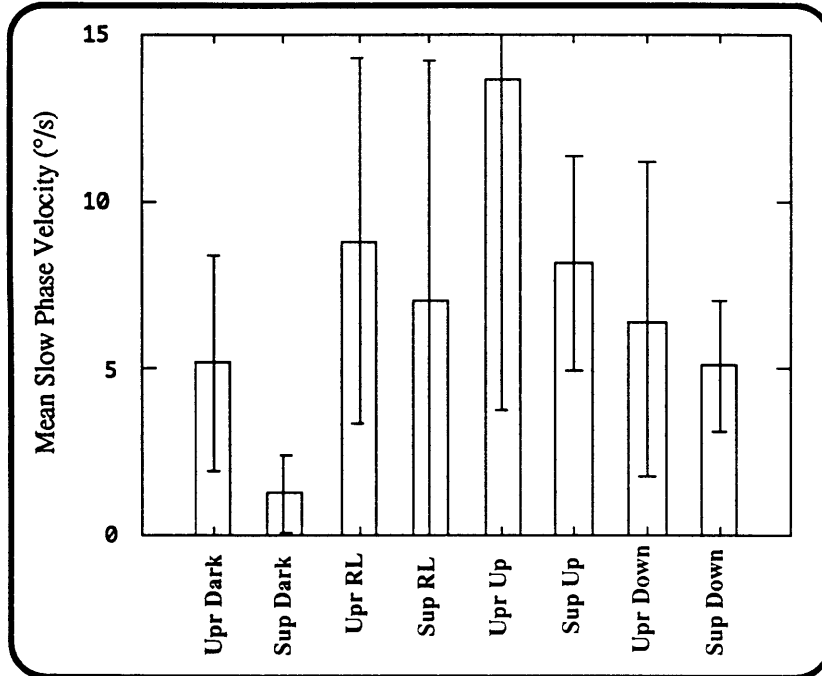
Figure 4.47: Mean Slow Phase Velocity in Dark and Constant Velocity Optokinetic Trials. The means are obtained across subjects. Standard deviations for each trial are also indicated. The differences in Dark (Upr:5.20±3.20°/s, Sup: 1.25±1.15°/s) and in Up are (Upr: 13.64±9.90°/s, Sup: 8.14±3.21°/s) are the largest ones.
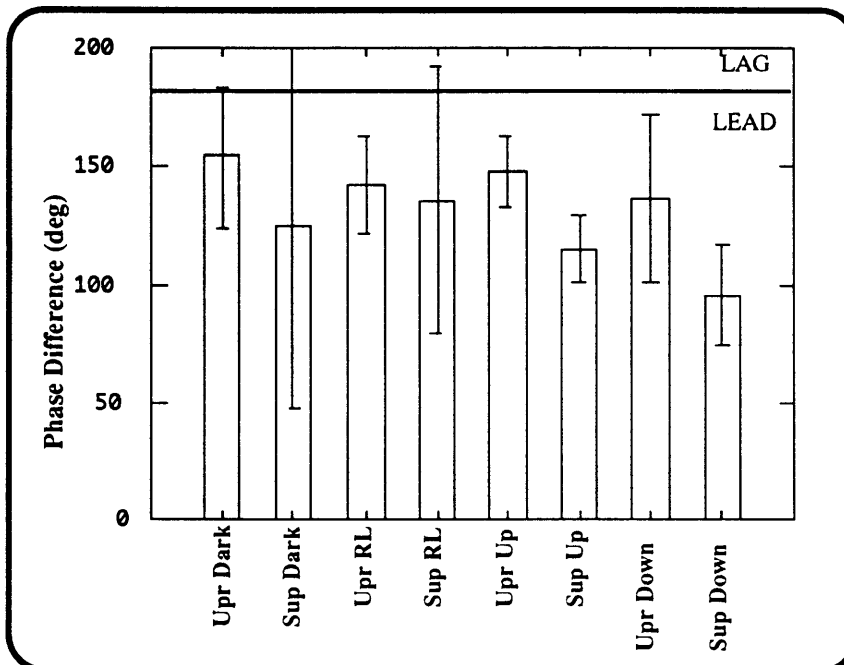
Figure 4.48: Mean Phase Difference in Dark and Constant Velocity Optokinetic Trials. The means are obtained across subjects. Standard deviations for each trial are also indicated. The horizontal line marks the 180° axis which separates lagging (above 180°) and leading responses (below 180°).

132
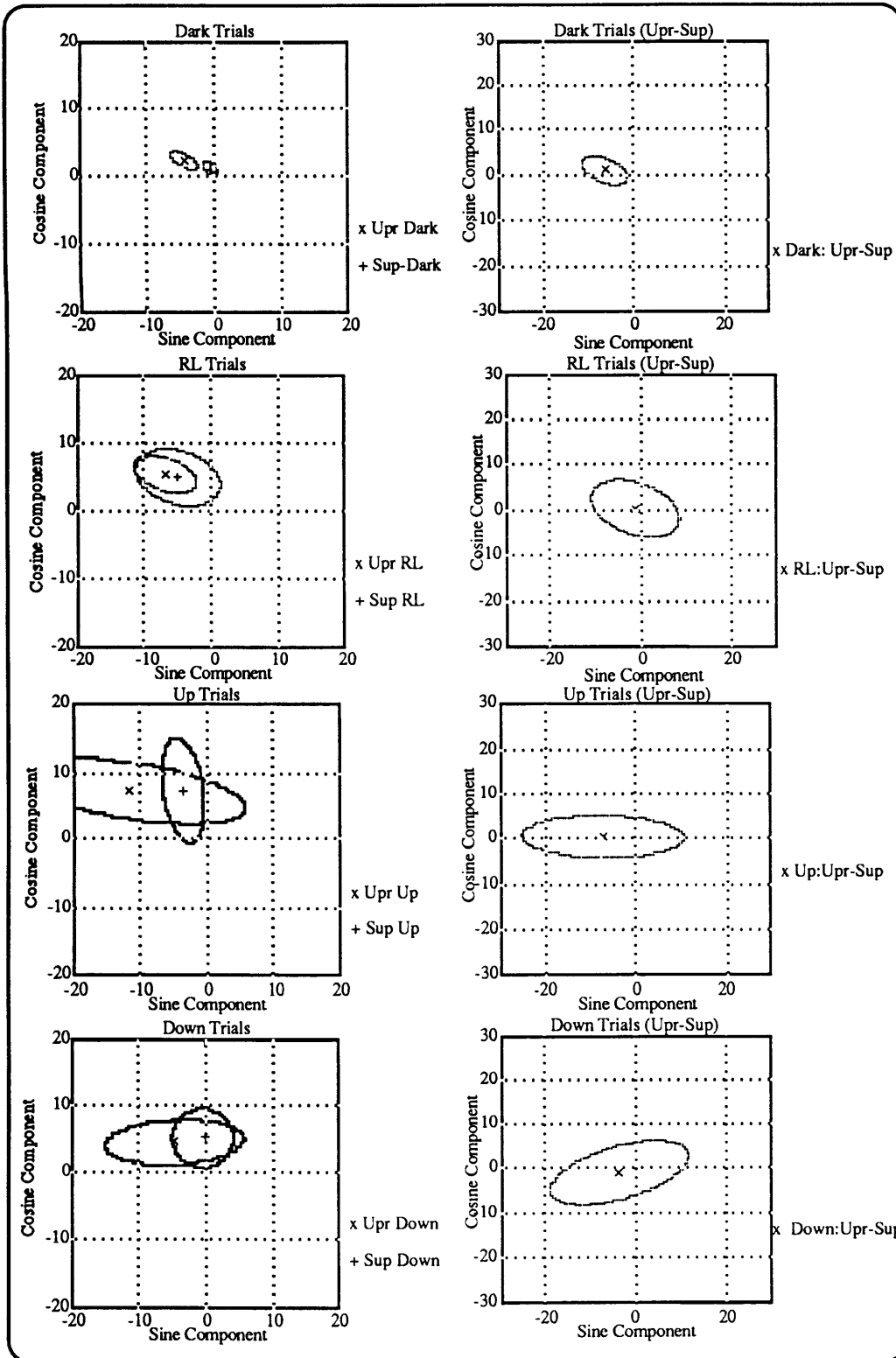
***Figure 4.49 Confidence Areas for Differences (in °/s) between responses in Upright
and Supine.*** The differences were calculated within each subject (upright-supine) for
each condition and then the confidence area is obtained using those. The ellipses in the
left column were obtained from all the subjects tested in each condition, while ellipses in
the right are obtained from the five subjects that were tested in both orientations.

133

4.3.2 Sinusoidal Optokinetic Trials

Figures 4.50 and 4.51 show the mean amplitude and phase (with standard deviations indicated in each case) of these trials in the upright and the supine position. The pattern followed by the three trials (*OK*, *OK+V*, and *OK-V*) is remarkably similar both in the upright and the supine position. *OK+V* had the largest amplitude, while *OK-V* and *OK* had relatively similar lower amplitude. Phasewise, *OK* showed a small lag, while *OK-V* showed a small lead that increases in *OK+V*.
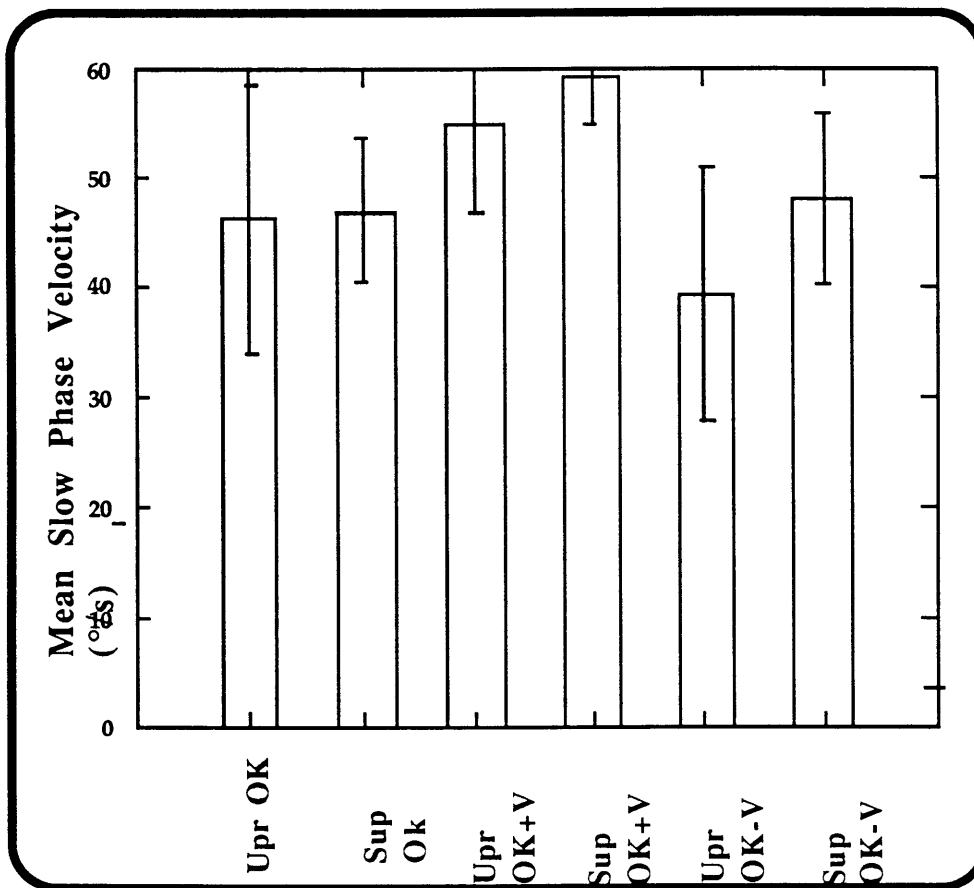
Figure 4.50: Mean Slow Phase Velocity in Sinusoidal Optokinetic Trials. The means are obtained across subjects. Standard deviations for each trial are also indicated. The differences between same trials in different positions was small and the one with the largest difference (*OK-V*) also showed the largest variability (Upr: 39.45±11.58°/s, Sup: 48.03±7.72°/s).
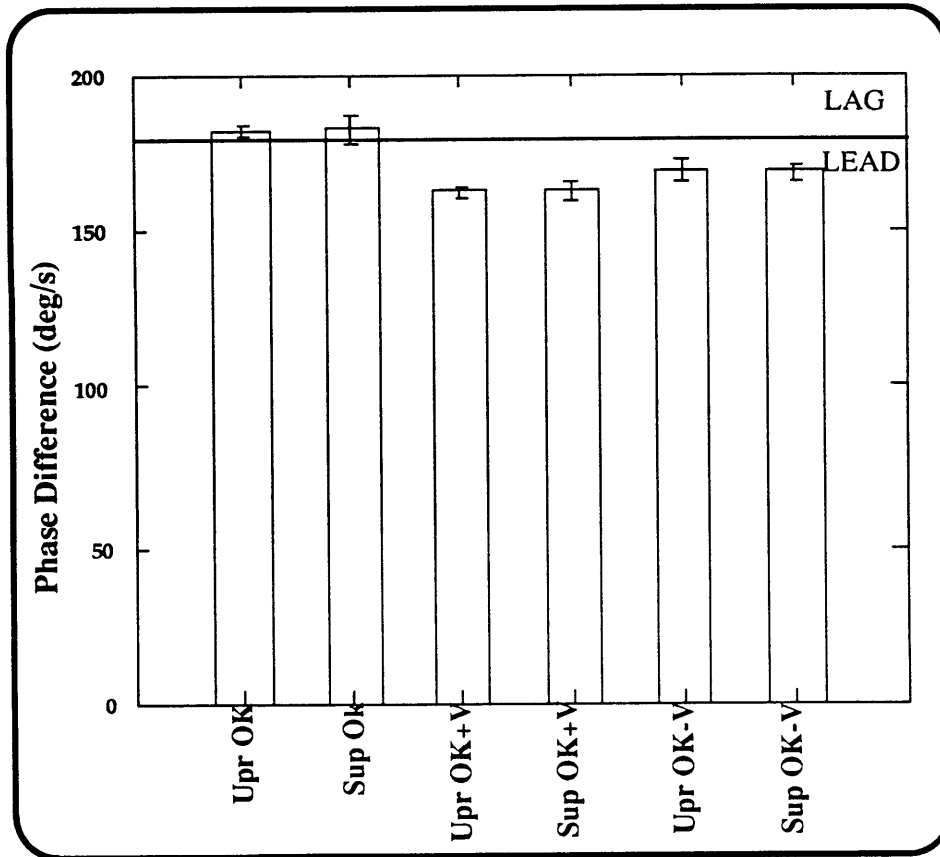
Figure 4.51 Mean Phase Difference in Sinusoidal Optokinetic Trials. The means are obtained across subjects. Standard deviations for each trial are also indicated. The horizontal line marks the 180° axis which separates lagging (above 180°) and leading responses (below 180°). Note the very small standard deviations and differences between the two positions.

Figure 4.52 shows the confidence areas of the differences between the two orientations in the three conditions. None of them was statistically different, suggesting that the position of the subject with respect to the gravity vector does not heavily influence these visual-vestibular interactions.
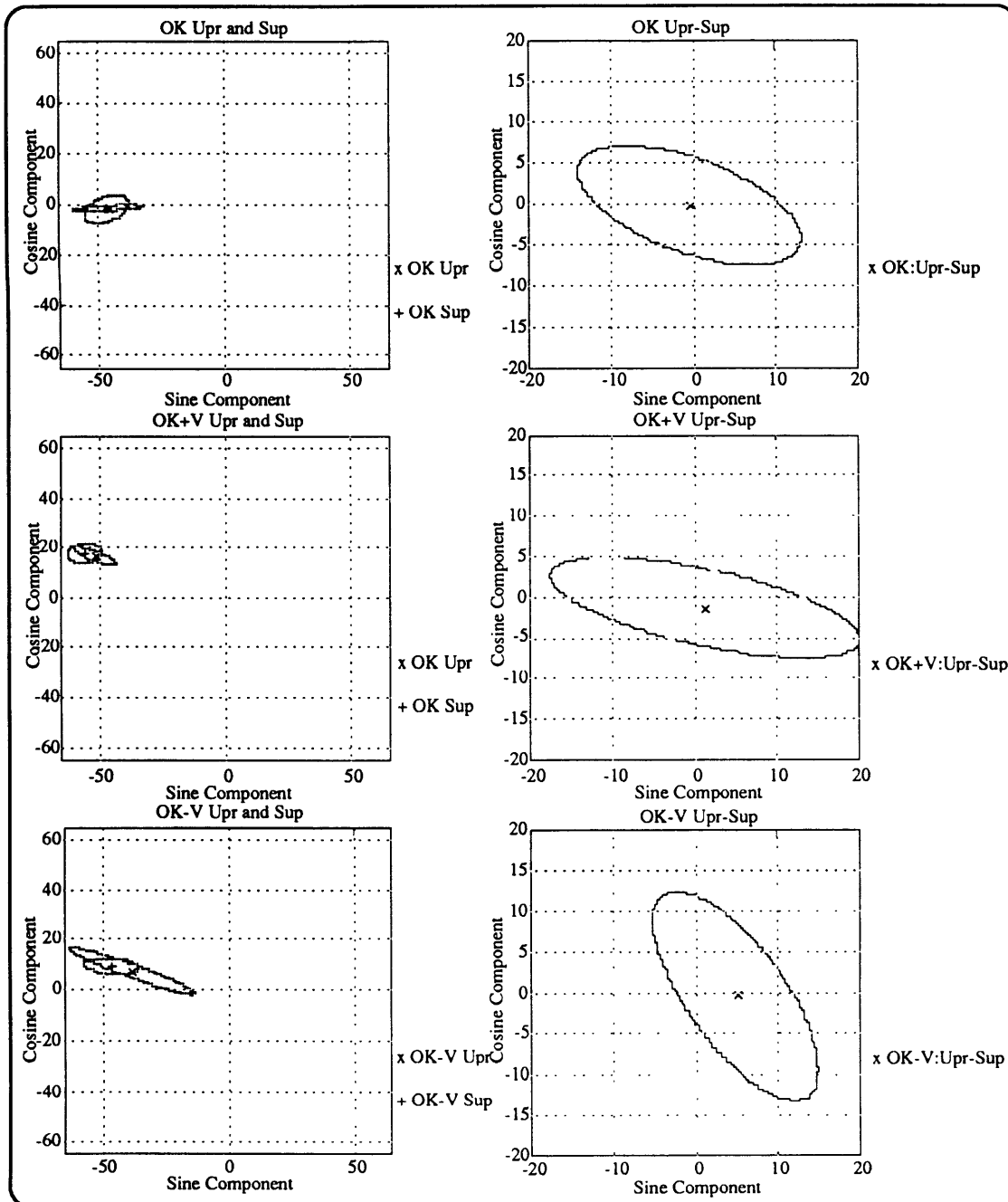
Figure 4.52 Confidence Areas for Differences (in °/s) between responses in same type of trials in the Upright and the Supine Position. The differences were calculated within each subject (upright-supine) for each condition and then the confidence area is obtained using those. The ellipses in the left column were obtained from all the subjects tested in each condition, while ellipses in the right are obtained from the five subjects that were tested in both orientations. Neither one of the three differences are statistically significant from zero.

136

Chapter 5

Discussion and Conclusions

After a brief summary, the discussion will begin by assessing the importance of the new statistical signal processing tools developed to analyze oculomotor dynamic responses. Then, the results presented in chapter four will be discussed starting with the affects of the subject's orientation on the ocular response and the characteristics and differences between the responses in each trial.

In the conclusion section, some of the observed phenomena will be explained in the light of existent models of oculomotor behavior (for a general description of oculomotor signals see Robinson, 1974; for reviews of specific models, see Henn et al., 1980; Zuber, 1981; and Merfeld, 1990) and their relationship with vestibular adaptation experiments in the Space Shuttle.

Finally, as is the case for many engineering and science problems, the new questions that arose from this project are translated into suggestions for future research.

5.1 Summary of Results

A new method of signal processing to analyze oculomotor responses was developed based on multi-variate statistics. Significant ($p<0.05$) horizontal responses at the frequency of the stimulus were observed in all trials. Horizontal responses at the second harmonic of the stimulus as well as vertical responses at the frequency of the

stimulus and the second harmonic were analyzed and no consistent and significant responses were observed

In the upright position, trials in the dark showed a horizontal oscillation with a mean and standard deviation of 5.19°/s±3.26°/s and a phase lead with respect to the perfect compensatory response of 29.16°±29.88°. When subjects were viewing an OK display moving at a constant velocity, these oscillations increased to approximately 5°/s to 6°/s, even when the display was moving in the vertical direction while subjects were interaurally accelerated. The phase lead remained similar to the one in the dark. In addition to the increase in amplitude of the oscillations, the DC offset - a response to the visual stimulus - tended to increase (not significantly, p=0.07) after vestibular stimulation began.

When subjects viewed an OK display moving sinusoidally in a complementary fashion to the sled velocity, the mean amplitude of the response (54.82°/s±7.90°/s) and phase lead (17.68°±1.86°) increased with respect to the mean response when the subjects viewed the sinusoidal display without sled acceleration (46.35°/s±12.52°/s with a phase lag of 1.52°±1.65°). An anti-complementary visual display also produced the same effect in phase as the complementary case (lead increased to 11.05°) but an opposite effect in magnitude (decreased to 39.45°/s±11.58°/s) with respect to the only OK case.

Vergence measurements upright showed that subjects verged on the plane of the OK display, even during the dark trials.

In the supine position, the response in the dark was significantly smaller than upright. The supine dark response had an amplitude of 1.25°/s and a phase lead of 54.4°±77.19°. With the subjects viewing the constant velocity OK display, the amplitudes increased to levels similar to those seen upright (7°/s-8°/s) but the phase lead increased to approximately 60°. The DC offset of the horizontal visual response to the constant velocity OK display increased slightly (10%) but significantly (p<0.05) after vestibular stimulation began.

As in the upright position, both the complementary and anti-complementary OK stimulation increased the phase lead of the response ($17.5°\pm3.23°$ lead in OK+V and $11.4°\pm2.78°$ in OK-V) when compared to responses during pure sinusoidal OK stimulation (lag of $2.13°$). A similar behavior was observed in the magnitude, with both the complementary ($59.24°/s\pm4.60°/s$) and anti-complementary ($48.03°/s\pm7.72°/s$) responses showing a larger amplitude than the purely OK case ($47.00°/s\pm6.33°/s$).

The only subject from which vergence measurements were taken in supine showed vergence levels similar to those found upright, with eyes verging near the plane of the OK display.

5.2 Statistical Analysis of Oculomotor Responses

Oculomotor responses to dynamic stimuli are characterized by magnitude and phase. The correlation between these two parameters had not been fully addressed analytically in previous statistical analysis of eye responses. The use of multi-variate statistics proved to be a very effective way to solve this problem by simultaneously accounting for magnitude and phase when assessing the statistical significance of the responses as well as the statistical difference between them.

Using these methods in future eye movement research will increase the validity of quantitative analysis in this area. This shows once again, the important and beneficial role engineers can play in physiological research.

5.3 Effects of Subject Orientation

As was discussed in chapter two, ocular responses can be affected by the input to several sensory systems in addition to the vestibular system (e.g., proprioceptive system). Consequently, any changes in the ocular response seen between the upright and supine trials can in principle be affected by parameters such as the different tactile and proprioceptive information coming to the CNS due to the different orientation of the

139

body. However, this discussion will analyze the changes from the perspective of the vestibular system which is a primary sensory system of spatial orientation.

The only condition that was significantly different for the two orientations was *Dark*, suggesting that the vestibular pathways might decrease in gain in the supine orientation. This is consistent with previous studies of ocular torsion (Arrott, 1985) which showed a decrease in vestibularly mediated torsional ocular response in the supine position with respect to the upright position when subjects underwent linear acceleration along the inter-aural axis.

Another observed trend, though not large enough to make the responses statistically different was that responses in the supine position had larger phase leads in the dark as well as in the constant velocity optokinetic trials. Therefore, responses provided less accurate compensation supine than upright.

Robinson (1977) proposed a model of visual-canal interaction which contains a "perseverance" loop. This is an internal positive feedback loop with a gain k that keeps feeding into itself as long as the stimulus continues and dies out with a time constant determined by k (since k is a finite value, this loop is responsible for the OKAN and also for the extension of the vestibular nystagmus). Because of its characteristics, the action of this loop is called velocity storage. Hain (1986) extended Robinson's model to a three-dimensional model of otolith-canal vestibular interaction in which the gain of velocity storage is modulated by the linear acceleration vector, including the gravity vector. His model predicts shorter time constants (smaller gain k) of VOR and OKAN when subjects are stimulated with their head in the supine position when compared to the upright position. His predictions have been partially confirmed in monkeys (Raphan and Cohen, 1988), and cats (Angelaki and Anderson, 1991).

A previous study using squirrel monkeys (Paige and Tomko, 1991) found the gain of the LVOR to be independent of head orientation during inter-aural acceleration. This discrepancy with the results presented in this thesis could be the product of the

higher frequencies used in that study (0.5, 1.5, and 5.0 Hz) since they also showed that the reflex is frequency-dependent, with higher gains at higher frequencies.

My results suggest that a gain, k, similar to the one described by Hain, exists for the direct vestibular pathways, and that this gain is modulated by otolith information indicating the position of the gravity vector, and that this gravity effect is more important at low frequencies.

The functional need for this orientation dependent gain of the LVOR is not clear. Hain suggests that the purpose of the LVOR is to supplement the AVOR during off-axis rotation. Since AVOR responses depend on the orientation with respect to gravity, the results presented in this thesis might support his hypothesis that the LVOR is functionally connected to the AVOR and that the observed low gains of ocular responses are caused by the lack of stimulation to the canals in this experimental protocol.

The lower gain and the larger phase error seen supine may also be the product of the fact that the reflexes have adapted primarily for sensory patterns in the upright position, the configuration in which humans normally move. The fact that Paige and Tomko did not find this orientation-dependent characteristic at higher frequencies also suggests that the LVOR might be more capable of performing its functional task (stabilizing images on the retina) at higher frequencies.

5.4 Effect of Constant Velocity Optokinetic Stimulus vs Dark

Dark responses while upright showed a sensitivity of approximately 12°/s/g which compares to the 9.5°/s/g found by Christie (1991) but is smaller to the one found by Buizza and his associates of more than 20°/s/g (Buizza et al., 1980).

The enhancement in the amplitude of the ocular oscillation in the light when compared to dark is not as large as the ones previously reported in other studies (Buizza et al., 1980; Christie, 1991) in the upright position but the change is very significant in the supine position since the *Dark* gains are so small.

Several differences exist between this study and those mentioned above. The larger sensitivity to acceleration observed by Buizza and his collaborators is the products of the small accelerations they used (0.10 G-0.16 G). The oscillations they observed had mean amplitudes of less than 2.5°/s, values close to the resolution limit of the system they used to measure ocular movements (corneal reflection technique, reported to have an accuracy of 0.5° of eye position).

Christie's (1992) results were obtained from only two subjects in which responses were measured using scleral coils, and the rest of the results come from EOG measurements taken in four other subjects. Results were reported individually for each subject and no attempts were made to pool subjects in order to obtain independent samples. Christie also reported in some subjects the presence of vertical oscillations at the second harmonic and the large amplitude of those (eye position oscillations with peak-to-peak amplitudes of approximately 40°) suggests that these may be saccadic movements and not smooth reflexes. Unfortunately, the true significance of this observation cannot be obtained due to the lack of across-subject statistical analyses.

Horizontal oscillations in *Right, Left, Up*, and *Down* were similar in both the upright and the supine position (no statistical differences were found among them, though the supine responses had the tendency to larger leads). Of special relevance is the fact that even when the visual stimulation was orthogonal to the vestibular stimulation (*Up* and *Down* trials) the vestibularly mediated horizontal ocular oscillations remained unchanged. This result suggests that the vestibular and optokinetic responses are indirectly connected in the sense that the enhancement in gain observed from the dark to the light trials might be the product of a vestibular arousal mechanism triggered by the presence of a visual stimulus.

The DC offset of the ocular response to the constant velocity OK stimulus tended to increase after the sled began its sinusoidal motion. This suggests that a reciprocal mechanism of arousal between the visual and vestibular channels might exist, possibly in

combination with other factors such as the central arousal and increase in attention produced by the motion or the somatosensory inputs caused by the vibration of the sled. In particular, the activation of the vestibular system might lead to a higher gain of the visual system, even during the half-cycles of sled motion where the vestibular and visual information are non-complementary. However, the mechanism of reciprocity is not exactly the same in all conditions since vertical visual stimulation enhances the horizontal LVOR, but the horizontal LVOR does not always enhance the vertical visual responses.

The velocity of the horizontal oscillations in the dark as well as in the constant velocity OK trials led the perfectly compensatory response in phase . Since the otoliths sense acceleration, the neural system must integrate the sensory signals in order to calculate velocity as required for a compensatory velocity response. That the responses fall between acceleration and velocity implies an imperfect neural integration. This explanation is consistent with our data and other studies showing imperfection in neural integration (Robinson, 1989).

5.5 Effect of Complementary and Anti-Complementary Vestibular Stimulation vs. Visual Stimulation Only. Sinusoidal Optokinetic Trials.

These trials were essentially not affected by the orientation of the subject, which supports the idea that visual information keeps the gain of the vestibular response the same when the subject is positioned in different orientations.

When compared to the trials with only visual information, the change in the response caused by complementary and anti-complementary vestibular inputs has two distinctive characteristics. Phasewise, both of them increased the lead with respect to the OK alone condition. On the other hand, while the complementary stimulation increased the amplitude of the response, the anti-complementary case left it unchanged (supine) or in the upright case, showed a tendency to decrease it.

When the overall response is studied using confidence ellipses, which take into account both magnitude and phase, the inclusion of vestibular stimulation changes the responses in similar fashion independent of whether or not the information coming from the vestibular pathways is in agreement or in disagreement with the visual information. Both complementary and anti-complementary visual-vestibular input increased the lag of the response, a result that would not be expected if the direct visual and direct vestibular pathways were linearly added since the acceleration stimulus is opposite in these two cases. At the end of this chapter, experiments are suggested to further investigate this result in order to obtain models that will explain this unexpected phase behavior.

5.6 Conclusions

The visual and vestibular systems reciprocally enhance each other in the task of keeping images stable in the retina. This is not achieved by only summing the two responses to send a unique oculomotor signal, but by the change of the gain of one by the other before the summation takes place. To a first approximation, the results can be explained by the model proposed in figure 5.1. The vestibular pathways have two gains, one modulated by the gravity vector (Kv) and another modulated by the visual pathway (Kvvi). In similar fashion, the visual pathways has a constant gain (Kvi) and a gain modulated by the vestibular pathway (Kviv).

This simple model would explain the a) the enhancement of the LVOR in the light compared to the dark trials, b) the variation of LVOR in the dark in the supine vs. the upright position, c) the increase in DC offset of the visual response to constant optokinetic stimulation when vestibular stimulation is added, d)the increase in amplitude of the response during complementary sinusoidal stimulation, and e) the unchanged magnitude in the anti-complementary phase.
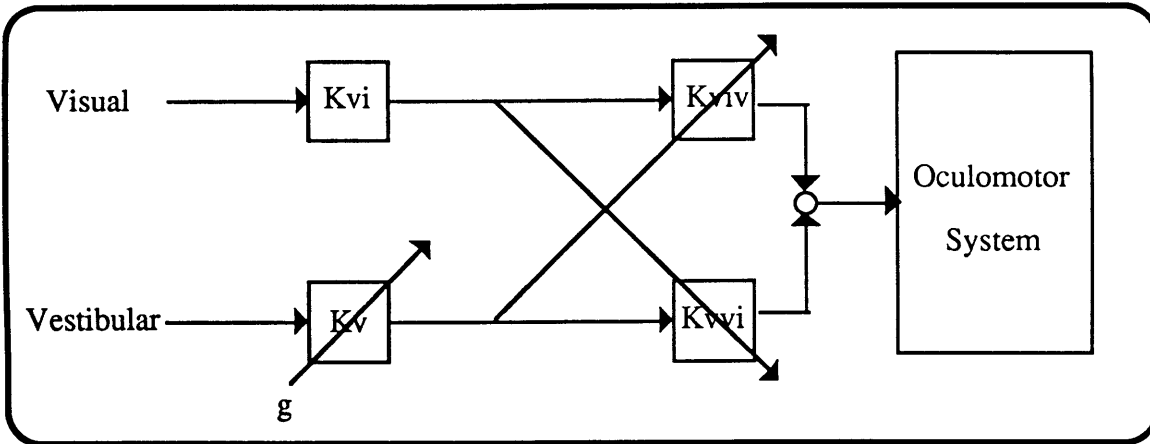
Figure 5.1: **Basic Model of Visual-Vestibular Interaction.** The perpendicular arrows are used to indicate that the gain depends on the signal carried by that arrow. The vestibular pathways have two gains, one modulated by the gravity vector (Kv) and another modulated by the visual pathway (Kvvi). In similar fashion, the visual pathways have a constant gain (Kvi) and a gain modulated by the vestibular pathway (Kviv).

The fact that this is the first step in the development of a model cannot be overemphasized. For example, the fact that visual responses which are perpendicular to the vestibular responses are not affected by the vestibular pathway must be accounted for by appropriately choosing matrices to represent these gains in a multidimensional model implementation.

Another very important consideration is the fact that from a black box point of view this model might seem feasible, but no strong evidence of modulation of the rate of firing by other neurons has been found in the vestibular or oculomotor pathways.

5.7 Implications for Space Research

Christie (1991) suggested that the otolith component of the vestibular pathway decreased its gain following a week of space flight. Young (1986) has also proposed that the CNS increases the weight of the visual information during microgravity in order to correct for the conflicting signals coming from the vestibular system.

The results presented demonstrate the interaction of these sensory systems. These interactions will be further investigated by testing subjects before and after space flight on the Spacelab Life Sciences 2 (SLS-2) mission. Based on the results presented in this

145

thesis, changes in the experimental protocol as well as in the scientific questions to be addressed will be made. In particular, the effects of complementary and anti-complementary visual-vestibular stimulation can be a very productive line of scientific inquiry since the relationship between the two stimuli is clearly defined. However, the relative significance of changes in the vestibular and visual pathways after spaceflight might become impossible to distinguish during these two types of trials (e.g., is an increase in gain post-flight in the anti-complementary case the product of enhanced visual gain or reduced vestibular gain?). Consequently, trials in the dark as well as during constant velocity optokinetic stimulation will be needed to also observe the adaptation of the visual and vestibular systems separately.

5.8 Suggestions for Future Research

The effect of frequency was not evaluated in this study. Previous studies (Paige and Tomko, 1991; Benson and Bodin, 1966) have suggested that the LVOR has a higher gain and smaller phase error at higher frequencies. A protocol similar to the one used in this thesis might be implemented at higher frequencies in order to characterize the sensitivity of the response to frequency and to see if the independence of the response on head orientation seen in monkeys by Paige and Tomko is due to the higher frequencies that they used.

Shelhamer (1990) showed that smooth pursuit in response to a moving visual target is enhanced by complementary acceleration. This result suggests that a purpose of the LVOR is to enhance smooth pursuit responses, especially at higher frequencies (where LVOR has higher gain) which are beyond the effective range of the saccadic system. To further investigate this (Shelhamer used EOG measurements, a technique that can be affected by external parameters such as illumination) the OK, $OK+V$, and $OK-V$ trials could be implemented with ta subject tracking a target on the windowshade while using scleral coils to measure eye movements.

When comparing DC offset pre and per sled motion, a limited amount of pre data, eight seconds, was available. Full trials with constant velocity OK stimulus should be obtained without sled motion to have a better way to assess the effects of periodical vestibular stimulation on the oculomotor response to constant velocity visual stimulation.

Complementary and anti-complementary vestibular stimulation had similar phase effects on the response when compared to the purely visual OK trial. It is evident that this result is counter-intuitive to the expected results if the two pathways generating the response, visual and vestibular, were simply summing their responses. To elucidate the effect of the relative phase between vestibular and visual stimuli on the phase of the oculomotor response, a series of trials in which the relative phase (of sled motion with respect to windowshade motion) is varied between OK+V and OK-V should be run. This will allow us to expand the proposed model into a more formal model that clearly shows the mechanisms that generate the observed phase leads.

REFERENCES

Angelaki DE and Anderson JH (1991): The horizontal vestibulo-ocular reflex during linear acceleration in the frontal plane of the cat. *Experimental Brain Research,* 86:40-46

Arrott AP (1985): *Ocular Torsion and Gravitational Force.* MIT - Biomedical Engineering Program Ph.D Thesis, May 1985

Balkwill MD (1992): *Changes in Human Horizontal Angular VOR After the Spacelab SLS-1 Mission.* MIT - Dept of Aeronautics and Astronautics Masters Thesis, February 1992

Baloh RW and Honrubia V (1979): *Clinical Neurophysiology of the Vestibular System,* Philadelphia: F.A. Davis Company.

Baloh RW, Beykirch K, Honrubia V, Yee RD (1988): Eye Movements Induced by Linear Acceleration on a Parallel Swing. *Journal of Neurophysiology,* 60: 2000-2013.

Barr CC, Schultheis LW, and Robinson DA (1976): Voluntary, Non-Visual Control of the Human Vestibulo-ocular Reflex. *Acta Otolaryngologica* 81:365-375.

Berthoz A, Israël I, Viéville T, and Zee D (1987): Linear head displacement measured by the otoliths can be reproduced through the saccadic system. *Neuroscience Letters,* 82:285-290

Bles W and Kapteyn TS (1973): Separate recording of the movements of the human eyes during parallel swing tests. *Acta Otolaryngologica* 75: 6-9

Boff KR and Lincoln JE (1988): *Engineering Data Compendium: Human Perception and Performance.* Wright-Patterson AFB, OH: AAMRL

Bos JH, Jongkees LBW, and Philipszoon AJ (1963): On the action of linear acceleration upon the otoliths. *Acta Otolaryngologica* 56: 477-489

Buizza A, Léger A, Droulez J, Berthoz A, Schmid R (1980): Influence of Otolithic

Stimulation by Horizontal Linear Acceleration on Optokinetic Nystagmus and

Visual Motion Perception. *Experimental Brain Research*, 39:165-176

Christie JRI (1991): *Modulation of Optokinetic Nystagmus in Humans by Linear*

Acceleration, and the Effects of Spaceflight. MIT, Masters Theses in

Aeronautics and Astronautics.

Clément G & Lathan CE (1991): Effects of static tilt about the roll axis on

horizontal and vertical optokinetic nystagmus and optokinetic after-

nystagmus in humans, *Experimental Brain Research*, 84:335-341.

Clément G & Reschke MF (1992): Response of the Neurovestibular System. In S.

Churchill (Ed.) *Introduction to Space Life Science*. MIT Course Material.

Cohen B, Matsuo V, and Raphan T (1977): Quantitative Analysis of the Velocity

Characteristics of Optokinetic Nystagmus and Optokinetic After-Nystagmus.

Journal of Neurophysiology 270: 321-344.

Cohen B, Henn V, Raphan T, and Dennett D (1981): Velocity storage, nystagmus

and visual-vestibular interactions in humans. *Annals of the New York*

Academy of Sciences, 374: 421-433

Cohen B (1984): Erasmus Darwin's observations on rotation and vertigo. *Human*

Neurobiology 3:121-128

Cohen B, Kozlovskaya I, Raphan T, Solomon D, Helwig D, Cohen N, Sirota M, and

Yakushin S (1992): Vestibuloocular reflex of rhesus monkeys after spaceflight.

Supplement of the Journal of Applied Physiology, August 1992: 121-131.

Correia MJ, Perachio AA, Dickman JD, Kozlovskaya IB, Sirota MG, Yakushin SB,

and Beloozerova IN (1992): Changes in Monkey Horizontal Semicircular

Canal Afferent Responses Following Space Flight. *Supplement of the*

Journal of Applied Physiology, August 1992.

Demer JL (1992): Mechanisms of Human Vertical Visual-Vestibular Interaction. *Journal of Neurophysiology,* 68: 2128-2146

Dichgans J, Nauck B, and Wolpert E (1973): The influence of attention, vigilance and stimulus area on optokinetic and vestibular nystagmus and voluntary saccades. In: *The Oculomotor System and Brain Function.* Zikmund V, ed. London: Butterworths, pp 281-294.

Engström H and Engström B (1981): The Structure of the Vestibular Sensory Epithelia. In Gualtierotti T (Ed.), *The Vestibular System: Function and Morphology,* New York: Springer-Verlag, pp 3-38.

Flourens P (1842): *Recherches expérimentales sur les propriétés et les fonctions du systéme nerveux dans les animaux vertébrés,* Paris: Bailliére, cited in Mach (1875).

Gacek RR (1981): The Afferent and Efferent Vestibular Pathways: Morphologic Aspects. In: Gualtierotti T (Ed.), *The Vestibular System: Function and Morphology,* New York: Springer-Verlag, pp 3-38.

Ghez C and Fahn S (1985): The Cerebellum. In: Kandel ER and Schwartz JH (Eds.), *Principles of Neural Science,* New York: Elsevier

Goltz F (1870): Uber die physiologische Bedeutung der Bogengänge del Ohrlabyrinths. *Pflügers Arch. ges. Physiol.* 3: 172-192, cited in Mach (1875).

Grüsser OJ (1984): J.E. Purkinje's contributions to the physiology of the visual, the vestibular and the oculomotor systems. *Human Neurobiology* 3:129-144

Guyton AC (1991): *Medical Physiology,* Philadelphia: W.B. Saunders.

Hain TC (1986): A Model of the Nystagmus Induced by Off Vertical Axis Rotation. *Biological Cybernetics,* 54:337-350

Henn V, Young LR, and Finley C (1974): Vestibular nucleus units in alert monkeys are also influenced by moving visual fields. *Brain Research,* 71: 144-149

Henn V, Cohen B, and Young LR (1980): Visual-Vestibular Interaction in Motion

Perception and the Generation of Nystagmus. *Neurosciences Research*

Program Bulletin. Vol. 18, No. 4.

Howard IP (1982): *Human Visual Orientation,* New York: John Wiley & Sons

Jell RM, Sett S, and Ireland DJ (1987): Human Optokinetic Afternystagmus. Is the Fast

Component of OKAN Decay due to smooth pursuit? *Acta Oto-Laryngologica,*

104:298-306.

Johnson RA & Wichern DW (1982): *Applied Multivariate Statistical Analysis.*

Englewood Cliffs, NJ: Prentice-Hall, Inc.

Jongkees LBW (1961): The influence of some drugs upon the function of the

labyrinth. *Acta Otolaryngologica* 53: 281-286

Kelly JP (1985): The Vestibular System. In: Kandel ER and Schwartz JH (Eds.),

Principles of Neural Science, New York: Elsevier

Koening E and Dichgans J (1981): Aftereffects of Vestibular and Optokinetic

Stimulation and their Interactions. In Cohen B (Ed.), *Vestibular and*

Oculomotor Physiology: International Meeting of the Bárány Society. Annals of

the New York Academy of Sciences, Vol. 374.

Lathan CE, Wall III C, and Harris LR (1993): The Effect of Linear Acceleration on the

Range of Optokinetic Performance in Humans (Abstract). To be published in

Aerospace Medical Association Meeting Abstracts, Toronto, May 23-27, 1993.

Lisberger SG (1988): The Neural Basis for Learning of Simple Motor Skills.

Science, 242:728-735.

Mach E (1875): *Outlines of the Theory of the Motor Sensations,* Private translation of

Grundlinien der Lehre von den Bewegungsempfindungen, Leipzig: Engelmann.

Massoumnia MA (1983): *Detection of fast phases of nystagmus using digital filtering.*

M.S. Thesis, Department of Aeronautics and Astronautics, MIT

151

Merfeld DM (1990): *Spatial Orientation in the Squirrel Monkey: An Experimental and Theoretical Investigation.* MIT, - Biomedical Engineering Program Ph.D Thesis.

Merfeld DM, Christie JRI, and Young LR (1992): Horizontal and Vertical Eye Movements in Humans During Inter-Aural Linear Acceleration. Presented at the *XVII Barany Society Meeting,* Prague, Czechoslovakia

Miles FA and Eighmy BB (1980): Long-Term Adaptive Changes in Primate Vestibuloocular Reflex. I. Behavioral Observations. *Journal of Neurophysiology,* 43: 1406-1424.

Niven JI, Hixson WC, and Correia MH (1966): Elicitation of Horizontal Nystagmus by Periodic Linear Acceleration. *Acta oto-laryngologica,* 62:429-441

Oman CM and Kulbaski MJ (1988): Spaceflight Affects the 1-g Postrotatory VOR. *Adv. Oto-Rhino-Laryng..* 42:5-8.

Oman CM and Weigl H (1989): Postflight VOR Changes in Space Shuttle/Spacelab D-1 Crew. Aerospace Medical Association Abstract, 1989

Paige GD (1989): The influence of target distance on eye movement responses during vertical linear motion. *Experimental Brain Research,* 77:583-593.

Paige GD and Tomko DL (1991): Eye Movement Responses to Linear Head Motion in the Squirrel Monkey. I. Basic Characteristics. *Journal of Neurophysiology,* 65:1170-1182

Parker DE (1980): The Vestibular Apparatus. *Scientific America,* 243: 118-135

Post RB, and Leibowithz HW (1982): The Effect of Convergence on the Vestibulo-Ocular Reflex and Implications for Perceived Movement. *Vision Research,* 22: 461-465

Pretch W (1975): Vestibular system. In: Hunt CC (Ed.), *MTP International Review of Science. Phsyiology Series Oner, Vol. 3. Neurophsysiology.*London: Butterworth, pp 82-149.

Pulaski PD, Zee DS, and Robinson DA (1981): The behavior of the vestibulo-ocular reflex at high velocities of head rotation. *Brain Research,* 222: 159-65

Raphan T, and Cohen B (1988): Organization principles of velocity storage in three dimensions. The effect of gravity on crosscoupling of optokinetic after-nystagmus. *Annals of the New York Academy of Sciences,* 545:74-92.

Roberts TDM (1973): Reflex Balance. *Nature* 244:156-158

Robinson DA (1974): Oculomotor Control Signals. In *Basic Mechanisms of Ocular Motility and their Clinical Implications* (Lennerstand and Bach-y-Rita, Eds.). London: Pergamon Press.

Robinson DA (1977): Vestibular and Optokinetic Symbiosis: An Example of Explaining by Modelling. In *Control of Gaze by Brain Stem Neurons,* Barker and Berthoz (Eds), Elsevier/North-Holland Biomedical Press.

Robinson DA (1989): Integrating with Neurons. *Ann Rev Neurosci,* 12:33-45

Rosner B (1990): *Fundamentals of Biostatistics.* Boston: PWS-KENT Publishing Co.

Schwarz U and Miles FA (1991): Ocular Responses to Translation and Their Dependence on Viewing Distance. I. Motion of the Observer. *Journal of Neurophysiology,* 66:851-864.

Shelhamer M, Young LR (1991): Linear Acceleration and Horizontal Eye Movements in Man. *Acta Otolaryngologica Supplement,* 481:277-281

Shelhamer M, Merfeld DM, Mendoza JC (1993): The Gain of the Linear Vestibulo-Ocular Reflex is Independent of Vergence. To be submitted.

Skipper JJ and Barnes GR (1989): Eye movements induced by linear acceleration are modified by visualisation of imaginary targets. *Acta Otolaryngologica Suppl.,* 468:289-293

Snyder LH and King WM (1988): Vertical Vestibuloocular Reflex in Cat: Asymmertry and Adaptation. *Journal of Neurophysiology,* 59: 279-298.

Tokunaga O (1977): The Influence of Linear Acceleration on Optokinetic

   Nystagmus in Human Subjects. *Acta Otolaryngologica,* 84:338-343

Viirre E, Tweed D, Milner K and Vilis T (1986): A Reexamination of the Gain of

   the Vestibuloocular Reflex. *Journal of Neurophysiology,* 56:439-450.

Wall III C, Harris LR, and Lathan CE (1992): Otolith-Visual Z-Axis Sensory

   Interactions (Abstract). *Association for Research in Otolaryngology,* Fifteenth

   Midwinter Research Meeting, St. Petersburg Beach, Florida, February   1992.

Westheimer G (1984): Helmholtz on eye Movements. *Human Neurobiology,* 3: 149-

   152

Wilson VJ and Melvill-Jones G (1979): *Mammalian Vestibular Physiology,* New

   York: Plenum Press.

Young LR, Shelhamer M, and Modestino S (1986): M.I.T./Canadian vestibular

   experiments on the Spacelab-1 mission: 2. Visual vestibular tilt interaction

   in weightlessness. *Experimental Brain Research,* 64:299-307

Zasorin NL, Baloh RW, Yee RD, and Honrubia V (1983): Influence of Vestibulo-Ocular

   Reflex Gain on Human Optokinetic Responses. *Experimental Brain Research,*

   51:271-274

Zuber BL (1981) (Ed.): *Models of Oculomotor Behavior and Control.* Boca Raton, FL:

   CRC Press Inc.

Appendix A

Individual Results

A.1 Upright Results

Tables A.1 through A.12 present the individual measurements for each subject run in the upright position, subjects A, B, C, D, E, and F. Format is similar to the one used in Tables 4.1 and 4.2. For each subject, DC offsets, oscillations at the fundamental frequency (0.25Hz) and the second harmonic (0.50Hz) are listed for both horizontal and vertical eye movements. Vergence is also reported when it was measured. Due to time constraints some conditions were not run in some subjects, this is indicated by asterisks (***) in the corresponding colums.

Condition	DC Values		Fundamental Frequency				Vergence		Second Harmonic			
	Ampl	StdDev	Ampl	StdDev	Phase	StdDev	Mean	StdDev	Ampl	StdDev	Phase	StdDev
	(deg/s)	(deg/s)	(deg/s)	(deg/s)	(deg)	(deg)	(deg)	(deg)	(deg/s)	(deg/s)	(deg)	(deg)
Dark1	-0.34	1.87	13.71	2.72	148.48	6.43	2.52	0.59	0.95	2.07	22.58	128.70
Dark2	-1.43	2.99	9.60	3.26	141.68	26.11	5.87	1.24	0.84	1.56	-9.00	107.65
OK	0.49	1.62	43.36	5.91	179.02	4.20	10.69	0.49	0.55	0.44	76.65	65.41
OK+V	1.69	0.85	53.07	1.11	159.38	1.08	12.10	2.98	0.93	0.88	9.86	158.23
OK-V	3.72	3.14	30.94	8.97	174.07	122.02	11.90	0.21	6.27	2.87	-55.75	104.53
Right	48.96	7.25	12.70	9.60	112.18	38.51	***	***	4.44	4.34	-13.92	130.80
Left	-37.55	10.96	18.78	7.62	147.03	29.69	***	***	3.37	4.67	36.42	127.14
Up	0.82	1.56	11.27	2.00	150.60	12.26	***	***	3.54	4.70	103.55	79.84
Down	-0.95	2.33	9.90	3.81	135.59	21.64	***	***	1.90	3.57	38.26	110.61

Table A.1: Mean resultant amplitude and phase of horizontal responses for subject A - upright. Phase differences are with respect to sled velocity except for trials OK, OK+V, and OK-V where the phase difference with respect to shade velocity is presented. Asterisks (***) indicate measurements that were not taken or condition that were not run due to time constraints.

Condition	DC Values		Fundamental Frequency				Second Harmonic			
	Ampl	StdDev	Ampl	StdDev	Phase	StdDev	Ampl	StdDev	Phase	StdDev
	(deg/s)	(deg/s)	(deg/s)	(deg/s)	(deg)	(deg)	(deg/s)	(deg/s)	(deg)	(deg)
Dark1	-1.21	1.19	0.45	0.78	15.53	113.64	0.77	1.37	161.13	73.43
Dark2	-1.15	2.02	0.45	1.80	11.73	117.26	1.37	3.13	-125.01	97.37
OK	-0.44	0.40	1.73	0.34	6.91	174.36	0.82	0.89	-2.20	131.55
OK+V	-0.28	0.19	2.44	0.23	-4.46	123.32	0.56	0.45	-159.12	55.47
OK-V	-0.22	0.37	0.49	0.51	147.83	89.69	0.82	0.40	-89.73	28.80
Right	-2.59	1.21	2.34	1.11	71.38	42.71	0.69	2.08	110.24	102.17
Left	0.48	2.99	0.57	3.83	50.68	111.31	2.45	2.88	176.26	65.01
Up	10.56	2.01	2.75	3.36	51.10	110.80	2.15	2.54	-100.58	65.01
Down	-20.18	3.59	0.51	3.05	-99.57	130.79	1.99	3.04	95.71	87.99

Table A.2: Mean resultant amplitude and phase of vertical responses for subject A - upright. Phase differences are with respect to sled velocity except for trials OK, OK+V, and OK-V where the phase difference with respect to shade velocity is presented.

Condition	DC Values		Fundamental Frequency				Vergence		Second Harmonic			
	Ampl	StdDev	Ampl	StdDev	Phase	StdDev	Mean	StdDev	Ampl	StdDev	Phase	StdDev
	(deg/s)	(deg/s)	(deg/s)	(deg/s)	(deg)	(deg)	(deg)	(deg)	(deg/s)	(deg/s)	(deg)	(deg)
Dark1	0.45	0.80	7.67	1.94	151.89	13.05	11.75	0.45	0.55	0.86	101.20	87.85
Dark2	1.12	1.24	6.85	1.43	173.15	9.22	11.77	0.62	1.17	1.79	-155.56	76.03
OK	-0.79	2.16	23.40	3.69	179.63	3.39	1.85	0.54	2.48	2.01	167.89	54.70
OK+V	-0.36	0.83	39.98	1.54	164.96	2.01	2.34	1.40	0.52	0.93	16.17	122.60
OK-V	0.08	1.18	31.67	3.02	171.57	1.99	2.33	0.93	1.03	0.45	-161.09	50.05
Right	36.86	4.48	9.01	6.84	164.85	68.58	***	***	2.63	1.75	-70.70	50.16
Left	-35.81	8.88	8.79	4.59	133.33	38.41	***	***	4.56	5.67	134.81	99.36
Up	0.53	1.71	9.24	2.14	136.74	17.14	***	***	1.75	1.33	46.04	138.93
Down	-1.25	2.09	3.65	1.87	128.57	48.66	***	***	2.03	1.87	65.81	88.82

Table A.3: Mean resultant amplitude and phase of <u>horizontal</u> responses for subject B - upright. Phase differences are with respect to sled velocity except for trials OK, OK+V, and OK-V where the phase difference with respect to shade velocity is presented. Asterisks (***) indicate measurements that were not taken or condition that were not run due to time constraints.

Condition	DC Values		Fundamental Frequency				Second Harmonic			
	Ampl	StdDev	Ampl	StdDev	Phase	StdDev	Ampl	StdDev	Phase	StdDev
	(deg/s)	(deg/s)	(deg/s)	(deg/s)	(deg)	(deg)	(deg/s)	(deg/s)	(deg)	(deg)
Dark1	1.61	0.42	1.62	0.35	46.41	20.88	0.57	0.53	177.97	49.57
Dark2	-1.21	1.42	1.66	2.10	2.86	144.11	1.79	2.85	-90.68	66.59
OK	-0.44	1.02	0.84	0.91	-40.12	112.30	0.32	0.69	166.94	92.12
OK+V	-1.01	0.32	0.46	0.47	159.42	54.82	0.80	0.48	76.34	94.96
OK-V	-1.08	0.17	1.04	0.17	-18.24	112.12	0.42	0.29	97.10	47.23
Right	-2.26	0.69	2.07	0.60	8.50	151.43	1.34	0.93	155.37	49.81
Left	-0.47	0.36	2.24	1.26	146.24	26.38	1.19	0.61	144.77	34.83
Up	36.16	2.49	2.53	5.29	58.07	103.09	2.49	5.77	173.25	80.43
Down	-20.79	7.86	1.78	3.10	98.67	116.48	2.10	3.33	60.71	118.61

Table A.4: Mean resultant amplitude and phase of <u>vertical</u> responses for subject B - upright. Phase differences are with respect to sled velocity except for trials OK, OK+V, and OK-V where the phase difference with respect to shade velocity is presented.

Condition	DC Values		Fundamental Frequency				Vergence		Second Harmonic			
	Ampl	StdDev	Ampl	StdDev	Phase	StdDev	Mean	StdDev	Ampl	StdDev	Phase	StdDev
	(deg/s)	(deg/s)	(deg/s)	(deg/s)	(deg)	(deg)	(deg)	(deg)	(deg/s)	(deg/s)	(deg)	(deg)
Dark1	0.04	0.37	0.53	0.18	50.19	35.58	***	***	0.31	0.20	-70.86	109.76
Dark2	-0.64	0.34	2.81	0.67	124.23	12.58	***	***	0.19	0.55	9.18	130.75
OK	0.45	1.51	46.02	2.39	179.93	1.48	***	***	0.26	1.72	-110.62	102.21
OK+V	0.76	0.78	55.26	1.57	161.33	1.91	***	***	1.18	2.28	-170.34	73.80
OK-V	***	***	***	***	***	***	***	***	***	***	***	***
Right	44.56	2.64	3.99	2.79	152.50	44.19	***	***	2.81	1.31	-133.20	52.76
Left	-37.16	2.27	3.82	1.39	113.22	40.07	***	***	1.27	1.94	62.57	98.64
Up	-1.68	2.49	16.27	6.33	135.68	7.61	***	***	1.14	2.10	-18.22	121.85
Down	-4.97	1.32	5.53	1.58	74.37	20.93	***	***	1.51	1.17	-64.27	82.15

Table A.5: Mean resultant amplitude and phase of horizontal responses for subject C - upright. Phase differences are with respect to sled velocity except for trials OK, OK+V, and OK-V where the phase difference with respect to shade velocity is presented. Asterisks (***) indicate measurements that were not taken or condition that were not run due to time constraints.

Condition	DC Values		Fundamental Frequency				Second Harmonic			
	Ampl	StdDev	Ampl	StdDev	Phase	StdDev	Ampl	StdDev	Phase	StdDev
	(deg/s)	(deg/s)	(deg/s)	(deg/s)	(deg)	(deg)	(deg/s)	(deg/s)	(deg)	(deg)
Dark1	-0.16	0.26	0.79	0.45	23.00	154.26	0.34	0.19	-154.90	43.62
Dark2	1.85	0.32	0.23	0.27	-108.69	75.93	0.28	0.55	-132.54	72.64
OK	0.61	0.43	1.51	0.66	169.59	25.62	0.46	0.55	-27.68	140.09
OK+V	0.58	0.46	1.12	1.10	178.14	51.85	0.84	0.42	172.88	45.42
OK-V	***	***	***	***	***	***	***	***	***	***
Right	3.14	1.48	1.53	1.84	-10.89	123.61	0.91	0.78	-178.93	52.56
Left	1.35	0.78	0.78	0.65	-85.76	57.95	0.32	0.75	171.83	92.77
Up	22.92	4.55	1.39	2.81	-115.41	81.75	2.00	2.28	96.78	76.19
Down	-19.36	3.75	1.29	3.09	87.13	82.09	1.88	2.13	72.44	93.50

Table A.6: Mean resultant amplitude and phase of vertical responses for subject C - upright. Phase differences are with respect to sled velocity except for trials OK, OK+V, and OK-V where the phase difference with respect to shade velocity is presented. Asterisks (***) indicate measurements that were not taken or condition that were not run due to time constraints.

Condition	DC Values		Fundamental Frequency				Vergence		Second Harmonic			
	Ampl	StdDev	Ampl	StdDev	Phase	StdDev	Mean	StdDev	Ampl	StdDev	Phase	StdDev
	(deg/s)	(deg/s)	(deg/s)	(deg/s)	(deg)	(deg)	(deg)	(deg)	(deg/s)	(deg/s)	(deg)	(deg)
Dark1	0.20	1.01	3.70	2.38	155.99	45.05	5.42	1.12	0.20	0.87	-30.63	111.10
Dark2	-0.21	1.17	6.94	1.71	157.19	5.43	5.34	0.78	1.84	0.71	-20.18	124.05
OK	0.88	1.37	52.53	2.87	-178.96	2.41	6.84	1.08	1.42	1.06	-104.18	62.47
OK+V	0.33	1.04	54.02	9.93	163.07	3.20	6.57	1.23	0.58	2.20	122.88	93.77
OK-V	0.96	3.14	42.76	6.50	166.92	3.11	6.22	1.14	2.07	3.96	173.54	85.03
Right	38.39	3.54	20.31	4.58	158.00	19.41	***	***	3.46	3.03	77.87	98.30
Left	-48.51	1.26	8.06	2.66	139.33	16.53	***	***	1.37	1.91	113.92	91.28
Up	0.58	4.72	33.01	6.18	163.35	15.64	***	***	2.50	2.79	-63.86	90.79
Down	6.88	3.92	16.06	7.09	167.03	32.60	***	***	2.51	4.04	6.74	143.31

Table A.7: Mean resultant amplitude and phase of horizontal responses for subject D - upright. Phase differences are with respect to sled velocity except for trials OK, OK+V, and OK-V where the phase difference with respect to shade velocity is presented. Asterisks (***) indicate measurements that were not taken or condition that were not run due to time constraints.

Condition	DC Values		Fundamental Frequency				Second Harmonic			
	Ampl	StdDev	Ampl	StdDev	Phase	StdDev	Ampl	StdDev	Phase	StdDev
	(deg/s)	(deg/s)	(deg/s)	(deg/s)	(deg)	(deg)	(deg/s)	(deg/s)	(deg)	(deg)
Dark1	-0.98	0.46	1.14	0.81	-7.19	162.23	0.33	0.75	-155.53	80.13
Dark2	-2.49	0.76	0.61	0.52	-16.76	148.30	0.41	0.56	165.69	64.64
OK	-0.43	0.27	1.37	0.47	8.02	162.32	0.79	0.38	2.68	137.13
OK+V	-0.46	0.76	0.98	0.67	19.22	151.89	1.46	0.91	113.60	45.25
OK-V	0.31	0.60	0.83	0.52	120.97	45.70	1.08	0.69	-60.82	54.50
Right	-1.73	0.71	1.19	1.12	2.28	133.39	0.29	0.42	5.88	132.96
Left	-4.29	0.46	0.53	0.83	-83.49	103.46	1.04	0.72	8.25	152.37
Up	22.51	6.90	4.26	3.18	-118.49	58.30	2.64	1.75	-121.87	53.74
Down	-34.16	5.89	2.62	2.26	-162.86	56.26	0.33	4.68	-142.82	132.13

Table A.8: Mean resultant amplitude and phase of vertical responses for subject D - upright. Phase differences are with respect to sled velocity except for trials OK, OK+V, and OK-V where the phase difference with respect to shade velocity is presented.

Condition	DC Values		Fundamental Frequency				Vergence		Second Harmonic			
	Ampl	StdDev	Ampl	StdDev	Phase	StdDev	Mean	StdDev	Ampl	StdDev	Phase	StdDev
	(deg/s)	(deg/s)	(deg/s)	(deg/s)	(deg)	(deg)	(deg)	(deg)	(deg/s)	(deg/s)	(deg)	(deg)
Dark1	0.66	1.05	4.95	1.28	-175.10	9.45	6.06	0.78	0.89	0.88	30.88	147.56
Dark2	0.65	0.66	3.97	0.91	175.94	9.99	5.46	0.90	0.67	0.43	25.71	147.80
OK	0.08	1.48	33.03	4.31	-179.88	2.73	4.35	0.40	1.18	1.31	68.14	123.00
OK+V	-1.46	2.81	46.16	4.07	162.52	3.29	4.36	0.51	2.25	2.67	119.60	66.42
OK-V	-1.06	0.98	33.73	4.68	168.19	1.71	4.46	0.60	2.49	1.24	40.58	106.21
Right	26.60	5.31	5.86	5.25	152.27	67.16	4.52	0.49	1.45	2.24	117.58	65.33
Left	-29.97	2.29	9.31	3.20	160.79	14.56	4.48	0.44	2.19	1.61	22.55	152.35
Up	3.64	0.79	5.66	1.78	144.89	7.95	4.91	0.78	1.27	0.97	53.92	108.93
Down	-1.88	0.67	4.20	1.23	152.89	18.86	4.90	0.71	1.21	0.45	49.39	100.37

Table A.9: Mean resultant amplitude and phase of horizontal responses for subject E - upright. Phase differences are with respect to sled velocity except for trials OK, OK+V, and OK-V where the phase difference with respect to shade velocity is presented.

Condition	DC Values		Fundamental Frequency				Second Harmonic			
	Ampl	StdDev	Ampl	StdDev	Phase	StdDev	Ampl	StdDev	Phase	StdDev
	(deg/s)	(deg/s)	(deg/s)	(deg/s)	(deg)	(deg)	(deg/s)	(deg/s)	(deg)	(deg)
Dark1	1.43	0.53	0.29	0.40	-14.66	139.00	0.58	0.40	28.30	114.04
Dark2	3.42	0.37	0.66	0.57	50.21	138.18	0.41	0.68	36.29	78.52
OK	0.96	0.26	0.62	0.30	-80.37	24.69	0.64	0.28	-167.88	17.37
OK+V	0.05	0.28	0.35	0.35	-169.66	72.90	0.74	0.41	116.20	20.92
OK-V	1.13	0.34	0.20	0.33	136.97	89.46	0.51	0.34	-118.84	47.11
Right	1.04	0.33	1.31	0.47	41.31	28.48	0.42	0.40	90.60	82.64
Left	1.09	0.79	0.88	0.27	165.00	16.50	0.44	0.50	69.81	61.66
Up	17.37	4.37	2.11	2.48	47.53	115.10	0.30	2.18	-46.15	115.74
Down	-10.53	4.06	0.53	1.68	-167.38	93.49	1.74	1.19	89.66	44.86

Table A.10: Mean resultant amplitude and phase of vertical responses for subject E - upright. Phase differences are with respect to sled velocity except for trials OK, OK+V, and OK-V where the phase difference with respect to shade velocity is presented.

Condition	DC Values		Fundamental Frequency				Vergence		Second Harmonic			
	Ampl	StdDev	Ampl	StdDev	Phase	StdDev	Mean	StdDev	Ampl	StdDev	Phase	StdDev
	(deg/s)	(deg/s)	(deg/s)	(deg/s)	(deg)	(deg)	(deg)	(deg)	(deg/s)	(deg/s)	(deg)	(deg)
Dark1	0.16	0.30	3.77	0.97	142.72	7.00	7.40	1.24	0.40	0.67	-89.91	84.78
Dark2	***	***	***	***	***	***	***	***	***	***	***	***
OK	0.24	0.73	59.15	0.80	-177.44	0.98	5.40	0.43	0.04	0.88	87.82	125.12
OK+V	1.17	1.29	63.64	1.95	164.74	0.90	5.11	0.92	2.57	1.10	-46.52	24.62
OK-V	0.05	1.10	58.41	1.39	166.73	1.35	5.17	0.77	1.20	1.50	-63.23	110.63
Right	43.54	5.56	5.20	3.91	113.11	44.25	***	***	2.83	4.92	-70.22	95.80
Left	-49.83	2.56	5.24	3.11	118.27	31.44	***	***	0.53	1.40	10.22	114.11
Up	5.87	0.66	9.11	1.81	121.34	6.63	***	***	0.68	1.08	-110.81	82.93
Down	-2.26	0.67	6.24	1.51	95.95	20.94	***	***	1.00	0.72	117.55	59.99

Table A.11: Mean resultant amplitude and phase of horizontal responses for subject F - upright. Phase differences are with respect to sled velocity except for trials OK, OK+V, and OK-V where the phase difference with respect to shade velocity is presented. Asterisks (***) indicate measurements that were not taken or condition that were not run due to time constraints.

Condition	DC Values		Fundamental Frequency				Second Harmonic			
	Ampl	StdDev	Ampl	StdDev	Phase	StdDev	Ampl	StdDev	Phase	StdDev
	(deg/s)	(deg/s)	(deg/s)	(deg/s)	(deg)	(deg)	(deg/s)	(deg/s)	(deg)	(deg)
Dark1	-2.59	0.48	0.65	0.31	-82.00	48.07	0.23	0.40	-111.25	108.78
Dark2	***	***	***	***	***	***	***	***	***	***
OK	-0.73	0.17	0.83	0.32	-16.96	162.40	0.97	0.48	-11.98	155.88
OK+V	-1.02	0.22	0.38	0.28	0.56	161.80	0.20	0.40	-90.64	114.45
OK-V	-1.07	0.26	0.30	0.27	68.20	124.35	1.36	0.43	-31.23	14.95
Right	-2.29	0.61	0.71	1.08	113.78	88.00	0.47	0.32	80.55	69.35
Left	-1.69	0.61	0.65	0.24	-135.11	56.91	1.02	0.65	162.38	56.12
Up	34.62	4.69	1.93	5.04	-23.13	132.01	2.49	4.10	-111.87	110.23
Down	-33.36	2.57	0.30	3.32	5.74	114.48	2.96	2.17	-141.15	63.62

Table A.12 Mean resultant amplitude and phase of vertical responses for subject F - upright. Phase differences are with respect to sled velocity except for trials OK, OK+V, and OK-V where the phase difference with respect to shade velocity is presented. Asterisks (***) indicate measurements that were not taken or condition that were not run due to time constraints.

A.2 Supine Results

Tables A.13 through A.26 present the individual measurements for each subject run in the supine position, subjects B, C, D, E, F, G, and H. Format is similar to the one used in Tables 4.1 and 4.2. For each subject, DC offsets, oscillations at the fundamental frequency (0.25Hz) and the second harmonic (0.50Hz) are listed for both horizontal and vertical eye movements. Vergence was only measured in subject C. Due to time constraints some conditions were not run in some subjects, this is indicated by asterisks (***) in the corresponding colums.

Condition	DC Values		Fundamental Frequency				Second Harmonic			
	Ampl (deg/s)	StdDev (deg/s)	Ampl (deg/s)	StdDev (deg/s)	Phase (deg)	StdDev (deg)	Ampl (deg/s)	StdDev (deg/s)	Phase (deg)	StdDev (deg)
Dark1	-0.25	0.91	2.66	0.79	107.31	21.32	1.00	0.46	24.67	115.23
Dark2	-0.89	0.25	1.63	0.90	106.46	21.40	0.37	0.45	-117.18	63.75
OK	3.18	5.12	45.05	7.35	177.23	3.03	4.88	3.29	-35.92	141.49
OK+V	-0.94	1.23	52.20	4.66	160.99	1.47	1.77	1.83	29.31	110.74
OK-V	1.03	4.25	40.88	5.91	166.65	2.20	1.63	2.46	-18.22	130.83
Right	31.30	2.49	7.62	2.64	96.39	43.83	5.18	5.00	22.89	136.07
Left	-28.82	4.03	9.20	5.28	99.84	42.17	1.36	3.55	153.10	79.82
Up	-1.43	1.08	5.35	1.96	135.95	22.09	1.17	0.93	-51.48	145.10
Down	-1.62	0.96	2.18	0.93	99.88	44.26	0.28	0.41	101.23	131.55

Table A.13: Mean resultant amplitude and phase of horizontal responses for subject B - supine. Phase differences are with respect to sled velocity except for trials OK, OK+V, and OK-V where the phase difference with respect to shade velocity is presented.

Condition	DC Values		Fundamental Frequency				Second Harmonic			
	Ampl (deg/s)	StdDev (deg/s)	Ampl (deg/s)	StdDev (deg/s)	Phase (deg)	StdDev (deg)	Ampl (deg/s)	StdDev (deg/s)	Phase (deg)	StdDev (deg)
Dark1	1.86	0.38	0.42	0.38	134.04	65.57	0.40	0.21	136.53	49.07
Dark2	-0.09	0.72	0.91	0.52	15.54	153.70	0.66	0.75	-106.87	63.96
OK	0.08	0.55	4.00	1.34	-22.30	7.75	1.77	0.80	-19.55	119.46
OK+V	-1.32	0.99	1.67	0.67	41.75	30.42	2.44	0.55	34.02	8.67
OK-V	0.99	0.32	2.01	0.83	136.44	22.78	0.64	0.62	-57.40	59.45
Right	-1.77	0.30	0.88	0.85	0.42	142.35	0.34	0.98	39.15	113.98
Left	0.47	0.81	2.14	0.72	140.01	22.80	0.60	0.34	20.78	152.27
Up	23.40	7.54	3.15	3.97	-90.52	55.08	0.85	3.30	-2.91	115.70
Down	-12.33	3.48	1.68	1.97	29.79	130.80	0.63	2.40	-160.30	93.90

Table A.14: Mean resultant amplitude and phase of vertical responses for subject B - supine. Phase differences are with respect to sled velocity except for trials OK, OK+V, and OK-V where the phase difference with respect to shade velocity is presented.

Condition	DC Values		Fundamental Frequency				Vergence		Second Harmonic			
	Ampl	StdDev	Ampl	StdDev	Phase	StdDev	Mean	StdDev	Ampl	StdDev	Phase	StdDev
	(deg/s)	(deg/s)	(deg/s)	(deg/s)	(deg)	(deg)	(deg)	(deg)	(deg/s)	(deg/s)	(deg)	(deg)
Dark1	0.42	0.53	0.74	0.61	-173.78	57.20	7.58	0.65	0.51	0.36	-119.01	54.14
Dark2	0.37	0.38	2.64	1.04	143.74	16.86	8.40	0.80	0.40	1.26	-36.04	123.63
OK	0.70	2.41	45.90	2.96	175.19	2.60	6.42	0.50	3.20	2.30	-9.94	151.76
OK+V	0.07	1.74	55.15	1.60	156.65	2.68	6.40	0.56	1.06	2.97	20.26	120.33
OK-V	0.72	2.20	49.21	5.47	165.80	4.44	6.39	0.56	1.12	3.43	-39.48	125.55
Right	34.39	2.58	3.43	2.70	140.59	52.30	6.15	0.64	1.00	2.55	-138.33	87.08
Left	-21.65	6.30	5.20	5.44	99.17	95.08	6.61	0.70	1.21	3.05	-139.49	91.65
Up	-3.54	2.15	7.32	2.96	91.69	18.36	8.06	0.64	1.76	1.47	-21.68	140.25
Down	-0.93	1.81	13.63	4.02	111.95	6.87	8.23	0.70	2.31	1.94	-48.52	128.52

Table A.15: Mean resultant amplitude and phase of horizontal responses for subject C - supine. Phase differences are with respect to sled velocity except for trials OK, OK+V, and OK-V where the phase difference with respect to shade velocity is presented.

Condition	DC Values		Fundamental Sinusoid				Second Harmonic			
	Ampl	StdDev	Ampl	StdDev	Phase	StdDev	Ampl	StdDev	Phase	StdDev
	(deg/s)	(deg/s)	(deg/s)	(deg/s)	(deg)	(deg)	(deg/s)	(deg/s)	(deg)	(deg)
Dark1	-0.15	0.84	0.45	0.75	-83.73	129.73	0.40	0.81	-122.33	107.08
Dark2	0.33	0.54	0.22	1.13	-79.95	118.66	0.12	0.19	129.31	82.93
OK	0.56	0.46	3.38	1.04	2.95	177.41	1.06	0.65	35.63	118.97
OK+V	1.13	1.14	1.70	1.42	-19.77	103.02	0.22	1.58	-92.26	109.16
OK-V	1.96	0.73	1.78	0.82	174.44	26.27	1.09	0.64	-37.18	130.70
Right	0.30	1.05	1.94	1.41	-36.20	80.58	0.37	0.59	135.34	83.16
Left	2.68	0.60	0.63	0.57	-78.37	100.10	0.75	1.09	156.44	75.54
Up	29.27	2.74	3.36	1.87	-98.00	39.82	2.69	2.39	-4.93	142.43
Down	-26.00	3.40	0.61	1.45	75.45	112.76	4.45	2.95	69.42	45.62

Table A.16: Mean resultant amplitude and phase of vertical responses for subject C - supine. Phase differences are with respect to sled velocity except for trials OK, OK+V, and OK-V where the phase difference with respect to shade velocity is presented.

Condition	DC Values		Fundamental Frequency				Second Harmonic			
	Ampl	StdDev	Ampl	StdDev	Phase	StdDev	Ampl	StdDev	Phase	StdDev
	(deg/s)	(deg/s)	(deg/s)	(deg/s)	(deg)	(deg)	(deg/s)	(deg/s)	(deg)	(deg)
Dark1	-0.41	0.50	2.91	1.51	111.13	26.46	0.17	0.72	-47.32	102.21
Dark2	-0.51	0.45	4.93	1.30	132.35	14.25	0.45	0.74	150.55	85.65
OK	0.60	2.12	55.62	6.50	-176.07	1.13	1.95	2.36	-136.61	57.76
OK+V	1.31	1.39	64.58	6.67	163.73	1.29	1.86	1.23	-81.25	55.93
OK-V	-1.18	3.99	47.33	9.97	171.21	3.23	1.17	3.12	101.80	101.21
Right	40.11	2.81	25.07	3.65	177.62	9.78	4.92	5.39	98.75	63.34
Left	-37.92	3.69	24.74	5.98	148.46	19.81	1.34	2.90	-104.46	84.44
Up	***	***	***	***	***	***	***	***	***	***
Down	***	***	***	***	***	***	***	***	***	***

Table A.17: Mean resultant amplitude and phase of horizontal responses for subject D - supine Phase differences are with respect to sled velocity except for trials OK, OK+V, and OK-V where the phase difference with respect to shade velocity is presented. Asterisks (***) indicate measurements that were not taken or condition that were not run due to time constraints.

Condition	DC Values		Fundamental Frequency				Second Harmonic			
	Ampl	StdDev	Ampl	StdDev	Phase	StdDev	Ampl	StdDev	Phase	StdDev
	(deg/s)	(deg/s)	(deg/s)	(deg/s)	(deg)	(deg)	(deg/s)	(deg/s)	(deg)	(deg)
Dark1	-3.31	0.65	0.26	0.88	95.23	112.98	0.15	0.74	170.92	94.96
Dark2	-3.73	0.52	0.36	0.86	70.88	114.84	0.27	0.35	-71.92	128.91
OK	-2.40	0.60	0.95	0.53	176.01	34.80	2.08	0.71	86.73	16.76
OK+V	-2.39	0.51	1.99	0.78	163.38	12.20	1.82	0.48	36.18	12.43
OK-V	-2.98	0.44	1.22	0.91	-32.44	54.78	1.53	0.77	63.39	29.28
Right	-4.17	0.53	2.03	0.97	-18.91	112.27	0.70	0.66	-24.11	128.18
Left	-6.38	0.57	3.63	1.26	152.99	22.82	0.78	0.99	-65.87	63.06
Up	***	***	***	***	***	***	***	***	***	***
Down	***	***	***	***	***	***	***	***	***	***

Table A.18: Mean resultant amplitude and phase of vertical responses for subject D - supine. Phase differences are with respect to sled velocity except for trials OK, OK+V, and OK-V where the phase difference with respect to shade velocity is presented. Asterisks (***) indicate measurements that were not taken or condition that were not run due to time constraints.

Condition	DC Values		Fundamental Frequency				Second Harmonic			
	Ampl	StdDev	Ampl	StdDev	Phase	StdDev	Ampl	StdDev	Phase	StdDev
	(deg/s)	(deg/s)	(deg/s)	(deg/s)	(deg)	(deg)	(deg/s)	(deg/s)	(deg)	(deg)
Dark1	-0.44	0.36	2.07	0.65	167.93	8.89	0.44	0.27	32.26	47.42
Dark2	-0.41	0.42	2.70	0.37	141.90	11.71	0.25	0.29	97.14	85.61
OK	-0.85	1.76	35.17	6.96	-178.52	3.32	1.85	1.51	37.89	112.68
OK+V	-0.26	1.88	60.11	2.90	162.77	1.65	1.67	1.18	-55.58	133.64
OK-V	-0.68	1.07	36.89	3.48	167.47	2.66	1.02	0.96	69.54	67.68
Right	27.59	4.66	10.00	4.51	128.16	16.25	2.17	3.28	113.22	88.77
Left	-31.17	2.39	8.51	3.60	-67.97	27.44	1.20	2.12	-72.79	120.66
Up	***	***	***	***	***	***	***	***	***	***
Down	***	***	***	***	***	***	***	***	***	***

Table A.19: Mean resultant amplitude and phase of horizontal responses for subject E - supine. Phase differences are with respect to sled velocity except for trials OK, OK+V, and OK-V where the phase difference with respect to shade velocity is presented. Asterisks (***) indicate measurements that were not taken or condition that were not run due to time constraints.

Condition	DC Values		Fundamental Frequency				Second Harmonic			
	Ampl	StdDev	Ampl	StdDev	Phase	StdDev	Ampl	StdDev	Phase	StdDev
	(deg/s)	(deg/s)	(deg/s)	(deg/s)	(deg)	(deg)	(deg/s)	(deg/s)	(deg)	(deg)
Dark1	-0.19	0.15	0.27	0.42	-81.75	100.21	0.34	0.27	100.46	54.28
Dark2	0.10	0.59	0.15	0.59	-103.00	116.58	0.33	0.23	27.95	126.86
OK	0.43	0.24	1.30	0.42	-19.80	10.09	0.76	0.42	160.92	33.50
OK+V	-0.34	0.24	1.08	0.47	-6.87	150.04	0.74	0.22	61.90	32.73
OK-V	0.30	0.46	1.97	0.25	149.33	9.55	0.49	0.46	159.56	68.33
Right	-1.43	0.77	0.38	0.54	25.95	145.80	0.24	0.40	24.64	138.85
Left	-0.02	0.21	1.98	0.45	-82.98	13.92	0.46	0.49	-4.13	149.27
Up	***	***	***	***	***	***	***	***	***	***
Down	***	***	***	***	***	***	***	***	***	***

Table A.20: Mean resultant amplitude and phase of vertical responses for subject E - supine. Phase differences are with respect to sled velocity except for trials OK, OK+V, and OK-V where the phase difference with respect to shade velocity is presented. Asterisks (***) indicate measurements that were not taken or condition that were not run due to time constraints.

Condition	DC Values		Fundamental Frequency				Second Harmonic			
	Ampl	StdDev	Ampl	StdDev	Phase	StdDev	Ampl	StdDev	Phase	StdDev
	(deg/s)	(deg/s)	(deg/s)	(deg/s)	(deg)	(deg)	(deg/s)	(deg/s)	(deg)	(deg)
Dark1	0.23	1.01	0.94	0.90	-159.78	69.08	0.05	0.81	-94.95	124.31
Dark2	-0.13	1.20	1.45	1.75	65.56	119.10	0.67	1.46	-134.62	77.77
OK	0.17	5.06	49.74	12.40	-171.55	5.04	2.18	2.63	75.57	114.45
OK+V	-0.51	1.48	58.14	1.89	165.21	1.53	2.45	1.02	0.31	158.21
OK-V	-0.23	2.45	60.62	2.24	169.24	2.92	4.62	2.85	-30.83	99.47
Right	44.34	5.23	3.77	2.53	104.48	34.94	0.42	4.18	-59.99	103.09
Left	-43.88	4.38	4.31	3.88	95.74	62.69	1.83	4.56	103.44	100.74
Up	3.82	1.31	7.62	0.93	99.37	9.28	0.39	0.72	131.99	93.87
Down	-1.96	1.03	5.22	2.06	65.27	34.91	0.60	2.09	-3.86	120.79

Table A.21: Mean resultant amplitude and phase of horizontal responses for subject F - supine. Phase differences are with respect to sled velocity except for trials OK, OK+V, and OK-V where the phase difference with respect to shade velocity is presented.

Condition	DC Values		Fundamental Frequency				Second Harmonic			
	Ampl	StdDev	Ampl	StdDev	Phase	StdDev	Ampl	StdDev	Phase	StdDev
	(deg/s)	(deg/s)	(deg/s)	(deg/s)	(deg)	(deg)	(deg/s)	(deg/s)	(deg)	(deg)
Dark1	-1.66	1.58	0.86	1.80	136.21	96.59	0.19	1.04	-86.67	78.04
Dark2	-3.65	1.23	0.71	1.82	-86.90	104.58	0.36	0.94	-142.60	101.59
OK	-1.16	0.99	1.79	0.80	11.86	162.87	1.76	1.52	49.34	56.48
OK+V	-1.45	0.25	1.66	0.80	-8.57	121.54	1.01	1.07	4.93	149.06
OK-V	-1.59	0.55	2.34	0.89	156.63	13.89	2.24	0.80	3.33	174.53
Right	-5.19	0.70	0.70	0.62	161.47	56.07	0.24	0.97	118.95	124.20
Left	-1.34	0.34	0.23	1.21	-170.69	91.33	0.49	0.73	44.33	116.72
Up	33.98	5.02	1.14	4.61	24.09	119.05	4.36	6.71	16.53	135.24
Down	-31.34	3.42	3.00	6.24	-122.64	104.66	2.29	3.70	147.10	83.88

Table A.22: Mean resultant amplitude and phase of vertical responses for subject F - supine. Phase differences are with respect to sled velocity except for trials OK, OK+V, and OK-V where the phase difference with respect to shade velocity is presented.

Condition	DC Values		Fundamental Frequency				Second Harmonic			
	Ampl	StdDev	Ampl	StdDev	Phase	StdDev	Ampl	StdDev	Phase	StdDev
	(deg/s)	(deg/s)	(deg/s)	(deg/s)	(deg)	(deg)	(deg/s)	(deg/s)	(deg)	(deg)
Dark1	-0.03	0.42	0.89	0.37	-161.47	38.92	0.45	0.35	107.07	53.78
Dark2	-0.39	0.93	0.65	0.67	-97.06	66.31	0.26	0.43	177.60	73.22
OK	1.23	1.67	50.68	3.07	-173.97	1.37	0.88	1.16	-68.23	84.92
OK+V	0.53	0.60	60.42	1.95	166.40	1.35	1.18	2.18	91.67	111.88
OK-V	-0.53	2.03	52.65	1.88	172.99	2.15	1.05	2.07	-168.24	107.20
Right	46.79	5.43	4.33	4.19	85.34	72.08	0.09	3.66	144.62	133.28
Left	-47.91	2.83	11.52	2.84	102.30	14.22	3.68	4.51	-147.80	69.98
Up	-1.61	1.03	6.39	1.35	128.15	5.90	0.47	0.57	113.90	98.33
Down	-0.23	1.01	6.28	1.59	95.53	12.41	0.79	0.52	64.20	55.72

Table A.23: Mean resultant amplitude and phase of horizontal responses for subject G - supine. Phase differences are with respect to sled velocity except for trials OK, OK+V, and OK-V where the phase difference with respect to shade velocity is presented.

Condition	DC Values		Fundamental Frequency				Second Harmonic			
	Ampl	StdDev	Ampl	StdDev	Phase	StdDev	Ampl	StdDev	Phase	StdDev
	(deg/s)	(deg/s)	(deg/s)	(deg/s)	(deg)	(deg)	(deg/s)	(deg/s)	(deg)	(deg)
Dark1	-2.39	0.75	0.91	0.85	168.33	56.81	0.14	0.32	107.52	110.45
Dark2	-2.72	0.50	1.07	0.56	-178.59	37.28	0.50	0.32	115.47	46.19
OK	-1.83	0.19	0.78	0.58	166.89	50.17	1.44	0.19	74.71	13.29
OK+V	-2.33	0.55	0.65	0.57	-141.85	55.78	1.25	0.46	60.00	17.40
OK-V	-2.11	0.48	0.26	0.69	15.64	123.56	1.30	0.30	29.68	121.93
Right	-4.79	0.71	0.79	0.68	-98.45	62.15	0.22	0.55	-94.35	99.95
Left	-4.75	0.68	0.94	1.08	-144.25	89.47	0.80	0.69	-173.36	72.55
Up	31.68	6.14	4.69	5.56	143.85	75.94	1.17	1.31	-116.65	78.25
Down	-42.60	12.62	2.36	4.49	-175.25	88.76	0.56	1.80	97.76	117.18

Table A.24 : Mean resultant amplitude and phase of vertical responses for subject G - supine. Phase differences are with respect to sled velocity except for trials OK, OK+V, and OK-V where the phase difference with respect to shade velocity is presented.

Condition	DC Values		Fundamental Frequency				Second Harmonic			
	Ampl	StdDev	Ampl	StdDev	Phase	StdDev	Ampl	StdDev	Phase	StdDev
	(deg/s)	(deg/s)	(deg/s)	(deg/s)	(deg)	(deg)	(deg/s)	(deg/s)	(deg)	(deg)
Dark1	-0.61	0.48	2.56	1.02	-25.33	121.76	0.45	0.73	91.32	92.94
Dark2	0.46	0.70	1.81	0.88	40.40	24.94	0.30	0.66	-96.45	116.59
OK	3.08	4.33	47.77	13.03	-178.94	2.32	6.11	4.55	-100.62	68.46
OK+V	-2.16	1.54	64.63	3.30	161.11	3.75	2.55	2.17	-50.30	149.56
OK-V	-0.62	2.18	48.98	7.46	165.94	3.05	1.12	3.01	-83.40	103.88
Right	30.03	7.23	3.84	4.48	-162.79	78.26	1.33	4.70	8.27	112.28
Left	-20.25	7.88	11.83	6.84	135.96	42.33	0.52	3.74	31.79	110.96
Up	5.65	0.94	8.55	1.34	114.19	7.39	0.22	0.61	-140.49	84.13
Down	-3.79	1.75	5.95	2.85	125.86	16.80	0.67	0.88	113.11	82.15

Table A.25: Mean resultant amplitude and phase of horizontal responses for subject H - supine. Phase differences are with respect to sled velocity except for trials OK, OK+V, and OK-V where the phase difference with respect to shade velocity is presented.

Condition	DC Values		Fundamental Frequency				Second Harmonic			
	Ampl	StdDev	Ampl	StdDev	Phase	StdDev	Ampl	StdDev	Phase	StdDev
	(deg/s)	(deg/s)	(deg/s)	(deg/s)	(deg)	(deg)	(deg/s)	(deg/s)	(deg)	(deg)
Dark1	0.04	0.25	1.59	0.29	140.28	16.98	0.77	0.36	146.09	33.19
Dark2	1.03	0.28	0.44	0.37	143.96	51.37	0.50	0.27	132.41	41.31
OK	-0.30	0.35	4.57	0.93	-4.97	181.54	1.87	0.66	43.57	113.35
OK+V	0.82	0.32	5.03	0.65	-14.56	10.79	1.42	0.70	11.88	179.40
OK-V	0.42	0.38	4.42	0.46	156.26	5.35	0.95	0.77	7.11	167.29
Right	-2.13	0.58	0.31	0.82	112.10	114.42	0.90	0.78	115.55	56.67
Left	2.60	1.02	1.07	0.87	55.29	128.29	0.34	1.02	58.89	100.54
Up	22.73	2.05	2.64	2.10	73.65	45.07	0.96	2.20	-147.33	90.97
Down	-16.40	3.64	0.36	3.81	105.49	108.40	2.04	2.01	59.80	125.57

Table A.26: Mean resultant amplitude and phase of vertical responses for subject H - supine. Phase differences are with respect to sled velocity except for trials OK, OK+V, and OK-V where the phase difference with respect to shade velocity is presented.

List of MatLab Scripts written for this Thesis

All of the Nysa programs used in this thesis have been described before (Balkwill, 1992). The MatLab scripts files written for this thesis performed frequency and statistical analyses on the SPV files generated by Nysa.

B.1 Frequency Analysis

This task is performed by the script *freq_analysis*, which was written based on the script *jc_sines* (Christie, 1992). This programs fits a curve to the SPV data which is a combination of a DC offset and sinuoids at the fundamental frequency, the second, third, and fourth harmonic. Its output is a statiscs file containing the amplitude of the response at each one of these harmonics, as well as their phase difference with respect to a negative sine at each frequency. This analysis is done for each one of the seven cycles analyzed per trial.

B.2 Statistical Analysis

Two scripts files implement the Hotelling's T distribution confidence areas that are used as statistical tools. *Mult_sbj* takes the statistics files generated by *freq_analysis*, and calls the scripts *conf_sbj* which plots the confidence areas using the data as well as the F distribution which is contained in that script.

```
% Title: freq_analysis
% Fits sinusoids at the fundamental frequency plus 2nd,3rd, and 4th
% harmonics to the eye SPV data
% Written by Juan Carlos Mendoza (July, 92) based on
% Jock Christie's jc_sines
% Output is sent to the Statistics directory and contains
% the coefficient at each frequency.  It also generates polar plots of the
% responses.
clear;
hold off;

if (exist('nysa_path') ~= 1)
    nysa_path = get_path;
end
eval(['load ',nysa_path,'bookkeeping:vel_filter.mat']);   % contains sample


% % % % % % % % % % % % % % % % % % % %
ALT = 1;              % 1 Turns on alternate curve fitting for whole trial
bias_flag = 0;        % bias_flag = 1; will calculate pos/neg bias.
discard = 0.0;        % Number of seconds to discard at start of trial
dn = 1;               % Axis for analysis. dn=1 Horiz. dn=2 Vert.;
EDV = 1;              % set EDV = 1 for edited values, else it loads SPV
eye_vel_sign = +1;    % = +/- 1 to correct for sign conventions.
freq_stim = [0.25,0.5,0.75,1.0];   % Should be in ascending order.
G_LEVEL = 0.4;        % Maximum sinusoidal G level.
N = 4;                % Allows user to chose the number of harmonics.
Ok_Stim=0;% Set to 1 if windowshade is the stimulus as in the OK trial
pick = 'n';           % 'y' allows user to manually select starting point.
run_code = 'Sxxxxxxx';      % Should have the same legth as file name.
sample = 200;                       % Sampling rate in Hertz
STATS = 'y';          % 'y' produces statistics about the phase and amp.
stim_offset = 0;      % This is the zero value for the A/D board.
stim_scale = 0.00253517;   % This is used to scale the stimulus data.
old_start = 1/200;    % Estimated time at which stimulus starts.
top = 100;            % Used for plotting.
T_run = 8.0;          % Duration of data to be analyzed in seconds.
vel_scale = 0.00253517;   % Calculated by JC for use with the MITsled.
wolfie = 'y';         % 'y' is used to plot the curve fits.
% % % % % % % % % % % % % % % % % % % %

name = input(['Enter exp. code [ default = ', run_code, ' ] '],'s');
if (~isempty(name))
    run_code(1:length(run_code)) = CAPS(name);
end
i

file_specs_2
if (Ok_Stim==1)
                fileS = file_name(Okn_File_raw,run_code);
                eval(['load ',data_path,fileS]);
                %eval(['stim = ',Sled_Var,';']);
                eval(['stim = Okn_scale*(',Okn_Var,'-stim_offset);']);
                eval(['clear ',Sled_Var]);
else
                fileS = file_name(Sled_File_raw,run_code);
                eval(['load ',data_path,fileS]);
                %eval(['stim = ',Sled_Var,';']);
```

171

```
                    eval(['stim = stim_scale*(',Sled_Var,'-stim_offset);']);
                    eval(['clear ',Sled_Var]);
end
file_len = length(stim);
eval(['filespv = file_name(Edited',int2str(dn),'_File,run_code);']);
if (EDV) & (exist([data_path,filespv]) == 2)
   eval(['load ',data_path,filespv]);
   if exist(['edited',int2str(dn)])
      eval(['SPV = eye_vel_sign*edited',int2str(dn),';']);
   else
      eval(['SPV = eye_vel_sign*',eval(['Edited',int2str(dn),'_Var']),';']);
   end
   eval(['clear ',eval(['Edited',int2str(dn),'_Var'])]);
else
   eval(['filespv = file_name(SPV',int2str(dn),'_File,run_code);']);
   eval(['load ',data_path,filespv]);
   eval(['SPV = eye_vel_sign*',eval(['SPV',int2str(dn),'_Var']),';']);
   eval(['clear ',eval(['SPV',int2str(dn),'_Var'])]);
end
run_code = [prefix, run_code];
clear fileS filespv name A B
clear_specs_jc
if ((pick == 'y')|(pick == 'Y'))
   hold off
   clg
   plot((1:file_len/2)/sample,stim(1:file_len/2))
   hold on
   plot((1:file_len/2)/sample,ones(file_len/2,1)*mean(stim(1:200)),'b')
   hold off
   xlabel('Time in seconds.');
   fprintf('\nClick at the point where the stimulus starts\n');
   [xx,yy] = ginput(1);
   old_start = round(xx*sample);
else
% This set to a constant as a trial (JM 8/2/92)
   old_start = old_start*sample;
   if (old_start==0)
                                    old_start=1;
   end
end

total_ticks = T_run*sample;
num_freq = length(freq_stim);
NNN = 2^floor(log(min(length(stim)-old_start,total_ticks))/log(2));
v = stim(old_start:old_start+NNN-1) - mean(stim(old_start:old_start+NNN-1));
mag = (2*abs(fft(v,NNN))/NNN);
[AMP,b] = max(mag);
guess = sample*(b-1)/NNN;
clear b mag NNN v
if (AMP < 0.25)|(guess > 2*max(freq_stim))
   dyn_cal = 1;
   AMP = 0;
   known_freq = min(freq_stim);
   step = sample/known_freq;
   title_string = ['File code = ',run_code,'  Dynamic Calibration    SPV in red   Curve fit in blue.'];
else
   dyn_cal = 0;
   known_freq = freq_stim(pick_a_freq(freq_stim,guess));
```

172

```
    step = sample/known_freq;
    %  old_start = zero_cross(stim,old_start+step) - step;    % Avoids transients.
    title_string = ['File code = ',run_code,'  ',num2str(known_freq),' Hz    SPV in red    Curve fit in blue.'];
end


start = old_start + discard*sample;
last_pt = old_start + total_ticks;  % Point at which sled motion ends

num_steps = round((last_pt - start)/step);    % Should be 6 or 24
% Revised by JC and LM    26 April 1991    Should be 5 or 20
sum_error = 0;
coeff_stim = zeros(num_steps,2*N+2);    % Matrix of coeff. for each cycle
coeff_spv = zeros(num_steps,2*N+2);     % Ditto  (may need space for two freq.
time = [0:(step - 1)]'/step;
K = ones(time);


% Note, All terms must be orthogonal, so drift was removed in March 1991    JC
% Second order Harmonics added 26 April 1991 JC
% Fourth order Harmonics added 06 July  1991  JC
for i = 1:N
    S = [S, -sin(2*i*pi*time)];
    C = [C, cos(2*i*pi*time)];
end



linear_part = zeros(file_len,1);   % Used to calculate residues.
curves = zeros(file_len,N);


pointer = start;
final = num_steps;
for loop = 1:num_steps,
    if ((pointer+step) > length(SPV))|(sqrt(2)*rms(stim(pointer+1:pointer+step)) < (0.75 * AMP))
fprintf('\nYou moron! OK up to here');
        final = loop - 1;    % ie. aborting due to sled crash.
        fprintf('\nAborting after cycle %2.0f out of %2.0f \n',final ,num_steps);
        break
    end

    temp_stim = ([S C]\stim(pointer+1:pointer+step))';
    coeff_stim(loop,1) = loop;    % Loads coefficients into Sled Matrix
    coeff_stim(loop,2) = (K\stim(pointer+1:pointer+step))';
    coeff_stim(loop,3:2:(2*N+1)) = sqrt(temp_stim(1:N).^2+temp_stim(N+1:2*N).^2);
    coeff_stim(loop,4:2:(2*N+2)) = atan2(temp_stim(N+1:2*N),temp_stim(1:N));
    temp_spv = ([S C]\SPV(pointer+1:pointer+step))';
    coeff_spv(loop,1) = loop;     % Loads coefficients into Spv Matrix
    coeff_spv(loop,2) = (K\SPV(pointer+1:pointer+step))';
    coeff_spv(loop,3:2:(2*N+1)) = sqrt(temp_spv(1:N).^2+temp_spv(N+1:2*N).^2);
    coeff_spv(loop,4:2:(2*N+2)) = atan2(temp_spv(N+1:2*N),temp_spv(1:N));

    linear_part(pointer+1:pointer+step) = coeff_spv(loop,2)*K;
    curves(pointer+1:pointer+step,:) = sin((2*pi*time*[1:N]) +
(ones(step,1)*coeff_spv(loop,4:2:(2*N+2))))*diag(coeff_spv(loop,3:2:(2*N+1)));


    pointer = pointer + step;  % increment for next round
end
clear K S C sled time temp_stim temp_spv


if final < num_steps
```

173

```
    coeff_stim = coeff_stim(1:final,:);
    coeff_spv = coeff_spv(1:final,:);
end

% This section repositions the branch cut to 2*pi.
coeff_stim(:,4:2:2*N+2) = coeff_stim(:,4:2:2*N+2) - 2*pi*round((sign(coeff_stim(:,4:2:2*N+2))-
1+eps)/2);

coeff_spv(:,4:2:2*N+2) = coeff_spv(:,4:2:2*N+2) - 2*pi*round((sign(coeff_spv(:,4:2:2*N+2))-1+eps)/2);

fprintf(['\n',title_string,'\n']);
fprintf('\n Stim cycle #   const   amp   phase    2amp   2phase\n')
disp(coeff_stim(:,1:6)*diag([1, 1, 1, (180/pi), 1, (180/pi)]));

fprintf('\n Eye cycle #   const   amp   phase    2amp   2phase\n')
disp(coeff_spv(:,1:6)*diag([1, 1, 1, (180/pi), 1, (180/pi)]));
%summary(:,:)=coeff_spv(:,3:10);
%Do t test for DC values:
break
[zdc,prdc]=T_test(coeff_spv(:,2));
for i=1:N,
for k =1:num_steps,
  vect(k,2*i-1)=coeff_spv(k,1+2*i)*cos(coeff_spv(k,2+2*i));
  vect(k,2*i)=coeff_spv(k,1+2*i)*sin(coeff_spv(k,2+2*i));
end
end
vect(num_steps+1,:)=sum(vect);
JUNK = [' FIRST ';'SECOND ';' THIRD ';' FOURTH';' FIFTH ';' SIXTH ';'SEVENTH'];
  for i = 1:N,
%      fprintf(['\n\nTESTING THE ',JUNK(i,:),' HARMONIC at %2.2f HERTZ.'], %known_freq*i);
    mag(i)=sqrt(vect(num_steps+1,2*i-1)^2+vect(num_steps+1,2*i)^2)/num_steps;
    ang(i)=atan2(vect(num_steps+1,2*i),vect(num_steps+1,2*i-1));
    for k=1:num_steps,
      prj(k,i)=coeff_spv(k,1+2*i)*cos(coeff_spv(k,2+2*i)-ang(i));
    end
% To check it, sum(prj)=mag
    [z, pr] = T_test(prj(:,i));
xx(i)=z;
pp(i)=pr;
clear z,pr
%fprintf('T = %3.3f \nProb = %3.3f \n',xx(i), pp(i));
  end
gain= mean(prj(:,1));
 phase=(ang(1)-mean(coeff_stim(:,4)))*(180/pi);
  if (abs(phase)>180)
     phase=phase-360*sign(phase);
  end
savemat=[coeff_stim(:,1:6) coeff_spv(:,1:6)];
if bias_flag
                    [pos,neg]=find_bias(SPV(old_start:last_pt));
                    fprintf('The positive bias = %3.3f deg/sec \nThe negative bias = %3.3f deg/sec
\n',pos, neg);
else
  neg=0;
  pos=0;
end
xx=[zdc xx];
pp=[prdc pp];
```

174

```matlab
% Add t test results
eval(['save ',stat_path,run_code,int2str(dn),'.newstat savemat mag ang prj phase xx pp ']);
% From here on, polar plots
  clg;
  subplot(221);
polar(coeff_spv(1:num_steps,4),coeff_spv(1:num_steps,3),'+',ang(1),mag(1),'o');
                        title ('First Harmonic');
  xlabel('SPV Amplitude (deg/s)');
  grid;
  subplot(222);
 polar(coeff_spv(1:num_steps,6),coeff_spv(1:num_steps,5),'+',ang(2),mag(2),'o');
                        title ('Second Harmonic');
  xlabel('SPV Amplitude (deg/s)');
  grid;
  subplot(223);
polar(coeff_spv(1:num_steps,8),coeff_spv(1:num_steps,7),'+',ang(3),mag(3),'o');
                        title ('Third Harmonic');
  xlabel('SPV Amplitude (deg/s)');
  grid;
  subplot(224);
polar(coeff_spv(1:num_steps,10),coeff_spv(1:num_steps,9),'+',ang(4),mag(4),'o');
                        title ('Fourth Harmonic');
  xlabel('SPV Amplitude (deg/s)');
  grid;
  text(0.44,.65,'File: ','sc');
  text(0.5,.65,run_code,'sc');
  text (0.44,.55,' Axis: ','sc');
  if (dn == 1)
                        text (.52,.55,'Horizontal','sc');
                        else
                                        text (.52,.55,'Vertical','sc');

  end
hold;
end;
```

175

```matlab
% Title: mult_sbj
% Gathers data from multiple subjects to generate confidence area plots
% Loads files from the statistics files, takes data from amplitude and phase format
% and puts it into sine and cosine component format and send it to conf_sbj under the
% variable a to be plotted
clear
clg
hold off
fl=0;
stat_path = 'Sherry:MatLab:Nysa:scripts:'
v=[-20 20 -20 20];
axis('square')
axis(v)
title('Sinusoidal OK Trials (Upr-Sup)')
xlabel('Sine Component')
ylabel('Cosine Component')
eval(['load ',stat_path,'okpos']);
fl1='.';
fl2='x';
%a(:,1)=hdark1(:,7).*cos(hdark1(:,9));
%a(:,2)=hdark1(:,7).*sin(hdark1(:,9));
a=okpos;
conf_sbj
hold on
clear a
text(16*(20/15),-7*(20/15),'x OK:Upr-Sup')
text(16*(20/15),-11*(20/15),'+ OK+V:Upr-Sup')
text(16*(20/15),-15*(200/15),'o OK-V:Upr-Sup')
title('Sinusoidal OK Trials (Upr-Sup)')
xlabel('Sine Component')
ylabel('Cosine Component')
%text(16*(20/15),-19*(20/15),'* Down')
eval(['load ',stat_path,'okpvpos']);
a=okpvpos;
%a(:,1)=hdark2(:,7).*cos(hdark2(:,9));
%a(:,2)=hdark2(:,7).*sin(hdark2(:,9));
fl1='.';
fl2='+';
conf_sbj
hold on
clear a
eval(['load ',stat_path,'okmpos']);
%a(:,1)=hokmv(:,3).*cos(hokmv(:,5));
%a(:,2)=hokmv(:,3).*sin(hokmv(:,5));
a=okmpos;
fl1='.';
fl2='o';
conf_sbj
hold on
clear a
%eval(['load ',stat_path,'hdown.summ2']);
%a(:,1)=hdown(:,3).*cos(hdown(:,5));
%a(:,2)=hdown(:,3).*sin(hdown(:,5));
%fl1='-.';
%fl2='*';
%conf_sbj
break
```

176

```matlab
% Title: conf_sbj
% Plots Confidence areas
[R C]=size(a);
%a=a(1:(R-1),:);
F=[199.5 19.00 9.55 6.94 5.79 5.14 4.74 4.46 4.26 4.10 3.98 3.89 3.81 3.74 3.68 3.63 3.59 3.55 3.52 3.49
3.47 3.44];
%if fl==1,
%  a=-a;
%end
b=inv(cov(a));
alfa=.5*atan2((2*b(2,1)),(b(1,1)-b(2,2)));
c1=b(1,1)*cos(alfa)^2+2*b(2,1)*cos(alfa)*sin(alfa)+b(2,2)*sin(alfa)^2;
c2=b(1,1)*sin(alfa)^2-2*b(2,1)*cos(alfa)*sin(alfa)+b(2,2)*cos(alfa)^2;
c3=(2*(R-1)/(R*(R-2)))*F(R-2);
%clear y1,y2;
x=-sqrt(c3/c1):.002:sqrt(c3/c1);
y1=sqrt((c3-c1*x.^2)/c2);
y2=-sqrt((c3-c1*x.^2)/c2);
%plot(x,y1,x,y2)
xf1=cos(alfa).*x-sin(alfa).*y1;
yf1=sin(alfa).*x+cos(alfa).*y1;
xf2=cos(alfa).*x-sin(alfa).*y2;
yf2=sin(alfa).*x+cos(alfa).*y2;
xf1=mean(a(:,1))+xf1;
yf1=mean(a(:,2))+yf1;
xf2=mean(a(:,1))+xf2;
yf2=mean(a(:,2))+yf2;
%axis('square')
%axis(v)
plot(xf1,yf1,fl1,xf2,yf2,fl1,mean(a(:,1)),mean(a(:,2)),fl2)
grid
```